Oil & Natural Gas Technology

DOE Award No.: DE-FG26-04NT-15533

Final Report

Synthesis and Evaluation of CO_2 Thickeners Designed with Molecular Modeling

Submitted by:
Dr. Robert M. Enick, Dr. Eric J. Beckman, Dr. J. Karl Johnson
Chemical and Petroleum Engineering
1249 Benedum Hall, Swanson School of Engineering, University of Pittsburgh
Pittsburgh PA 15261

Prepared for:
United States Department of Energy
National Energy Technology Laboratory

February 1, 2010

Office of Fossil Energy

Synthesis and Evaluation of CO_2 Thickeners Designed with Molecular Modeling

Final Report

Start Date: Sept. 1, 2004
End Date: August 31, 2009

Dr. Robert M. Enick
Dr. Eric J. Beckman
Dr. J. Karl Johnson
Chemical and Petroleum Engineering
University of Pittsburgh

Dr. Andrew Hamilton
Chemistry
Yale University

Date Issued: Feb. 1, 2010

DE-FG26-04NT-15533

Dr. Robert M. Enick and Dr. Eric J. Beckman
Department of Chemical and Petroleum Engineering
University of Pittsburgh
1249 Benedum Engineering Hall
Pittsburgh, PA 15261

Disclaimer

This report was prepared as an account of work sponsored by an agency of the United States Government. Neither the United States Government nor any agency therefore, nor any of their employees, makes any warranty, express or implied, or assumes any legal liability or responsibility for the accuracy, completeness, or usefulness of any information, apparatus, product or process disclosed, or represents that its use would not infringe privately owned rights. Reference herein to any specific commercial product, process or service by trade name, trademark, manufacturer, or otherwise does not necessarily constitute or imply its endorsement, recommendation, or favoring by the United States Government or any agency thereof. The views and opinions of authors expressed herein do not necessarily state or reflect those of the United States Government or any agency thereof.

Abstract

The objective of this research was to use molecular modeling techniques, coupled with our prior experimental results, to design, synthesize and evaluate inexpensive, non-fluorous carbon dioxide thickening agents.

The first type of thickener that was considered was *associating polymers.* Typically, these thickeners are copolymers that contain a highly CO_2-philic monomer, and a small concentration of a CO_2-phobic associating monomer.

Yale University was solely responsible for the synthesis of a second type of thickener; *small, hydrogen bonding compounds.* These molecules have a core that contains one or more hydrogen-bonding groups, such as urea or amide groups. Non-fluorous, CO_2-philic functional groups were attached to the hydrogen bonding core of the compound to impart CO_2 stability and macromolecular stability to the linear "stack" of these compounds.

The third type of compound initially considered for this investigation was *CO_2-soluble surfactants*. These surfactants contain conventional ionic head groups and composed of CO_2-philic oligomers (short polymers) or small compounds (sugar acetates) previously identified by our research team. Mobility reduction could occur as these surfactant solutions contacted reservoir brine and formed mobility control foams in-situ.

The vast majority of the work conducted in this study was devoted to the copolymeric thickeners and the small hydrogen-bonding thickeners; these thickeners were intended to dissolve completely in CO_2 and increase the fluid viscosity. A small but important amount of work was done establishing the groundwork for CO_2-soluble surfactants that reduced mobility by generating foams in-situ as the CO_2+surfactant solution mixed with in-situ brine.

Polymers

In this final report, we review our entire co-polymeric thickener effort and detail, for the first time, the phase behavior and viscosity results *of* ***the first non-fluorous, oxygenated hydrocarbon-based, associating polymer CO_2 thickener, poly(vinyl acetate – co – benzoyl$_{5\%}$).*** The CO_2-philic monomer was vinyl acetate, and the associative thickener monomer was vinyl benzoate. Poly(vinyl acetate – co – benzoyl$_{5\%}$), Mw ~ 12000, is capable of increasing the viscosity of CO_2 by 70% at a concentration of 2wt%, a shear rate of ~5000s $^{-1}$, 298K and 9500 psia. Unfortunately, poly(vinyl acetate – co – benzoyl$_{5\%}$) is ***not capable of dissolving in CO_2 at pressures close to the MMP***, roughly 1200 psia at 298 K. In fact, we are now convinced that a ***non-fluorous, hydrocarbon-based co-polymeric thickener cannot be designed*** that will dissolve in CO_2 at typical reservoir conditions. Why? Every polymer that we designed using molecular modeling tools was indeed CO_2 soluble, a somewhat remarkable achievement given the small number of CO_2 soluble surfactants that have ever been identified, but each one was less soluble in CO_2 than poly(vinyl acetate). Therefore co-polymeric thickeners based on any CO_2 soluble polymer will undoubtedly be less soluble in CO_2 (i.e. require even greater pressures than 9500 psia) than poly(vinyl acetate – co – benzoyl$_{5\%}$). We even considered co-polymeric thickeners based on poly(dimethylsiloxane)(PDMS) because PDMS is much more CO_2-soluble than PVAc. Poly(phenyl methyl – siloxane), a copolymer containing the CO_2-philic siloxane and the CO_2-phobic, pendant, associating, methyl phenyl group, was found to be CO_2 insoluble at pressures up to 10000 psia.

Despite our inability to design a CO_2-soluble copolymeric thickener, were made significant progress in identifying CO_2 soluble polymers and oligomers. Specific high molecular weight polymers that have been designed/identified as CO_2 soluble included the following (listed in order of most CO_2 soluble to less CO_2 soluble); poly(fluoroacrylate)(PFA), poly(dimethylsiloxane)(PDMS), poly(vinyl acetate) (PVAc), poly(1-O-(vinyloxy)ethyl-2,3,4,6-tetra-O-acetyl-β-D-glucopyranoside) (PAcGIcVE), amorphous poly(lactic acid)(PLA) and poly(methyl acrylate)(PMA). Oligomers that exhibit CO_2 solubility include poly(propyleneoxide)(PPO), poly(vinyl ethyl ether)(PVEE), poly(vinyl methoxymethyl ether)PVMME, cellulose triacetate oligomers (CTA), peracetylated cyclodextrins (PACD), poly(acetoxy oxetane)(PAO), and poly(vinyl methoxy ethyl ether)(PVMEE).

Small hydrogen-bonding compounds

We were able to synthesize the first non-fluorous, small, hydrogen-bonding molecule that was soluble in CO_2 to about 1 wt% at elevated temperature (high temperature weakens hydrogen bonding, which facilitates dissolution)

and remained in solution upon cooling. The compound contained two ureas for hydrogen bonding, two highly acetylated tails for CO_2 solubility, and a small alkyl chain in the middle as a spacer. This compound did **not** appreciably thicken CO_2. Interestingly, upon depressurization (removal of the CO_2) this compound formed a brittle, free-standing microfibrillar monolith; direct evidence that the small compounds were indeed aligned or "stacked" in solution. We were also able to synthesize the first CO_2 soluble dendrimer, a bisurea with four highly acetylated arms. This compound was very soluble in CO_2 at 298K but did **not** induce any change in viscosity and did not yield fibers upon depressurization. Apparently the steric hindrance associated with the four acetylated arms prevented the two cetral urea groups from associating with neighboring molecules.

Surfactants

In an attempt to identify surfactants that could dissolve in CO_2 and then form CO_2-in-brine mobility controls foams in-situ, we successfully identified numerous non-fluorous ionic surfactants that were CO_2 soluble. The fundamental characteristic of these surfactants was the presence of CO_2-philic oligomers. These oligomers included acetyl gluconic, oligo(propylene glycol), oligo(vinyl acetate), and highly branched alkyl groups. Although we were successful in the identification of ionic surfactants that were soluble to several weight percent in CO_2, they required pressures far in excess of typical CO_2 MMP values. It appears that future efforts in the design of CO_2 soluble surfactants (including our current NETL IAES project on this subject) should be directed at non-ionic surfactants with ethoxylated (i.e. PEG) hydrophiles and hydrocarbon-based or oxygenated hydrocarbon-based CO_2 philes.

Table of Contents

Executive Summary

In this report, we present a summary of all of our work, including new results from the last twelve months. These most recent results from the last year of the project include the findings that poly(vinyl acetoxy acetate), which has a "double" acetate side chain, is insoluble in CO_2 to 10000 psia. A hyperbranched PVAc polymer, similar to poly(vinyl acetate) but very branched, was determined to be insoluble in CO_2 to 10000 psia rather than linear. We were able to synthesize another sample of poly(acetoxy oxetane) with the assistance of GE Global; this sample was particularly well characterized and clean due to the care taken to begin with a very pure starting material and a reduction in the number of steps required to make the product. Unfortunately, despite the promising molecular modeling results, this oligomer was not more CO_2 soluble than previously identified oligomers such as oligo(propylene oxide), and could not be produced as a high molecular weight polymer. In summary, the results of our final year did not include the identification of a polymer more CO_2 philic than poly(vinyl acetate) that could have served as the "base" polymer for a copolymeric CO_2 thickener.

With regards to the entire project, the objective of this research was to use molecular modeling techniques, coupled with our prior experimental results, to design, synthesize and evaluate inexpensive, non-fluorous carbon dioxide thickening agents. The first type of thickener that was considered was *associating polymers*. Typically, these thickeners are copolymers that contain a highly CO_2-philic monomer, and a small concentration of a CO_2-phobic associating monomer.
Yale University was solely responsible for the synthesis of a second type of thickener; *small, hydrogen bonding compounds*. These molecules have a core that contains one or more hydrogen-bonding groups, such as urea or amide groups. Non-fluorous, CO_2-philic functional groups were attached to the hydrogen bonding core of the compound to impart CO_2 stability and macromolecular stability to the linear "stack" of these compounds. The third type of compound initially considered for this investigation was *CO_2-soluble surfactants*. These surfactants contain conventional ionic head groups and composed of CO_2-philic oligomers (short polymers) or small compounds (sugar acetates) previously identified by our research team. Mobility reduction could occur as these surfactant solutions contacted reservoir brine and formed mobility control foams in-situ. During these studies we also identified small compounds that were extraordinarily CO_2 soluble, such as tritertbutylbenzene, tritertbutylphenol, and peracetylated sugars,

The vast majority of the work conducted in this study was devoted to the copolymeric thickeners and the small hydrogen-bonding thickeners; these thickeners were intended to dissolve completely in CO_2 and increase the fluid viscosity. A small but important amount of work was done establishing the groundwork for CO_2-soluble surfactants that reduced mobility by generating foams in-situ as the CO_2+surfactant solution mixed with in-situ brine.

Polymers

In this final report, we review our entire co-polymeric thickener effort and detail, for the first time, the phase behavior and viscosity results *of* ***the first non-fluorous, oxygenated hydrocarbon-based, associating polymer CO_2 thickener, poly(vinyl acetate – co – benzoyl$_{5\%}$).*** The CO_2-philic monomer was vinyl acetate, and the associative thickener monomer was vinyl benzoate. Poly(vinyl acetate – co – benzoyl$_{5\%}$), Mw ~ 12000, is capable of increasing the viscosity of CO_2 by 70% at a concentration of 2wt%, a shear rate of ~5000s $^{-1}$, 298K and 9500 psia. Unfortunately, poly(vinyl acetate – co – benzoyl$_{5\%}$) is ***not capable of dissolving in CO_2 at pressures close to the MMP***, roughly 1200 psia at 298 K. In fact, we are now convinced that a ***non-fluorous, hydrocarbon-based co-polymeric thickener cannot be designed*** that will dissolve in CO_2 at typical reservoir conditions. Why? Every polymer that we designed using molecular modeling tools was indeed CO_2 soluble, a somewhat remarkable achievement given the small number of CO_2 soluble surfactants that have ever been identified, but each one was less soluble in CO_2 than poly(vinyl acetate). Therefore co-polymeric thickeners based on any CO_2 soluble polymer will undoubtedly be less soluble in CO_2 (i.e. require even greater pressures than 9500 psia) than poly(vinyl acetate – co – benzoyl$_{5\%}$). We even considered co-polymeric thickeners based on poly(dimethylsiloxane)(PDMS) because PDMS is much more CO_2-soluble than PVAc. Poly(phenyl methyl – siloxane), a copolymer containing the CO_2-philic siloxane and the CO_2-phobic, pendant, associating, methyl phenyl group, was found to be CO_2 insoluble at pressures up to 10000 psia.

Despite our inability to design a CO_2-soluble copolymeric thickener, were made significant progress in identifying CO_2 soluble polymers and oligomers. Specific high molecular weight polymers that have been designed/identified

as CO_2 soluble included the following (listed in order of most CO_2 soluble to less CO_2 soluble); poly(fluoroacrylate)(PFA), poly(dimethylsiloxane)(PDMS), poly(vinyl acetate) (PVAc), poly(1-O-(vinyloxy)ethyl-2,3,4,6-tetra-O-acetyl-β-D-glucopyranoside) (PAcGIcVE), amorphous poly(lactic acid)(PLA) and poly(methyl acrylate)(PMA). Oligomers that exhibit CO_2 solubility include poly(propyleneoxide)(PPO), poly(vinyl ethyl ether)(PVEE), poly(vinyl methoxymethyl ether)(PVMME), cellulose triacetate oligomers oligoo(CTA), peracetylated cyclodextrins (PACD), poly(acetoxy oxetane)(PAO), and poly(vinyl methoxy ethyl ether)(PVMEE).

Small hydrogen-bonding compounds

We were able to synthesize the first non-fluorous, small, hydrogen-bonding molecule that was soluble in CO_2 to about 1 wt% at elevated temperature (high temperature weakens hydrogen bonding, which facilitates dissolution) and remained in solution upon cooling. The compound contained two ureas for hydrogen bonding, two highly acetylated (acetyl gluconic) tails for CO_2 solubility, and a small alkyl chain in the middle as a spacer. This compound did **not** appreciably thicken CO_2. Interestingly, upon depressurization (removal of the CO_2) this compound formed a brittle, free-standing microfibrillar monolith; direct evidence that the small compounds were indeed aligned or "stacked" in solution. We were also able to synthesize the first CO_2 soluble dendrimer, a bisurea with four highly acetylated arms. This compound was very soluble in CO_2 at 298K but did **not** induce any change in viscosity and did not yield fibers upon depressurization. Apparently the steric hindrance associated with the four acetylated arms prevented the two cetral urea groups from associating with neighboring molecules.

Surfactants

In an attempt to identify surfactants that could dissolve in CO_2 and then form CO_2-in-brine mobility controls foams in-situ, we successfully identified numerous non-fluorous ionic surfactants that were CO_2 soluble. The fundamental characteristic of these surfactants was the presence of CO_2-philic oligomers. These oligomers included acetyl gluconic, oligo(propylene glycol), oligo(vinyl acetate), and highly branched alkyl groups. Although we were successful in the identification of ionic surfactants that were soluble to several weight percent in CO_2, they required pressures far in excess of typical CO_2 MMP values. It appears that future efforts in the design of CO_2 soluble surfactants (including our current NETL IAES project on this subject) should be directed at non-ionic surfactants with ethoxylated (i.e. PEG) hydrophiles and hydrocarbon-based or oxygenated hydrocarbon-based CO_2 philes.

In summary, it is extremely unlikely that a polymeric or copolymeric CO_2 thickener that dissolves in CO_2 at typical MMP values can be designed. We have investigated numerous highly oxygenated hydrocarbon-based polymers and have designed and synthesized new polymers that were even richer in CO_2-philic functionalities. These polymers were all CO_2 soluble, with PVAc being the most CO_2 philic. Unfortunately, the pressure required to dissolve modest concentrations of PVAc are many thousands of psia above typical MMP values. None of these polymers even comes close to the CO_2 solubility of the fluorinated polymers that we intended to replace.

Further, it is appearing increasingly unlikely that a small hydrogen rich hydrogen bonding compound can be identified. We did design one, but it required extensive heating and mixing at pressures of nearly 10000 psia to dissolve in CO_2; the notion of heating CO_2 to such conditions in the oilfield is not feasible. These compounds were built with the most CO_2 philic chemical groups known, yet the CO_2 phobic urea groups inhibited their dissolution. Further, no discernible viscosity increase occurred.

Clearly, the most viable remaining alternative for the reduction of CO_2 mobility is the identification of CO_2 soluble, extremely water soluble, nonionic, liquid surfactants with PEG hydrophiles and non-fluorous, CO_2 philic segments. It appears that a few inexpensive, commercially available, mass-produced surfactants may be capable of dissolving in the injected CO_2 at typical CO_2 flooding pressures. This single phase CO_2 + surfactant solution will then form a mobility control foam in-situ as the surfactant partitions into the brine already residing in the pores of the porous media and stabilizes the lamellae that bridge across pores, thereby encapsulating the CO_2 into small droplets/bubbles which have a low mobility in porous media. Specific examples suggested for future investigation during this study included surfactants with linear or branched alkyl, or linear or branched alkyl aryl CO_2-philic segments, and poly(propylene glycol), poly(ethyleneglycol) or diblock PPG-PEG hydrophilic segments.

The results of this project have already proven useful in three of Dr. Enick's current DOE IAES projects. Most importantly, the current IAES project that focuses solely on decreasing CO_2 solubility via the addition of CO_2

soluble, water soluble surfactants that can act to form in-situ foams (as discussed in the last paragraph). Alternately, one can attempt to design CO_2 soluble, water insoluble surfactants that not only dissolve in CO_2, but also form viscosity-enhancing cylindrical or rodlike micelles (must like the water-insoluble surfactant that is dissolved in gasoline to make Napalm). In both strategies, the results of this study are being used to design the surfactants for mobility control. Our early results for this project indicate that there may be several commercially available surfactants for in-situ foam generation, while the identification of a viscosity-enhancing surfactants is proving to be elusive. Dr. Enick has a second IAES project related to the identification of new liquid solvents for the absorption of CO_2 that have little if any capacity to absorb either water or hydrogen. The most common commercial oligomeric CO_2 physical solvent is Selexol, a mixture that is rich in poly(ethyleneglycol)dimethylethers (methyl ethers are much more CO_2 philic than the hydroxyl groups that terminate PEG). Selexol is a good CO_2 solvent but is completely miscible with water. CO_2 philic oligomers used in the current study, including oligo(propylene glycol)dimethyl ether and oligo(dimethylsiloxane), have already been shown to be just as good at absorbiong CO_2 as Selexol, yet they exhibit little if any affinity for water. Dr. Enick's third IAES project relates to the design of CO_2 permeable, CO_2 selective polymeric membranes composed of highly CO_2 philic polymers of oligomers. Both supported liquid membranes and flexible crosslinked membranes based on end-functionalized liquid oligomers are being assessed. At this point in time, crosslinked PEG-based membranes appear to be superior, although higher CO_2 permeability and lower CO_2 selectivity can be achieved with PDMS-based and poly(butyleneglycol)-based membranes.

Milestones, Decision Points

Our original proposal listed the following decision points and milestones. A review of our progress during this entire project is provided after each decision point and milestone.

Decision point for CO_2-CO_2 philic monomer molecular modeling: If the CO_2-novel monomer interactions are weaker than those exhibited by CO_2-vinyl acetate monomer, the monomer will not be considered a viable monomer for polymerization or inclusion in the hydrogen bonding compounds.
We did identify (using ab initio calculations) several monomers that exhibit stronger interactions with CO_2 –than vinyl acetate. These include acetoxy oxetane, methoxy methyl ether, and methoxy ethyl ether. We have been able to qualitatively establish that the interaction of CO_2 with sugar acetates is of comparable strength. This work was successfully completed.

Decision point for CO_2 philic polymers: If a polymer less CO_2 soluble than PVAc, it will no longer be considered as a successful advance or a viable candidate.
We synthesized the monomers and polymers, and completed testing the solubility of these polymers in CO_2. None of the polymers tested in this project, including PMME, PMEE, PAO, amorphous PLA, PAcGIcVE (a polymer with pendant sugar acetates), or polymers with a "double" acetate side chain (polyvinyl acetoxy acetate), or highly branched (rather than linear) PVAc has been found to be more CO_2-soluble than PVAc.

***Decision point for CO_2 thickeners*:** If the co-polymeric thickener or small hydrogen bonding compound cannot increase the viscosity of CO_2 at pressures by a factor of 2-3 at concentrations below 0.5wt%, it will not be considered a success

We did not identified a polymer that is more CO_2-soluble than poly(vinyl acetate), therefore we synthesized and testing a 95%vinyl acetate-5%benzoyl copolymer and proved that CO_2 can be thickened by 70% at a 2wt% concentration of vinylacetate-benzoyl copolymer at a shear rate of ~5000 s^{-1}. Even though we are capable of thickening CO_2 with this hydrocarbon-based polymer and it is very likely that we can get more substantial increases this copolymer by increasing its benzoyl content, it will not dissolve at pressures near the MMP. (Remember that the pressure required to dissolve high molecular weight PVAc in CO_2 greatly exceeds the MMP, and that the inclusion of a CO_2 phobic monomer such as benzoyl will only further diminish the CO_2 solubility of the copolymeric thickener). It is therefore our conclusion that while it is indeed possible to thicken CO_2 at pressures of ~9,000-10,000 psia, it is not possible to thicken CO_2 at typical MMP values using a hydrocarbon-based thickener. Our efforts at identifying a silicon-based thickener were also unsuccessful. We assessed several PDMS-based copolymers with pendant aromatic groups because PDMS is the second-most CO_2-soluble polymer after perfluoroacrylates, and PDMS is much more CO_2-soluble than PVAc. These PDMS-based copolymers did not dissolve at 10000 psia, however.

We therefore recommend that future efforts at decreasing CO_2 mobility be directed at the design of CO_2 soluble nonionic surfactants capable of forming mobility control foams in-situ. The strategy would be to inject a CO_2 + surfactant solution that would mix with reservoir (post-waterflood) brine and generate CO_2 foams in-situ; alternate slugs of brine or aqueous surfactant solutions would ***not*** *be required.) As shown in our report R03, it is possible to dissolve nonionic surfactants in CO_2 at pressures close to the MMP; we were not able to identify nonionics that were excellent foam stabilizers, however. Future efforts should be directed at identifying nonionics that are capable of stabilizing CO_2-brine foams as effectively as surfactants such as the water-soluble (CO_2-insoluble) Chaser surfactants used during the testing of CO_2 foams that required the injection of alternating slugs of surfactant solution.*

***Milestone 1*:** The identification of oxygenated hydrocarbon monomers that interact more favorably with CO_2 (according to molecular modeling) than vinyl acetate
Several monomers were more CO_2 philic than vinyl acetate, including the monomers for PAO, PVMME, PVMEE, and sugar acetate-rich polymers.

***Milestone 2*:** The synthesis of novel oxygenated hydrocarbon polymers that are more CO_2 soluble than poly(vinyl acetate).

None of the polymers based on these monomers were more CO_2 soluble than PVAc. PMME, PMEE, PAO, poly((1-O-(vinyloxy) ethyl-2,3,4,6-tetra-O-acetyl-β-D-glucopyranoside), *PLA, branched PVAc or poly(acetoxy acetate) are less CO_2 soluble than PVAc.*

***Milestone 3*:** The synthesis of novel oxygenated hydrocarbons that can dissolve in CO_2 at pressures at or below the MMP
Because none of the polymers made during this project is more CO_2 soluble than PVAc, we did not achieve this goal.

***Milestone 4*:** The synthesis of novel oxygenated hydrocarbon thickeners (copolymers or small H-bonding compounds) that can dramatically increase the viscosity of CO_2 by a factor of 2-20 at a concentration of 0.1-0.25wt% at pressures at or below the MMP.
With regards to copolymer CO_2 thickeners, we were able to design a hydrocarbon-based copolymeric CO_2 thickener, poly(vinyl acetate-co-benzoyl), but it was not be soluble in CO_2 at the MMP; it required ~9500 psia to dissolve in CO_2.
With regards to small hydrogen bonding compounds, we have also successfully designed the first CO_2 soluble, non-fluorous hydrogen bonding compound (5R,6R,7S,8R,27R,28S,29R,30R)-5,6,7-triacetoxy-2,9,14,21,26-pentaoxo-3,10,25-trioxa-13,15,20,22-tetraazahentriacontane-8,27,28,29,30,31-hexayl hexaacetate. This compound has a C4 chain in the middle, a urea group on each end of the C4 chain, and a highly acetylated "arms" extending out from each urea groups. *We also successfully designed the first non-fluorous dendrimer* (5R,6R,7S,8R,27S,28R,29S,30S)-5,6,7,8-tetraacetoxy-2,9,14,21,26-pentaoxo-12-(((2R,3S,4S,5R)-2,3,4,5,6-pentaacetoxy-hexanoyloxy)methyl)-23-(((2S,3R,4S,5S)-2,3,4,5,6-pentaacetoxy-hexanoyloxy)methyl)-3,10,25-trioxa-13,15,20,22-tetraazahentriacontane-27,28,29,30,31-pentayl pentaacetate. *This compound has a similar structure, but with two acetylated groups attached to each urea. Unfortunately, neither is soluble at conditions close to reservoir temperature and MMP, and neither appears to be capable of thickening CO_2 even when the compounds are in solution at elevated pressure.*

With regards to CO_2 soluble ionic surfactants that may be capable of generating CO_2 foams in-situ, we did identify several CO_2 soluble hydrocarbon-based ionic surfactants, but these ionic surfactants were not CO_2 soluble at typical reservoir conditions. We did lay the groundwork for the identification of CO_2 soluble nonionic surfactants that would dissolve in CO_2 at MMP in a concentration high enough to stabilize a CO_2 in brine foam. We suggested that the following classes of surfactants be studied in the future; non-ionic surfactants with ethoxylated (i.e. PEG) hydrophiles and hydrocarbon-based or oxygenated hydrocarbon-based CO_2 philes. For example, water-soluble nonyl phenol ethoxylates appear to be promising (as has been verified in our current IAES project with the DOE).

Significant Accomplishments

1. The design, synthesis and characterization of the first polymer designed for CO_2-solubility using molecular modeling, *poly(methoxy methyl ether), PMME.*
2. The design and synthesis of the second polymer designed using molecular modeling, *poly(3-acetoxy oxetane), PAO*.
3. The design and synthesis of a novel polymer, poly (1-O-(vinyloxy)ethyl-2,3,4,6-tetra-O-acetyl-β-D-glucopyranoside), P(AcGIcVE), which is is amorphous and capable of readily dissolving in CO_2. It is the second-most CO_2 soluble polymer that has yet been identified.
4. The determination that amorphous PLA is the third-most CO_2 soluble polymer.
5. The design and synthesis of the first hydrocarbon-based CO_2 thickener. The CO_2-philic monomer was vinyl acetate, and the associative thickener monomer was vinyl benzoate. **Poly(vinyl acetate – co – benzoyl$_{5\%}$)**, a.k.a. **poly(vinyl acetate – co – vinyl benzoate$_{5\%}$),** Mw ~ 12000, is capable of increasing the viscosity of CO_2 by 70% at a concentration of 2wt%, a shear rate of ~5000s $^{-1}$, 298K and 9500 psia. Unfortunately, poly(vinyl acetate – co – benzoyl$_{5\%}$) is <u>not</u> capable of dissolving in CO_2 at pressures close to the MMP.
6. The discovery that tritertbutyl phenol (TTBP) is extremely soluble in CO_2. This compound melts in dense CO_2, exhibits extraordinary solubility in CO_2 and is commercially available in bulk quantities at a cost of about $3/lb. It appears that a polymeric thickener cannot be based on this group, however, although <u>highly branched short alkyl tails may enhance the solubility of surfactants in CO_2</u>.
7. The design, synthesis and characterization of the first series of non-fluorous, ionic, highly CO_2-soluble surfactants that has been reported. (Specific tails include acetyl gluconic, oligo(vinyl acetate), sugar acetates, and oligo(propylene oxide). The surfactants with vinyl acetate tails were particularly CO_2 soluble.
8. The observations of CO_2 foams generated by mixing of CO_2, water and a CO_2-soluble surfactant. Specific tails include oligo(vinyl acetate), sugar acetates, and oligo(propylene oxide).
9. The phase behavior of the two novel polymers designed with molecular modeling: PMME and low MW branched PAO.
10. The detailed phase behavior of a sugar acetate with CO_2 has been shown to illustrate the complex phase behavior of compounds that melt in the presence of CO_2 and are extremely CO_2 soluble.
11. The first report of a highly CO_2-soluble, non-fluorous hydrogen-bonding compound, and the first report of a non-fluorous dendrimer designed for solubility in CO_2.

Technology Transfer

Refereed journal articles

1. Enick, R., Hong, L., Thies, M., "CO_2 + β-*D*-Maltose Octaacetate System Exhibits a Global Phase Behavior of CO_2-Philic Solids That Melt in Dense, CO_2-Rich Fluids" Journal of Supercritical Fluids Vol 34/1, 11-16, 2005
2. Fan, X.; Potluri, V. K.; McLeod, M. C.; Wang, Y.; Liu, J.; Enick, R. M.; Hamilton, A. D.; Roberts, C. B.; Johnson, J. K.; Beckman, E. J.; Oxygenated Hydrocarbon Ionic Surfactants Exhibit CO_2 Solubility,; *Journal of the American Chemical Society***;** (Article); 2005; *127*(33); 11754-11762
3. Sevgi Kilic, Stephen Michalik, Yang Wang, J. Karl Johnson, Robert M. Enick, Eric J. Beckman, "Phase Behavior of Oxygen-Containing Polymers in CO_2", *Macromolecules* 40 (4): 1332-1341 FEB 20 2007
4. Fan, X.; Mcleod, M. C.; Enick, R. M.; Beckman, E. J.; Roberts, C. B. Preparation of Silver Nanoparticles via Reduction of a Highly CO_2-Soluble Hydrocarbon-Based Metal Precursor. *Industrial & Engineering Chemistry Research*.45(10) May 2006, 3343-3347
5. Bell, P. W.; Anand, M.; Fan, X.; Enick, R. M.; Roberts, C. B. Stable Dispersions of Silver Nanoparticles in Carbon Dioxide with Fluorine-Free Ligands. *Langmuir* 2005 21, 11608-11613.
6. Eastoe, J., Gold, S., Rogers, S., Wyatt, P., Steytler, D., Gurgei, A., Heenan, R., Fan. X., Beckman, E., Enick, R., Designed CO_2-philes Stabilized Water-in-Carbon Dioxide Microemulsions, *Angewandte Chemie International Edition*, 2006, ON 1521-3773, PN: 1433-7851
7. Yang Wang, Lei Hong, Inchul Kim, Jacob Crosthwaite, Andy Hamilton, Mark Thies, Eric J. Beckman, Robert M. Enick, J. Karl Johnson, Design and Evaluation of Non-fluorous CO_2-Soluble Polymers, submitted to Polymer, Dec 2008
8. Hong L, Fidler E, Enick R, et al. Tri-tert-butylphenol: A highly CO_2-soluble sand binder, J of Supercritical Fluids, Volume**:** 44 Issue: 1**,** 1-7, 2008

9. Madhu Anand, Philip W. Bell, Xin Fan[†], Robert M. Enick[†], Christopher B. Roberts; Synthesis and Steric Stabilization of Silver Nanoparticles in Neat CO_2 Solvent Using Fluorine-Free Compounds, J Phys Chem B 110 (30): 14693-14701 August 3, 2006
10. Ik-Hyeon Paik, Deepak Tapriyal, Robert Enick, Andrew Hamilton, Fiber formation by Highly CO_2-Soluble Bis-Ureas based on peracetylated carbohydrate groups; Angewandte Chemie International Edition 46 (18): 3284-3287 2007
11. Tapriyal, D.; Enick R.; Poly(vinyl acetate), Poly((1-O-(vinyloxy) ethyl-2,3,4,6-tetra-O-acetyl-β-D-glucopyranoside) and Amorphous Poly(lactic acid) are the Most CO_2-soluble Oxygenated Hydrocarbon-Based Polymers, Journal of Supercritical Fluids 46 (2008) 252-257
12. Hong, L., Enick, R.; CTA Oligomers Exhibit High CO_2 Solubility, Green Chemistry 10 (7) 756-761, 2008
13. Lei Hong, Deepak Tapriyal, and Robert M. Enick; Phase Behavior of Polypropylene Glycol MonoButylEthers in Dense CO_2, J of Chem and Eng Data, 53(6) 1342-1345, June 2008
14. CO_2-Miscibility of Polymers Possessing Tert-Amine Groups; Sevgi Kilic, Yang Wang, J. Karl Johnson, Eric J. Beckman, Robert M. Enick, Polymer, 50: 11, 2436-2444, May 22 2009
15. Yang Wang, Lei Hong, In Chul Kim, Ik-Hyeon Paik, Jacob M. Crosthwaite, Andrew D. Hamilton, Mark Thies, Eric J. Beckman, Robert M. Enick, J. Karl Johnson, Tapriyal; Design and Evaluation of Non-fluorous CO_2-Soluble Polymers, Polymer (in press)

Presentations

1. Hong, L., Enick, R., The Design of Oxygenated Hydrocarbon-Based CO_2 Soluble Polymers, 7th International Symposium on Supercritical Fluids (ISSF2005) Orlando May 1 - 4, 2005 Rosen Centre Hotel, Orlando, Florida USA
2. CO_2 Soluble polymers and compounds – Wayne State University, May 2004
3. CO_2 Soluble polymers and compounds – Clemson University, October 2004
4. Enick, R., Beckman, E., Design of CO_2 Soluble Compounds – PACChem, Hawaii, Dec. 2005
5. Fan, X., Enick, R., The Design of Oxygenated Hydrocarbon-Based CO2 Soluble Surfactants, 7th International Symposium on Supercritical Fluids (ISSF2005), Orlando May 1 - 4, 2005 Rosen Centre Hotel, Orlando, Florida USA
6. Enick, R., Hong, L., Manke, C., Gulari, E., Dilek, C., "Carbon Dioxide Soluble Binders for Metal Casting Applications" to the organizers of the symposium Green Engineering for Materials Processing, Materials Science and Technology 2006 Conference and Exhibition, October 15-19, 2006, Cincinnati, OH
7. Tapriyal, D., Enick, R., Non-fluorous, CO_2-philic Polymers, Oligomers and Small Compounds for Chemical and Petroleum Engineering Applications, 5th International Symposium on High Presure Processes Technology and Chemical Engineering, Segovia, Spain, June 22-28, 2007
8. CO_2 Soluble Polymers, Oligomers and Dendrimers, National AIChE Conference, Salt Lake City, Nov. 200724. Enick, R.; Designing Molecules that Love CO_2, CMU, Dec 2, 2008
9. Enick, R., CO_2 Soluble Surfactants for Improved Mobility Control of CO_2 EOR, KinderMorgan, Oct 26, 2009
10. Xing, D.; Enick, R.; Eastoe, J.; Trickett, K.; Soong, Y.; "Forming Cylindrical, Viscosity-Enhancing Micelles in Dense CO2 with Fluorinated Surfactants" has been accepted as an oral presentation for the 19th Winter Fluorine Conference being held on January 11-16, 2009 at the TradeWinds Island Grand Beach Resort in St. Pete Beach, FL.
11. Miller, M., Enick, R., Luebke, D., Assessing the Solubility of CO_2 in Highly CO_2-philic Liquids, 9th International Symposium on Supercritical Fluids, May 18-20, 2009, Bordeaux, France
12. Xing, D., Enick, R., Soong, Y., Increasing the Viscosity of CO_2 with Surfactants to Improve EOR Performance, 9th International Symposium on Supercritical Fluids, May 18-20, 2009, Bordeaux, France
13. Kieran Trickett, Julian Eastoe, Robert Enick, Dazun Xing; Modifying the Properties of Liquid CO_2, Session: Surfactants and Supermolecular Assemblies: Manipulating Supramolecular Structures, IACIS/83rd ACS Colloid & Surface Science Symposium; Friday, June 19, 2009
14. Enick, Barillas, Morreale, CO_2-selective Polymeric Membranes AIChE National Conference, Nashville TN, November 8-13, 2009
15. Enick, Xing, Wei and Soong, CO_2-soluble surfactants for improved mobility control, AIChE National Conference, Nashville TN, November 8-13, 2009
16. Xing and Enick, CO_2 soluble surfactants for improved mobility control, SPE IOR Conference, Tulsa, OK March 2010

Conclusions

The objective of this project was to use molecular modeling tools, along with previously elucidated design heuristics, to design non-fluorous, hydrocarbon-based, CO_2 soluble compounds capable of improving mobility control during EOR. We considered three types of compounds: copolymeric associating polymer CO_2 thickeners, small hydrogen-bonding compound CO_2 thickeners, and surfactants capable of generating CO_2-in-brine foams upon introduction to the porous media that contains brine. Our findings, detailed in the remainder of this report, have led us to draw the following conclusions.

We were successful in using *ab initio* calculations to identify highly CO_2 philic monomers, from which we were able to design, synthesize and characterize novel polymers and oligomers. These oligomers and polymers were intended to be the CO_2 philic segments of the copolymers, H-bonding compounds, and surfactants. Each oligomer and polymer that we designed was indeed CO_2 soluble; a noteworthy accomplishment given the sparcity of polymers known to be CO_2 soluble. However, each polymer that we assessed was less CO_2 soluble than poly(vinyl acetate), which our previously DOE-funded research had shown was the most CO_2 philic, low- or high-molecular weight, hydrocarbon-based polymer. Therefore we designed a non-fluorous CO_2 thickener based on PVAc, which remains the most CO_2-philic, CO_2-soluble polymer that we have yet identified. Although the resultant copolymeric thickener, ***poly(vinyl acetate – co – benzoyl$_{5\%}$)***, induced a modest increase in CO_2 viscosity, it required pressures of over 9000 psia at 25C for dissolution; a pressure far in excess of that attainable during CO_2 EOR. ***We have therefore concluded that it is not feasible to thicken CO_2 at typical reservoir conditions with a non-fluorous copolymer.***

We aere also successful in identifying two "small" (i.e. non-polymeric) CO_2 soluble compounds that containing two or four CO_2-philic oligomers and two CO_2 phobic hydrogen-bonding urea groups. The idea was to dissolve these relatively small molecules in CO_2, and then let the compounds self-assemble into viscosity-enhancing linear macromolecules via H-bonding interactions. The compound with two CO_2-philic segments, (5R,6R,7S,8R,27R,28S,29R,30R)-5,6,7-triacetoxy-2,9,14,21,26-pentaoxo-3,10,25-trioxa-13,15,20,22-tetraazahentriacontane-8,27,28,29,30,31-hexayl hexaacetate, is the first CO_2 soluble H-bonding compound that has been identified. This compound dissolved to ~1wt% in CO_2 at very high pressures, but did not induce any viscosity increase. A four-armed version of this compound, which can be considered as a small dendrimer, (5R,6R,7S,8R,27S,28R,29S,30S)-5,6,7,8-tetraacetoxy-2,9,14,21,26-pentaoxo-12-(((2R,3S,4S,5R)-2,3,4,5,6-pentaacetoxy-hexanoyloxy)methyl)-23-(((2S,3R,4S,5S)-2,3,4,5,6-pentaacetoxy-hexanoyloxy)methyl)-3,10,25-trioxa-13,15,20,22-tetraazahentriacontane-27,28,29,30,31-pentayl pentaacetate, was also synthesized. This dendrimer dissolved readily on CO_2, but did not increase the viscosity; apparently steric hindrance associated with the four bulky CO_2 philic segments prevented the urea groups from associating with one another. ***We have therefore concluded that small hydrogen-bonding compounds are unlikely to be capable of thickening CO_2.***

We also designed several CO_2-soluble ionic surfactants. The method of mobility reduction associated with these surfactants was *not* to directly increase the viscosity of CO_2. Rather it was to design a CO_2+surfactant solution that would, upon injection into sandstone or limestone that contains brine (original in-situ brine or brine from waterflooding), form mix with the in-situ brine, providing an opportunity for the surfactant to partition into the brine. This resultant foam would consist of a large volume fraction of supercritical CO_2 bubbles separated by thin films of surfactant stabilized brine stretching across pore throats. ALthoughwe successfully made hydrocarbon-based ionic surfactants with remarkably high CO_2 solubility of several wt%, none of these surfactants could dissolve in CO_2 to an appreciable extent at typical CO_2 flooding conditions. ***We have therefore concluded that hydrocarbon-based ionic surfactants are unlikely to be capable of dissolving in CO_2 during EOR and forming CO_2-in-brine foams.*** We did, however, lay the groundwork for the identification or design or liquid, non-ionic, CO_2 soluble, water soluble, low viscosity, inexpensive surfactants that could be assessed for this technology. We suggested that the following classes of surfactants be studied in the future; non-ionic surfactants with ethoxylated (i.e. PEG) hydrophiles and hydrocarbon-based or oxygenated hydrocarbon-based CO_2 philes. For example, water-soluble nonyl phenol ethoxylates appear to be promising (as has been verified in our current IAES project with the DOE). ***We therefore conclude that the design of non-ionic CO_2 soluble surfactants for mobility control via the in-situ generation of CO_2-in-brine foams is clearly the most technically promising and economically viable technology for reducing the mobility of CO_2 during EOR.***

Copolymers and Small Hydrogen Bonding Compounds as Potential CO_2 Thickeners

TABLE OF CONTENTS

List of figures

Introduction

Oil is an important source of energy. Currently, it supplies more than 40% of total energy demands and more than 99% of the fuel used in cars and trucks. All over the world, the oil production is on decline. One way to prevent a domestic oil supply shortage is to ensure that domestic oil production is maintained or increased. Since much of easy to find oil has been recovered, the present oil production is becoming increasingly costly. According to recently published data, oil output from all major oil companies is on decline trend. Exxon Mobil, for example, announced that its average oil output has fallen by 614,000 barrels per day in 2008. As for new projects, BP's Thunder Horse project in the Gulf of Mexico, for example, is finally coming online in 2008, with an anticipated output of nearly 250,000 barrels per day. But this one project has taken almost 20 years to complete, at a cost in excess of $6 billion. And Chevron's recent success with its Jack 2 project in the Gulf came at a cost of over $240 million for just one test well. The Jack 2 project is still years away from being a successful oil-producing prospect. With present technology, which depends on the natural pressure within the formation and subsequent injection of water in the formation to displace oil, nearly two barrels remain in the ground for every barrel produced. So it becomes extremely important to increase the production of oil by increasing the efficiency of enhanced oil recovery techniques (those used after the production from natural pressure and waterflooding approach uneconomic levels).

Enhanced Oil Recovery

Oil recovery techniques have been grouped into three basic categories i.e. primary, secondary and tertiary oil recovery. Primary recovery techniques exploit the pressure within the reservoir and use pumps to drive oil to surface form production wells. When the reservoir natural pressure becomes too low to maintain economical production rate, then secondary recovery methods are applied. In secondary recovery an external force is applied to drive the oil to production well. This is typically done by injecting high pressure water or nitrogen into the reservoir. On average, the recovery of original oil after primary and secondary recovery operations is between 30 to 40%, depending upon reservoir characteristics. Tertiary or enhanced oil recovery (EOR) is done towards the end of secondary recovery to maintain oil production rates and thereby increase the amount of oil ultimately recovered from the reservoir. It typically involves injecting of $scCO_2$, steam, polymer solutions or surfactant solutions to improve oil flow from the reservoir.

Recent reports from the US DOE suggest that in total there is 1,332 billion barrels of domestic oil resources which include original, developed and undeveloped fields, as shown in Figure 1.1. Out of this only 208 billion barrels is recovered by primary and secondary recovery. An additional 400 billion barrels can be technically recovered by using present enhanced oil recovery techniques. Still, there is 724 billion barrels unrecoverable oil in place for which we need the technology to recover.

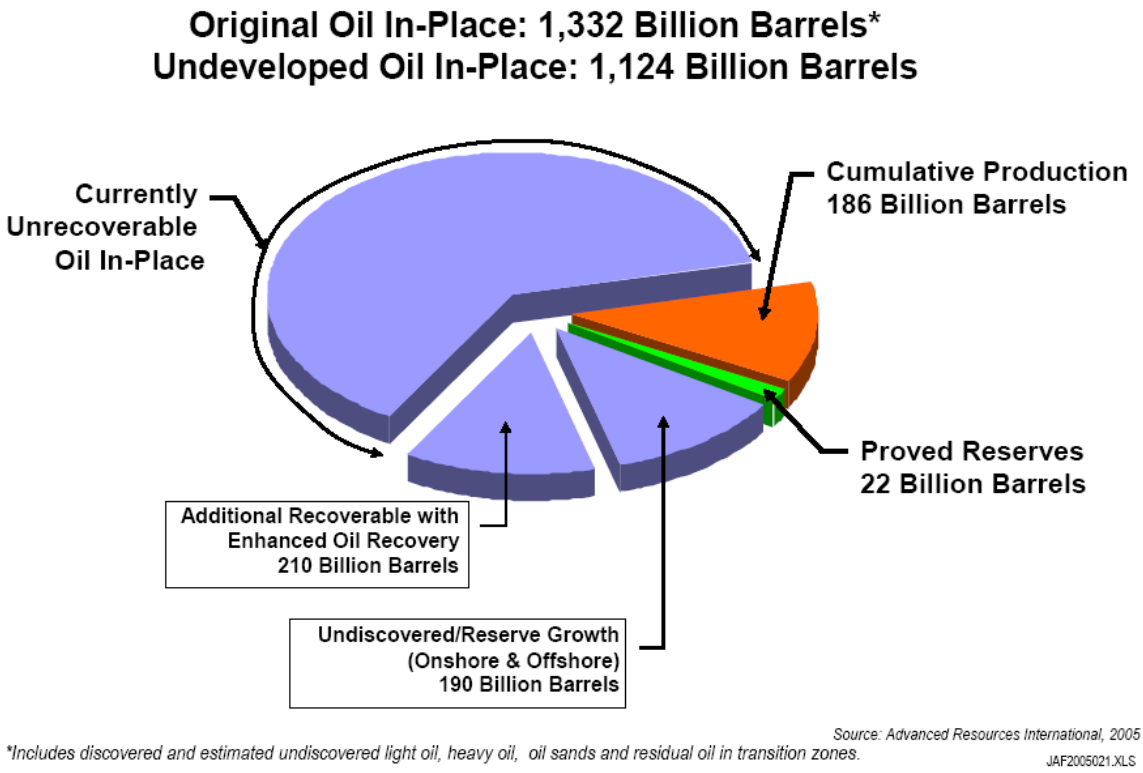

Figure 1.1 : Original, Developed and Undeveloped Domestic Oil Resources.

All EOR methods fall into three major categories: chemical, gas and thermal as shown in Figure 1.2. Propose of injecting material into the reservoir is to recover the trapped oil by reducing its viscosity or interfacial surface tension, increasing sweep efficiency, maintaining reservoir pressure or swelling oil.

Thermal Method: Viscosity of oil decreases dramatically with increase in temperature. Therefore, hot water or high pressure steam is injected to increase the reservoir temperature. As a result oil expands slightly and becomes significantly less viscous and moves towards the production well. This method is usually employed in the reservoir with heavy crude oil. In-situ combustion also aims at viscosity reduction and expansion. In this process air is injected and then ignited in the reservoir. This combustion reaction consumes a small amount of oil and produces heat and which helps to dramatically lower the viscosity of the remaining oil.

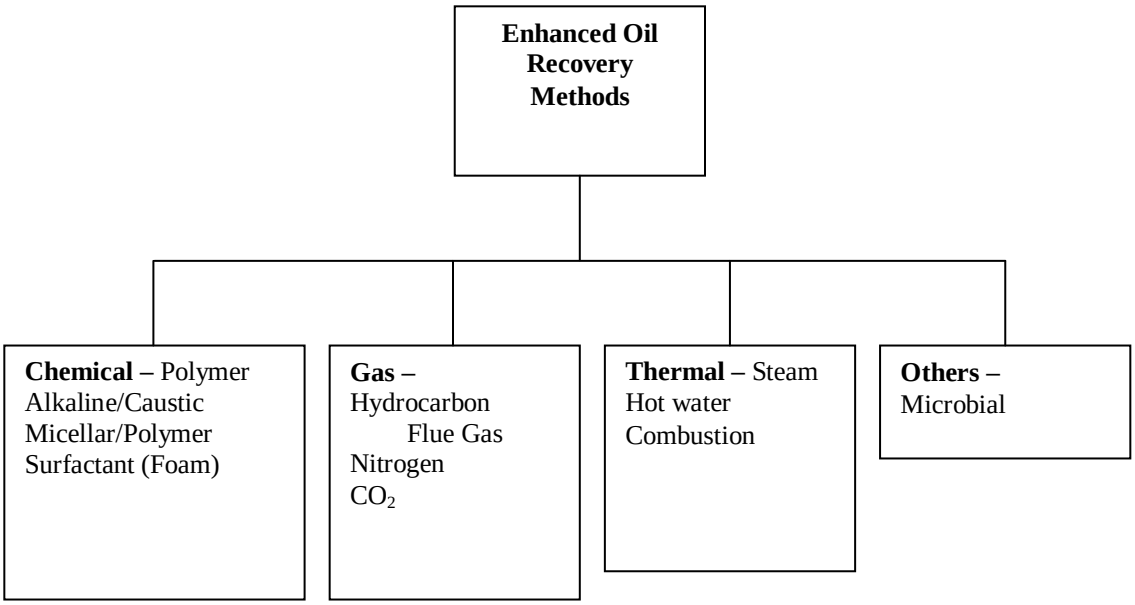

Figure 1.2 : Enhanced oil recovery categories

Chemical Method: This method involves addition of alcohols, surfactants, polymers, or bases in the reservoir. Micellar solutions are mixture of surfactants (surface active agents), co-surfactants (alcohols for stability), electrolytes (salts for viscosity and interfacial tension control) and water. First the surfactant solution is injected in the reservoir followed by polymer thickened water for mobility control. Caustic flooding is effective for the crude that has organic acid like naphthenic acids. It involves in-situ surfactant formation as a result of reaction between injected alkaline solution and acid present in the reservoir. This emulsification process helps to mobilize trapped oil. In polymer flooding, an aqueous solution of ultra-high molecular weight polymers is added to decrease the mobility of water in oil reservoir by increasing its viscosity.

Gas Injection: Depending on the properties of crude oil, rock and reservoir pressure different gases are injection to recover reaming oil. Gases like LPG or propane are miscible with oil upon first contact and are effective at low reservoir pressure. Methane rich gas, with some proportion of ethane, propane and butane are not miscible with oil on first contact but can be effectively used for oil recovery. For example, for heavy crude oil, these gases get absorbed in the crude and develop a zone with is rich in C_1-C_4 and then form a miscible zone that moves towards

production well. For crude oil rich in light components (C_2-C_6), at high pressure, methane-rich gases strip light components from the crude and develops a miscible front. In CO_2 flooding, the dense CO_2 saturates the crude oil as a result oil swells, the viscosity decreases, the high pressure re-pressurizes the reservoir, and a miscible zone forms as the dense CO_2 extracts the lighter components from the crude oil. This multi-component fluid is indeed miscible with the crude oil.

One of the most important and successful uses of CO_2 is in enhanced oil recovery (EOR) because it provides a way to recover substantial portion remaining oil present. An Oil and Gas journal survey shows that EOR contributed 649,000 bpd to US oil production in 2006[1]. Table 1.1 shows the US EOR production summary from 1986 to 2006. CO_2 flooding is the second most common EOR process used, next to steam flooding. However Table 1 shows that the oil production by steam flooding is now decreasing, while CO_2 flooding is flourishing. The total number of CO_2 injection projects for EOR has increased which has resulted in an increase in oil recovery by CO_2 injection (243,000b/d). CO_2 flooding is likely to continue expanding. Although current CO_2 projects obtain CO_2 from high pressure natural reservoirs of CO_2, future EOR projects may use anthropogenic CO_2. Since CO_2 flooding technology is mature and a valuable product (oil) is recovered, CO_2 EOR will be an economically, technically and politically viable means of sequestering CO_2 in the near future.

Table 1.1 : EOR survey from oil and gas journal

	1986	1988	1990	1992	1994	1996	1998	2000	2002	2004	2006
Thermal											
Steam	468,692	455,484	444,137	454,009	415,801	419,349	439,010	417,675	365,717	340,253	286,668
Combustion insitu	10,272	6,525	6,090	4,702	2,520	4,485	4,760	2,781	2,384	1,901	1,3260
Hot water	705	2,896	3,985	1,980	250	250	2,200	306	3,360	3,360	1,776
Total	**479,669**	**464,905**	**454,212**	**460,691**	**418,571**	**424,084**	**445,970**	**417,675**	**371,461**	**345,514**	**301,704**
Chemical											
Micellar-polymer	1,403	1,409	617	254	64						
Polymer	15,313	20,992	11,219	1,940	1,828	139	139	1,598			
Caustic/alkaline	185										
Surfactant			20					60	60	60	
Total	**16,901**	**22,501**	**11,856**	**2,194**	**1,892**	**139**	**139**	**1,658**	**60**	**60**	**0**
Gas											
Hydrocarbon	33,767	25,935	55,386	113,072	99,693	96,263	102,053	124,500	95,300	97,300	95,800
CO2 miscible	28,440	64,192	95,591	144,973	161,486	170,715	179,024	189,493	187,410	205,775	234,420
CO2 immiscible	1,349	420	95	95				66	66	102	2,698
Nitrogen	18,510	19,050	22,260	22,580	23,050	28,017	28,117	14,700	14,700	14,700	14,700
Flue gas	26,150	21,400	17,300	11,000							
Other				6,300	4,400	4,350	4,350				
Total	**108,216**	**130,997**	**190,632**	**298,020**	**288,629**	**299,345**	**313,544**	**328,759**	**297,476**	**317,877**	**347,618**
Other											
Carbonated Water flood											
Microbial				2	2						
Total				2	2						
Grand Total	**604,786**	**618,403**	**656,700**	**760,907**	**709,094**	**723,568**	**759,653**	**748,092**	**668,997**	**663,451**	**649,322**

CO_2 in Enhanced Oil Recovery

CO_2 in EOR has been used by oil industry well over 50 years. CO_2 flooding has gained attention as one of the most technologically viable means of recovering undeveloped oil in place. CO_2 flooding efficiency strongly depends on reservoir temperature, pressure and crude oil composition. Figure 1.3 shows the effect of reservoir temperature and pressure on CO_2 flooding mechanisms. These mechanisms are broadly divided into 5 categories: -

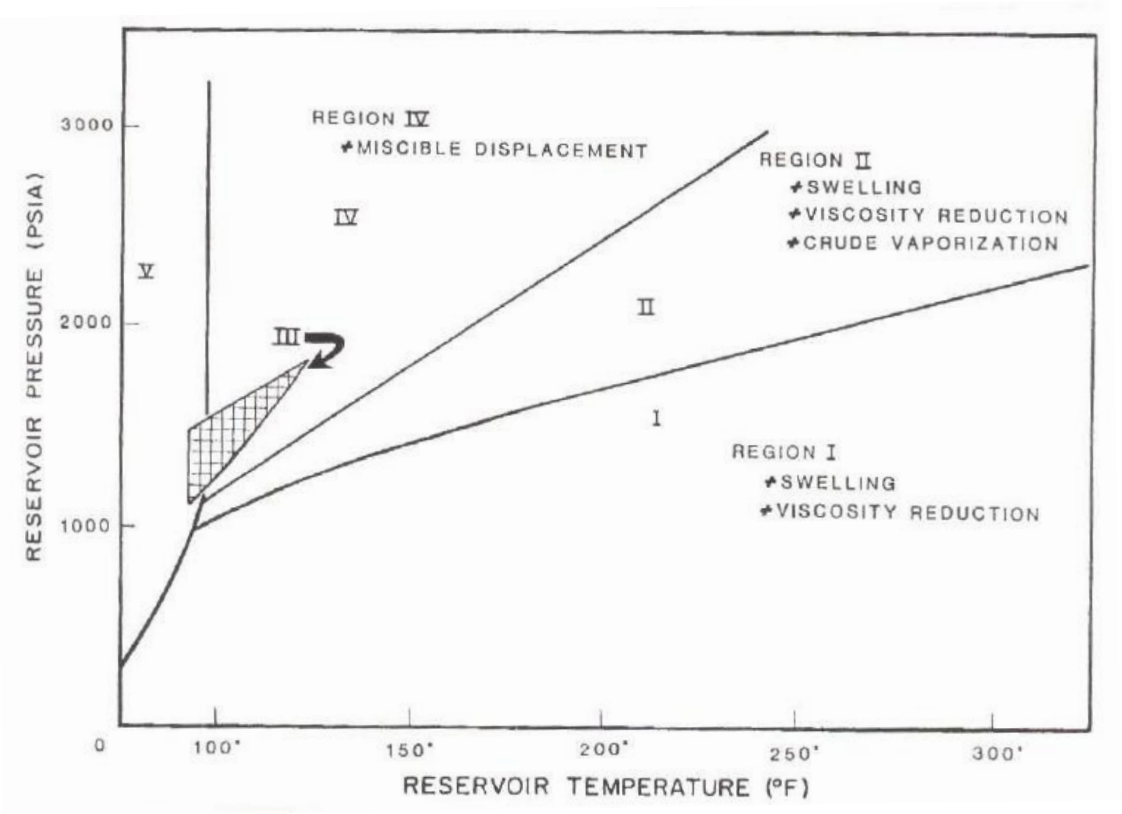

Figure 1.3 : Temperature and Pressure effect on CO_2 flooding

Low Pressure (Region I): At low pressure reservoir, CO_2 flooding depends on the solubility of oil in the crude oil. Once the injected CO_2 comes in contact with crude oil, it dissolves in CO_2

and swells. Swollen oil droplets force water out from the pores and create favorable flow conditions for the oil by increasing its relative permeability. As crude oil becomes saturated with CO_2, there is drastic decrease in the crude oil viscosity (about one-tenth to one-hundredth of original viscosity), which facilitates the displacement of the oil to the production wells. Once the CO_2 injection is stopped, CO_2 comes out from the solution and continue to drive oil towards production well.

Intermediate Pressure and High Temperature (Region II): Mixture of CO_2+oil swells up to certain pressure. At even higher pressure values, the crude oil starts vaporizing in the CO_2 rich phase. Therefore, in addition to swelling of oil and viscosity reduction, as in region I, vaporization of hydrocarbon into gas phase takes place at high temperature. Holm et al has demonstrated this swelling and vaporization behavior. At high temperature CO_2 can dissolve up to C_{30} hydrocarbon components of typical crude oil, facilitating multiple contact miscibility [2].

Intermediate Pressure and Low Temperature (Region III): This region is very similar to region II. At same pressure as region 2 but at lower temperatures, CO_2 + oil mixture demonstrate the swelling and viscosity reduction behavior but instead of vaporization CO_2 extracts the lighter components of crude oil and form CO_2 rich liquid region. Then this CO_2 rich phase comes in contact with crude and extracts lighter components. This process is called multiple contact miscibility.

High Pressure (Region IV): In this region also CO_2 swells oil, reduces it viscosity and vaporizes crude oil. But this vaporization, multiple contact miscibility, of crude oil is so fast that it occurs in very short time and reservoir distance. Therefore it is considered that CO_2 is essentially “first contact” miscible with oil.

Based on the above mechanisms CO_2 can be effectively used for EOR. For practical proposes CO_2-EOR is divided into two processes: miscible displacement and immiscible displacement. Miscible CO_2 displacement takes place under favorable temperature, pressure and crude oil composition, at which CO_2 become miscible with crude oil in all proportions shown in Figure 1.4. As described above, CO_2 is not miscible with oil on first contact. However, displacement tests in long cores and sand packed slim tubes indicate that dynamic displacement is possible above minimum miscibility pressure (MMP)[3] (the pressure at which oil recovery is essentially complete i.e. compressing CO_2 above MMP does not result in increase in oil recovery). When CO_2 is injected and is brought in contact with crude oil, initially its composition is enriched with vaporized intermediate components of the oil. This local change in the composition near the injection well results in the development of a miscible zone between oil and CO_2, within a relatively short distance from the injection well. For the effective mixing of oil and CO_2, this process should take place above MMP. The value for MMP depends on reservoir temperature, pressure and crude properties. This CO_2-oil interaction makes oil swell and reduces its viscosity. As a result it improves the oil recovery rate and ultimate amount of oil recovery (relative to continued water flooding).

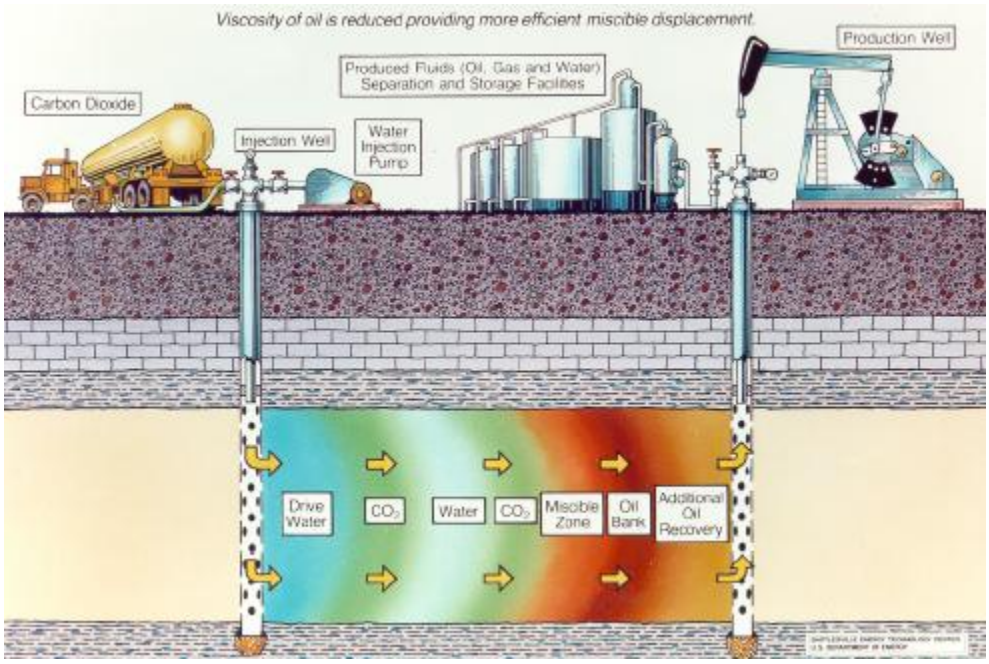

Figure 1.4 : A schematic of water-CO_2 EOR operation

Immiscible CO_2 displacement takes place when the reservoir pressure is below the MMP or the crude oil is not miscible with CO_2, typically because the reservoir is so shallow that it cannot withstand the MMP requirement. Even when crude oil is not miscible with CO_2, increased oil recovery occur due to oil viscosity reduction, oil swelling and reduction in surface tension.[4]

Mobility Reduction

Water-alternating-gas process (WAG): Current Industrial State of the Art: Dense CO_2 is much less viscous than the oil and water in the reservoir. As a result, the mobility (relative permeability/viscosity) of CO_2 is very high as compared to the oil and brine. Although a fluorinated thickener has been developed at the University of Pittsburgh, no commercial CO_2 thickener has ever been identified, therefore industry efforts have been directed at reducing the relative permeability of CO_2 using other techniques. The simplest way to accomplish this is by

introducing alternative slugs of brine and CO_2. This reduces the CO_2 saturation in the reservoir, which diminishes the relative permeability[5] and the CO_2 mobility. This process is shown in Figure 1.4. WAG requires water injection equipment, delays the injection of the specified amount of CO_2, may inhibit the mixing of CO_2 and oil within the porous media, increases the amount of water production, necessitates post-production water-oil separation processes and water re-injection equipment.

CO_2 Foam Flooding: Mobility reduction has also been proposed via generation of CO_2 forms in-situ. This concept involves the alternate injection of CO_2 and aqueous surfactant solutions. Foams can exhibit remarkable mobility reduction in porous media, especially at the lab scale[6,7]. Further oil recovery could have increased due to emulsification, wettability changes and interfacial tension reduction. Pilot test results, however, were discouraging primarily due to surfactant loss due to adsorption. Further, the CO_2 may not flow into the surfactant solution as desired, especially in heterogeneous formations. Therefore CO_2 foam floods are not commercially used at this time.

CO_2 Fracturing

CO_2 containing propping agent (such as sand) is used for the production of natural gas from reservoirs with low permeability. Further, it is typically undesirable to employ aqueous solutions as fracturing fluids in the candidate reservoir due to permeability reduction along the vertical fracture faces that form when the formation is fractured. In this process, CO_2 is injected into the formation at extremely high pressure (e.g. 10,000 psia) until the formation fractures as indicated by a sudden and dramatic decrease in pressure. At this point, a slurry of CO_2 and sand is injected

into the well in order to prop the 1/8" – 1/4" wide fracture open before it collapses upon itself, which typically takes a minute. This creates a narrow, high permeability, sand-packed channel for the gas to flow from the formation to the well. This process is efficient when the fracture is deep, wide and propped open with large sand particles. The advantage of the CO_2 fracturing is that it eliminates the formation damage associated with conventional aqueous fluids or aqueous foams and reduces the cost of frac fluid cleanup and disposal. The main disadvantage of CO_2 fracturing is the low viscosity of CO_2. As a result CO_2 is not able to carry high concentrations of large proppant particles, which would yield a dramatically more permeable fracture.

Problems with CO_2 Flooding

Theoretically, nearly all the oil remaining in the reservoir after a CO_2 flood could possibly be recovered if it is swept by the CO_2 (this is achieved in small core lab tests), but in the field recovery is limited to about 20%. Reasons for this low recovery are:

- Unstable flow (fingering, shown in Figure 1.5) of CO_2 i.e. CO_2 is more mobile than oil or water being displaced. (Mobility is permeability/viscosity.) Early breakthrough of CO_2 results; i.e. CO_2 coming out of production well long before all the oil is removed due high CO_2 mobility. (shown in Figure 1.6)
- Low density of CO_2 (at MMP) relative to oil causes gravity override, which inhibits the contact of CO_2 with oil in the lower portion of reservoirs.

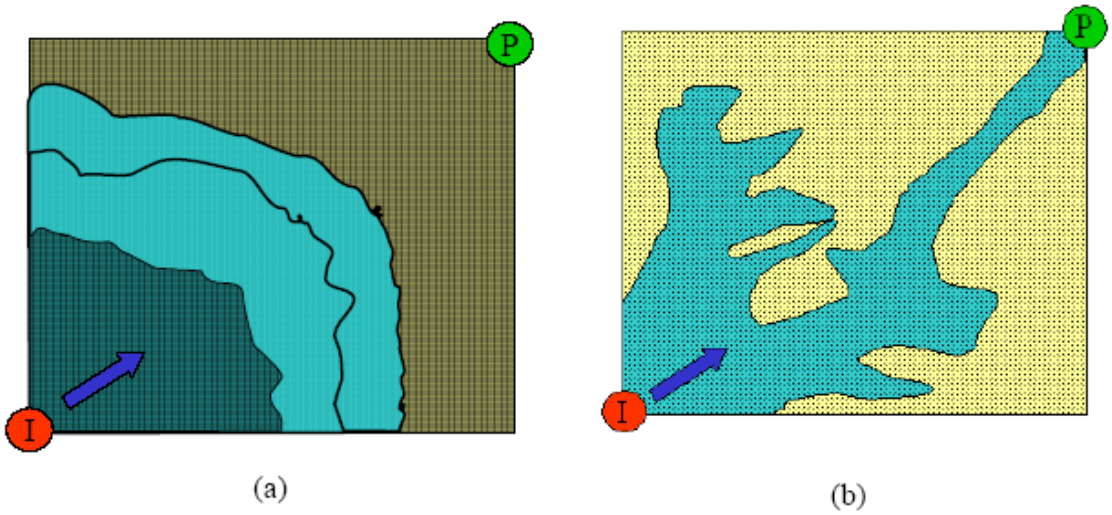

Figure 1.5: a) Ideal flow of CO_2 from injection well (I) to Production well (P) for maximum oil recovery b) Viscous fingering of CO_2 leaving behind large volume of oil trapped

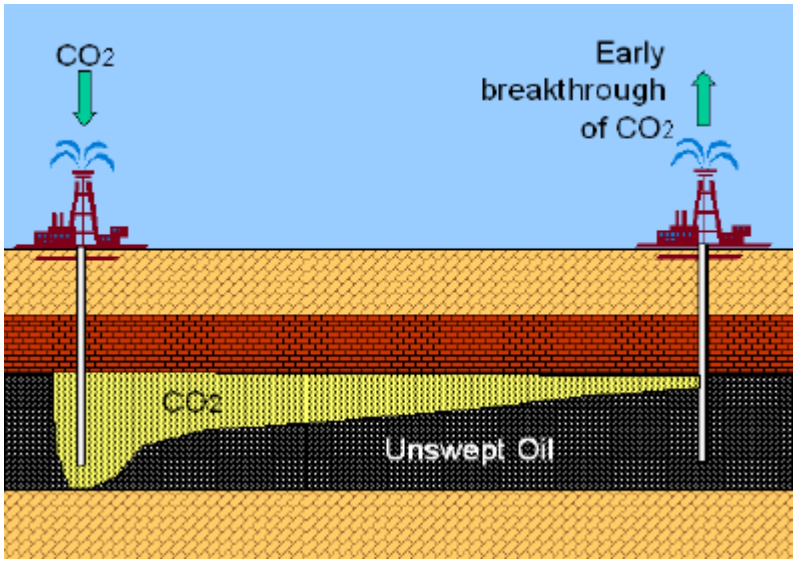

Figure 1.6: Early breakthrough of CO2 resulting in low areal and vertical sweep efficiencies.

It is not practical to increase the density of CO_2 by several tenths of a g/cc at a specified temperature and pressure via use of dilute concentration of additives, nor is it feasible to significantly decrease the permeability of CO_2 in the formation without introducing large volumes of brine (WAG). It *is* conceivable, however, to make significant increase in viscosity via the introduction of dilute amounts of a thickener (oil and water thickeners that are effective at concentrations of 0.1-1 wt% are commonplace). **Therefore this work will focus on increasing**

the viscosity of CO_2 to a level comparable to the viscosity of the oil being displaced via the introduction of a dilute concentration of a hydrocarbon-based thickener.

CO_2 as a Solvent

Carbon dioxide is a small, linear, and symmetric molecule where carbon is covalently bonded to oxygen. In the past few decades there has been a great deal of development in the use of supercritical carbon dioxide ($scCO_2$), especially in petroleum engineering applications. The supercritical phase actually bridges the gap between liquid and gaseous states by offering gas-like diffusion rates and liquid-like solvent densities. Figure 2.1 represent the phase diagram for CO_2.

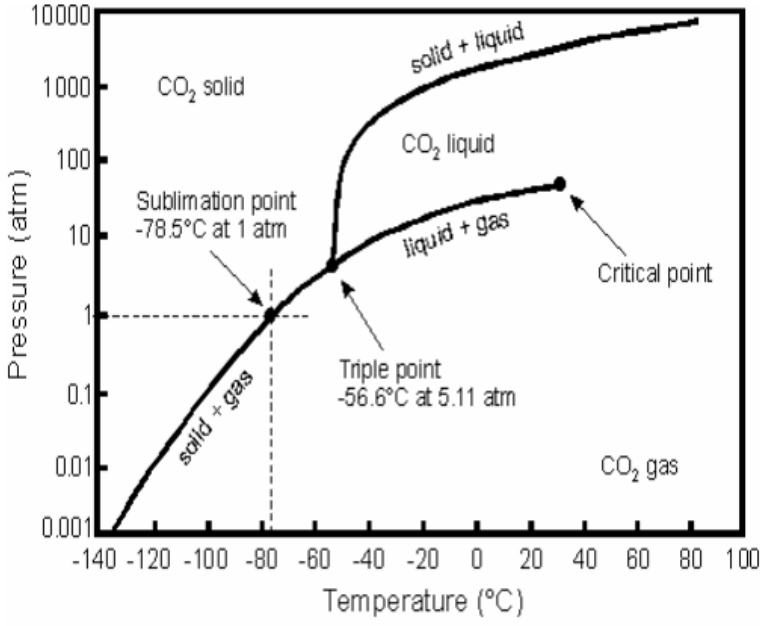

Figure 2.1: - Temperature phase diagram for CO_2

Supercritical carbon dioxide has gained a considerable attention as an environmentally acceptable alternative to organic solvents in many chemical and petroleum engineering processes. CO_2 is non-toxic, inexpensive, non-flammable, readily available and easy to remove

(and recover) at the end of the process via de-pressurization (and re-compression). It is also high pressure process (roughly 1000 or more psi, however, that often requires significant capital costs). Because of these properties, CO_2 is widely recognized as a green solvent. Some of the industrial examples where CO_2 has replaced organic solvents are the Dupont facility for producing floropolymers in $scCO_2$-based solvent, coffee decaffeination, and dry cleaning technology based on liquid CO_2[8]. CO_2 flooding is the largest industrial use of CO_2 as a solvent in the country; about 1.5 billion scf/d of natural CO_2 are used for EOR. Polymer, food and pharmaceutical industries may use CO_2 for extraction/separation steps because of its pressure-adjustable solvent strength and non-toxic nature. There has been an on-going effort to develop new CO_2-philic polymers, oligomers, dispersants chelating agents, catalysts and surfactants which could enhance the potential of CO_2 as a processing fluid[9,10,11].

Table 2.1: Physical properties of CO_2

T_c(K)	P_c(bar)	ρ_c(g/cm3)	$\alpha \times 10^{25}$ (cm^3)	μ(D)	$Q \times 10^{26}$ ($erg^{1/2}cm^{5/2}$)
304.2	73.8	0.468	27.6	0.0	-4.3

Thermodynamic properties of CO_2

Despite these successes in niche markets, $scCO_2$ technology has not been as successful in many other technologies, primarily because CO_2 is weak solvent for polar and/or high molecular weight compounds. Physical properties of CO_2 are shown in Table 2.1. CO_2 was considered as an alternative solvent for hydrocarbon because of its low dielectric constant as compare to hydrocarbons. But it is not good solvent for long chain hydrocarbon systems. Raveendran et al has described CO_2 as a non-dipolar solvent system. Although carbon dioxide has no permanent

dipole moment but large electronegative oxygen atoms, impart CO_2 molecule an especially large quadrupole moment. It is this quadrupole[12] moment that gives CO_2 solvent properties, that may enhance the solubility of certain polar solutes in the fluid. There is a charge separation in the CO_2 molecule with the bond electron density being polarized more toward the oxygen atoms, leaving the carbon atom with a partial positive charge and the two oxygen atoms with partial negative charges as shown in Figure 2.1.

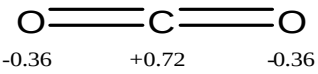

Figure 2.2 : Charge distribution in CO_2

CO_2 is a good solvent for non-polar and some low molecular weight polar molecules. It has very limited solubility for high molecular weight molecules. In order for a polymeric material or any other solute to dissolve in a given solvent, the Gibbs free energy of mixing, ΔG_{mix}, must be negative and at a minimum. The Gibbs free energy of mixing is given by

$$\Delta G_{mix} = \Delta H_{mix} - T\Delta S_{mix} \qquad \textbf{Equation 1}$$

where ΔH_{mix} and ΔS_{mix} are the change of enthalpy and entropy of mixing, respectively. The enthalpy of the system depends on the polymer segment-segment, solvent-solvent and polymer segment-solvent interaction energies. Thus the CO_2 soluble polymer is required to have weak polymer segment-segment interactions and strong polymer segment - CO_2 interactions. The balance of these interactions in a solution is described by the interchange energy[13], ω, defined as

$$\omega = z\left[\Gamma_{ij}(r,T) - \frac{1}{2}(\Gamma_{ii}(r,T) + \Gamma_{jj}(r,T)\right] \qquad \textbf{Equation 2}$$

where z is the coordination number and Γ is the potential energy, which is defined as

$$\Gamma_{ij} \approx -\left[C_1\frac{\alpha_i\alpha_j}{r^6} + C_2\frac{\mu_i^2\mu_j^2}{r^6kT} + C_3\frac{\mu_i^2Q_j^2}{r^8kT} + C_4\frac{\mu_j^2Q_i^2}{r^8kT} + C_5\frac{Q_i^2Q_j^2}{r^{10}kT} + \text{complex. formation}\right] \qquad \textbf{Equation 3}$$

where α is the polarizability, μ is the dipole moment, Q is the quadrupole moment, $C_{1\text{-}5}$ are constants[14], r is distance between the molecules, k is Boltzmann's constant and T is absolute temperature. Equation 3 only gives us the qualitative idea of polymer segment-CO_2 interaction because the polymer chain length is not taken into consideration. Dispersion interaction, the first term in equation 3, depends only on polarizability of the compound and the distance between them. Because CO_2 has low polarizability (table 2), the polymer should have high polarizability in order to be soluble in CO_2 otherwise high pressure will be required to dissolve it in CO_2. The next three terms in equation 3 represent dipole-dipole, dipole-quadrupole and quadrupole-quadrupole interactions. Although CO_2 has zero dipole moment but it has substantial quadrupole moment over short distances. This quadrupole moment has negative effect when a non-polar polymer is dissolved in CO_2 at low temperature because CO_2 quadrupole interactions will dominate the interchange energy (equation 3). CO_2 is a reasonable solvent for slightly polar molecules. The critical point of the mixture, i.e. lowest pressure at which molecule is soluble in CO_2, rises sharply with the increase in molecular size. Therefore high molecular weight polymers exhibit limited solubility.

Very limited amount of work has been done on CO_2 dimer and trimer systems to study CO_2 self interactions. Miller et al and others have shown that CO_2 dimer can interact in parallel and T-shape geometry as shown in Figure 2.3.

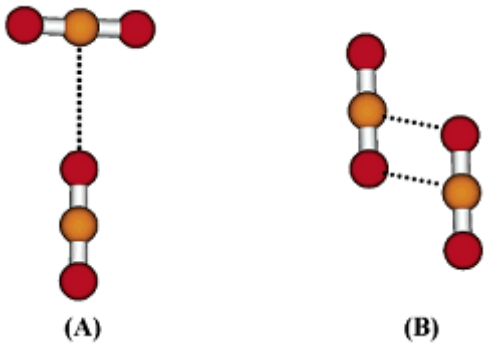

Figure 2. 3: - Optimized geometries (A) T-shape and (B) parallel of CO_2 dimer.[15]

To study the CO_2 interactions in liquid state, modeling of CO_2 trimer was done by Nesbitt et al. By doing IR spectral studies they demonstrated that CO_2 can foam cyclic and non-cyclic trimers; but the cyclic trimer was more abundant. Tsuzuki et al have done *ab initio* calculation on these structures and concluded that non-cyclic structure is more thermodynamically stable.

Another complex interaction which is electron accepter-donor interaction also plays very important part in making polymers CO_2 soluble. It has been shown through the use of IR spectroscopy[16] that polymers possessing electron-donating functional groups display Lewis acid-base interaction with carbon dioxide with carbonyls, acetates and ethers. The interaction is between carbon of CO_2 which acts as Lewis acid and the oxygen present in the side chain of the polymer which acts as Lewis base. Hydrogen bonding (C-H…O) is also reported[17] which act along with Lewis acid-base interaction in a systems having hydrogen atom attached to carbonyl carbon or α carbon. Figure 2.4 shows three different type in which CO2 can interact with carbonyl group.

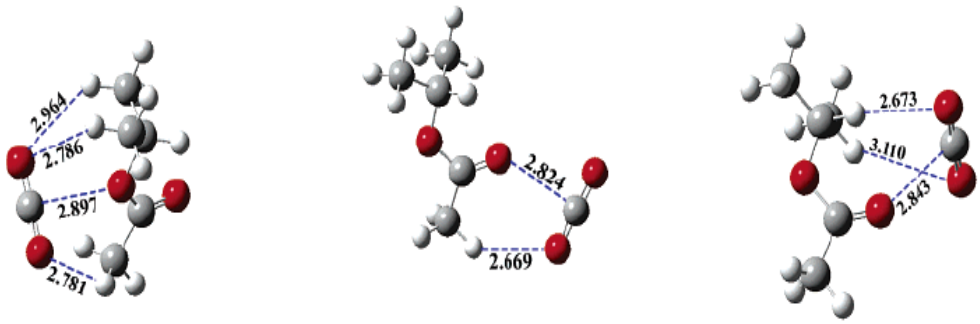

Figure 2.4: CO_2 complex involving hydrogen bonding and CO_2 – Lewis acid-base interactions. Red represents oxygen, dark grey is carbon and small light grey is hydrogen.

Kazarian et al[18] investigated the interaction of carbon dioxide with polymers and demonstrated that the polymers possessing the electron-donating group (e.g. carbonyl groups) exhibit specific interactions with CO_2 which are Lewis acid-base nature. Raveendran et al[17] showed that in addition to Lewis acid-base interaction there is an additional stabilizing interaction (hydrogen bonding) which helps in solvation of polycarbonyl moieties with hydrogen atoms attached directly to the carbonyl carbon. McHugh et al were the first to note that polyvinyl acetate exhibited remarkable solubility in CO_2. Our group along with Mark McHugh and Zhihua Shen of Virginia Commonwealth University, studied a wide range of polymers and found that only three oxygenated hydrocarbon polymers are capable of dissolving in CO_2 at 5 wt % or more[19]. Those are, in order of decreasing CO_2 solubility, poly(vinyl acetate), amorphous poly(lactic acid) and poly(methyl acrylate).

Entropy of mixing is also plays an important in creating a single phase solutions. For high entropy polymer should have high free volume and high chain flexibility which results in low glass transition temperature of the polymer (Tg). Polymers with low Tg are more likely to dissolve in $scCO_2$ then with high Tg. Entropy becomes more important in polymers with high molecular weight because at high molecular weight chain flexibility decreases which results in less no of conformation. Branching of the polymer helps to increase the free volume.

From a thermodynamic point of view, a balance between enthalpy and entropy is required for successful design of a CO_2-soluble polymer. A polymer with low glass transition temperature, branching and CO_2-philic functional group is an ideal candidate that will dissolve in CO_2.

Viscosity of CO_2

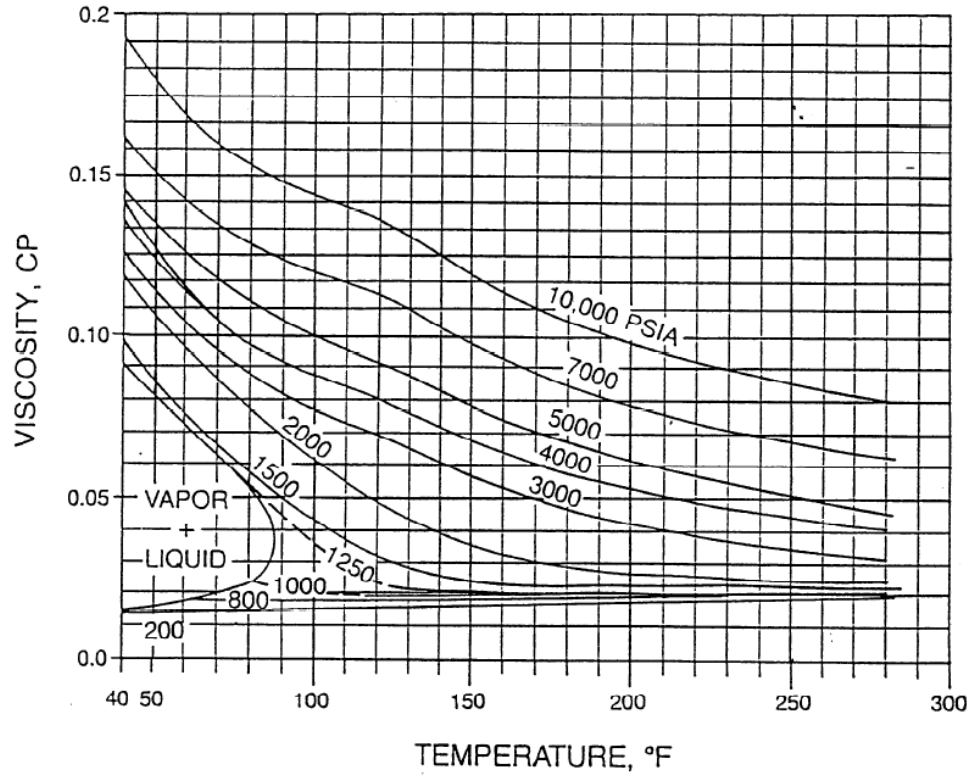

Research Objective

Previous attempts to thicken CO_2

The efficiency of CO_2 flooding and CO_2 fracturing can be increased if we can decrease the mobility of dense CO_2. Two ways of doing this are to either use a surfactant to form a foam (emulsion) or to use a thickener to directly enhance the viscosity of the single-phase CO_2 solution. Surfactant solutions have been used in the lab and a pilot test to generate a form when it is injected into the reservoir in alternating slugs with CO_2. (Current research in Dr. Enick's group is directed toward the use of CO_2-soluble surfactants for in-situ foam generation.) The two benefits of using surfactant are that it can decrease the mobility of CO_2 and it can also be used to block the permeable zone created in water flooding. Direct thickeners are designed to dissolve in the CO_2 and increase the viscosity of CO_2 by a factor of 2-50. Furthermore, the thickener should tend to partition in the CO_2 rich phase rather than the oil or brine in the reservoir. Many attempts have been made to thicken CO_2 during the last two decades. ***The objective of this work is to identify an oxygenated hydrocarbon-based direct CO_2 thickener; foams will not be considered.*** In the 1980's, John Heller was the first group to work on the use of direct thickeners for CO_2. He and his coworkers evaluated the solubility of several commercially available polymers in liquid and supercritical CO_2. It was unsuccessful the search for polymers which can increase the

viscosity of CO_2 but they made some generalization about the CO_2 soluble polymers. They found that CO_2 soluble polymers should be amorphous and atactic and the polymers which are soluble in water or are isotactic are not highly soluble in CO_2[20]. Taking these things into consideration, they also synthesized amorphous, atactic polymers but they were only slightly soluble in CO_2. They also synthesis hydrocarbon based telechelic ionomers for CO_2 thickener. These are low molecular weight polymer with ionic groups at each end of the chain. These polymers were successful thickeners for some non-polar solvents but had essentially no solubility in CO_2[21].

Heller et al. also tried to increase the viscosity by gelation of variety of organic fluids and supercritical CO_2 with 12-hydroxysteric acid (HSA). HSA is insoluble in CO_2 but when used with co-solvent, 10-15% ethanol; it is completely soluble in CO_2 and formed translucent or opaque gels[22]. For controlling the mobility ratio, Heller group also tested various commercially available surfactants which form foams in dense CO_2. These foams did not have much influence on CO_2 mobility[23].

Terry et al[24] attempted to increase the viscosity of CO_2 via in-situ polymerization of CO_2-soluble monomers. They found that the resulting polymers were insoluble in CO_2. Llave et al[25] used entrainers to improve CO_2 mobility. Entrainers are low molecular weight, CO_2-soluble compounds such as isooctane, 2-ethylhexanol and ethoxylated alcohol. Entrainers improved the viscosity of CO_2 but very high concentrations, for example, 44 mole% of 2-ethylhexanol resulted in 1565% increase in viscosity of CO_2. Irani et al[26] considerably increase the viscosity of CO_2 by using silicone polymers. They were able to increase the viscosity of CO_2 by a factor of 90 by dissolving 6 wt% polydimethylsiloxane (MW = 197000) and 20 wt% toluene into the CO_2.

In the last decade, DeSimone et al[27]. reported that silicones and fluoropolymers exhibit higher degree of solubility in CO_2 as compare to other non-fluorous polymers. Soon this group

identified first CO_2 thickener which can be used without co-solvent. They reported that 5-10 wt% of a fluoroacrylate homopolymer[28] can increase CO_2 viscosity by 3-8 fold . Shi et al[29] synthesized CO_2-soluble fluorinated polyurethane telechelic disulfates which are soluble in CO_2 up to 4 wt % and can increase the viscosity ay 2.7 fold. Semi-Florinated trialkytin fluorides were soluble in CO2 below 18 MPa at 4wt% and increased the viscosity of CO2 by the factor of 3.3 times at 4 wt%.

To date only a single CO_2 thickener has been identified that is capable of order-of-magnitude type increases; a random copolymer of **f**luoro**a**crylate and **st**yrene, dubbed polyFAST, developed by Enick, Beckman and coworkers[30]. The increase in viscosity was due to intrernolecular π-π stacking of aromatic side chain functional groups. This was demonstrated indirectly in that analogous copolymer that had linear, rather than aromatic, side chains induced no viscosity increase. The optimum composition of the copolymer was found to be 29 mol% styrene and 71 mol% fluoroacrylate. Addition of 1.2 wt% of the copolymer increased the viscosity of CO_2 by the factor of 19 relative to neat CO_2 at the velocity of 0.00035m/s in a sandstone core[31]. Increases in velocity resulted in smaller increase in CO_2 viscosity. This fluorinated thickener is too costly and environmentally persistent to be used commercially.

Research objective and strategy

The ultimate objective of this work is to make a thickener with CO_2-philic segments composed solely of carbon, oxygen and hydrogen that is soluble in CO_2 and can significantly increase the viscosity of CO_2 at concentrations less than 1 wt%. This work does **not** investigate the use of surfactants as foaming agents for mobility reduction.

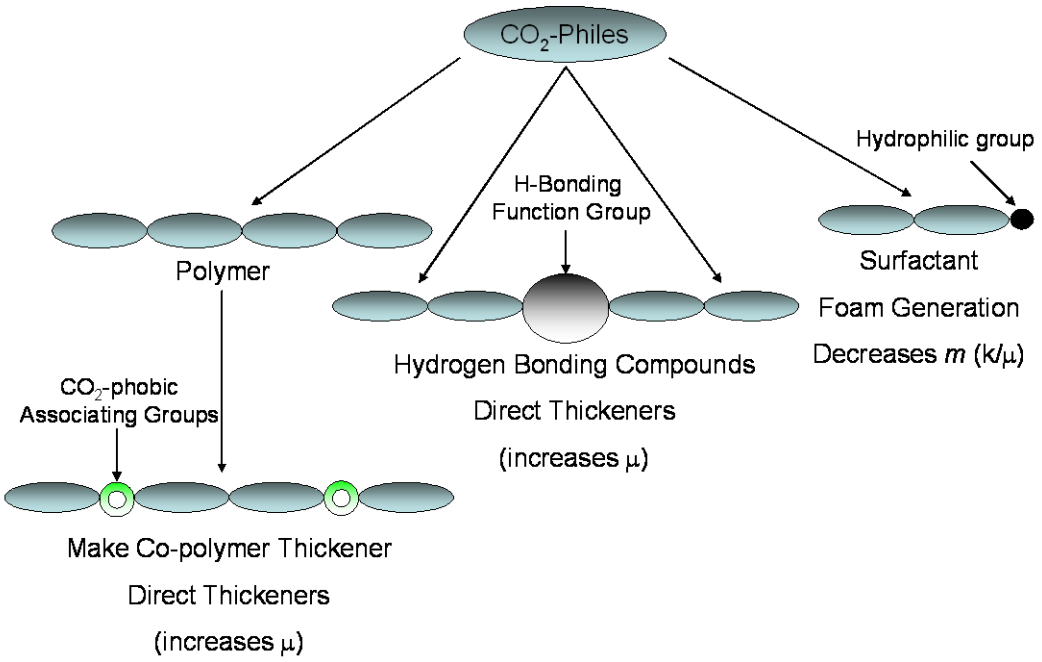

Figure 3 1: Strategy

The specific goal of this project is to **first** identify or design a highly CO_2-soluble oxygenated hydrocarbon oligomer. The **second** objective is to incorporate this oligomer as the CO_2-philic segment of thickeners, including copolymers and hydrogen bonding compounds that may increase the viscosity of CO_2 via intermolecular associations. The thickener, for example, should contain slightly CO_2-phobic associating groups, thereby allowing the thickener to dissolve in CO_2 and to associate and form viscosity-enhancing macromolecular networks. Two candidates will be considered; hydrogen bonding compounds and co-polymers.

The main emphasis of this DOE-sponsored research is the design of a co-polymeric thickener. The first step in the design of the copolymer is to design or identify CO_2-philic oligomers. The second step is to use that oligomer to make high molecular weight polymers. If the polymer is CO_2-soluble, it will then be modified to become a CO_2 copolymeric thickener. Such modifications make the thickener less CO_2-philic because the associating groups are inherently

CO_2-phobic, therefore the identification of CO_2 soluble polymer does not necessarily insure that a CO_2 thickener based on that polymer will dissolve in CO_2.

We have also assessed the ability of small hydrogen-bonding compounds to dissolve in CO_2 and then associate, thereby increasing the CO_2 viscosity. These compounds have one or two hydrogen bonding functional groups and at least two highly CO_2-philic "arms". This type of compound has been previously designed by Enick, Beckman, Hamilton and co-workers. Urea groups and fluoroalkyl "arms" were used to make a compound that dissolved in CO_2, made modest changes in viscosity, and then made low-density microfibrillar, brittle foam upon depressurization[32]. Our colleagues at Yale provided similar compounds for this project with non-fluorous, sugar acetate-rich arms. One of the H-bonding compounds, which will be detailed in a subsequent chapter, can be considered as a simple dendrimer.

In both cases (and even in the case of the CO_2-soluble surfactants that will be studied in the future), the identification of highly CO_2 soluble oligomers is required to design a CO_2-soluble thickener.

General Guidelines for Making CO_2 Soluble Polymers

a) **Acetylation** usually increases the CO_2 solubility. For example poly(vinyl acetate) is the most CO_2-soluble, high molecular weight, oxygenated hydrocarbon polymer. Per-acetylated monosaccharides, disaccharides, cyclodextrins and oligomers with up to four acetylated sugar repeat units are highly soluble in CO_2.

b) **Acetylation alone does not ensure CO_2 solubility**. Crystalline per-acetylated polysaccharides (e.g. cellulose triacetate) are CO_2 insoluble. PVAc, which has a pendant acetate associated with every other C in the polymer backbone, is very CO_2-soluble, yet poly(methoxy acetate), which has a pendant acetate associated with every C in the polymer backbone, is not soluble in CO_2 probably due to its extremely high melting point.

c) The polymer should be **amorphous** i.e. it should have flexible chains and high free volume. These properties are necessary to have high entropy of mixing and thus high solubility in CO_2. Previous research has shown that branching increases the free volume of solute there by decreasing the intermolecular interaction between polymer segments.

d) **Carbonyl and ether groups** can also be used to design CO_2 soluble polymers. Molecular modeling has shown that interaction energy of ether-CO_2 is comparable with interaction energy of carbonyl-CO_2.

e) **Amine functional groups and hydroxyl groups should be avoided** in designing CO_2 soluble polymer. Self interactions between amine groups dominate all the interactions between CO_2 and polymer[33]. Similarly, hydroxyl groups are well known to be CO_2-phobic.

f) **Methylene spacer**s between polymer backbone and acetate group or any other pendent group should be avoided. For example, poly (allyl acetate), which has a methylene spacer backbone and acetate group, was completely insoluble in CO_2. This is probably the most poorly understood, yet indisputable, effect in the design of CO_2-soluble polymers.

Polymers

In an attempt to develop less expensive and environmentally persistent CO_2-soluble compounds, several investigators have investigated highly CO_2-philic derivative, composed solely of carbon, hydrogen and oxygen. Poly(ether-carbonate), (240 repeat units, 15.4 mole % carbonate) was soluble in CO_2 at 1 wt % at low pressure (14 MPa) and was comparable to poly(hexafluoropropylene) oxide with 175 repeat units (soluble for 1 wt % at 18 MPa). The solubility of poly(ether-carbonate) in scCO_2 is partly due to the high concentration of negative charge density on the oxygen atoms of each carbonate functional group.[8] The solubility of these polymers in CO_2 is strongly dependent upon the ratio of carbonates to ethers, it is somewhat difficult to synthesize polymers with a precisely desired ratio, and the cloud point pressures required to dissolve these polymers at concentrations as great as 5wt% have not been reported. (Cloud point pressures at 5wt% are commonly used to gage the CO_2-solubility of polymers.) Therefore, poly(ether-carbonates) were not further studied in this work. The acetate group was also recognized as having the potential to be very CO_2-philic and has the advantage of easy introduction into polymers or small compounds. As expected, an increase in the CO_2-solubility of siloxanes was observed with the addition of acetate side chains to silicone oil[11,12]. McHugh et. al. observed the significantly lower cloud point pressure of poly(vinyl acetate) relative to its isomer poly(methyl acrylate)[13], even though the molecular weight of the PVAc was significantly less than the PMA. Our subsequent joint study with McHugh

substantiated that PVAc was more CO_2-soluble than any other polymer composed solely of C, H and O [14] over a very broad molecular weight range. The later design of CO_2-soluble acetylated ionic surfactants[15,16], and high CO_2-solubility of peracetylated sugars such as sorbitol[17], sugar amides, high molecular weight peracetylated cyclodextrins[18], and maltose octaacetate[19] successfully demonstrated the CO_2-philic nature of acetate group. The enhancement of CO_2 solubility via acetylation has also been studied by Wallen[20], who first reported the high solubility of glucose pentaacetate and galactose pentaacetate. Manke and co-workers recently provided a very detailed phase diagram for galactose pentaacetate in CO_2 by dew-point and bubble-point measurements and confirmed a substantial solubility of galactose pentaacetate in CO_2[21]. A two-point association involving, (1) a Lewis acid:Lewis base interaction between the oxygen in the acetate carbonyl group and the carbon of the CO_2; (2) a weak hydrogen bonding between the acetate methyl groups and the oxygen of the CO_2 is believed to be responsible for the thermodynamic affinity of the acetate group for carbon dioxide[22].

Based on the favorable CO_2-polymers interactions CO_2-philes were identified. The polymers were synthesized and phase behavior studies were done to check the solubility of polymer in CO_2.

Phase Behavior Experiment

Polymers were evaluated in CO_2 at 298K and 70 MPa from 5wt % to 1wt %. Some of these polymers might be soluble in CO_2 at less than 1 wt % but those polymers that were not soluble to 1 wt % were highly unlikely to remain CO_2 soluble when modified by the inclusion of CO_2-

phobic associating groups. Therefore any polymer that was not at least one weight percent soluble in CO_2 is regarded as insoluble in this research. For the polymers which were soluble in CO_2, cloud point pressures were determined using a standard non-sampling technique involving slow, isothermal compression and expansion of binary mixtures of known overall composition. The cloud point pressure is designated as the highest pressure at which a minute amount of the denser, polymer-, H-bonding compounds- or dendrimer-rich phase remains in equilibrium with the CO_2-rich fluid phase. Typically, when this pressure is realized, the transparent single-phase solution becomes essentially opaque as the "cloud" of the second phase appears.

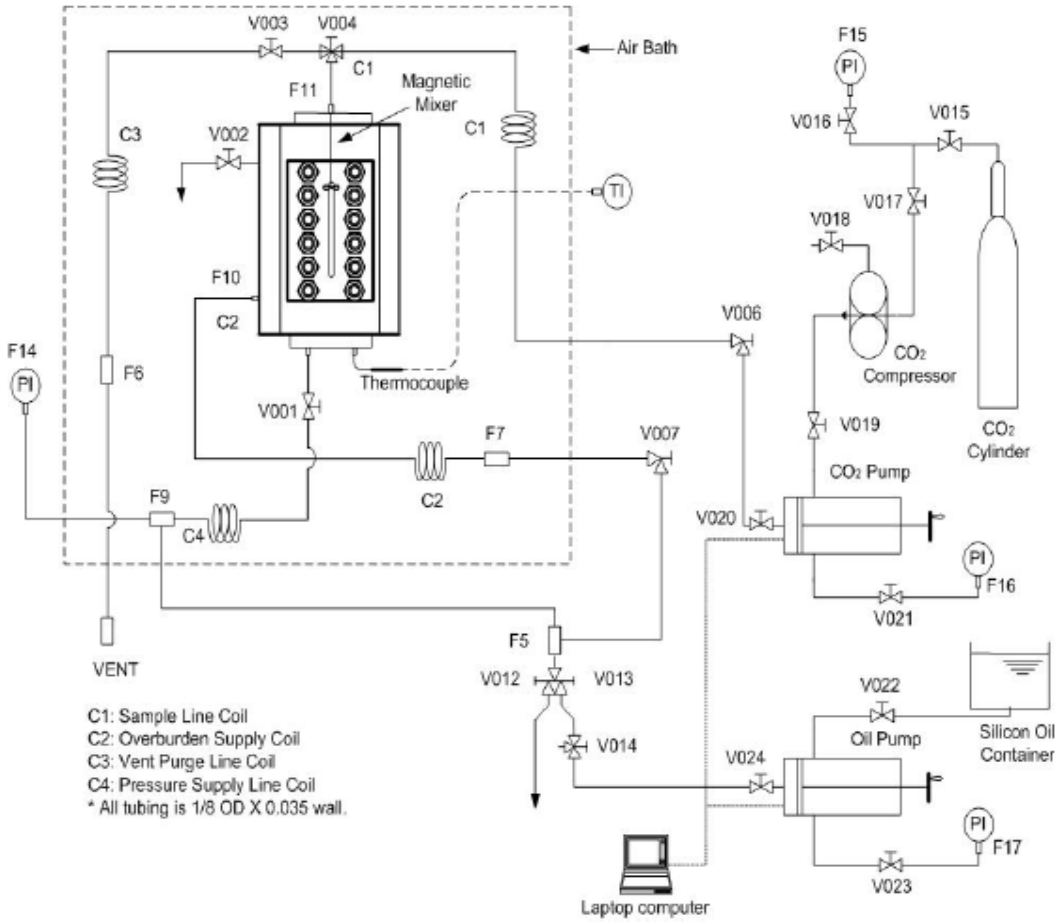

Figure 4.1: Schematic of phase behavior apparatus (Robinson cell)

Phase behavior studies were performed using high pressure, variable-volume, windowed cell, Figure 4.1, (formerly DB Robinson and Associates, now Schlumberger) retained in a constant

temperature air bath. Temperature range for the cell is -20^{o}C to 180^{o}C and can be pressurized up to 10000 psi. The maximum volume of the cell is about 110 cc. To do the phase behavior experiment, a known amount of polymer sample is place on the piston inside the glass quartz as shown in figure 4.3. The piston can be moved up or down, thereby decreasing or increasing the volume of the sample chamber, by adding or withdrawing the overburden fluid (silicone oil) using a positive displacements pump. CO_2 is added to the cell and constant pressure is maintained by withdrawing overburden fluid. When the required amount of CO_2 is added, the cell is pressurized and mixed using magnetically driven stirrer until the single phase is obtained at very high pressure (up to 70 MPa). Then cell is then slowly depressurized by withdrawing overburden fluid until two phases were observed; the second phase may be droplets of liquid polymer or fine particles of a solid polymer. At the when no light can transmit through the sample, the pressure is considered to be the cloud point pressure, also known as the dew point pressure for liquid polymer droplets. The particles or droplets of the second phase would accumulate at the bottom of the cell for cloud or dew point measurements. The system is pressurized again and mixed to obtain single phase and depressurized until the two-phase pressure is again observed. For each weight percent, this process is repeated 3-4 times to obtain a consistent reading. Bubble point pressures were easily detected as the pressure at which the first bubble of a CO_2-rich vapor appeared. Liquid-liquid "bubble" points appeared as cloud points, but were distinguished by the droplets of the second liquid phase floating *up* to the top of the sample volume. Three phase pressures were easily detected as the pressure at which the first bubble of a CO_2-rich vapor would appear from a liquid-liquid system.

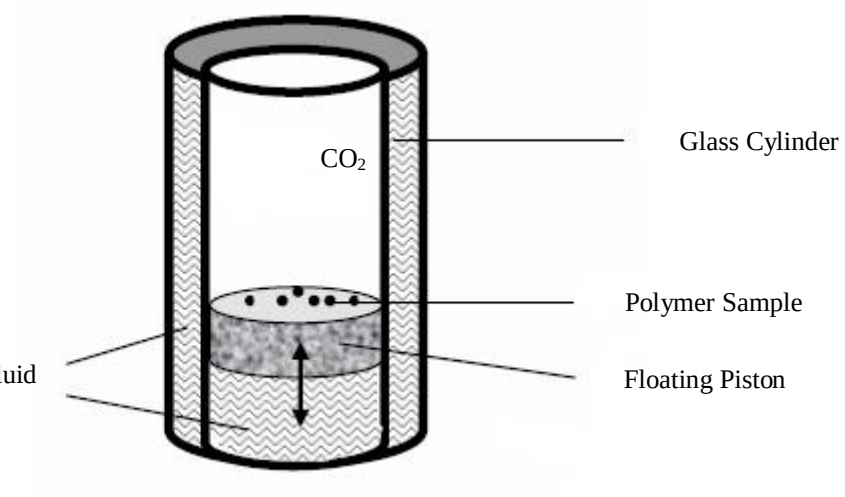

Figure 4.2: Schematic of glass cylinder with piston, polymer and CO_2

Based on the guidelines provided in the previous section new oxygenated polymers were tried.

Poly (vinyl propionate)

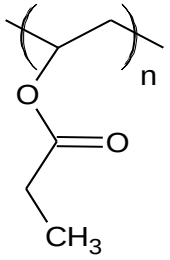

Figure 4. 3: Poly (vinyl propionate)

Poly (vinyl propionate) (PVPp) is very similar to poly (vinyl acetate) (PVAc) but has a side chain terminated with ethyl group instead of methyl group. It was thought that increase in the length of side will increase the free volume of the polymer which will lower the glass transition temperature and thus might be more soluble in CO_2 than PVAc. Poly (vinyl propionate) (30000 molecular weight and melting point 35°C) was purchased from Aldrich and was tested for its solubility in CO_2. It was found that poly (vinyl propionate) was not soluble in CO_2 although it did become a free flowing liquid in CO_2. An increase in the side chain length in PVPp apparently

acted as a hindrance to the Lewis acid-base interaction between polymer and CO_2, which are responsible for making PVAc CO_2 soluble. As result PVPp was not soluble in CO_2.

Poly (propylene fumaric acid)

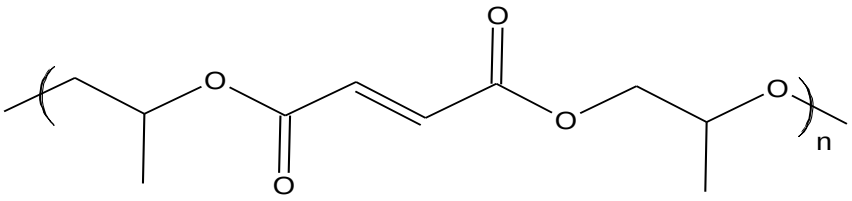

Figure 4. 4: Poly (propylene fumaric acid)

Poly (propylene fumaric acid) (5000 molecular weight) has highly oxygenated backbone. This polymer was tried to detertmine the effects of oxygen in the backbone rather than on the pendent group. It melted in CO_2 but was not soluble.

Poly (acetoxymethylsiloxane)

The objective is to design a highly CO_2-philic polymer solely composed of C, O and H. Given the challenge of this task and remarkable solubility of siloxane polymers in CO_2, we decided to determine if acetylation of PDMS would further enhance the solubility of this polymer. This was the only Si-containing polymer that was studied.

Synthesis of poly (acetoxymethylsiloxane)

Material: Polymethylhydrosiloxane of average molecular weight 1600 was bought from Gelest and palladium acetate, acetic acid, and benzene was purchased from Aldrich and used without any purification

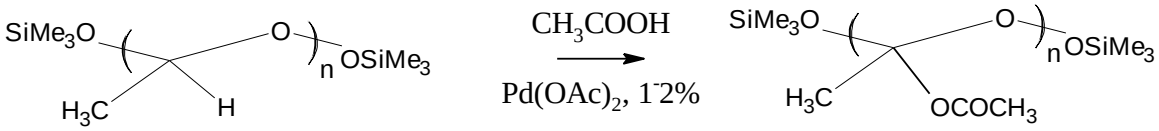

Figure 4.5: Reaction of poly (methylhydrosiloxane) with acetic acid to give poly (acetoxymethylsiloxane)

Synthesis: A mixture of palladium acetate (0.5mmol) and acetic acid (50mmol) in12 ml benzene was degassed by freeze-pump-thaw cycle. Poly (methylhydrosiloxane) (50mmol) was added to the mixture at 70°C. Evolution of gas (presumably H_2) was observed and the reaction mixture turned from yellow to black. The progress of the reaction was observed by IR by disappearance of the Si-H band at 2166 cm^{-1}.After the completion of the reaction, the catalyst precipitated and from the remaining colorless solution benzene was removed under vacuum to get poly (acetoxymethylsiloxane).

The resultant poly (acetoxymethylsiloxane) was very unstable and very quickly hydrolyzed to produce acetic acid while forming a cross-linked network which was not soluble in CO_2.

Poly(Lactic Acid) (PLA)

Amorphous PLA, composed of a racemic mixture of the D- and L- isomers, was selected rather than crystalline sample because high melting point polymers are notorious for being difficult to dissolve in CO_2. A previous study by Mark McHugh [9] has demonstrated that high molecular

weight (Mw = 84500 and 128450) PLA is soluble in CO_2 at pressures far in excess of those required for the dissolution of PVAc. However, in our study, the CO_2 solubility of PLA was contrasted over a wider range of molecular weight to determine if lower molecular weight PLA exhibited cloud point pressures more comparable to that of PVAc of comparable molecular weights. The effect of the end group composition on the CO_2 solubility of several very low molecular weight oligomers, Figure 4.6, was also determined.

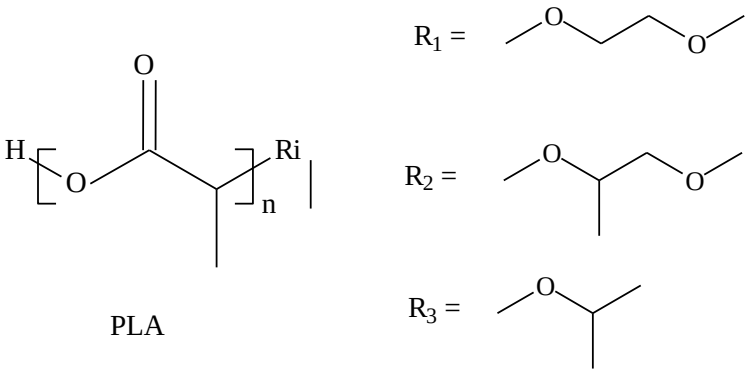

Figure 4.6: PLA oligomers with different end groups

Material: Amorphous PLA with acid end groups and inherent viscosity 0.17 dL/g, 0.45 dL/g and, 0.66 dL/g, which correspond to weight molecular weight of 12000, 55400 and 94500, respectively, were purchased from Lakeshore Biomaterials. PLA with different end groups (R_1 Mw = 5700 and 8300; R_2 Mw = 1265 and R_3 Mw = 900), Figure 2, were purchased from Polymer Source.

PLA phase behavior results

Different molecular weight samples of amorphous, acid-terminated PLA were dissolved in CO_2 at room temperature at a concentration of 5wt%. The resultant phase behavior is shown in Figure 4.7. As with PVAc, the cloud point curve corresponding to PLA is relatively flat over a

broad range of molecular weight. However the pressure required to dissolve PLA ranges between 120 – 140 MPa at 298K; more than twice that required to dissolve PVAc in dense CO_2.

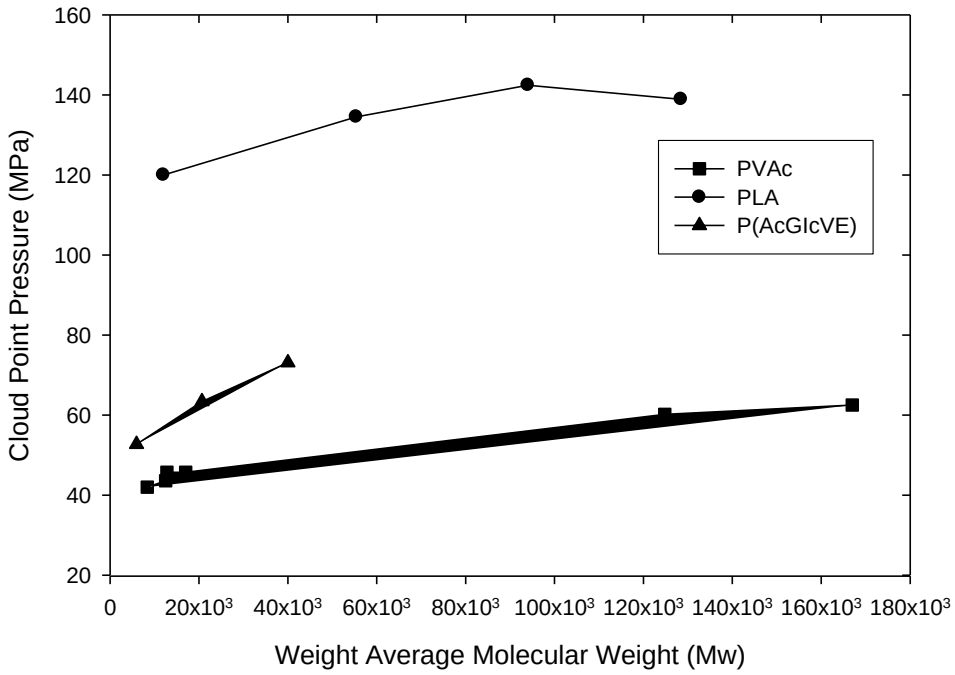

Figure 4.7: Cloud-point pressures at 5 wt% polymer concentration and 298 K for binary mixtures of CO_2 with poly vinyl acetate (■), polylactic acid (●) and P(AcGIcVE) (▲) as a function of weight average molecular weight. Data for Mw = 84500 and 128450 previously published by McHugh. PVAc data previously published [6].

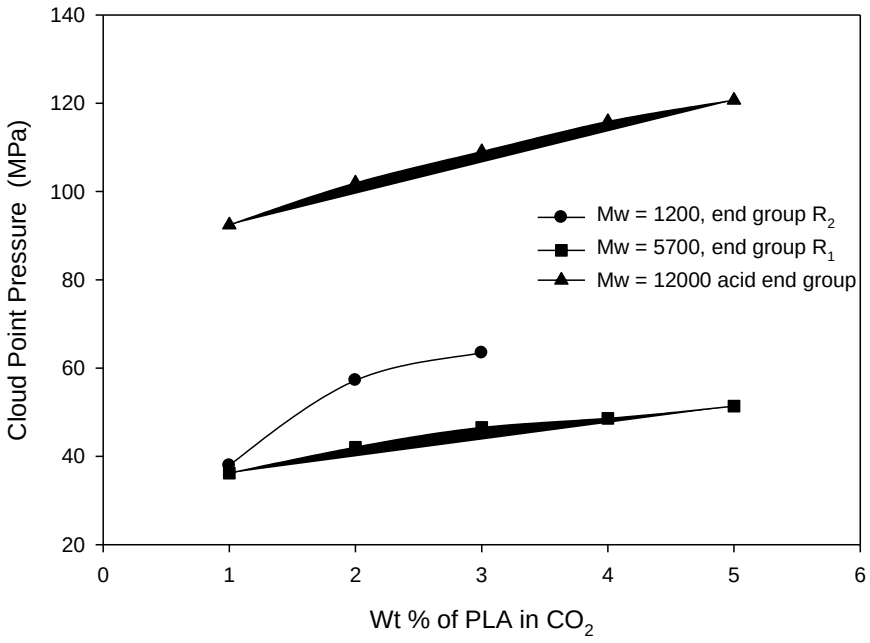

Figure 4.8: Phase behavior of low molecular weight PLA with different end group in CO2, cloud point data at 1- 5wt% PLA and 298K.

The CO_2 solubility of several very low molecular weight PLA oligomers was also determined over the 1-5 wt% range, Figure 4.8. (Because these samples were not acid terminated and the effect of the end group is recognized to be most significant at low molecular weights, the 5wt% cloud point data were not provided in Figure 4.7, which contains the higher molecular weight, acid terminated PLA data.) The R_1 end group, which is linear with two ether oxygens, seems to impart the greatest degree of CO_2 solubility. This is evidenced by a decrease in cloud point pressure, despite a molecular weight increase from 1200 to 4700, when the R_2 end group, which had two ether oxygen and a pendent methyl group, was replaced with the R_1 end group. When the end group contains only single ether oxygen, R_3, the PLA with Mw = 900 was insoluble in CO_2.

It is observed that solubility of low molecular weight PLA is quite comparable to low molecular weight PVAc. However with increase in molecular weight, the pressure required to dissolve PLA in CO_2 is almost double of PVAc for same molecular weight and weight percent.

Molecular Modeling

In an attempt to determine attain a more accurate understanding of why PVAc was remarkably more CO_2 soluble in CO_2 than amorphous PLA, *ab initio* calculations were employed.

Computational Methods: We constructed a model for poly(lactide) consisting of two repeat units, hereafter referred to as the PLA dimer (shown in Figure 4.9). The PLA dimer model was used to compute the interaction energies and binding configurations with CO_2. In order to compare PLA with PVAc on an equal footing in our calculations, we used an IPA dimer as a reference for PVAc, which we have studied previously [7]. The IPA dimer, which will also be referred to as the PVAc dimer, is shown in Figure 4.10.

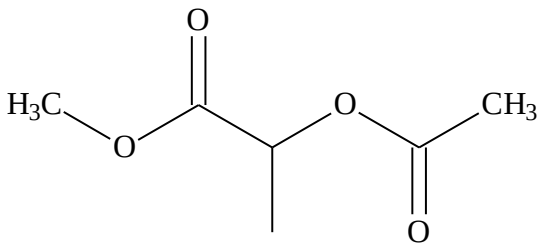

Figure 4.9: The structure of a compound with two repeat units of poly(lactide), (PLA dimer)

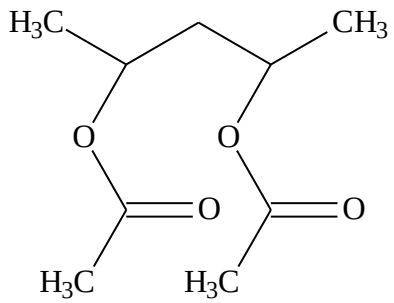

Figure 4.10: The structure of a compound with two repeat units of poly(vinyl acetate), PVAc dimmer

We have used *ab initio* quantum chemical methods to calculate the interactions between CO_2 and the molecules of interest. The calculations include three steps. First, we made initial guesses for the binding configurations by randomly placing a CO_2 molecule around the important functional groups (ester and carbonyl oxygens) of the model molecules. Second, we used second order Møller-Plesset (MP2) perturbation theory along with the 6-31+G(d) basis set to optimize the configurations of the CO_2+model molecule systems. Finally, we used a larger basis set, aug-cc-pVDZ, to compute the binding energy for the optimized systems to improve the accuracy of the results. We have used counterpoise (CP) corrections to account for basis set superposition error (BSSE) [15]. We have used the average values of raw and CP corrected energies to approximate the complete basis set limit binding energies. This method has been shown to give reasonable estimates for the complete basis set limit binding energies [16; 17].

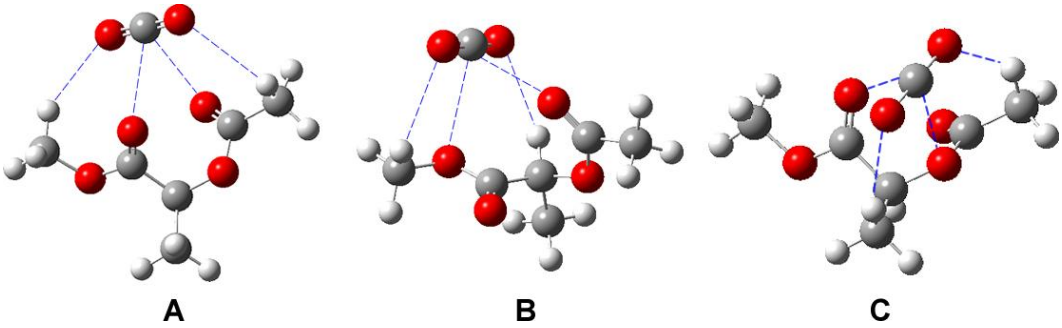

Figure 4.11: Three distinct binding configurations of CO_2/PLA dimer systems

PLA dimer: -We have identified three distinct binding configurations for CO_2/PLA dimer system, starting from six initial structures. The final binding configurations are shown in Figure 4.11. The calculated energies are listed in Table 1 along with the previously published results for three (different) configurations of the CO_2/isopropyl acetate (IPA) monomer (also referred to as the VAc monomer) system from Kilic et al [7] We can see from Table 1 that the interactions energies between CO_2 and the PLA dimer are much stronger than those between CO_2 and the IPA (VAc monomer) molecule. This is expected because the PLA dimer contains two acetate-like structures while IPA in this prior reference only has one. We note that the carbon atom in CO_2 molecule always binds with two oxygen atoms in the PLA dimer molecule and only binds with one oxygen atom in IPA molecule. The additional C-O interaction pair is responsible for the stronger interactions.

Table 4.1: The interaction energies for the CO_2/PLA dimer and CO_2/IPA [7] systems. See Figure 8 for the definition of the configurations for the CO_2/PLA dimer system and [7] for the corresponding definitions for the CO_2/IPA system.

Configuration	Interaction energy (kJ/mol)	
	CO_2/PLA dimer	CO_2/IPA monomer
A	-23.2	-14.8
B	-22.0	-14.2
C	-21.8	-15.9
Average	-22.3	-15.0

In order to make a fairer comparison between PLA and PVAc, we subsequently carried out calculations for CO_2 interacting with the IPA dimer (PVAc dimer) shown in Figure 4.10.

PVAc dimer: The PVAc dimer has a greater degree of conformational flexibility than the PLA dimer, and therefore the two pendant groups give rise to a larger number of rotational isomers. We have identified five distinct conformations corresponding to minima for the PVAc dimer; these are shown in Figure 4.12. The conformations are numbered from 1 to 5 based on the calculated energies, from the lowest to the highest. We set the energy of conformation 1 to be zero. The relative energies are then 5.4, 6.7, 9.6 and 15.5 kJ/mol for conformations 2 through 5, respectively. We have optimized multiple configurations of the CO_2/PVAc dimer system, starting from the five conformations listed in Figure 4.12. We have obtained seven distinct optimized geometries for the CO_2/PVAc dimer system, shown in Figure 4.13. The calculated energies for these binding modes are listed in Table 4.2.

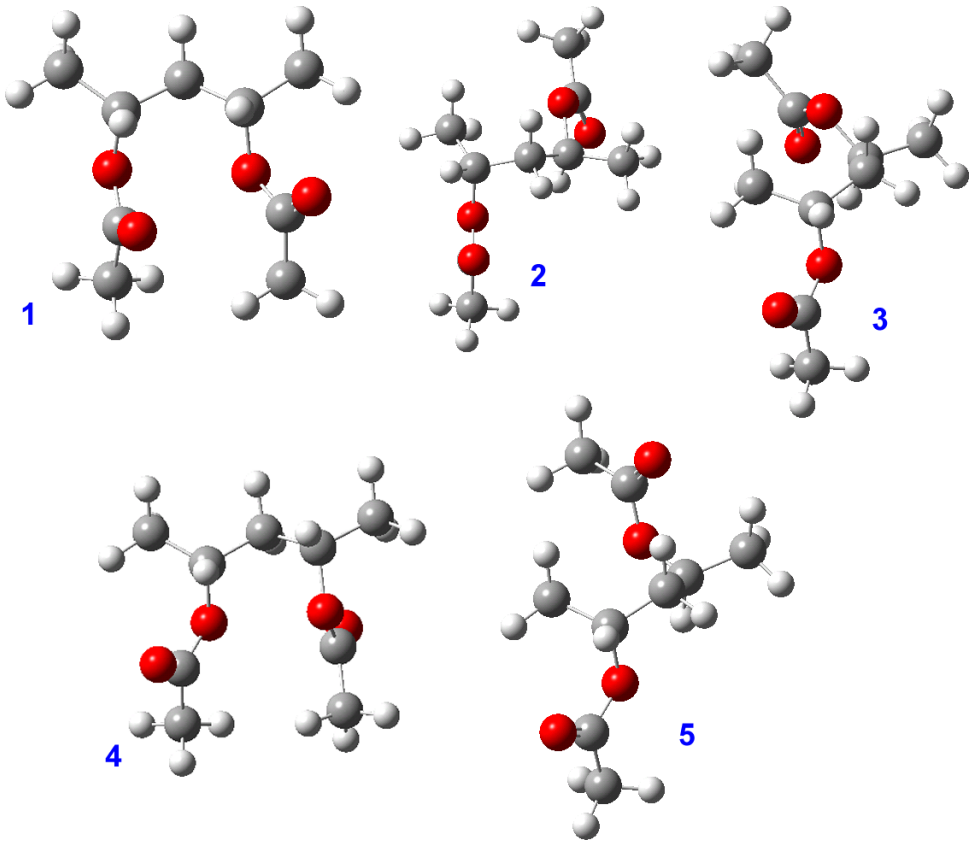

Figure 4.12: Five distinct conformational minima of the PVAc dimer molecule. They are numbered according to the calculated energies, from the lowest to the highest.

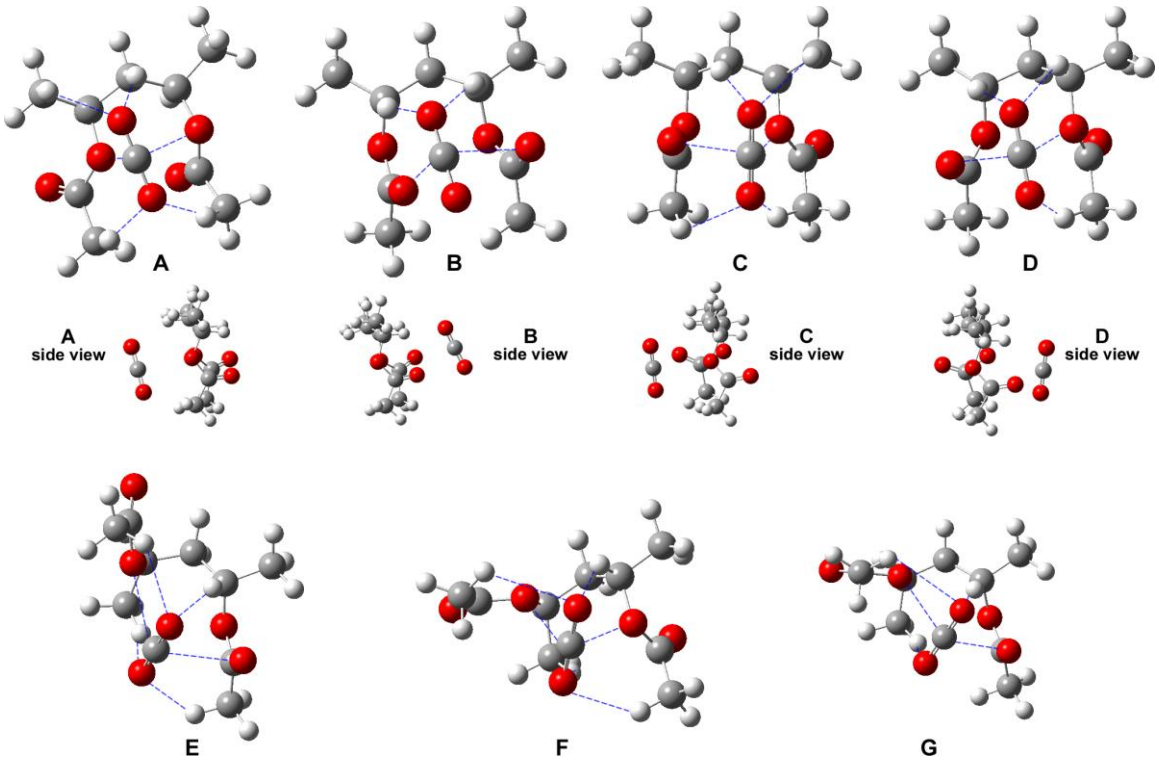

Figure 4.13: The optimized binding configurations for the CO_2/PVAc dimer system. The blue dashed lines indicate the primary interaction points between the two molecules.

Table 4. 2: Interaction energies of CO_2/PVAc dimer system.

Configuration	Interaction energy (kJ/mol)
A	-22.0
B	-25.0
C	-25.4
D	-26.1
E	-24.7
F	-24.4
G	-22.3
Average	-24.3

The PVAc dimer molecule in binding modes A and B adopts essentially the same geometry; the difference in binding energy is due to changes in the CO_2 location; binding modes A and B having CO_2 on opposite sides of the PVAc dimer. Therefore, these two binding modes can be simultaneously populated. This is also true for binding modes C and D. The average interaction energy for the CO_2/PVAc dimer is -24.3 kJ/mol. This is only slightly more favorable than the CO_2/PLA dimer average binding energy of -22.3 kJ/mol.

Molecular Modeling Discussions: Our calculations indicate that there is little difference in the average interaction energies for the CO_2/PLA dimer and the CO_2/PVAc dimer systems. There is a slight energetic preference for the CO_2/PVAc dimer system, but not enough to account for the observed differences in cloud point pressures for PLA and PVAc shown in Figure 4.7. There are, however, clues to the increased solubility of PVAc relative to PLA. First, the PVAc dimer has considerably more conformational freedom than the PLA dimer and correspondingly more binding modes than the PLA dimer (7 and 3, respectively). This leads to more configurational entropy and more favorable mixing. It is well known that crystalline polymers (with low configurational entropy) generally exhibit poor solubility in CO_2. Second, the PVAc dimer has binding modes that will readily accept multiple CO_2 molecules, whereas the PLA/CO_2 binding modes illustrated in Figure 4.11 can apparently only accommodate a single CO_2 molecule at a time.

Pendent Sugar Acetate

Many small peracetylated sugars (monosaccharides, disaccacharides, cyclodextrins) exhibit high solubility in CO_2.[10; 11] Although cellulose triacetate (CTA) is composed of peracetylated sugar that constitutes the backbone of the polymer, it is essentially CO_2 insoluble because of its crystallinity. Therefore we decided to evaluate a polymer with a polyethylene backbone and pendent peracetylated sugar groups because it was likely that such a polymer would not be crystalline. Therefore poly(1-O-(vinyloxy) ethyl-2,3,4,6-tetra-O-acetyl-β-D-glucopyranoside), AcGIcVE was synthesized at Yale following a recently published procedure. [12]

Polymerization of AcGIcVE

The polymerization [12] of AcGIcVE was carried out under nitrogen in a dry three neck round bottom flask. AcGIcVE (2.5 mmol, 1.06g) was combined with 10 ml of toluene at 0°C. Then chilled BF_3OEt_2 (0.05mmol) was added to the solution. After stirring the reaction mixture for 24 hrs, polymerization was stopped by adding ammoniacal methanol. The reaction mixture was washed with dilute HCl and then with water. During this washing, some of the polymer precipitated out and some remained in toluene. The precipitates were dissolved in dichloromethane. P(AcGIcVE) was obtained by removing dichloromethane and toluene under vacuum.

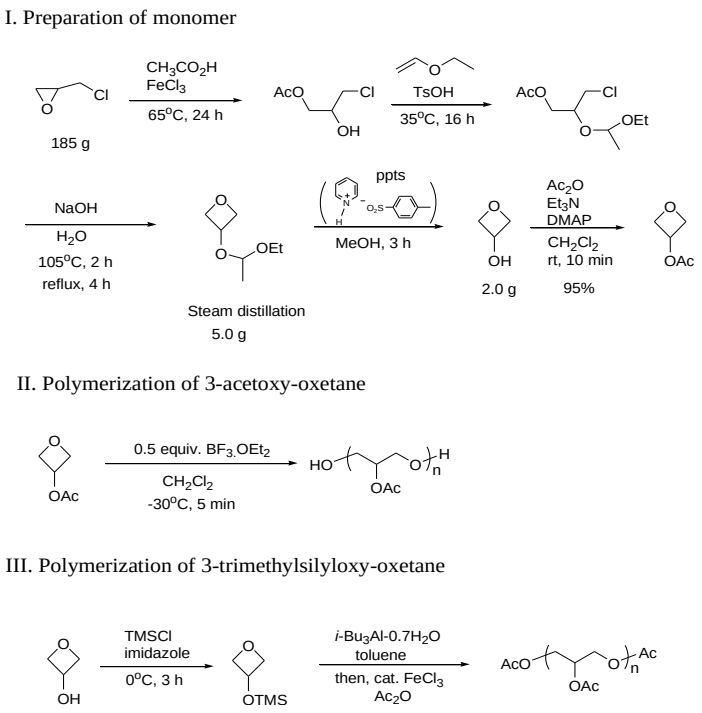

Figure 4.14: polymerization of AcGIcVE

The polymerization was confirmed by ^{1}H NMR on Bruker 300 MHz instrument. The NMR spectra were taken in $CDCl_3$ at 298 K which showed that vinyl double bond peak (δ = 6.44 (q, 1H, =CHO)) was absent. The weight average molecular weight was determined by GPC using THF was used as eluent at 298 K and polystyrene standard.

P(AcGIcVE) Phase Behavior

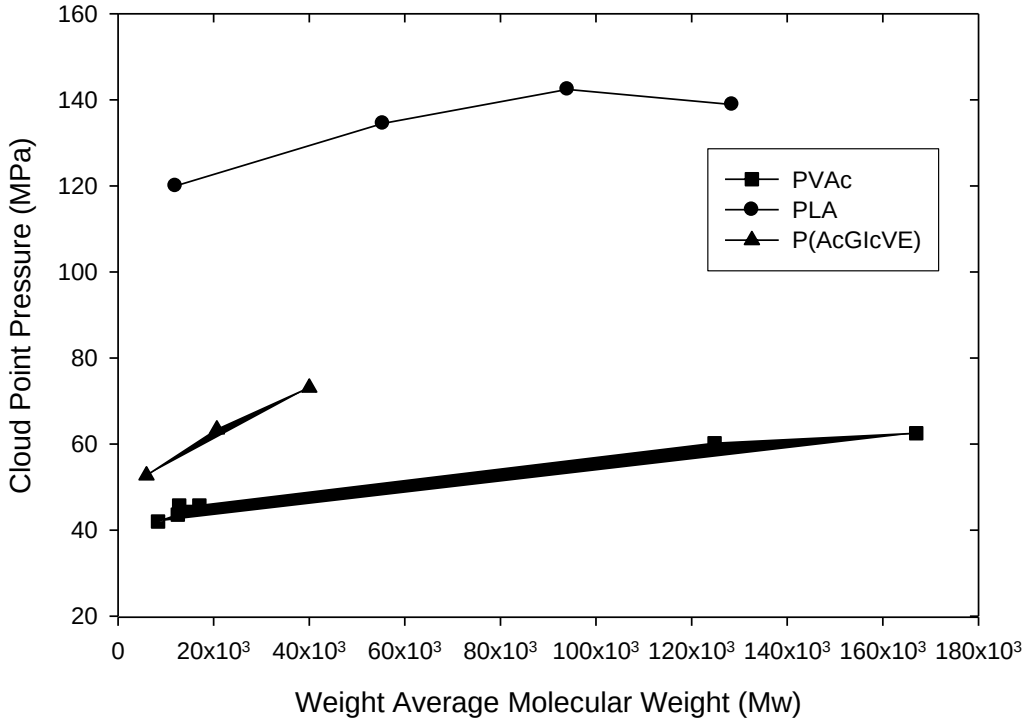

Figure 4.15: Cloud-point pressures at 5 wt% polymer concentration and 298 K for binary mixtures of CO_2 with poly vinyl acetate (■), polylactic acid (●) and P(AcGIcVE) (▲) as a function of weight average molecular weight. Data for Mw = 84500 and 128450 previously published by McHugh. PVAc data previously published [6].

The cloud point pressures for P(AcGIcVE) at 5wt% are also presented in Figure 4.15. These cloud point values are significantly less than those for PLA, but are about 10-20 MPa greater than the cloud point pressures associated with PVAc. It should be noted that the solubility of these polymers in CO_2 was based on polymer molecular weight rather than the number of repeat units because the monomeric unit for P(AcGIcVE) is 418 and contains 4 acetate groups, while the monomer of PVAc has a molecular weight of 84. Currently, P(AcGIcVE) is the second-most CO_2 soluble, high molecular weight, oxygenated hydrocarbon polymer, second to PVAc.

Comparison of PVAc, P(AcGIcVE) and PLA

It is apparent from the results illustrated in Figure 3 that PVAc remains the most CO_2 soluble, high molecular weight, oxygenated hydrocarbon polymer yet identified, followed by P(AcGIcVE) and amorphous PLA. Although the cloud point loci of 5wt% in CO_2 at 298K as a function of molecular weight is relatively flat over a broad range, the differences in pressure between these curves, particularly between PLA and PVAc, is dramatic. One may conjecture that over the molecular weight illustrated in Figure 4.15, PVAc and P(AcGIcVE) (318 - 338 K) relative to PLA (393 – 413K), combined with the more accessible -$OCOCH_3$ pendent groups of PVAc and P(AcGIcVE) rather then the –$OCOCHCH_3$ backbone of PLA account for this difference in miscibility.

Poly(acetoxyacetate)

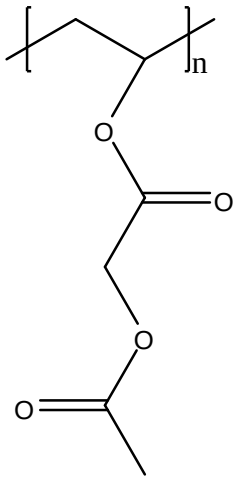

Figure 4.16 Poly acetoxy acetate

Poly (acetoxy acetate) was synthesized by Dr. Champan's group, in department of chemistry at University of Pittsburgh. It is very similar to poly (vinyl acetate). It has two acetate units in its

pendent group, Figure.. These two acetate units were expected to interact with CO_2 better than PVAc and make the polymer flexible. However the polymers were not soluble in CO_2. Lower molecular weight polymer melted in CO_2 but higher molecular weight did not melt and form a foam in CO_2.

Branched poly vinyl acetate

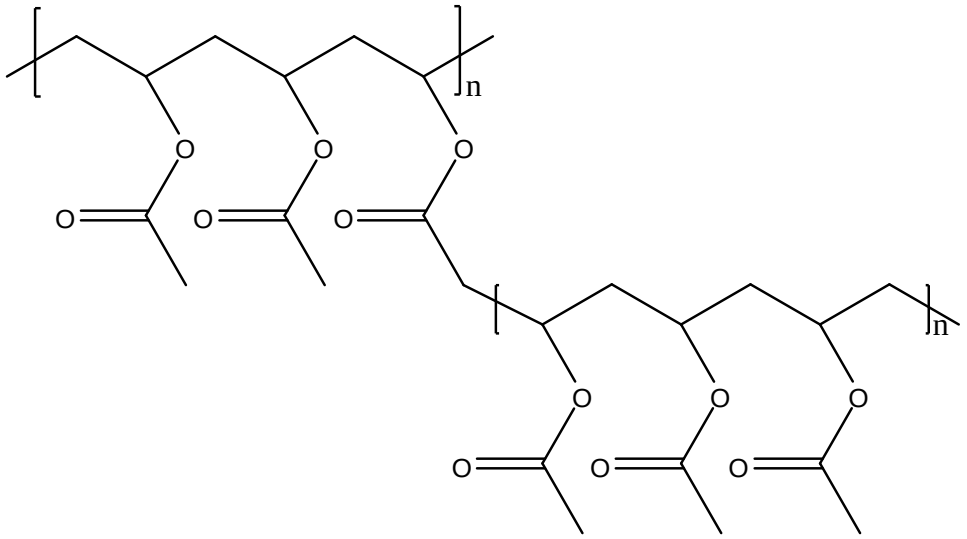

Figure 4.17: Branched poly vinyl acetate

Linear poly vinyl acetate is very CO_2 soluble polymers, however nobody had studied the effect of branching on the solubility of polymer in CO_2. In order to make branched polymer, first branching agent, vinyl xanthate was synthesized. To a solution of 30 gm potassium ethyl xanthogenate in 600 ml of acetone was added dropwise solution of 20gm vinyl chloroacetate in 70 ml of acetone at 0^oC. The reaction mixture was stirred for 4 hrs at room temperature. Reaction mixture was filtered and acetone was removed using vacuum. Crude product was dissolved in

dichloromethane and washed with water. Organic layer was separated and dichloromethane was removed under vacuum. Product was characterized by NMR.

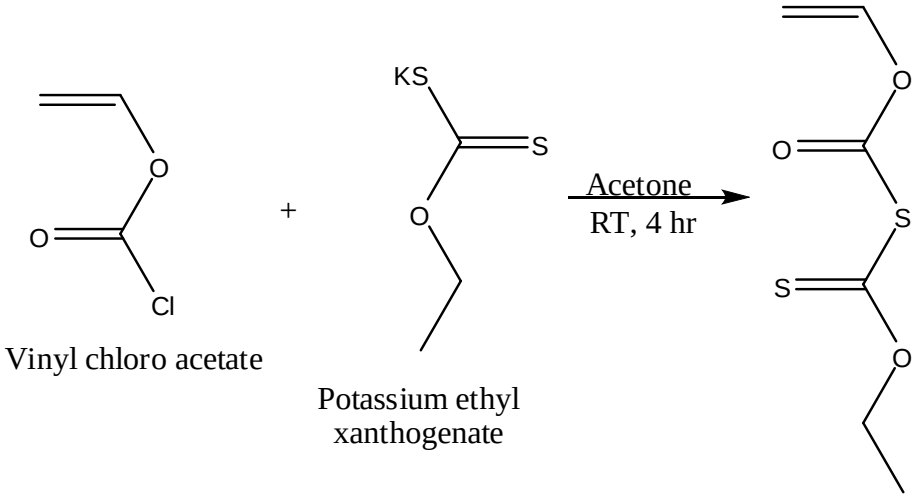

Figure 4.18: Syntheses of branching agent

Branched poly vinyl acetate was synthesized by copolymerization of vinyl acetate and vinyl xanthate.(5:1 mole ratio) using AIBN in THF at 50^{o}C for 12 hrs. Product was putified by precipitating it in hexane. It was characterized by NMR and the weight average molecular weight was determined by GPC using THF was used as eluent at 298 K and polystyrene standard.which was 6000. Branched Polyvinyl acetate was not soluble in CO_2 however it melted in CO_2.

Conclusions

Poly(vinyl acetate) remains the most CO_2-soluble, high molecular weight, oxygenated hydrocarbon-based polymer that has yet been identified. Although crystalline, high molecular weight peracetylated polysaccharides such as cellulose triacetate are CO_2 insoluble, we have

determined that P(AcGIcVE), a polymer with a polyethylene backbone, a flexible –OCH_2O- spacer and pendent sugar acetates, is more CO_2 soluble that any polymer other than PVAc. Amorphous PLA requires substantially higher pressures to attain miscibility with CO_2 with PVAc. However, molecular modeling calculations demonstrated that the average interaction energies between CO_2 with dimers of each polymer were comparable in magnitude. These calculations also demonstrated that PVAc has more conformational freedom than PLA and that (unlike PLA) PVAc has binding modes that will accept multiple CO_2 molecules. These may be responsible for the enhanced CO_2 solubility of PVAc.

Hydrogen Bonding Conpounds

It has been previously shown that self-aggregating organic compounds containing both hydrogen bonding urea groups and fluorinated CO_2-philic tails could modestly increase the viscosity of $scCO_2$.[9] Upon depressurization these solutions produced free-standing foams which represent organic analogs of silicate aerogels with sub-micron sized fibers and a bulk density reduction of greater than 90% of the parent material.[9] A critical feature of these molecules is the presence of strong and directional hydrogen bonding between carbonyl oxygen and hydrogen in the urea groups within each molecules leading to the formation of two-dimensional sheet like structures. (Figure 1a).[23] These molecules can form viscosity enhancing polymeric structures through non-covalent contact in solution, and subsequently free-standing foams upon the removal of the CO_2.

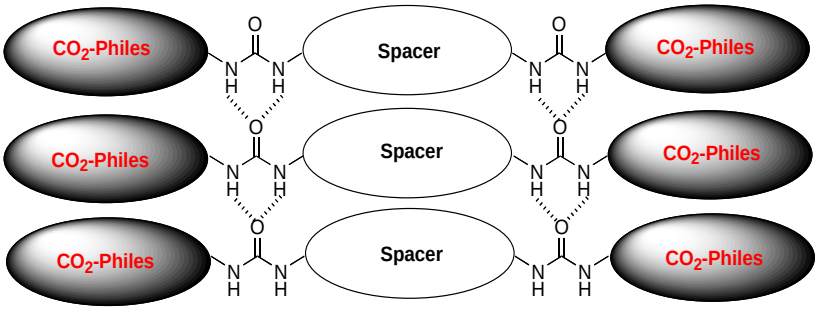

(a)

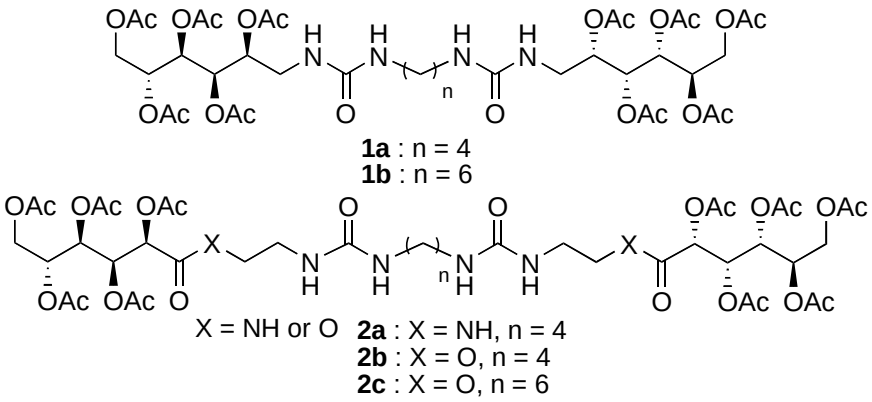

(b)

Figure 5.1: (a) Intermolecular hydrogen bonded network of bis-ureas with CO2-philes (b) Bis-ureas with two highly acetylated arms

The objective of the present work was to design non-fluorous hydrogen-binding derivatives capable of dissolving in CO_2. An inexpensive and readily available source of multiple hydroxyl groups is the family of mono-, di- and oligosaccharides. These can be readily converted into their peracetylated derivatives, which should have a similar density of electronegative groups to perfluoroalkanes. In particular, gluconic acid is readily available from glucose by oxidation and should be easily converted into its peracetylated derivative. Thus, peracetylated gluconic acid was chosen as the candidate for the non-fluorous CO_2-phililic appendage and commercially available D-glucamine was also chosen for easy access to the bis-urea family (Figure 5.1b).

Synthesis of Bis-urea compounds

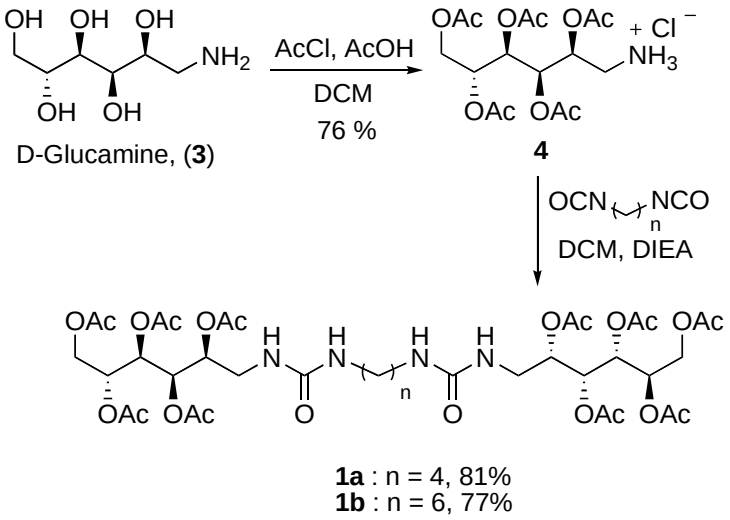

Figure 5.2: Synthesis of bis-ureas 1a and 1b

The synthesis of bis-urea 1 begins with the per-acetylation of commercially available D-glucamine (3). In contrast to the longer four step synthesis of acetylated glucamine, 4, reported by Hoeg-Jensen et. al.[24], we could selectively acetylate hydroxyl groups in glucamine with acetyl chloride under acidic conditions[25] directly. Penta-acetylated D-glucamine salt, which was easily purified through re-crystallization, reacted with various commercially available alkyl bis-isocyanates at room temperature to give the desired bis-ureas 1 in high yield (Figure 5.2). The CO_2-philic acetylated sugars are located adjacent to the bis-urea functionality in bis-ureas 1, and sterically hinder the formation of hydrogen bonded networks as in Figure 5.1a. An alternative design (shown in 2) places the peracetylgluconate groups more distant from the ureas through the insertion of ethanolamine or ethylenediamine spacers. Esters and amides of gluconic acid, 8, were synthesized by using a dehydrating agent such as the 1-(3-(dimethylamino)propyl)-3-ethylcarbodiimide hydrochloride (EDC hydrochloride). After deprotection of the Boc-

protected esters or amides in situ, the resulting free amines were reacted with bis-isocaynates to form the desired bis-ureas 2 in moderate to high yields (Figure 5.3).

The simplicity of this approach made it readily applicable to branched species, containing multiple acetylated gluconate groups. Cooper et. al. have previously shown that the fourth generation hydrophilic dendrimer, DAB-dendr-(NH2)32, functionalized with CO_2-philic per-fluoropolyether chains is highly CO_2 soluble.[10] A similar, albeit more limited approach could be taken to the dissolution of self-assembling bis-urea dendrimer in $scCO_2$ through the attachment of multiple CO_2-phlic groups, as in 10. The Boc-protected bis-ester amine, 9 was synthesized from the reaction of two equivalents of peracetylated gluconic acid with Boc-protected serinol. This was converted using the same reaction conditions, as in the synthesis of 1 and 2 to afford the bis-urea derivative with four CO_2-philic groups, 10. The yield was highly affected by the concentration of the reaction mixture. In order to avoid intramolecular side reactions and promote intermolecular reaction, the reaction was conducted at high concentration and resulted in the dendrimeric bis-urea in a moderate yield.

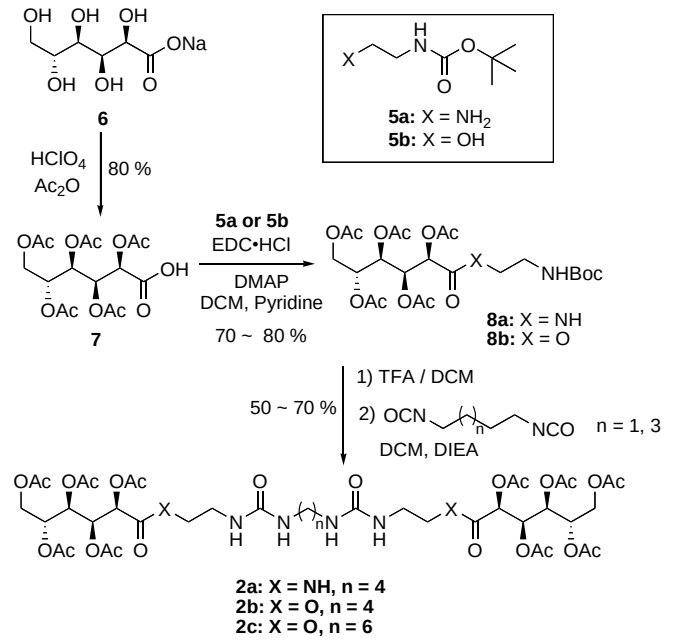

Figure 5.3: Synthesis of bis-ureas 2a, 2b, and 2c.

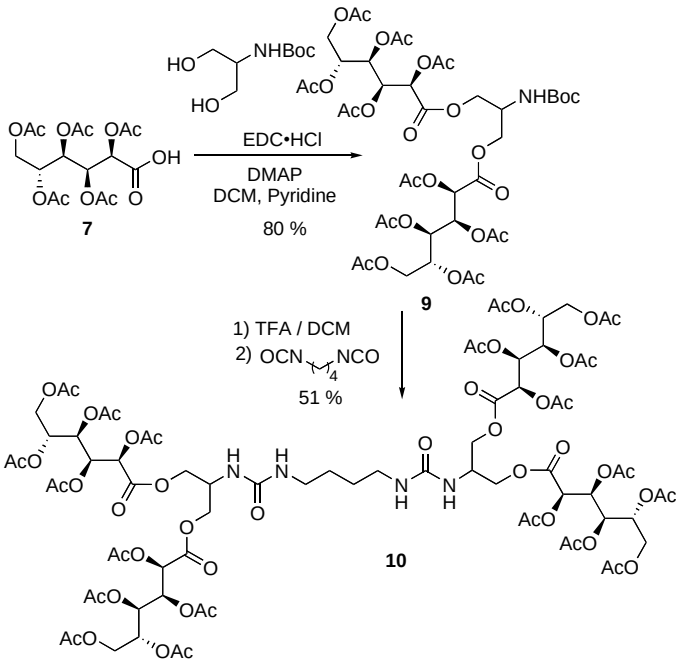

Figure 5.4: Synthesis of dendrimer 10

Phase Behavior

At ambient temperature, bis-ureas 1a and 1b were not soluble in $scCO_2$ even at pressures up to the limit of the instrument (68.95 MPa) or when heated to 100°C. Chain length (butane vs. hexane spacer) did not have any effect on the solubility of these compounds in $scCO_2$. It is possible that the close proximity of the acetates to the urea groups may inhibit both the insolvation by CO_2 as well as the inaggregation through hydrogen bondings.

Bis-ureas 2a - 2c containing an ethylene spacer between the CO_2-philic peracetates and the bis-urea groups were synthesized to test the effect of distance between the core and the tail in these molecules. Bis-urea 2a did not dissolve into CO_2 at any temperature and pressure, possibly due to the CO2-phobic nature of the amide group installed as a linkage. However, replacement of the amide by ester groups gave an oxygen rich and more CO_2-philic series in bis-ureas 2b and 2c (Figure 5.3). At 298 K, these highly acetylated bis-ureas dissolved in CO_2 at pressures of 62 MPa at 1 wt % for 2b and 65 MPa at 1 wt % for 2c.

The single phase, transparent solution attained under these conditions (e.g. 62 MPa, 298 K, 1 wt% of compound 2b) was apparently meta-stable. After 2-5 minutes, light suspension of fine fibers began to form in the solution. Apparently, at isothermal and isobaric conditions, the dissolved compound slowly aggregate due to hydrogen bonding and the macromolecule precipiattes, resulting in the formation of fibers. Within 20 minutes, the sample volume was filled with fibers and upon the removal of CO_2, very brittle, freestanding, micro-fibrillar foam formed, with an average fiber diameter of 1 - 3 microns. In the phase behavior studies at lower (13.5°C) and higher (37.5°C) temperature and a pressure of 65 MPa for bis-urea 2b, a single transparent phase was never attained. Nonetheless, the powdery compound initially charged into

the cell dissolved and then precipitated in the form of fibers. This compound appeared to be changing in morphology from a powder to fibers at isothermal, isobaric conditions.

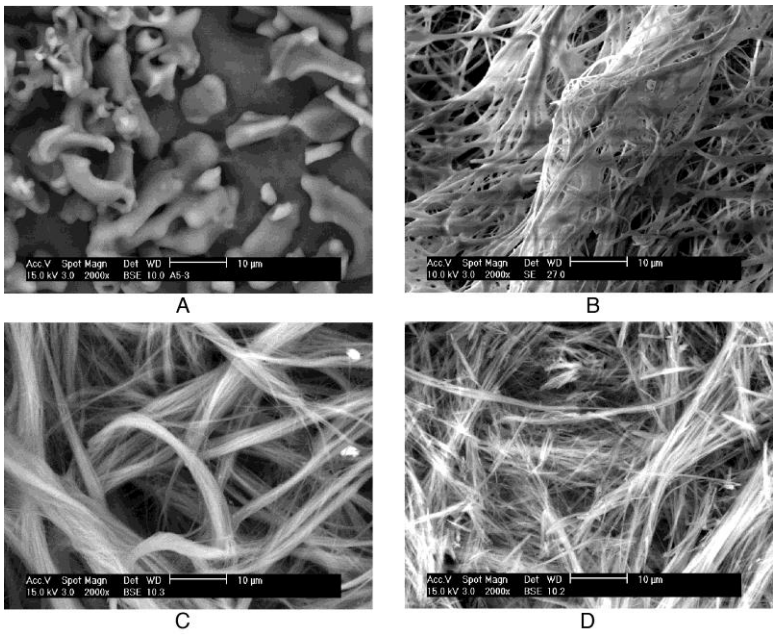

Figure 5. 5: SEM images of compound 2b before introduction of CO2 (A), and the fibers formed at pressure at 13°C (B), 25°C (C) and 37.5°C (D)

SEM images of all the fibrous material obtained at different temperatures are shown in Figures 2b-d and the morphology of the powder sample before mixing with CO_2 is shown in Figure 5.5a. At low temperature, compound 2b produced a foam with a highly interconnected micro-fibrillar structure with fiber diameters less than 1 micron (Figure 5.5b). The foam produced from compound 2b at ambient temperature has a major fiber diameter of 1 - 3 microns, which is composed of sub-micron fibers, and had higher porosity than that formed at low temperature (Figure 5.5c). The foam produced at 37.5°C was very brittle and had a fiber diameter around 1 micron (Figure 5.5d).

The improvements in CO_2 solubility seen in 2b and 2c encouraged us to prepare, a first generation dendrimer 10 containing four CO_2-philic peracetylated groups around a bis-urea core, shown in Figure 5.4. In contrast to the bis-ureas 2b or 2c (1% dissolution at 62 or 65 MPa), simple dendrimer 10 was more readily dissolved in CO_2 at a notably lower pressure of 27 MPa at 1 wt%. Compound 10 dissolved in the range of 1 - 5 wt % in liquid CO2 at 25°C as well as in supercritical CO_2 at 44°C. These are the first CO_2 soluble dendrimers composed solely of C, O, H and N. Unlike the linear, bis-ureas 2b or 2c discussed earlier, this dendrimer 10 formed a powder, not a rigid foam, upon the removal of CO_2. Both trends indicate that hydrogen bonding did *not* act to associate the dendrimers in solution,

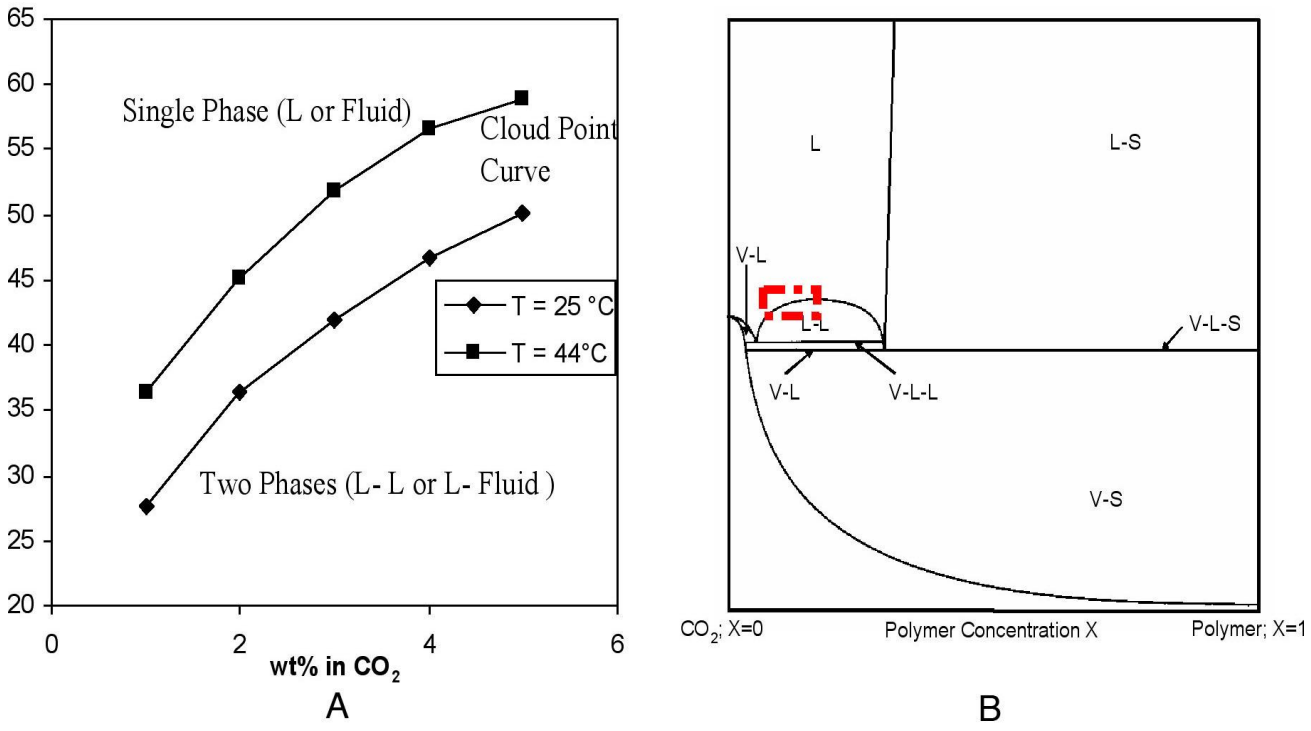

Figure 5.6: Cloud point curve of dendrimer in CO_2 at different temperature (A) General P-x isotherm of binary mixture in CO_2 (B).

Conclusion

In conclusion, a non-fluorous CO_2-philic compound with a core of two ureas separated by a short alkyl chain and two highly oxygenated "arms" derived from per-acetylated gluconic acid was dissolved to 1wt % in supercritical CO_2 at 298 K and 65 MPa. Upon dissolution, formation of micro-fibrillar foam with fiber diameters of approximately 1-3 microns was observed and this brittle networked material retained its integrity upon depressurization of the CO_2. A non-fluorous, first-generation highly CO_2-soluble dendrimer with four per-acetylated "arms" derived from acetylated gluconic acid and a bis-urea core was also synthesized. This dendrimer was soluble up to 5wt% in liquid and supercritical CO_2. The phase behavior of the dendrimer 12 in CO_2 is presented in Figure 5.6 in the form of a P-x isotherm. These results constitute a small portion of the overall phase Px diagram of this binary mixture, which is illustrated in Figure 5.6b. The small box within this figure represents the measured phase behavior shown in Figure 5.6a. These results indicate that acetylation provides an environmentally benign pathway to the generation of small, non-fluorous CO_2-soluble hydrogen-bonding compounds and dendrimers.

Design of CO_2 thickener

CO_2 soluble polymers, alone, cannot be used to increase the viscosity of CO_2 because (unlike water) ultra-high molecular weight polymers of any composition cannot, to the best of our understanding, dissolve in CO_2. Although significant viscosity increase may be attained using ultra-high molecular weight homopolymers, it is quite unlikely that a polymer with molecular weight of 1-10 million could dissolve in CO_2 at pressures less than minimum miscibility pressure, which is roughly 10 MPa at 295K.

Therefore first step in making a successful CO_2 thickener is to identify a CO_2 philic monomer based on oligomeric and/or polymeric phase behavior results. Then the CO_2-philic monomer can be copolymerized with a CO_2-phobic monomer which has the capacity to induce intermolecular associations such that when the copolymer is dissolved in CO_2, it can promote association among polymer chains. Alternately a copolymer consisting of the CO_2-philic monomer and a CO_2-phobic monomer can be purchased and transformed via replacement of the CO_2-phobic group (e.g. hydroxyl) with a more appropriate associating group.

To date only single CO_2 thickener has been identified, a random copolymer of **f**luoro**a**crylate and **st**yrene, dubbed. polyFAST, developed by Enick, Beckman and coworkers[34]. The increase in viscosity was due to π-π stacking of aromatic side chain functional groups. The optimum composition of the copolymer was found to be 29 mol% styrene and 71 mol% fluoroacrylate.

Addition of 1.2 wt% of the copolymer increased the viscosity of CO_2 by the factor of 19 relative to neat CO_2 as determined at low velocities in a sandstone core.

Styrene Association

It has been well known that the aromatic rings, for example benzene, associate via electrostatic, non bonding interactions which results into stacking of these rings [SV 57, 58]. This stacking is due to: -

- Delocalization of electrons in the pi orbital of benzene which creates a negative charge in a plane above and below the ring.
- Slight positive charge on the hydrogen atoms at the end of ring.

Due to this charge distribution, the hydrogen atoms of one ring are attracted towards the electron rich region above the other benzene ring, resulting in the stacking of benzene rings shown in Figure 6.1 [SV 57, 59,60,61]. Since benzene is non-polar and have zero dipole, these electrostatic interaction are attributed to their quadrupole –quadrupole interactions [63, 64]

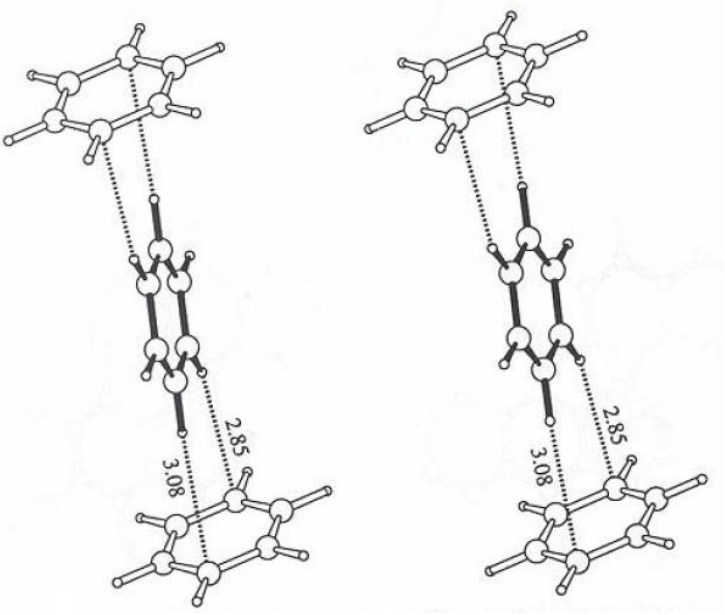

Figure 6.1: Stacking of benzene ring

This quadrupole - quadrupole interaction between the pendant phenyl groups of the (fluoroalkyl acrylate-co-styrene) polymer resulted in the individual copolymers not only dissolving in CO_2, but also interacting to form extremely high molecular weight viscosity-enhancing macromolecular structures.

Strategy of making a CO_2 thickener

The objective of this research is to make a CO_2 thickener only from carbon, hydrogen and oxygen. Therefore *vinyl acetate*, the monomer of the most CO_2-soluble oxygenated hydrocarbon polymer, poly(vinyl acetate) (PVAc), was selected as the CO_2-philic group. It is recognized that this PVAc-based copolymer will *not* be able to be used in the field because the pressure required to dissolve PVAc in CO_2 is much greater than the MMP of CO_2 EOR projects, and the inclusion of the CO_2-phobic associating groups will only serve to diminish its solubility in CO_2. Nonetheless, VAc remains the best CO_2 philic monomer, and the copolymer derived from this

compound will be used to demonstrate that a non-fluorous co-polymeric thickener can be designed for CO_2, albeit the pressure required for dissolution is too high for practical application.

The second step is the selection of an appropriate self associating monomer which can be co-polymerize with vinyl acetate. Styrene was successfully used in making fluorinated CO_2 thickener. As styrene is somewhat CO_2-phobic, the CO_2-solubility of co-polymeric thickener that includes styrene is expected to be less then the CO_2 philic homopolymer. Although styrene was successfully employed in the synthesis of polyFAST, styrene *cannot* be used for making copolymer with vinyl acetate because there is a large difference in there reactivity ratio (VAc = 0.001, Styrene = 42). Therefore simple radical copolymerization will give a mixture of homopolymers rather than random copolymers. The following monomers, each of which contains a pendant aromatic group, were selected for copolymerization with vinyl acetate.

Associating Groups

Vinyl Benzoate

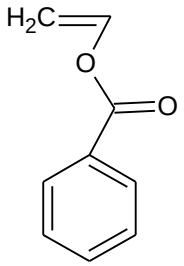

Figure 6. 2: Vinyl benzoate

As we know that PVAc is the most CO_2 soluble non-fluorous high molecular weight polymer, a methyl group at the end of side chain was replaced with benzene group to make a monomer that may be able to generate copolymers with VAc.

Material: Poly(vinyl alcohol) 78% hydrolyzed was bought from polymer science. Pyridine, benzol chloride and tetrahydrofuran was bought from Aldrich and used without purification.

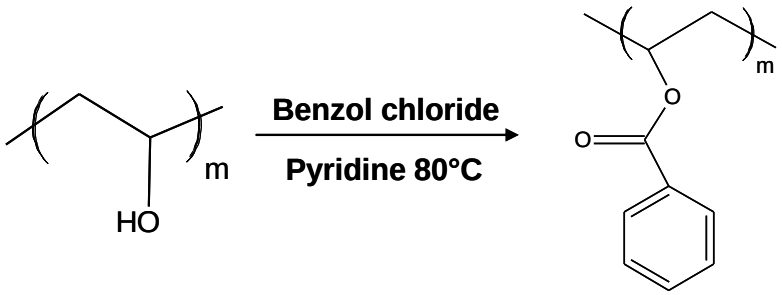

Figure 6. 3: Synthesis of Poly (vinyl benzoate)

Synthesis of Poly (vinyl benzoate): The reaction was carried under nitrogen atmosphere in a three neck round bottom flask. The mixture of pyridine(0.2 mol) and poly(vinyl alcohol) (0.035mol) was heated at 80°C for 12 hrs. Poly(vinyl alcohol) did not dissolved in pyridine After 12 hrs a solution of benzol chloride (0.045 mol) and pyridine (0.1 mol) was added to the reaction

mixture drop wise at 60°C and the reaction was monitored by IR (disappearance of C-OH band). Poly(vinyl benzoate) was obtained by precipitating the reaction solution in excess of water. Polymer was dissolved in tetrahydrofurane and re-precipitated in water for further purification.

Result: Poly (vinyl benzoate) of 6000 molecular weight was synthesized and tested for CO_2 solubility. It melted in CO_2 but was not soluble at 298 K and 70 MPa. The insolubility of this homopolymer was not surprising. However the melting point depression is a favorable indication that this monomer is more CO_2-philic than styrene.

Benzyl vinyl formate

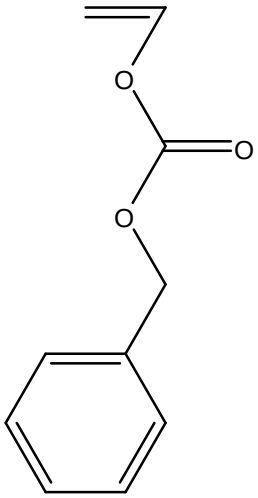

Its molecular structure is very similar to vinyl benzoate. In this monomer, the benzene ring is further away from the main chain by CO_2 philic -OCH_2- group. Additional CO2 philic group should make this monomer more CO_2 philic. Homopolymer of benzyl vinyl formate was not synthesized.

4-acetoxystyrene

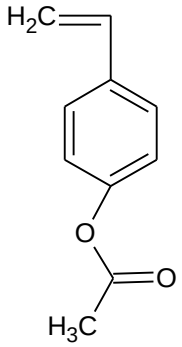

Figure 6.4: 4-acetoxystyrene

In order to increase the likelihood that VAc could copolymerize with a monomer containing an aromatic ring the structure of styrene monomer is modified by adding a CO_2-philic acetate group to the benzene ring. Poly (4-acetoxy styrene) of 32000 weight average molecular weight was purchased from polymer source and was tested for it CO_2 solubility. It melted and become sticky in CO_2 but was not soluble up to 70 MPa at room temperature. The insolubility of this homopolymer was not surprising. However the melting point depression is a favorable indication that this monomer is more CO_2-philic than styrene because polystyrene neither melts nor dissolves in dense CO_2.

Synthesis of Co-polymeric Thickeners

Usually the copolymers are made by the polymerization of two monomers in the presence of initiator. To synthesize copolymeric thickeners we modified the functional groups on the

commercially available polymers to our requirements. All the chemicals were from sigma-aldrich.

Synthesis of poly (vinyl acetate-co-benzoyl) copolymer (a.k.a. poly(vinyl acetate-co-vinyl benzoate)

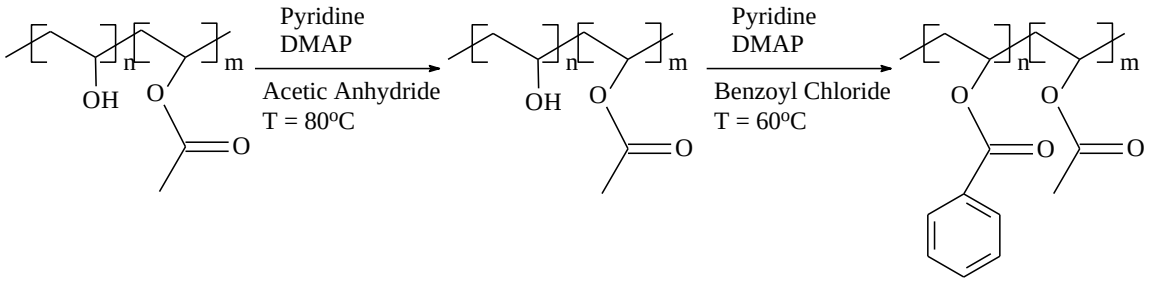

Figure 6. 5: a) Poly (vinyl alcohol) 80% hydrolyzed, b) Poly (vinyl acetate-co-vinyl alcohol) with 80% acetate groups, c) Poly (vinyl acetate-co-benzoyl)

This copolymer is made in two steps.

Step I: Making poly (vinyl acetate-co-vinyl alcohol) with 80 %acetate and 20 % alcohol groups: - Poly (vinyl alcohol) (10 gm, 6000 Mw, 80 % hydrolyzed) was dispersed in 80 ml of pyridine at 80°C. After 4 hr, acetic anhydride (16 ml, 50% excess) was added to the reaction mixture. Poly (vinyl alcohol) started to dissolve in pyridine as it acetylated. The reaction was run overnight at 80°C. Poly (vinyl acetate-co-vinyl alcohol), 80 % hydrolyzed, was obtained by precipitating the reaction mixture in water. The copolymer was further purified by dissolving it in THF and again precipitating in water. NMR showed that the polymer has about 80% acetate groups.

Step II: Adding benzene functionalized group to make thickener: - Above copolymer is dissolved in toluene. After adding pyridine, DMAP, and benzoyl chloride, the reaction mixture was stirred for 4 hr at 80°C.After that more pyridine, DMAP and acetic anhydride were added and the reaction was stirred at 80°C overnight. Polymer was obtained by precipitating the reaction

mixture in water. It was further purified by dissolving it in THF and again precipitating in water. NMR showed the polymer has about 5 % benzene functional group(Mw ~ . A copolymer with 10% benzene functional group was also synthesized.

Synthesis of poly (vinyl acetate-co-benzylformate) copolymer

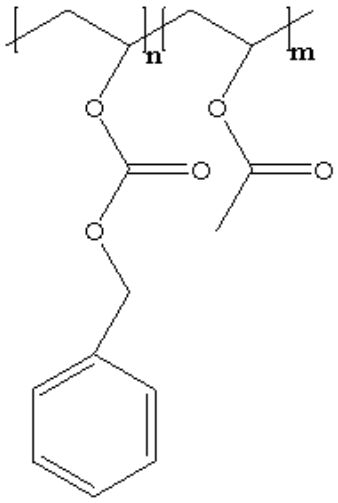

Figure 6.6: Poly (vinyl acetate co benzylformate)

The benzyl formate group is very similar to benzoyl group with the addition of $–OCH_2$ group in the side chain. Lengthening of the side chain will make copolymers more flexible and addition of oxygen will provide more sites for CO_2-polymer interactions. The same synthesis strategy that used for poly (vinyl acetate-co- benzoyl) was used to make this copolymer. Chloro benzylformate was used instead of benzoyl chloride to put aromatic group on the copolymer. Copolymer with 5% benzylformate group was synthesized and characterized by NMR.

Phase Behavior

The phase behavior curve for these copolymers in CO_2 is shown in figure 2. Poly (vinyl acetate-co-benzoyl) with 5% benzoyl group was soluble in CO_2 at 64 MPa for 3wt %. The pressure required to dissolve PVAc, of 11000 Mw and 5wt%, is around 40 MPa. As expected, the solubility of copolymer in CO_2 is decreased substantially on addition of aromatic groups. Poly (vinyl acetate-co- benzoyl) with 10% benzoyl group was not soluble in CO_2.

Poly (vinyl acetate-co-benzylformate) was soluble in CO_2 for only 0.5wt% at 63MPa

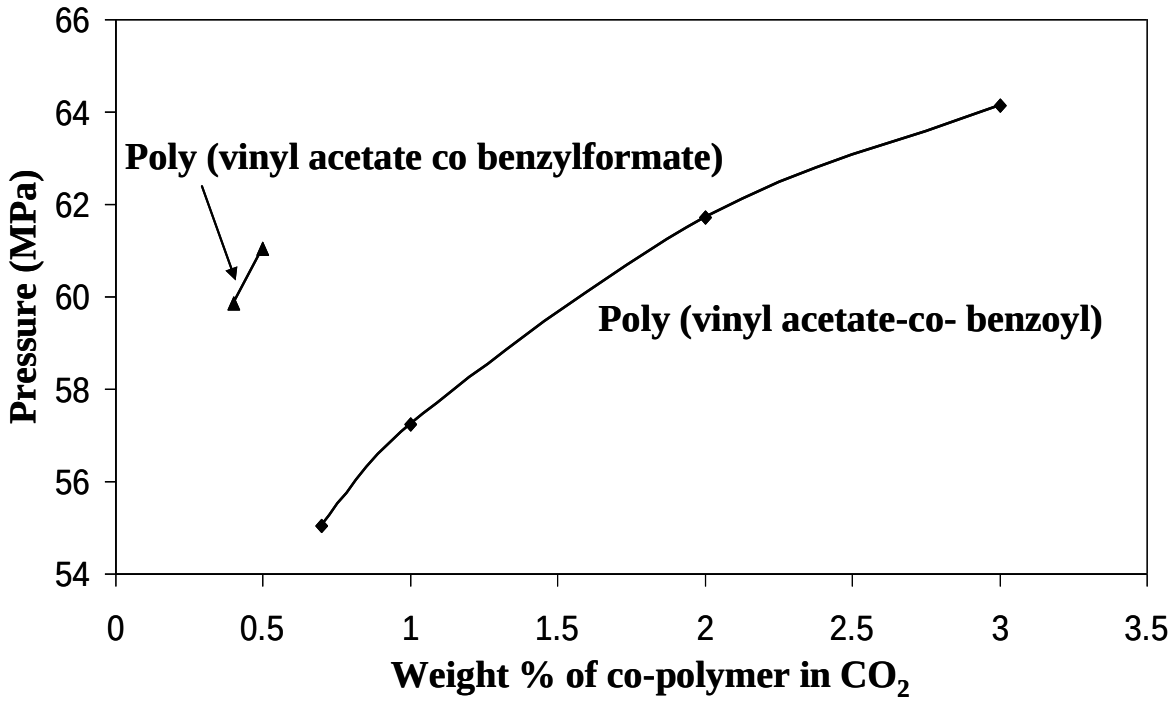

Figure 6. 7: Phase behavior of copolymers

Viscosity Measurement

Experimental setup

Falling cylinder test was used to measure the relative viscosity of a co polymeric thickener. The equipment used for phase behavior measurements (described in section 5.6).was used for this purpose. Aluminum cylinder with very smooth surfaces, height of 1 in and diameter of 1.245 in was used. This cylinder was put in the glass cell along with polymer and the system was pressurized and stirred until single phase was obtained. Once single phase is obtained stirring is stopped and cell is inverted and time taken by the cylinder to fall certain distance in measure Figure 6.8. First few centimeters of the falling cylinder are ignored to make sure that cylinder has reached its terminal velocity. This procedure is repeated about 10 times to get consistent reading. Same experiment is done for neat CO_2 also.

Relation between the velocity of falling cylinder and viscosity of the fluid is derived from Navier-stokes equation which has following assumptions:

- The cylinder and glass tube are always coaxial and concentric.
- The compressibility of fluid is low during the experiment.
- Density difference of the fluid above and below the piston is negligible
- Temperature and pressure are maintained constant during the experiment

The governing equation for the system is:

$$\eta = \kappa \frac{(\rho_c - \rho_f)}{V_t} \quad \textbf{Equation 6.1}$$

where η is the viscosity of fluid, ρ_c and ρ_f are the density of cylinder and fluid, V_t is the terminal velocity of the falling cylinder and κ is the viscometer constant which is determined by calibration by a fluid of known density and viscosity. Equation 6.1 stands good for Newtonian fluids but it can be used for non Newtonian fluids if shear rates are low and dependence of viscosity on shear is not considered. Comparison of viscosity of thickener added CO_2 and neat CO_2 gives us:

$$\frac{\eta_{solution}}{\eta_{CO_2}} = \frac{V_{CO_2}}{V_{solution}} = \frac{t_{solution}}{t_{CO_2}} \quad \textbf{Equation 6. 2}$$

where $t_{solution}$ and t_{CO2} are the time taken by the cylinder to fall particular distance through CO_2. Equation 6.2 gives us relative increase in the viscosity of CO_2 when thickener is added.

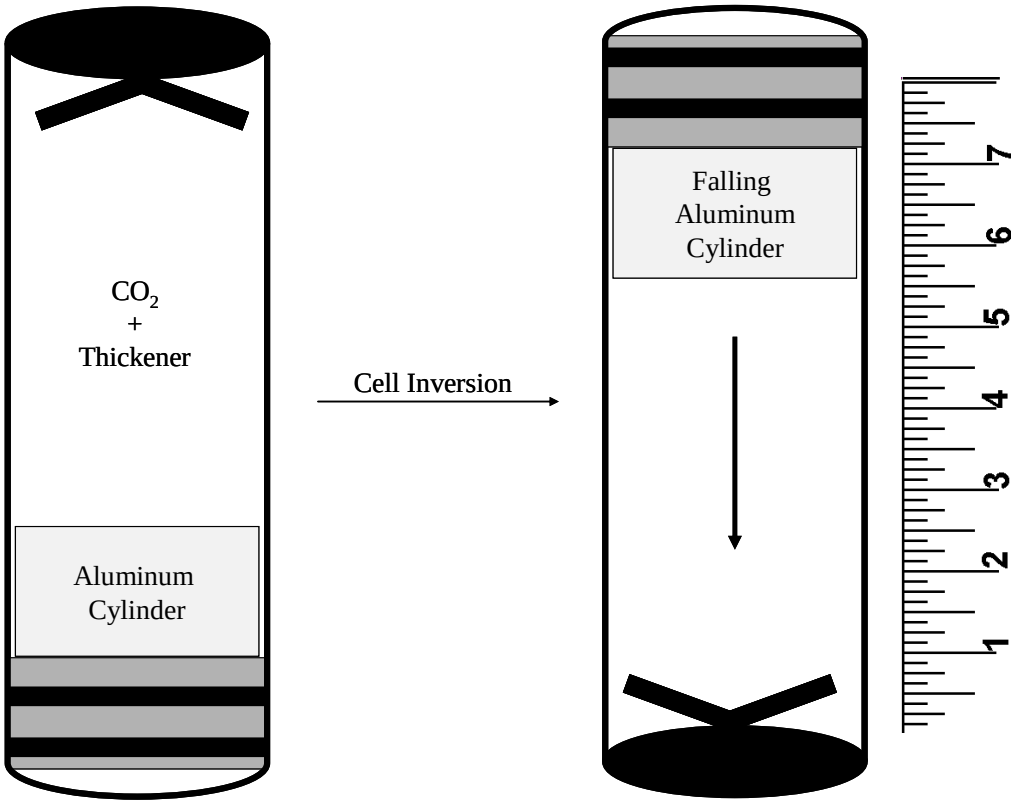

Figure 6.8: Viscosity measurement apparatus

Viscosity measurement results

Falling cylinder test results of Poly (vinyl acetate co benzoyl) and CO_2 solution for 2wt% and 1wt% at 25^{o}C and 64 MPa are shown in Figure 6.9. As a control terminal velocity of CO2 and poly (vinyl acetate), homopolymer, is measured at 25^{o}C and 63 MPa. No apparent decrease in the terminal velocity of aluminum cylinder was observed. However substantial decrease in the terminal velocity was observed for 2 wt% of Poly (vinyl acetate co benzoyl) in CO_2. As expected, terminal velocity increased when the 1 wt% of with Poly (vinyl acetate co benzoyl) was used but it was still less than pure CO_2. This result proves that benzene ring associate to generate a higher order macromolecule and produce thickening effect.

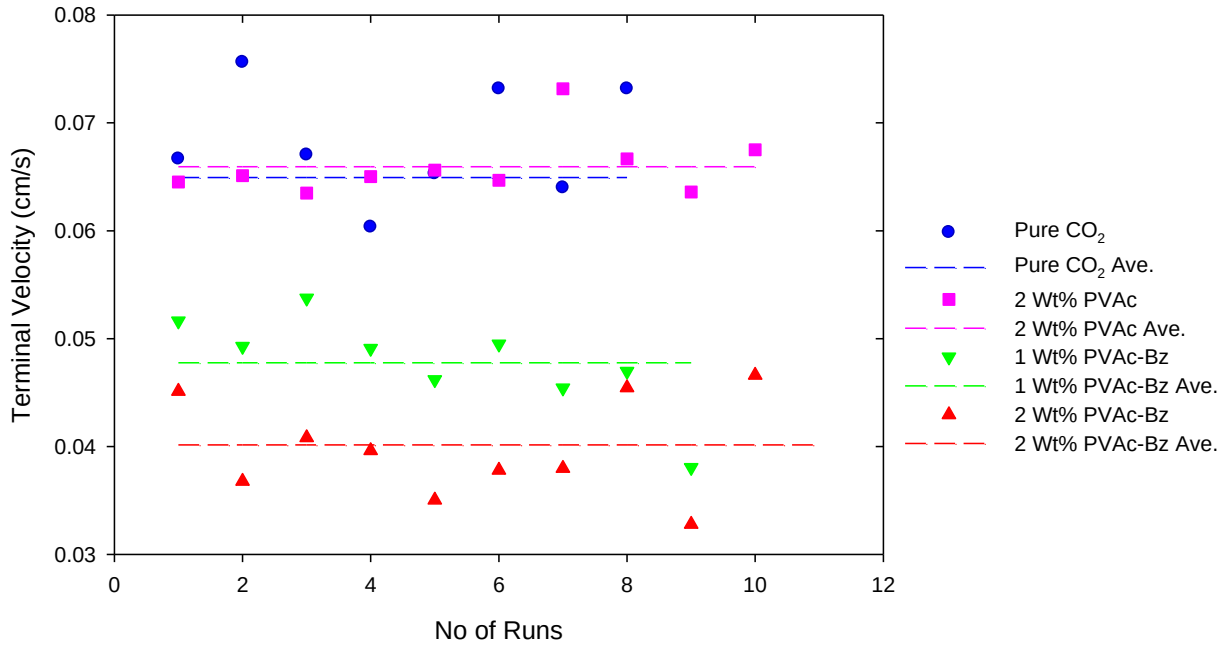

Figure 6.9: Terminal velocity of aluminum cylinder in CO_2, poly (vinyl acetate)+CO_2 solution, and CO_2+ poly vinyl acetate-co-vinyl benzoate solutions

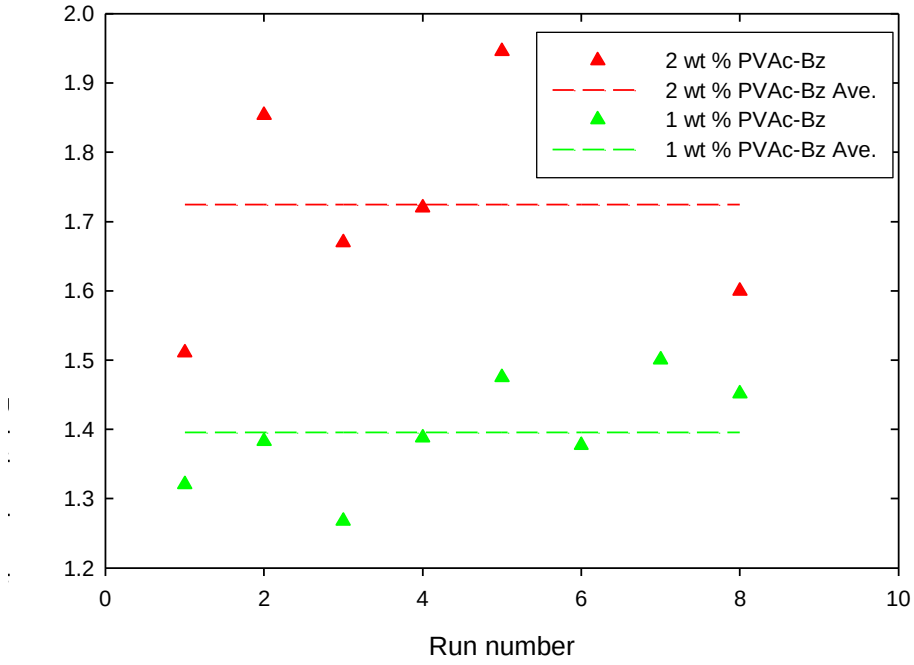

Figure 6. 10: Relative viscosity of copolymeric thickener

Using equation 6.2 relative viscosity of the co-polymeric solution was calculated and the comparison of relative viscosity increase for 2wt% and 1wt% is shown in Figure 6.10. The relative viscosity of CO_2 increased by roughly 40% at a copolymer concentration of 1wt% and 80% at 2wt% at a shear rate of ~5000 s^{-1}. **This is the first documented non-fluorous CO_2 thickener.**

CO_2 Soluble Surfactants as

Potential CO_2-in-Brine Foam Generators

Table of Contents for CO_2 Soluble Surfactants as

Potential CO_2-in-Brine Foam Generators

LIST OF TABLES

LIST OF FIGURES

1.0 INTRODUCTION

Supercritical carbon dioxide (sc-CO_2) is a potential alternative to organic solvents in many chemical processes because of its abundance, low cost, non-toxicity, non-flammability and easily accessible critical conditions (P_c = 7.38 MPa, T_c = 31.1 ^oC). Unfortunately, sc-CO_2 is a feeble solvent. Although it can solubilize low-molecular weight, volatile compounds at pressures below 10 MPa, polar and high-molecular weight materials are usually poorly soluble at tractable pressures. One strategy for enhancing the capabilities of CO_2 as a green solvent has been the identification of additives, such as surfactants,[1, 2] dispersants,[3, 4] chelating agents,[5, 6] thickeners[7] and polymers,[4, 8] that are designed to exhibit favorable thermodynamic interactions with CO_2. With regards to surfactants, nearly all conventional hydrocarbon-based ionic surfactants are essentially insoluble in sc-CO_2; however, because ionic head groups are CO_2-phobic and hydrocarbon surfactant tails are not designed for favorable interactions with dense CO_2.[9]

A number of groups began a search for CO_2-philic materials that would be soluble in CO_2 at moderate pressures. Beckman and Desimone's groups have shown experimentally that fluoralkyls,[10] fluorethers,[11] fluoracrylates,[12] and silicones [13, 14] are miscible with CO_2 at moderate pressures, while conventional alkyl functional polymers and oligomers are nearly insoluble. Ionic surfactants with CO_2-solubility of 1 wt% or more have been developed by

incorporating highly CO_2-philic fluorinated tails or silicone-based tails. For example, perfluorpolyether (PFPE) sodium and ammonium carboxylates with average molecular weights of 2500, 5000, and 7500 were soluble in supercritical CO_2 at 40 ^oC and pressures below 17 MPa.[11] Fluoroalkyl-tailed sulfosuccinate surfactants, such as di-CF3, di-CF4, and di-CF6 stabilized microemulsions at CO_2 bottle pressure (5.7 MPa) at 15 ^oC, with a W value ([water]/[surfactant]) of 10.[15] Silicone-based ionic surfactants, such as PDMS-based AOT analogue can dissolve in CO_2 at 65 ^oC and pressures below 31 MPa.[16, 17] Although these surfactants have been used successfully in supercritical fluid research such as emulsion polymerization, dispersion polymerization, and extraction, the environmental and biological persistence of these expensive fluorous and silicone-based surfactants (approaching $1/gram) has impeded their use in commercial applications, especially for large-scale applications in which the surfactant will be lost to the environment, such as enhanced oil recovery (EOR). Less expensive, biodegradable, CO_2-soluble surfactants composed of carbon, hydrogen, and oxygen would hasten the practical applications of CO_2 as a processing solvent.

2.0 BACKGROUND

2.1 PROPERTIES OF SUPERCRITICAL/LIQUID CO_2

A supercritical fluid (SCF) is a substance elevated above its critical temperature (Tc) and pressure (Pc). The critical temperature is defined as the temperature above which a pure, gaseous compound cannot be liquefied regardless of the pressure applied. The critical pressure is then defined as the vapor pressure of the gas at the critical temperature. The temperature and pressure at which the gas and liquid phases become identical is the critical point. In the supercritical region, only one phase exists; the supercritical fluid, as it is termed, is neither a gas nor a liquid and is best described as intermediate to the two extremes. A comparison of typical values for density, viscosity, and diffusivity of gases, supercritical fluids, and liquids is presented in Table 2.1.[18] Supercritical fluids have a density close to liquids, a viscosity close to gases, and a high diffusivity, which retain the solvent power common to liquids as well as the transport properties common to gases.

As carbon dioxide is the most commonly used SCF, the pressure-temperature phase diagram for carbon dioxide is presented in Figure 2.1 to illustrate the differences between the gas, liquid, and supercritical states. The critical point is marked at the end of the gas-liquid equilibrium curve, and the supercritical fluid region is indicated by the shaded area. CO_2 attains its supercritical state at near-ambient temperature (Tc=31 ^{o}C) and relatively moderate pressure

(Pc=7.4 MPa). Supercritical CO_2 (sc-CO_2), like all other supercritical fluids, offers many mass transfer advantages over conventional organic solvents due to its gas-like diffusivity, low viscosity, and negligible surface tension.

Table 2.1. Comparison of density, viscosity, and diffusivity of gases, supercritical fuids, and liquids.[18]

Property	Gas	Supercritical Fluid	Liquid
Density (g/ml)	0.001	0.1 – 1	1
Viscosity (cp)	0.01	0.05-0.1	0.5-1
Diffusivity (mm^2/s)	1-10	0.01-0.1	0.001

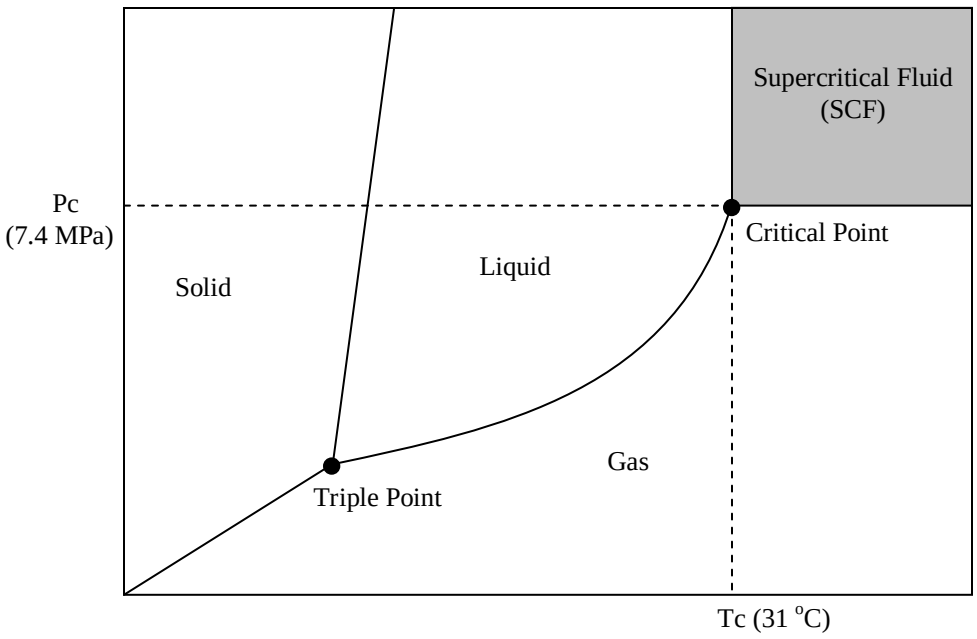

Figure 2.1. Pressure-temperature diagram for pure CO_2, showing the solid, liquid, gas, and supercritical regions.

Supercritical CO_2 has many properties that make it an interesting solvent; it is abundant, inexpensive, nontoxic, and nonflammable. It has been proposed as a green alternative to traditional organic solvents because it is not regulated as a volatile organic chemical (VOC). Moreover, supercritical fluids have a tunable solvent power, which increases as a function of increasing density.[19] As a result, the solvent power of supercritical CO_2 can be easily tuned simply by adjusting the operating temperature and/or pressure, which in turn affects the density of the supercritical CO_2. In addition to the tunable solvent power, a number of other physical properties such as dielectric constant, viscosity, and diffusivity change significantly near the critical point.[20, 21] One interesting characteristic of supercritical fluids is the extremely low surface tension possessed as a result of the gas-like transport properties of viscosity and diffusivity.[22] This imparts supercritical fluids the ability to easily penetrate very small surface areas and contributes to their attractiveness for extraction of solutes from porous media.[21] A particularly attractive advantage of using supercritical CO_2 is that the solvent can be removed by simply decompression. It is worth noting that liquid CO_2 can sometimes be used in the place of sc-CO_2 in certain procedures. Near the critical point, liquid CO_2 has many of the similar properties of the supercritical fluid and can be achieved at milder conditions. Overall, CO_2 has a great potential to be a valuable process solvent.

There is one major drawback to supercritical/liquid CO_2 as a solvent. CO_2 has an extremely low polarizability/volume ratio (a parameter to estimate solvent power) and hence is a somewhat feeble solvent for many polar and nonpolar compounds, although it can dissolve many small molecules.[23] It was once believed that CO_2 had solvent properties similar to those of hexane based on solubility parameters calculations, but in fact, Mcfann et al. have shown that the quadrupole moment of CO_2 serves to inflate the calculated solubility parameter by 20%.[24, 25]

Consequently, using the solubility parameter as a sole determination of solubility could be misleading. The polarizability/volume has been suggested as a better parameter on which to estimate the solvent power of CO_2, but the polarizability/volume of CO_2 indicates that it is a weak solvent.[25] Other properties of CO_2 include low polarizability and electron accepting capacity, since CO_2 is a Lewis acid and can participate in Lewis acid: Lewis base interactions. Fourier transform infrared (FTIR) spectroscopy has been used to show that CO_2 interacts with polymers containing electron-donating functional groups[26] and Lewis bases.[27] Specific interactions resulting from quadrupole-dipole interactions between CO_2 and certain polymers are also believed to influence solubility.[28, 29] O'Neill et al. suggest that cohesive energy density (CED), reflected by surface tension, of a polymer determines solubility in CO_2.[30]

2.2 SURFACTANTS

A surfactant (surface active agent) is an amphiphilic molecule containing both hydrophilic head group and lipophilic tail group. Typically, the hydrophilic head contains groups like water such as sulfonates, sulfates, and phosphonates while the lipophilic or hydrophobic tail group consists of a hydrocarbon chain. Figure 2.2 represents the structure of a common surfactant consists of a hydrophilic head group and a hydrophobic tail group.

The polar or ionic portion is solvated by water as a result of strong dipole-dipole or ion-dipole interactions. It is therefore said to be hydrophilic, and often simply called the head group. The hydrocarbon chain of the surfactant is typically called hydrophobic because of the hydrocarbon section's minimal interaction with the water in an aqueous environment.

Furthermore, the strong attractions between water molecules, arising from dispersion forces and hydrogen bonding, act to force the hydrocarbon out of the water. Since the nonpolar, hydrophobic part is usually an elongated alkyl chain, it is often simply called the tail. The balanced properties of both the hydrophilic and hydrophobic portions of surfactants combine to give the unique properties commonly associated with surface active agents.

Surfactants can be classified according to the charge present in the hydrophilic portion of the molecule (after dissociation in aqueous solution): anionic, cationic, nonionic, and amphoteric surfactants. Typically, these four kinds of surfactants are composed of similar lipophilic or hydrophobic tail group, such as a long hydrocarbon chain, however with different hydrophilic head groups.

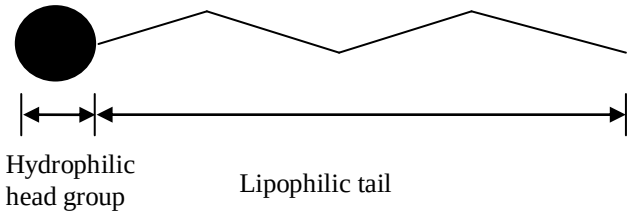

Figure 2.2 Example of a basic surfactant structure

AOT (Aerosol-OT, bis(2-ethyl-1-hexyl) sodium sulfosuccinate), as an anionic surfactant, has been extensively utilized and investigated in numerous alkane solvents for the formation of reverse micelles due to its ability to disperse large amount of water. The structure of AOT is shown in Figure 2.3. The rich phase behavior of AOT, and its ability to form microemulsions, is

often attributed to its twin hydrocarbon tails which impart a cone-like structure and encourage the molecule to pack into spherical aggregations.

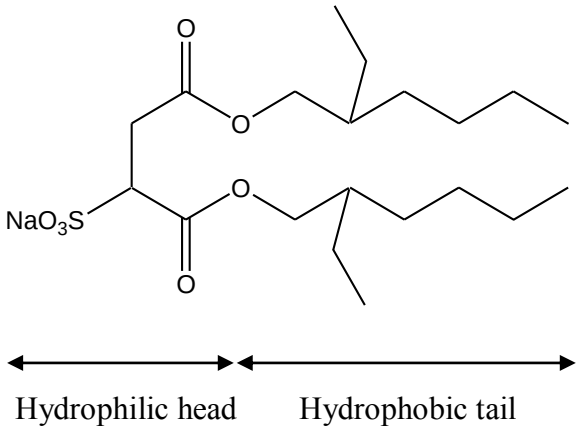

Figure 2.3. Structure of AOT (Aerosol-OT, sodium bis(2-ethyl-1-hexyl) sulfosuccinate)

2.3 CO_2-SOLUBLE SURFACTANTS

Sc-CO_2 is a feeble solvent, although it can solubilize low-molecular weight, volatile compounds at pressures below 10 MPa, polar and high molecular weight materials are usually poorly soluble at tractable pressures. One strategy to broaden the range of applications of CO_2 as a green solvent has been the identification of additives, such as surfactants,[1, 2] dispersants,[3, 4] chelating agents,[5, 6] thickeners[7] and polymers,[4, 8] that are designed to exhibit favorable thermodynamic interactions with CO_2. With regards to surfactants, nearly all conventional hydrocarbon-based ionic surfactants are essentially insoluble and could not form microemulsions in sc-CO_2; however, because ionic head groups are CO_2-phobic and hydrocarbon surfactant tails are not designed for favorable interactions with dense CO_2.[9] A CO_2-soluble surfactant would

be amphiphilic, like a traditional surfactant, but instead of hydrophilic and lipophilic segments, it would contain CO_2-philic and CO_2-phobic segments. Once the CO_2-philic portion of the surfactant has been identified, the CO_2-phobic segment can be chosen from conventional hydrophilic or lipophilic groups. The structure of a CO_2-soluble surfactant is presented in Figure 2.4.

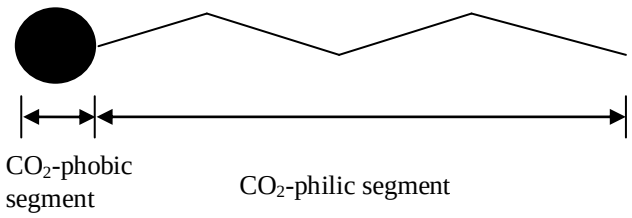

Figure 2.4. Example of a CO_2-soluble surfactant structure

Development of CO_2-philic surfactants has been a target of researchers for many years. Functional CO_2-soluble surfactants would allow the feeble solvent nature of CO_2 to be enhanced by the formation of a microemulsion with a polar water domain which can favorably dissolve polar solutes and high molecular weight molecules. The concept of a nm-scale water pool dispersed in CO_2 find applications in a variety of reaction chemistry and material synthesis.[31-34]

2.4 FLUORINATED AND SILICONE-BASED CO_2 SOLUBLE SURFACTANTS

Preliminary studies by Consani and Smith have shown that most conventional surfactants are insoluble in CO_2. They studied over 130 commercially available surfactants, among which only a few nonionic exhibited reasonable solubility in CO_2 [9]. Focus was then being given to fluorinated and silicone compounds as effective CO_2-philic agents. Followed the finding by Iezzi

et al. that fluorocarbons and CO_2 are compatible,[35] Beckman and Desimone's groups have shown experimentally that fluoalkyls,[10] fluoethers,[11] fluoacrylates,[12] and silicones [13, 14] are miscible with CO_2 at moderate pressures, while conventional alkyl functional polymers and oligomers are nearly insoluble. The fluorinated and silicon chains represent low cohesive energy density groups thereby promoting low solubility and low polarizability, which are more characteristic of carbon dioxide's properties. The structures of fluorinated and silicone CO_2-philes are shown in Figure 2.5, and these molecules have been used in the design and synthesis of surfactants for applications in CO_2. Ionic surfactants with CO_2-solubility of 1 wt% or more have been developed by incorporating highly CO_2-philic fluorinated tails or silicone-based tails.

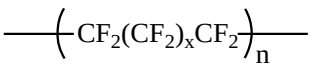

Fluoroalkyl

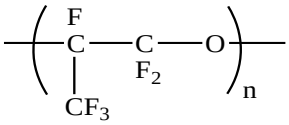

Fluoether

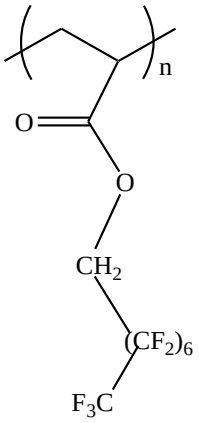

Fluoroarcylate

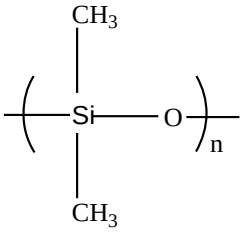

Silicone

Figure 2.5. Structures of fluorinated and silicones CO_2-philic functionalities.

Fluoroalkyls: Fluorocarbon-Based Ionic surfactants

Based on the fact that the fluorocarbons and CO_2 are compatible, Hoefling et al. designed the first effective fluoro-surfactants for CO_2, the pioneering work demonstrating solubility of a fluorinated analogue to AOT in CO_2.[10] Harrison et al. reported the first water-in-CO_2 (w/c) microemulsion using a double chain hybrid surfactant comprising of separate fluororocarbon and hydrocarbon chains: $(C_7F_{15})(C_7H_{15})CHOSO_3^-Na^+$ or F7H7. Water up W of 32 could be stabilized in w/c microemulsion at 35 ^oC, 26.2 MPa, and surfactant concentration of 1.9 wt%.[36] In 1997, Eastoe et al. launched a study of fluoroalkyl analogues to AOT. Twelve different linear chain fluoroalkyl AOT analogues were investigated, of which nine stabilized w/c microemulsions at 15 ^oC and CO_2 bottle pressure (5.7 MPa), with a W value of 10; these were di-HCF4, di-HCF6, di-CF3, di-CF4, di-CF6, di-CF4H, di-CF6H, di-CF4GLU and the cobalt salt of Co-HCF4.[37]

Fluoroethers: PFPE-Based Ionic Surfactants

In 1993, perfluoropolyether (PFPE) sodium and ammonium carboxylates with average molecular weights of 2500, 5000, and 7500, were reported to be soluble in liquid CO_2 up to 10 wt% at 40 ^oC and pressures below 17 MPa.[11] However, these high molecular weight polymers were not effective for stabilizing w/c microemulsions. Later, Johnston et al. formed w/c microemulsion with a PFPE ammonium carboxylate ($PFPE\text{-}COO^-NH_4^+$) surfactant of only 740 M_W.[38] Success with this class was attributed to the chemical structure itself. PFPE constitutes an extremely CO_2-philic tail group, accentuated by the presence of pendant fluoromethyl groups, which tend to increase the volume at the interface on the CO_2 side and thus favor curvature around water.

Fluoroacrylates: PFOA Block Copolymer Nonionic Surfactants

Fluorinated acrylate polymer, poly(1,1-dihydroperfluorooctylacrylate) or PFOA, was obtained from homopolymerization in sc-CO_2 at 60 ^oC and 20.7 MPa, with molecular weight of 270,000.[12] Small angle neutron and scattering (SANS) investigations of dilute solutions of PFOA in CO_2, over a wide range of temperatures and pressures, provided clear evidence for favorable interaction between PFOA and CO_2.[39] PFOA contains a lipophilic, acrylic backbone, and a CO_2-philic segment, rendering it amphiphilic, thus it can be used as a surfactant without modification. McClain et al used PFOA as the CO_2-philic segment of a nonionic surfactant, where PFOA was copolymerized with a CO_2-insoluble polystyrene (PS) segment to form a block copolymer of PFOA-b-PS. The micelles formed by PFOA-b-PS were used to solubilize CO_2-phobic hydrocarbon oligomers.[40] Copolymers composed of PFOA and poly(ethylene oxide) (PEO) were also able to form micelles in CO_2, in which small amount of water was able to be stabilized.[41]

Silicones: PDMS

For applications in CO_2, silicones are generally considered less effective than their fluoroinated counterparts. Solubility of poly(dimethyl siloxane) (PDMS) in CO_2 was first reported in 1996. At a level of 4 wt%, PDMS (Mn~13,000) is soluble in CO_2 at 35 ^oC and 27.7 MPa.[30] Block copolymer surfactants consisting of CO_2-philic PDMS and CO_2-phobic poly(methacrylic acid) (PMA) or poly(acrylic acid) (PAA) were used to form water-in-CO_2 (w/c) and CO_2-in-water (c/w) emulsions.[17] Recently, Fink's research in silicone-based ionic surfactants pointed that a PDMS-based AOT analogue can dissolve in CO_2 at 65 ^oC and and pressure below 31 MPa up to 1 wt%.[16]

Although these surfactants have been used successfully in supercritical CO_2 research, the environmental and biological persistence of these expensive fluorous and silicone-based surfactants (approaching $1/gram) has impeded their use in commercial applications, especially for large-scale applications in which the surfactant will be lost to the environment, such as enhanced oil recovery (EOR). The development of CO_2-soluble surfactants, which are composed of carbon, hydrogen, and oxygen, biodegradable and less expensive, would hasten the applications of CO_2, as they could represent significant advantages over the biological persistent and high-cost fluorinated or silicone counterparts.

2.5 OXYGENATED HYDROCARBON AND HYDROCARBON-BASED CO_2 SOLUBLE SURFACTANTS

2.5.1 Design of Oxygenated Hydrocarbon and Hydrocarbon-Based CO_2 Soluble Surfactants

Experimental results from several research groups have shown that the incorporation of CO_2-philic functionalities into the structures of surfactants, dispersants, and chelating agents has greatly enhanced their solubility, making it possible to use CO_2 for polymerization [4, 8], metal extraction [5, 6] and other more sustainable processes. It must be noted that combining a CO_2-philic tail to a conventional head group does not ensure the resultant surfactant will also exhibit CO_2-solubility, or that will be effective in the proposed application if it is solubility. CO_2 solubility is a necessary but insufficient property of the candidate surfactant. The interactions

between the tail and CO_2 must be strong enough to impart CO_2-philicity to a compound that contains a CO_2-phobic segment.

The characteristic of hydrocarbons most commonly associated with enhanced CO_2-solubility is the presence of polymer side chains [42] or a high degree of branching [43]. This enhanced solubility is usually attributed to the increased polymer free volume and the diminished intermolecular interactions [43]. Recently, Stone and Johnston found that the interaction between CO_2 and CH_2 is about the same as CO_2 and CF_2.[44] A level of 1 wt% surfactant soluble in CO_2, which would typically be needed for microemulsions, requires a moderate high, yet reasonable pressure. Clearly, solubility is a key factor that governs whether a surfactant will lead to water-in-CO_2 microemulsions. An additional factor, steric force, which plays an important role in designing hydrocarbon surfactants for w/c microemulsions, has been described recently. Stubby tails enhance the formation of w/c microemulsions as they raise surfactant solubility in CO_2 by weakening interactions between tails, weaken interactions between droplets, favor curvature of the interface bending toward water, and reduce the interfacial tension.[44-46] Ryoo and Johnston achieved about 1 wt% water, significant protein solubilities, and the presence of microemulsions as detected with dynamic light scattering formed by a methylated branched hydrocarbon nonionic surfactant. Furthermore, this study shows that the surfactant lowers the water-CO_2 interfacial tension significantly, which is an important requirement for forming microemulsions.[46]

2.5.2 Oxygenated Hydrocarbon and Hydrocarbon-Based CO_2-Philic Functionalities

Several oxygenated hydrocarbon and hydrocarbon-based groups previously shown to exhibit CO_2-philicity include acetylated sugars, poly (propylene oxide), acetate-rich compounds, and short alkyl group with t-butyl tip. These CO_2-philes are illustrated in Figure 2.6.

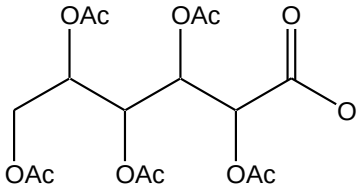

(a) per-acetylated glucose (Ac=$COCH_3$)

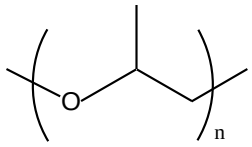

(b) Poly(propylene oxide)

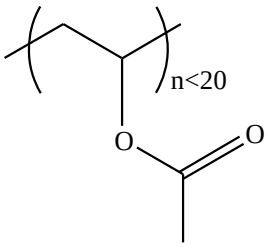

(c) Oligo(vinyl acetate)

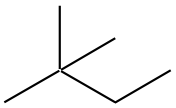

(d) Short alkyl group with tert-butyl tip

Figure 2.6. Oxygenated hydrocarbon-based and hydrocarbon-based CO_2-philic groups

Per-acetylated sugars

The replacement of the proton of every hydroxyl group (-OH) with an acetate group (-OCOCH3) can dramatically enhance the CO_2-philicity of sugar molecules. Acetylated sugars, such as per-acetylated glucose and galactose,[47] sorbitol,[48] maltose[49] and cyclodextrins,[50] have been shown to dissolve in CO_2 at low pressures up to 10-50 wt%. The high degree of CO_2 solubility has been attributed to a favorable two-point interaction between

CO_2 and the accessible acetate side chain, a Lewis acid–Lewis base interaction between the C of the CO_2 and the O of the acetate carbonyl, and a weak, complimentary hydrogen bond between the O of the CO_2 and a proton on the methyl group of the acetate,[51, 52] as shown in Figure 2.7.

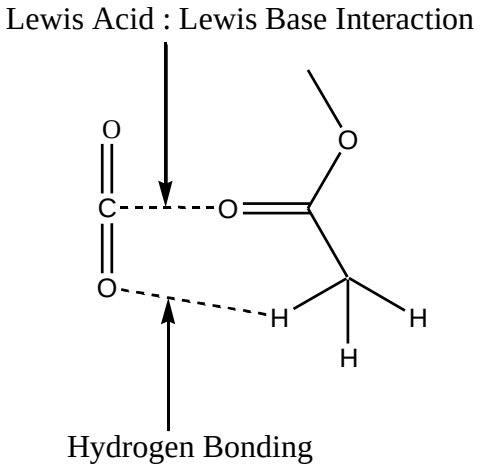

Figure 2.7. Two point interaction between CO_2 and acetate

Poly(propylene oxide) (PPO)

Low molecular weight PPO (Mn<2000) is quite CO_2-soluble at moderate temperature,[30] and higher MW PPO (>2000) is also soluble in CO_2 at elevated temperatures.[53] The solubility of the PPO oligomers has been attributed to the Lewis acid–Lewis base interaction between the carbon in CO_2 and the ether oxygen in poly(propylene oxide),[54] and the lower surface tension caused by the pendent methyl group on each monomer unit favoring solvation by CO_2.[30] The lowering of the interfacial tension at the water-CO_2 interface, emulsion formation and solubilities of block copolymers containing PPO segment were

reported.[30, 55] PPO has been used as a CO_2-philic segment in di-block and tri-block nonionic surfactants along with hydrophilic blocks of poly(ethylene oxide) (PEO).[56-59] For example, the tri-block nonionic surfactant, $(PO)_{15}(EO)_{10}(PO)_{15}$, composed of two CO_2-philic propylene oxide oligomers, and a single hydrophilic ethylene oxide oligomers, exhibit CO_2 solubility up to 0.6 wt% below 30 MPa at 25 ^oC.[59] Other CO_2 soluble nonionic triblock surfactants include those contain an alkyl group, an ethylene oxide block and a propylene oxide block, such as $C_{12}H_{25}$-$(EO)_3(PO)_6$-OH, which is 1 wt% soluble in CO_2 at 35–45 ^oC and pressures below10-15 MPa.[57]

Poly(vinyl acetate)

McHugh and coworkers were the first to note that poly(vinyl acetate) demonstrated remarkable solubility in dense CO_2.[29] Recently, poly(vinyl acetate) has been identified as the most CO_2 soluble, high molecular weight, oxygenated hydrocarbon-based homopolymer composed of solely of carbon, hydrogen and oxygen; however, only short oligomers of PVAc, $n<20$ are likely to be soluble in CO_2 at pressure below moderate pressure (35 MPa), as shown in Figure 2.8.[53] The interactions between poly(vinyl acetate) and CO_2 are similar to those of per-acetylated sugars and CO_2.

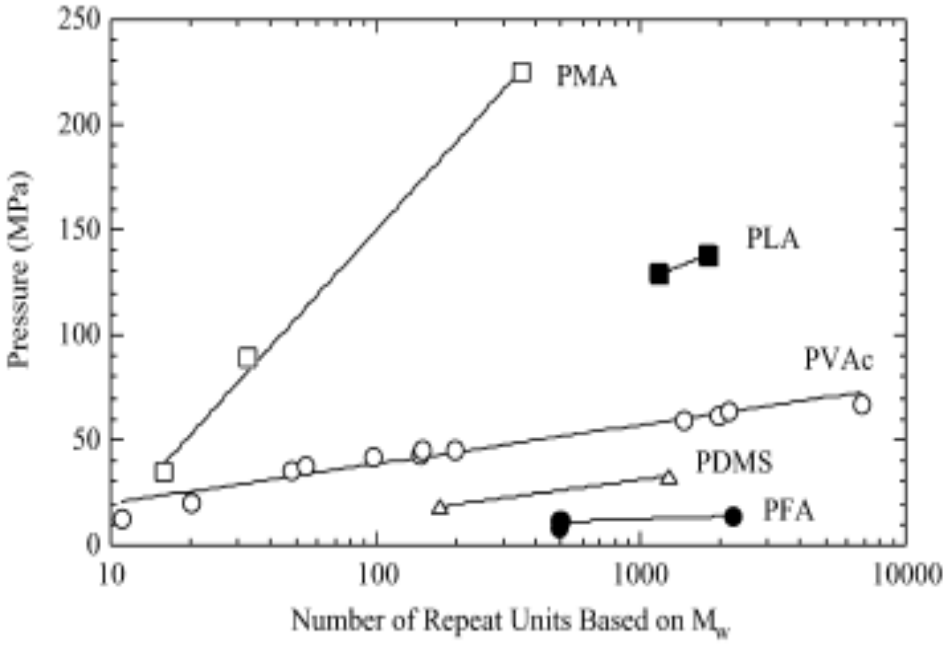

Figure 2.8. Cloud point pressure at ~ 5 wt% polymer concentration and 25 ^{o}C for binary mixture of CO_2 with poly(methyl acrylate) (PMA), poly(lactide) (PLA), poly(vinyl acetate) (PVAc), poly(dimethyl siloxane) (PDMS), and poly(fluoroalkyl acrylate) (PFA) as a function of number of repeat units based on Mw.[53]

Short Alkyl Chain with t-Butyl Tip

Recently, Eastoe and Johnston[60-62] described two branched hydrocarbon-based ionic surfactants, sodium bis(2,4,4-trimethyl-1-pentyl) sulfosuccinate and sodium bis(3,5,5-trimethyl-1-hexyl) sulfosuccinate, that exhibit CO_2 solubility. These twin tailed sodium succinates are similar in structure to the CO_2-insoluble surfactant AOT, sodium bis(2-ethyl-1-hexyl) sulfosuccinate, but they contain trimethyl pentyl or trimethyl hexyl tails and are referred to as AOT-TMP and AOT-TMH, respectively. This is illustrated as the "short alkyl chain with t-butyl tip" in Figure 2.6. AOT-TMH has been reported 0.1 wt% solubility in CO_2 at 40 ^{o}C, 50 ^{o}C, and

80 ^{o}C at 34.5 MPa, 31MPa, and 29 MPa, respectively.[62] Even though there are no specific sites for strong CO_2-alkyl interactions in this system, the favored solvation of the branched tail surfactants by CO_2 may be attributable to the surface energy of the pendant methyl groups being much lower than that of the CH_2 groups of linear tails.[30] Further, it was found the high degree of chain tip methylation do form water-in-carbon dioxide (w/c) reverse micelles [61].

2.6 MICELLES AND MICROEMULSIONS

Surfactants reduce interfacial tension and aid in the solubilization of hydrophobic compounds into hydrophilic solvents, or vice versa. A micelle or a microemulsion droplet is an aggregation of surfactant molecules, which can only form when the surfactant concentration is greater than the critical micellar concentration (CMC). Depending on the nature of the continuous phase, the micelles formed are termed oil-in-water (o/w, for a bulk water phase with dispersed organic phase) or water-in-oil (w/o, for a bulk organic phase with dispersed water phase). Water-in-CO_2 microemulsion (w/c) is formed for bulk CO_2 with dispersed water phase. The structure of typical oil-in-water (o/w) micelle is shown in Figure 2.9 a, in which the hydrophilic segment interacts with the aqueous phase and the lipophilic segment is oriented to interact with the organic phase. The opposite structure of water-in-oil (w/o), or water-in-CO_2 (w/c), called reverse micelle, is also formed whereby the lipophilic tail interacts with the continuous organic phase and the hydrophilic heads are directed to the core of the micelle, thus interacting with the aqueous phase, as shown in Figure 2.9 b. Micelles can exist in different shapes, including spherical, cylindrical, hexagonal, or lamellar.

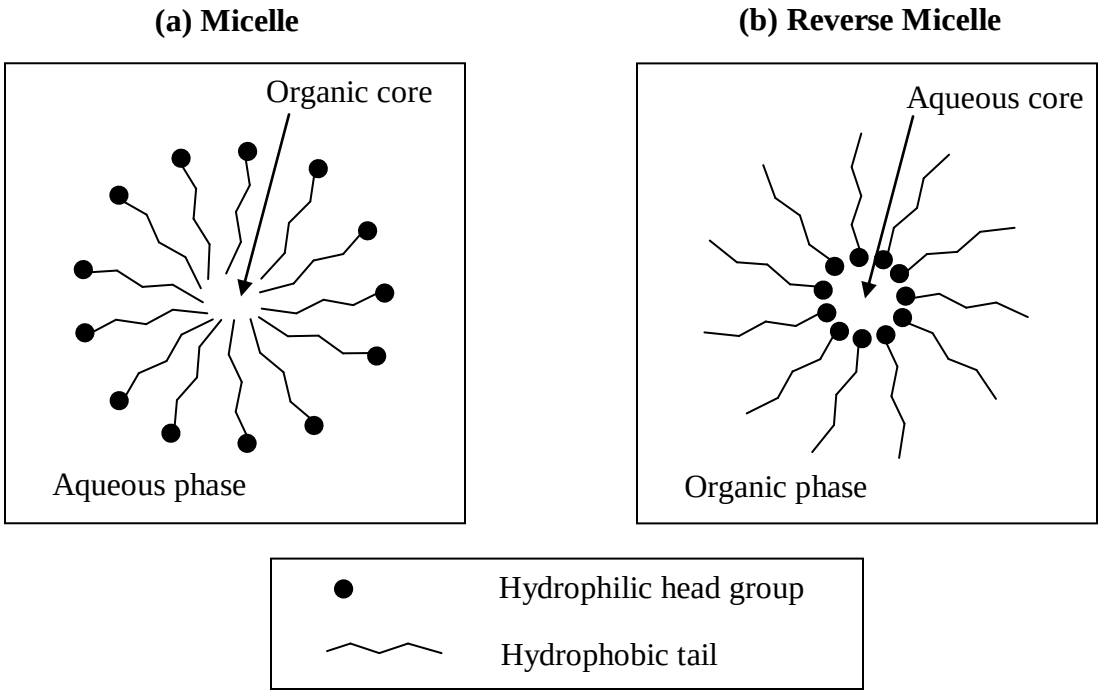

Figure 2.9. Representation of a micelle and a reverse micelle.

System containing micelles is referred to as emulsion, which is a dispersion of one liquid in another. Microemulsions are special kind of emulsions, which are thermodynamically stable and optically transparent, with the dispersed liquid droplets dimensions less than 100 nm. It has been long established that hydrophilic-hydrophobic balance plays a crucial role in the formation and stability of colloidal dispersions and self-assembly structures. An important efficiency factor for a surfactant to form water-in-CO_2 microemulsion is the water uptake W, defined as the molar ratio of water loading to the surfactant, which is highly dependent on the surfactant type and nature of the CO_2-philic chains, as well as CO_2 pressure and temperature. Another measure of efficiency is the minimum pressure that requires keeping the dispersion a stable single

transparent phase. Above this pressure the surfactant is able to stabilize w/c microemulsion, whereas below this pressure a phase separation occurs.

The formation of microemulsions in a scf continuous phase was first reported by Smith and co-workers using AOT in sub- and supercritical alkanes.[63] Since then, interest in surfactant/scf has grown steadily and produced a wide variety of research aimed at characterizing and applying these systems.[63-65] The most commonly used alkanes to form the scf continuous phase have been ethane and propane.[64] However, interest in using more environmentally benign solvents in chemical processes has pushed the forefront of surfactant/scf systems and formation of microemulsions to include CO_2 as the continuous phase.[61, 62, 66]

One interesting feature in the formation of water-in-CO_2 microemulsions is the creation of a nanosized water pool in a bulk CO_2 phase. The concept of a nano-scale water pool dispersed in CO_2 is particularly interesting in that there is tremendous potential for chemical applications. For example, the low viscosity (high diffusivity) of a scf makes scf-based microemulsions particularly attractive as separation media. Also, water pools formed in CO_2 find applications in a variety of reaction chemistry and material synthesis. The advantages of using sc-CO_2 to carry out these processes lies in one's ability to achieve more specific or selective control over separation and/or reactivity via the tunable solvent property. By changing the system pressure, one can selectively tune droplet-droplet interactions, thereby directly influencing the chemistry that takes place within the water domain.

Characterizations of Microemulsions

Various probing techniques such as FTIR, UV-vis, X-band electron parametic resonance (EPR), and time-resolved fluorescence depolarization have been used to characterize the nature

of the PFPE/CO_2 reverse micelles. EPR identified the micelle as having a bulk-like water core able to solvate ionic species while time-resolved fluorescence depolarization revealed an anisotropic/nonspherical reverse micelle.[67] FTIR and UV-vis spectroscopy by Johnston and coworkers[68, 69] showed that the w/c microemulsion consists of regions of "bulk" hydrogen bonded water, "interfacial" water, and "free" water dissolved in sc-CO_2. The UV-vis spectroscopic studies using methyl orange as a probe indicated that the PFPE/sc-CO_2/water reverse micelle cores have a polar environment as seen in dry PFPE reverse micelles, a bulk-like water region, and an acidic environment resulting from carbonic acid formation. Additionally, Lee et al.[70] observed the interaction strength between the droplets to be larger in water-in-CO_2 relative to water-in-oil microemulsions due to stronger tail-tail interactions resulting from the weak solvation by CO_2. As a result, it is more difficult to overcome droplet interactions to produce stable microemulsions. Lastly, SANS measurements performed by Zielinski et al.[71] show evidence of water-in-CO_2 microemulsion with a droplet radius ranging from 20 to 36 A.

2.7 APPLICATIONS OF SURFACTANTS IN CARBON DIOXIDE

Carbon dioxide is desirable as a process solvent because of its "green" characteristics and it has been considered as a replacement for organic solvents in numerous technologies, such as the production of nanoparticles, polymer processing, chemical reactions, and extractions due to the development of CO_2 soluble surfactants specifically for each application.

2.7.1 Nanoparticle Formation

There is a growing interest in the preparation of nanoparticles for use as catalysts, pharmaceuticals, sensors, semiconductors, optical materials, and others. Current techniques for producing nanoparticles involve harsh process conditions and do not provide adequate control over particle characteristics. Recently, CO_2 has been extensively investigated as a pressure-

tunable reaction medium for the manufacture of nanoparticles. Changes to CO_2 solvent properties through manipulation of the pressure can affect the growth rate of nanoparticles, their final size, and their size distribution, allowing fine control over nanoparticles. Several modes of nanoparticle synthesis have been explored in CO_2.

Nanoparticle Formation in w/c Microemulsions

One method provides for the formation of nanoparticles within w/c microemulsions by reducing metal salts dissolved in the nano aqueous core and has been demonstrated for copper,[33] silver,[33, 72-74] and palladium.[34] This technique employs CO_2-philic perfluoropolyether (PFPE) surfactants in order to form reverse micelles in CO_2 with a water core into which CO_2-phobic polar species (metal salts) can dissolve. Typically, by using this strategy, metallic nanoparticles having diameters from 2−15 nm were synthesized and stabilized in the water-in-CO_2 microemulsions formed by PFPE surfactants. In nanoparticle formation, a metal ion is introduced into a reverse micelle. A reducing agent within the CO_2 continuous phase diffuses into the micelle, reducing the metal ions to form very small metal particles. The inter-micellular exchange of the metal particles solubilized within the core of the micelles allows for the particles growth by the aggregation and coalescence of the very small particles. The particle growth continues until the particles reach a terminal size determined by the system and where the surfactant aids in stabilization of the particles.

The substitute of oxygenated hydrocarbon-based or hydrocarbon-based surfactants for fluorinated surfactants in the applications of nanoparticle formation in w/c microemulsion would mitigate the problems associated with the environmental and biological persistence associated with fluorinated surfactants. One of the objectives of this study was to design, synthesize, characterize, and evaluate the CO_2 solubility of ionic surfactants with oxygenated hydrocarbon

tails composed of acetylated sugar, PPO, or oligo(vinyl acetate). Additionally, these surfactants were examined for their ability to form stable microemulsions with polar microenvironments capable of dissolving polar species in the bulk non-polar CO_2 solvent.

Nanoparticle Formation via Reducing CO_2-Soluble Organometallic Precursors

An alternative technology forgoes the formation of the reverse micelles, and instead employs the reduction of fluorinated, CO_2-soluble organometallic precursors of Ag(1,1,1,5,5,5-hexafluoropentane-2-,4-dione)(tetraglyme) [Ag(hfpd)(tetraglyme)], palladium(II) hexafluoroacetylacetonate [$Pd(hfac)_2$],[75] and triphenylphosphine gold(I) perfluorooctanoate [TPAuFO].[76] After reduction, the metal atoms aggregate to form nanoparticles which are capped by the CO_2 soluble fluorinated thiols. The thiol binds to the surfaces of nanoparticles, quenches particle growth and provides a steric barrier to aggregation. In this manner, metallic silver, palladium, and gold nanoparticles with a size range of about 1–4 nm were dispersed in supercritical CO_2.

Another method involves reducing CO_2-soluble fluorinated, organometallic precursors, such as Ag(hfpd)(tetraamine), Ag(hfpd)(tetraglyme), and $Pd(hfac)_2$ in the absence of stabilizing thiols. Rather, the reduced silver nanoparticles were trapped in porous substrates, such as poly(styrene-divinlybenzene) and silica aerogels,[77] palladium nanoparticles were stabilized in swelled plastics.[78] In each of these cases, CO_2-soluble fluorinated metal complexes were required to make the metal nanoparticles.

The use of hydrocarbon-based or oxygenated hydrocarbon-based precursor complexes in supercritical CO_2 manufacture of metal nanoparticles would mitigate the problems associated with the environmental and biological persistence associated with fluorous compounds. Platinum, copper, and nickel film were successfully deposited onto polymer substrates or silicon

wafer by reducing CO_2-soluble hydrocarbon-based metal precursors, such as dimethyl(cyclooctadiene)platinum(II) [$CODPtMe_2$],[79] bis(2,2,6,6-tetramethyl-3,5-heptanedionato)copper (II) [$Cu(tmhd)_2$], and bis(cyclopentadienyl)nickel [$NiCp_2$].[80] Silver acetylacetonate, [Ag(acac)] was reported as a hydrocarbon-based precursor for the preparation of silver nanocrystals capped with fluorinated ligands of 1H,1H,2H,2H-perfluorooctanethiol.[81, 82] However, these prior reports of metallic nanoparticle synthesis by reducing hydrocarbon-based metal precursors did not contain any CO_2-metal precursor phase behavior data. Our objective was to produce silver nanoparticles capped with non-fluorinated ligands via the reduction of highly CO_2-solulbe hydrocarbon-based or oxygenated hydrocarbon-based metal precursors.

2.7.2 CO_2 in Enhanced Oil Recovery

The largest application of CO_2 is in the area of enhanced oil recovery. Carbon dioxide, being available at high purity and in large quantities from natural reservoirs, has been used in enhanced oil recovery for many years.

Enhanced Oil Recovery

In petroleum industry, primary recovery, producing oil under natural reservoir pressure, accounts 5-20% of original oil in place (OOIP). Subsequently, secondary recovery, the injection of water to displace oil, called water flooding, can recover up to 50% of OOIP. Much of the oil still remains behind in place due to inefficiency of these recovery processes. With the increasing demand for petroleum versus limited resources, tertiary recovery methods, referred to as enhanced or improved oil recovery (EOR/IOR) employ fluids other than water to displace additional oil from reservoir. Recent production trends show less than 10% of OOIP comes from

EOR processes. EOR processes include hydrocarbon miscible flooding, CO_2 flooding, polymer flooding, surfactant flooding, steam flooding, and immiscible gas injection. Different fluids are injected to displace additional oil from the reservoir, via several mechanisms including solvent extraction to achieve (or approach) miscibility, interfacial-tension (IFT) reduction, improved sweep efficiency, pressure maintenance, oil swelling, and viscosity reduction.[83]

CO_2 as a Flooding Agent in Enhanced Oil Recovery

During a CO_2 flooding, also called miscible displacement, because CO_2 is miscible with light oils under reservoir conditions. CO_2 is injected into the oil-bearing porous media, typically at a depth greater than 2000 ft and reservoir temperature usually between 300 K and 400 K. The working pressure is maintained slightly above the "minimum miscibility pressure" (MMP, approximately 7-30 MPa) as shown in Figure 2.10,[84] thus CO_2 can dynamically develop effective miscibility with oil and displace the oil left behind by water flooding.[85] As the reservoir fluids are produced form the production well, CO_2 can be easily separated from the oil simply by pressure reduction. Other properties of CO_2 such as low cost, nonflammable, nontoxic, and easy separation from the oil also contribute to make CO_2 flooding an attractive oil recovery procedure.

CO_2 flooding at nearly 70 projects sites in the U.S. produces more than 200,000 barrels per day, which is approximately 3% of the domestic oil production rate. About 1.3 billion standard cubic feet (SCF) of CO_2 is injected into domestic reservoirs each day, the majority of which are located in the Southwest. At typical reservoir conditions, CO_2 is a dense fluid and its utilization corresponds to 3 barrel of liquid CO_2 injected per barrel of oil rejected. Despite the large amount of CO_2 flooding injected into these formations, the recovery efficiency is typically

only 10-20% of the OOIP. Further, shallow reservoirs are not amenable to CO_2 flooding because the MMP exceeds the overburden pressure of the formation.

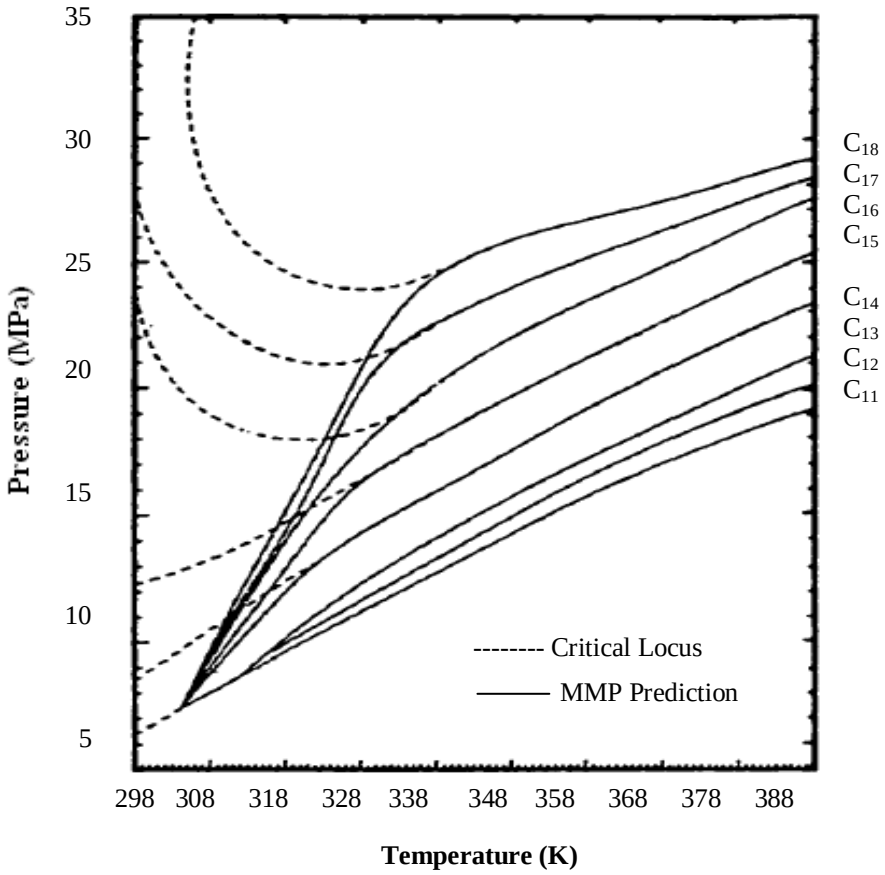

Figure 2.10. Working temperature and pressure for CO_2 flooding as a function of oil average molecular weight.[84]

The foremost disadvantage of CO_2 as an oil displacement fluid is its low viscosity, 0.03-0.1 cp at the reservoir conditions, as shown the shade area in Figure 2.11,[86] which is up to 100 times lower than that of the oil being displaced, varying from 0.1 cp to 50 cp. The low viscosity of CO_2 results in its much higher mobility (defined as permeability/viscosity of that fluid in porous media) compared to that of the oil, because the permeability of CO_2 and oil are comparable in magnitude. This unfavorable high mobility of CO_2 causes CO_2 "fingering" its way towards the production well, bypassing as much as 85% of the oil in the reservoir, which reduces the area sweep efficiency. Figure 2.12 shows the comparison of CO_2 fingering and the ideal case in EOR. Injection is in the lower left hand corner, and production is in the upper right hand corner, the curves show CO_2/oil interface as a function of time

Moreover, the low viscosity of CO_2 also contributes to the low vertical sweep efficiency, especially in stratified reservoirs that include two or more layers. The formation may contain a highly permeable water-rich zone caused by extensive water flooding, while the other layer is low permeability oil-rich zone. The high mobility of CO_2 prefers entering the highly permeable water-rich zone, leaving oil residing in the less permeable zones, which is not contacted by CO_2 and thus not efficiently displaced.

Furthermore, some shallow reservoirs are not amenable to CO_2 flooding because the MMP exceeds the overburden pressure of the formation. In this case, the displacement of oil by CO_2 would be conducted at pressures below the MMP, and the resultant displacement would be categorized as immiscible displacement. Such a process would benefit from a CO_2 thickener to improve sweep efficiency. The displacement efficiency would also be enhanced if there was a way to reduce the CO_2-oil interfacial tension.

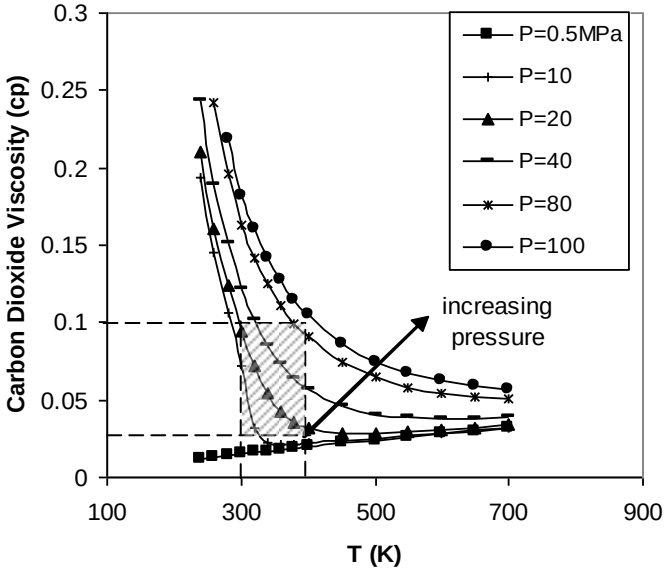

Figure 2.11. Viscosity of CO_2 as function of temperature and pressure.[86]

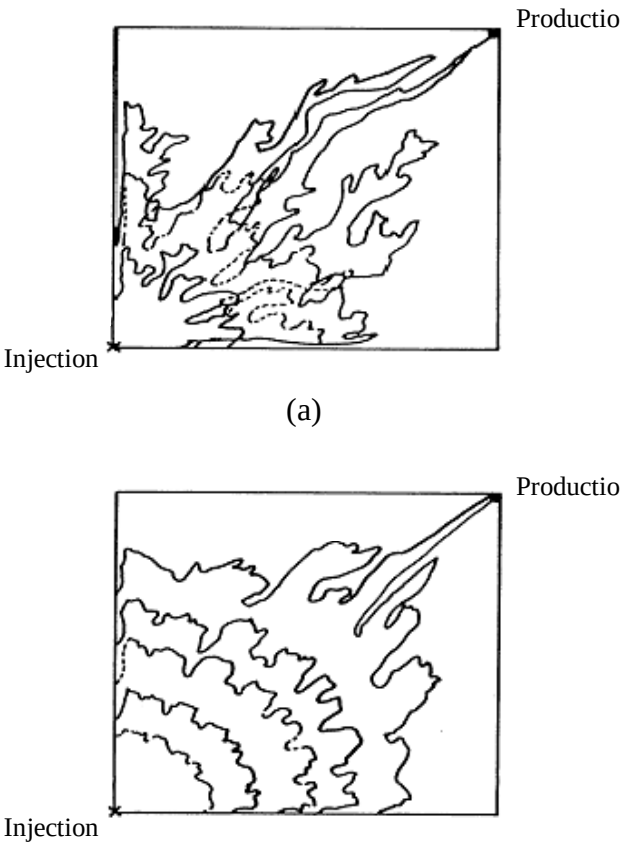

Figure 2.12. CO_2 flooding in EOR: (a) CO_2 "fingering" (b) ideal case.

Mobility Control Technologies to Improve the Efficiency of CO_2 Flooding

The high CO_2 utilization rate and low volumetric sweep efficiency are primarily attributing to the low viscosity and density of dense CO_2 relative to the oil being displaced. For example, the density of CO_2 at reservoir conditions may be 0.45-0.75 g/cm^3, while the oil density varies between 0.7-0.9 g/cm^3. The viscosity of CO_2, 0.03-1 cp at reservoir conditions, is commonly 2-20 times less than that of the oil being displaced. Although it is not feasible to significantly increase the density of CO_2, it is possible to significantly alter the relative viscosity of CO_2 using several technologies.

Water-Alternating-Gas (WAG) Technology

Currently, the water-alternating-gas (WAG) process remains the most common means of moderating CO_2 mobility.[87] The water slugs act as a blocking agent to impeding CO_2 flow in the porous medium. Alternating slugs of water and CO_2 are injected to improve the mobility of CO_2 by reducing the relative permeability of CO_2. The increased water saturation in the porous media decreases the relative permeability of CO_2; however, the high saturation of water may impede the contact of CO_2 with oil, and gravity segregation of CO_2 and water can impede the effectiveness of this process. The injection of water also extends the time required to inject the desired amount of carbon dioxide. Further, a significant amount of oil can still be left behind during the WAG process; recovery of only 10-20% of the oil is common.

CO_2 Foam Flooding or Surfactant Solution-Alternating-Gas (SAG) Technology

Foam is a dispersion of a gas in a liquid. CO_2 foams have also been studied by both academic groups[42, 88-90] and by industrial researchers.[91, 92] An aqueous surfactant solution is injected into the formation, followed by the CO_2, which is called surfactant-alternating-gas (SAG) process. The in-situ generation of foams results in high phase volume CO_2 foams in which bubbles of the CO_2 are separated by aqueous films. Foams show potential for both mobility control (modest decreases in mobility) and permeability modification (significantly decreases in mobility). Shorter cycles are recommended in the SAG process to obtain a more uniform foam quality. Problems associated with CO_2 foam flooding or SAG process includes corrosion, surfactant adsorption and control of foam mobility within the reservoir for extended periods of time.

CO_2-Soluble Polymeric Thickener Technology

A search for CO_2-soluble polymers or smaller associating compounds capable of directly enhancing the viscosity of dense CO_2 have been conducted by numerous research groups [42, 93]. Subsequently, Enick and co-workers identified the first CO_2 thickener, poly(**f**luoroalkyl**a**crylate-**st**yrene) copolymer, poly FAST, which successfully increased the viscosity of CO_2 by a factor of 10 in porous media at 1 wt%.[7, 94] Poly FAST isn't practical for field use; however due to its expensive and environment persistence.

These examples demonstrate the diversity applications of CO_2 from nanoparticle formation to enhanced oil recovery. Despite difficulties associated with its feeble solvent nature, application of creative engineering solutions can still enable its use, provided that CO_2 soluble surfactants can be specifically designed and synthesized for each application. Such surfactants contain a CO_2-philic segment such as a fluoroether, fluoroacrylate, or silicone-based compound and a CO_2-phobic segment made up of a hydrophilic or lipophilic molecule, depending on the application.

3.0 RESEARCH OBJECTIVES AND APPROACH

3.1 RESEARCH OBJECTIVES

The primary objective of this project is to enhance the performance of petroleum and chemical engineering CO_2-based processes using oxygenated hydrocarbon-based or hydrocarbon-based, novel, inexpensive, biodegradable CO_2 soluble surfactants with tails composed of C, H, and O (other elements may be used in ionic surfactant counterions).

3.1.1 CO_2 Soluble Surfactants for Nanoparticle Synthesis and Stabilization

Our objectives are to design, synthesize, characterize, and evaluate the CO_2 solubility of ionic surfactants with oxygenated hydrocarbon tails composed of acetylated sugar, PPO, or oligo(vinyl acetate). Additionally, these surfactants were examined for their ability to form stable microemulsions with polar microenvironments capable of dissolving polar species in the bulk non-polar CO_2 solvent. Other objectives for nanoparticle synthesis application were to design and determine the solubility of silver organometallic complex that could be used to form silver nanoparticles in CO_2 via reduction in the presence of fluorous or non-fluorous stabilizing ligands.

3.1.2 CO_2 Soluble Surfactants for Generating in-Situ EOR Foams

We proposed the use of CO_2 soluble surfactants that can be injected along with CO_2 into the oil reservoir for mobility control and/or permeability alteration. Upon mixing with the reservoir brine, foam would be generated in-situ; especially in watered out zones into which a significant fraction of the CO_2 typically flows with little economic benefit. The fundamental advantages of such a surfactant include (a) a reduction or elimination of the need to inject brine or aqueous surfactant solutions into the reservoir, and (b) the generation of foams along and at the tips of the CO_2 "fingers" where mobility control is needed the most, thereby acting as a "smart fluid" to divert the subsequently injected neat CO_2 to oil-rich zones.

The objective of this study was to form emulsions by mixing of CO_2, water and CO_2-soluble surfactants, and then to characterize the stability of the emulsion by measuring its rate of collapse. CO_2-soluble ionic surfactants with oxygenated hydrocarbon tails composed of acetylated sugar, PPO, or oligo(vinyl acetate) were evaluated along with two nonionic surfactants, iso-stearic carboxylic acid and PPG-PEG-PPG triblock polymer (Mn=3300). Nonionic surfactants are considered to be low-to-moderate foamers relative to ionic surfactants, and were therefore expected to yield less stable emulsions, but nonionic surfactants have less severe problems associated with adsorption or chemical degradation. The stability of the emulsions stabilized with CO2 soluble ionic surfactants was then contrasted with that the stability of emulsions formed using conventional water soluble ionic surfactants.

3.2 OUR APPROACH

We proposed to explore new types of oxygenated hydrocarbon-based or hydrocarbon-based, novel, inexpensive, biodegradable CO_2 soluble surfactants. Each surfactant will contain two types of segments, one of which will be a novel, highly CO_2-philic, oxygenated hydrocarbon-based or hydrocarbon-based segment. The other would be either a conventional non-ionic or ionic hydrophilic segment, or a nonionic lipophilic segment.

The CO_2 solubility of each surfactant will be evaluated, along with the ability of the surfactant to solubilize water or generate foams in a high pressure variable volume view cell. Auburn University will confirm the solubilization of water into the cores of micelles spectroscopically.

4.0 OXYGENATED HYDROCARBON-BASED IONIC SURFACTANTS

4.1 IONIC SURFACTANTS WITH PERACETYL GLUCONIC TAILS

4.1.1 Materials

Acetic anhydride, perchloric acid, D-glucose, triethylamine, 1,8-Diazabicyclo[5.4.0]undec-7-ene (DBU), 2-boromoethanol, pyridine sulfur trioxide, sodium bicarbonate, ammonium carbonate were purchased from Aldrich and used as received. All other reagent and solvents were obtained from Aldrich and used without further purification. N_2 (99.995%) and CO_2 (99.99%, Coleman grade) were purchased from Penn Oxygen.

4.1.2. Characterizations

The purities of the ionic surfactants were estimated by ^{1}H NMR spectra recorded on a Bruker 400 MHz NMR and IR spectra obtained on a Mattson Polaris FTIR. The molecular weights of the ionic surfactants were detected by mass spectra performed on a liquid chromatography/electrospray ionization/quadrupole time-of-flight mass spectrometer.

4.1.3 Synthesis

The synthesis of peracetyl gluconic (sugar acetate)-based ionic surfactants with ethyl sodium sulfate, sodium carboxylate and ammonium carboxylate head groups were carried out with the help of Dr. Hamilton's group of Chemistry Department at Yale University.[95] The structures of peracetyl gluconic-based ionic surfactants are shown in Figure 4.1.

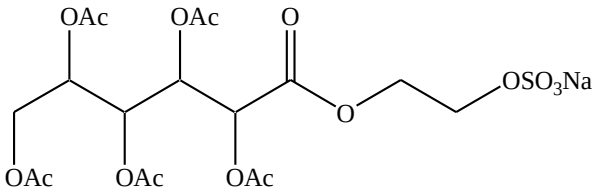

Peracetyl Gluconate Ethyl Sodium Sulfate (a)

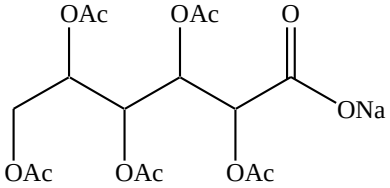

Peracetyl Gluconate Sodium Carboxylate (b)

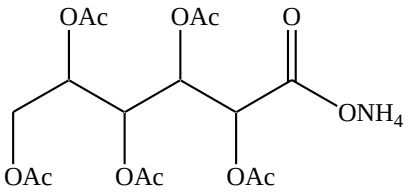

Peracetyl Gluconate Amonium Carboxylate (c)

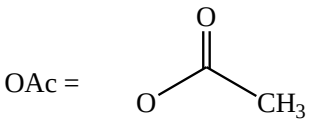

Figure 4.1 Structures of peracetyl gluconic-based ionic surfactants.

The reaction scheme is shown as follows in Figure 4.2, with the synthesis of peracetyl gluconic ethyl sodium sulfate as an example. Peracetyl gluconic carboxylic acid was prepared by

acetylation of D-glucose by acetic anhydride, followed by neutralization with sodium bicarbonate.

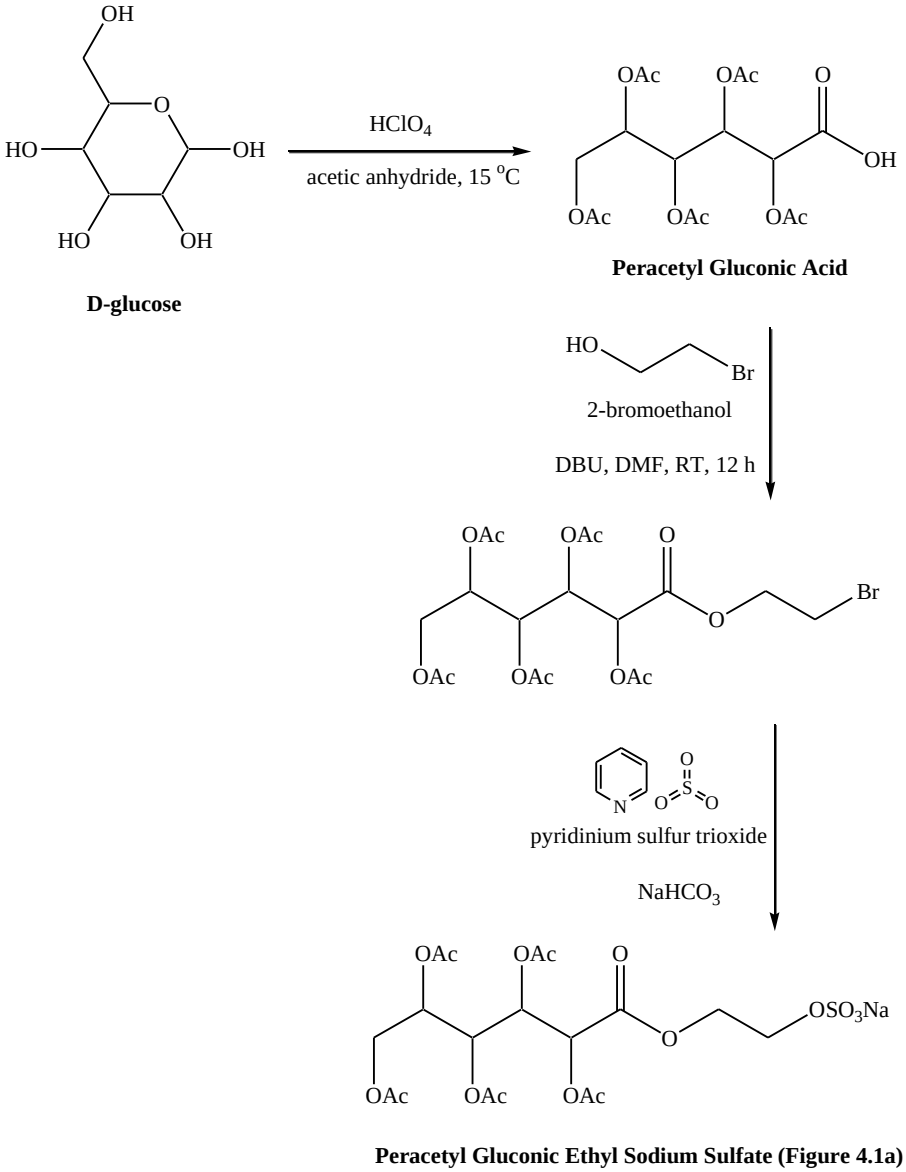

Figure 4.2 Reaction scheme for preparation of peracetyl gluconic ethyl sodium sulfate.

Synthesis of Peracetyl Gluconic Carboxylic Acid

Acetic anhydride (30 mL) was cooled to about 15 °C, 67% $HClO_4$ (4 g, 39.82 mmol) was then added to the cold acetic anhydride, followed by the addition of D-glucose (5 g, 25.23 mmol). The temperature of the mixture was kept below 40 °C. After brief heating to obtain a homogeneous solution, the mixture was poured on ice and extracted twice with $CHCl_3$ (2 x 100 mL). The organic layers were pooled and washed with ice-cold water. Water (50 mL) and triethylamine (4 mL) were added to the $CHCl_3$, followed by overnight stirring to hydrolyze any anhydride. The organic layer was separated and washed with 1 N HCl and dried over anhydrous Na_2SO_4, and $CHCl_3$ was removed in vacuo to yield 80% 2,3,4,5,6-penta-*O*-acetyl-D-gluconic acid. ^1H NMR δ_H ($CDCl_3$): 5.618 (t, J = 4.8 Hz, 1H), 5.510 (dt J = 6.4 Hz, 1H), 5.285 (d, J = 3.6 Hz, 1H), 5.055 (m, 1H), 4.301 (dd, J = 12.4 Hz, 4 Hz, 1H), 4.113 (dd, J = 12.4 Hz, 5.6 Hz, 1H), 2.249 (s, 3H), 2.085 (s, 3H), 2.077 (s, 3H), 2.072 (s, 3H), 2.044 (s, 3H).

Synthesis of Peracetyl Gluconic Ethyl Sodium Sulfate (Figure 4.2a)

1,8-Diazabicyclo[5.4.0]undec-7-ene (DBU) (4.8 g, 31.53 mmol) was added to a solution of peracetyl gluconic carboxylic acid (10 g, 24.63 mmol) and 2-bromoethanol (3.94 g, 31.53 mmol) in DMF(10 mL) and stirred at room temperature. After 12 h the mixture was poured into water (100 mL) and extracted with dichloromethane (3 x 50 mL). The organic layers were pooled, washed with water, and dried over anhydrous Na_2SO_4 prior to the removal of solvent. Column chromatographic purification of the crude product over silica gel using 50% ethyl acetate and hexanes as the eluent gave the pure product (9.4 g, yield 85%). The product was dissolved in anhydrous dichloromethane, pyridine sulfur trioxide (6.3 g, 39.58 mmol) was added, and the mixture was stirred at room temperature for 12 h. The mixture was filtered through a pad of Celite and solvent removed to give the pyridinium salt. The pyridinium salt was dissolved in

water (100 mL), and sodium bicarbonate (1.74 g, 20.71 mmol) was added. The resultant mixture was frozen and water was removed using a freeze-dryer to give a white color fluffy solid.

HRMS (ESI) calculated for $C_{18}H_{25}Na_2O_{16}S$ ($[M + Na]^+$) 575.0659, found 575.0630. (Appendix A Figure A.1)

Synthesis of Peracetyl Gluconic Sodium Carboxylate (Figure 4.2b).

Peracetyl gluconic carboxylic acid (5 g, 12.32 mmol) was dissolved in water (50 mL), and sodium bicarbonate (1.04 g, 12.38 mmol) dissolved in water (10 mL) was added. The resultant solution was frozen and water was removed using a freeze-dryer to give white color fluffy solid.

HRMS (ESI): calculated for $C_{16}H_{22}NaO_{12}$ ($[M + H]^+$) 429.1009, found 429.1016. (Appendix A Figure A.2)

Synthesis of Peracetyl Gluconic Ammonium Carboxylate (Figure 4.2c).

Ammonium carbonate (2.0 g, 20.81 mmol) was added to a solution of peracetoxy gluconic carboxylic acid (5 g, 12.32 mmol) dissolved in water (50 mL), and the mixture was stirred. The resultant solution was frozen and water was removed using a freeze-dryer to give a yellow color fluffy solid. HRMS (ESI) calculated for $C_{16}H_{26}NO_{12}$ ($[M + H]^+$) 424.1455, found 424.1422. (Appendix A Figure A.3)

4.1.4 Phase Behavior of Peracetyl Gluconic-Based Ionic Surfactants

4.1.4.1 Experimental Apparatus The CO_2 solubility of surfactants was determined by phase behavior study as function of temperature, pressure and concentration. The apparatus is a high pressure, windowed, variable volume view D. B. Robinson cell with magnetic mixer and temperature control. The schematic apparatus is shown in Figure 4.3 and the variable volume view D.B. Robinson cell with magnetic mixer is illustrated in Figure 4.4. The system is rated to 70 MPa and 200 ^{o}C.

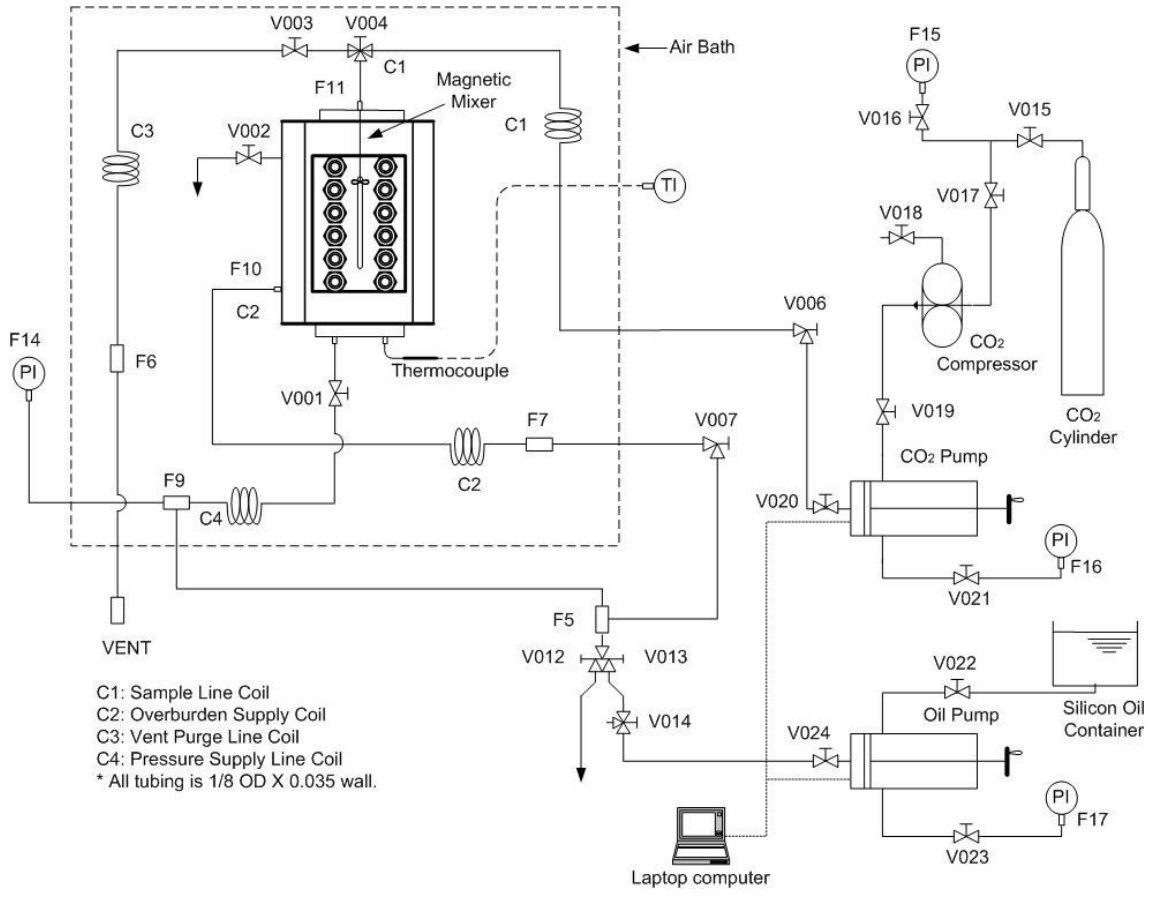

Figure 4.3 Schematic apparatus for solubility/phase behavior measurements.

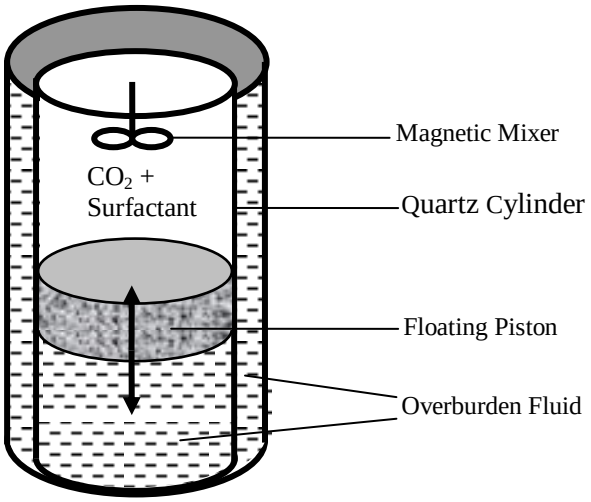

Figure 4.4 Variable volume view D. B. Robinson cell with magnetic mixer

A known amount of surfactant (e.g., 0.0700 ± 0.0001 g) was loaded into the sample volume of a high pressure, windowed, stirred, variable-volume view cell (DB Robinson & Assoc., 3.18 cm i.d., ~120 cm^3 working volume). In this cell, the sample volume is separated from the overburden fluid by a steel cylinder (floating piston) that retains an O-ring around its perimeter. The O-ring permits the cylinder to move while a seal is retained between the sample volume and the overburden fluid. After purging with carbon dioxide at 0.2 MPa, the sample volume was minimized by displacing the floating piston to the highest possible position within the cell that did not result in the displacement of surfactant out of the sample volume. High pressure liquid carbon dioxide (22 °C, 13.8 MPa) was then introduced to the sample volume as the silicone oil overburden fluid (which was maintained at the same pressure as the CO_2) was withdrawn at the equivalent flow rate using a dual-proportioning positive displacement pump (DB Robinson). This technique facilitated the isothermal, isobaric addition of a known volume of CO_2 (e.g., 12.50 ± 0.01 mL) into the sample volume. The mass of CO_2 introduced was

determined from the displaced volume, temperature, and pressure using an accurate equation of state for carbon dioxide.[96] On the basis of the uncertainties associated with the measurement of temperature, pressure, and volume, and the precision of the equation of state, compositions are estimated to be accurate to within 1% of the specified value (e.g., 0.5 ± 0.005 wt %). The surfactant-CO_2 mixture was compressed to high pressure (e.g., 60 MPa) and mixed thoroughly using a magnetic stirrer (DB Robinson, max. 2500 rpm). If the surfactant did not completely dissolve at these conditions, additional CO_2 was added to the system until a single transparent phase could be attained. Cloud points were determined by standard nonsampling techniques. The high-pressure, single-phase solution of known composition was subjected to a slow, isothermal expansion until the cloud point was attained. Cloud points were reproduced three times to within approximately ± 0.1 MPa for monodisperse surfactants and ± 0.5 MPa for polydisperse surfactants. Temperatures were measured with a type K thermocouple to an accuracy of ± 0.1 °C. Experiments with water were conducted by adding the specified amount of surfactant and double distilled and deionized water to the sample volume, followed by the introduction of CO_2. W is the molar ratio of total amount of loading water to surfactant in the mixture. The W value is "uncorrected" in that this value accounts for the total amount of water in the mixture that may dissolve into the bulk CO_2 and/or be solubilized in the core of reverse micelles. The corrected water/surfactant ratio, W^{corr}, for a transparent single phase mixture can be estimated by assuming that the bulk CO_2 is saturated with water, while the amount of the excess water, which is assumed to reside within the cores of the micelles, is used in the numerator of W^{corr}.[97]

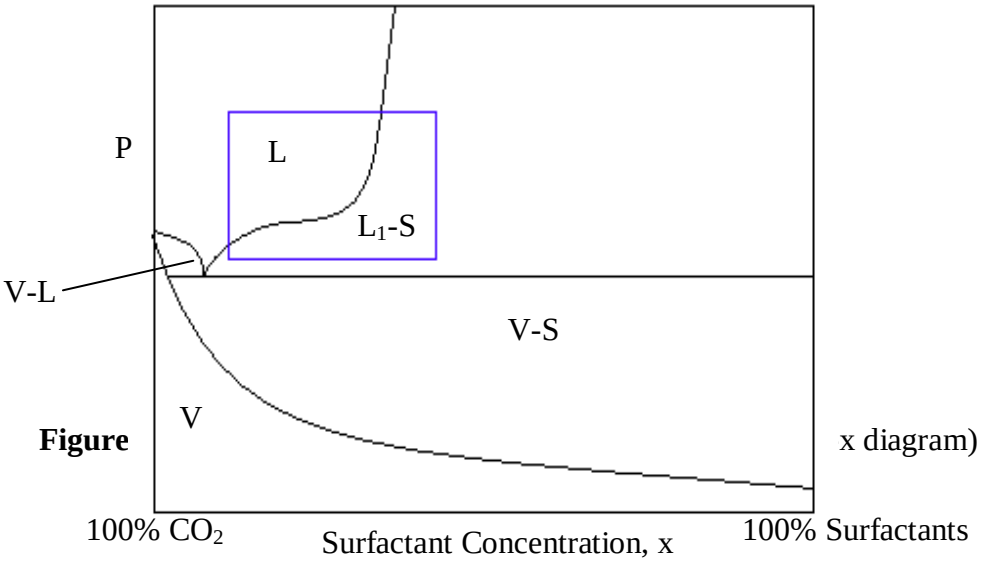

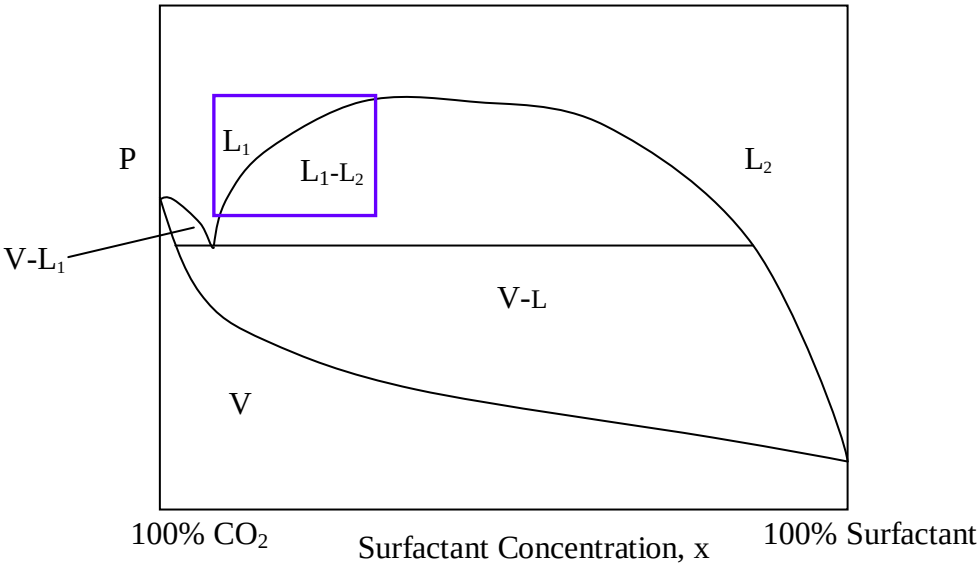

Figure 4.6. Phase diagram for liquid surfactant/CO_2 system (P-x diagram)

The cloud point pressure is the minimum pressure at which the sample is miscible with dense carbon dioxide at that particular temperature and composition. Below this pressure, the system consists of a sample-rich phase and a CO_2-rich phase. Thus we could obtain a point on

the two-phase boundary of a P-x diagram of solid surfactant/CO_2 system and liquid surfactant/CO_2 system, shown in Figure 4.5 and Figure 4.6. A series of these experiments were conducted over a range of overall compositions, enabling the two-phase boundary of the surfactants/CO_2 system to be established.

4.1.4.2 Phase Behavior Results The neat peracetyl gluconic-based surfactants with an ethyl spacer and a sodium sulfate, sodium carboxylate or ammonium carboxylate head group (Figures 4.1 a,b,c) are solids. Peracetyl gluconic ethyl sodium sulfate (PGESS) does not dissolve in CO_2 at 22 ^{o}C or 40 ^{o}C in the absence of water (W=0), but its solubility increases as water is added, as shown in Figure 4.7. The surfactant is up to 0.6 wt% soluble in CO_2 in the presence of water at a W value of 10 (W is the molar ratio of water to surfactant, uncorrected for dissolved water). At W values of 40 and 50; however, a water phase appeared at the bottom of the cell. Attempts to dissolve 0.7 wt% or more yielded an excess surfactant-rich phase at the bottom of the cell for all values of W. Table 4.1 lists W and W^{corr} for the PGESS surfactant in water and CO_2 mixture at different weight percent and temperature.

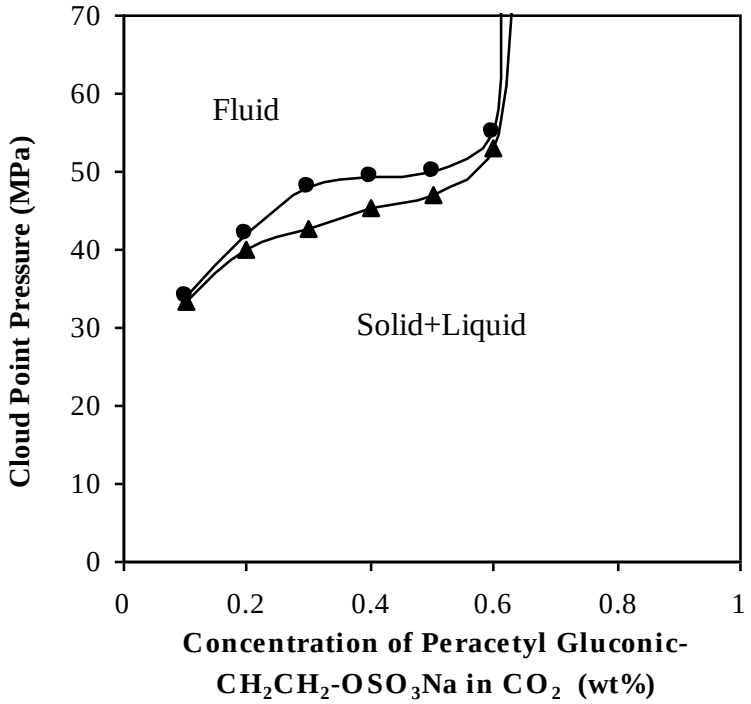

Figure 4.7. Phase behavior of peracetyl gluconic-CH_2CH_2-OSO_3Na/CO_2 mixtures. Insoluble at W = 0; 22 ^oC, W =10 (●); 40 ^oC, W=10 (▲). (Appendix A Figure A.4. Surfactant concentration in mM)

Table 4.1. W and W^{corr} for the PGESS surfactant in water and CO_2 mixture at different weight percents and temperature. *When the amount of water is not sufficient to saturate the CO_2, W^{corr} is reported as 0.

PGESS Concentration, wt%	Temperature, ^oC	W	W^{corr*}
0.1-0.5	25	10	0
0.6	25	10	0.8
0.1-0.6	40	10	0

Figure 4.8 shows that peracetyl gluconic sodium carboxylate (PGSC) appears to be more CO_2 soluble than PGESS because PGSC can dissolve at 40 ^oC in the absence of water. The solubility of PGSC decreases slightly with the addition of water. PGSC has a limiting solubility of approximately 0.4 wt% in CO_2 at W = 10. Single phase solutions could not be realized at W values of 40, even at surfactant concentrations as low as 0.1 wt%. W^{corr} is 0 at W value of 10 for PGSC surfactant in water and CO_2 mixture at concentration range of 0.1-0.5 wt% is 0 at 40 ^oC.

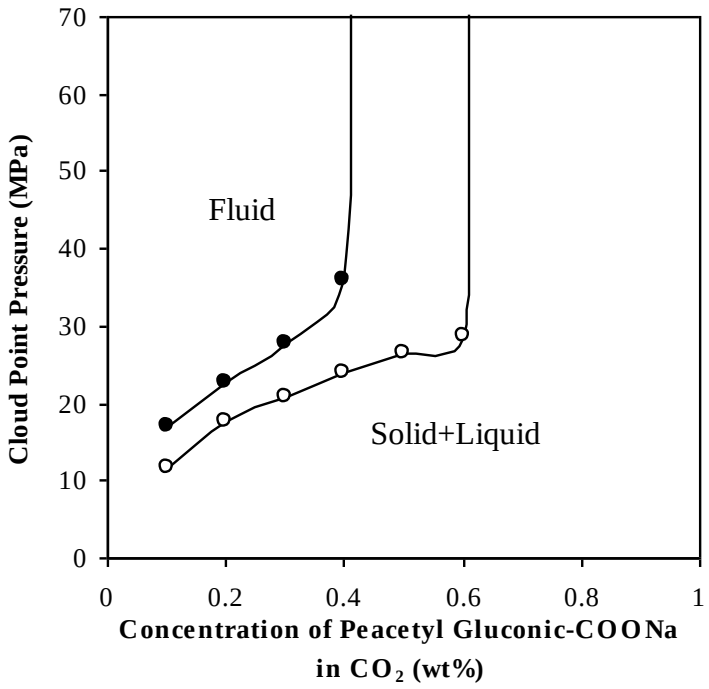

Figure 4.8. Phase behavior of peracetyl gluconic-COONa/CO_2 mixtures at 40 ^oC. W=0 (o); W=10 (•). (Appendix A Figure A.5. Surfactant concentration in mM).

Figure 4.9 illustrates that peracetyl gluconic ammonium carboxylate (PGAC) can dissolve in CO_2 up to 2 wt% at 40 ^oC without water. Although this limiting solubility value is significantly greater than those for either PGESS or PGSC, the pressure required to dissolve PGAC at dilute concentrations (up to 0.5 wt%) was greater than that required to dissolve PGSC. The solubility of PGAC decreases with the introduction of water, as does its limiting solubility in CO_2, which is about 0.5 wt% at W value of 10. Single phase solutions could not be realized at W values of 40, even at surfactant concentrations as low as 0.1 wt%. W^{corr} is 0 for W value of 10 over PGSC concentrations up to 0.5 wt% at 40 ^oC.

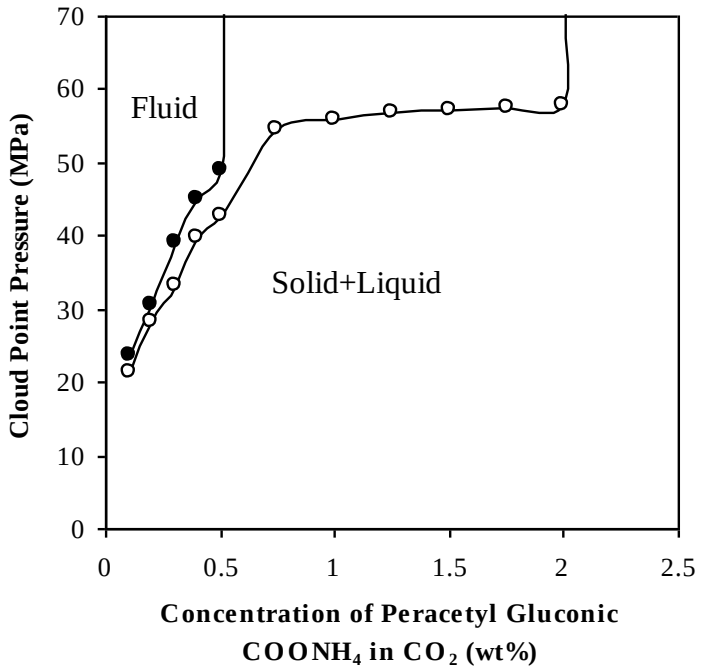

Figure 4.9. Phase behavior of peracetyl gluconic-$COONH_4/CO_2$ mixtures at 40 ^oC. W =0 (o); W =10 (•). (Appendix A Figure A.6. Surfactant concentration in mM).

4.1.5 Dye Solubilization and Spectroscopic Measurements

Dye solubilization and spectroscopic measurements were carried out with the help of Dr. Roberts' group in Chemical Engineering Department at Auburn University.[95]

The ability to form reverse micelles by these CO_2-soluble surfactants was investigated using the solvatochromic probe methyl orange at system concentration of ca. 4.7 x 10^{-5} M. Methyl orange is a polar probe that is insoluble in both carbon dioxide and water-saturated carbon dioxide. Furthermore, the location of its absorption maximum is dependent upon the polar environment in which it is dissolved. For instance, it has an absorption maximum at 416 in dry PFPE-NH_4/CO_2 reverse micelles, 421 in methanol, 464 in water, and 502 nm in CO_2-

saturated water.[68, 69] Hence, the solubility of methyl orange in an otherwise ineffective solvent, such as CO_2, indicates the presence of reverse micelles and it also functions as a probe of polarity of the water environment within CO_2 reverse micelles. Consequently, methyl orange has been used successfully to identify the presence of reverse micelles as well as their ability to uptake water in CO_2 reverse micelles.[68, 69, 98-103] It was indicated that the absorption maximum in water-in-CO_2 microemulsions formed by ammonium carboxylate PFPE surfactant approaches that of pure water ($\lambda_{max} = 460$ nm).[66]While a surfactant may show some solubility in CO_2 in the presence of dissolved water, this alone does not guarantee that a polar microenvironment is present. Verification of a polar microenvironment is necessary to confirm that the surfactant does indeed self-assemble in solution to form reverse micelles.

4.1.5.1 Experimental Apparatus A 32 mL stainless steel high-pressure vessel equipped with pressure gauge, resistance temperature detector (RTD), and parallel quartz windows for UV-vis characterization, which has been described previously,[73] was used to perform dye solubilization experiments. A magnetic stir bar was used to facilitate surfactant/CO_2 mixing. For a typical experiment, 100 μL freshly prepared 0.015 M methyl orange (MO) in methanol solution was added into the UV cell, and a gentle stream of N_2 was passed through the cell for ten minutes to fully evaporate the methanol while only maintaining the MO inside of the UV-cell. 0.15 wt% of surfactant was charged into the cell, then specific amount of double distilled and de-ionized water was injected into the cell using a syringe to reach the desired W value. After sealing the vessel, an ISCO syringe pump was used to add specific quantity of CO_2 to the vessel. Once the vessel was filled with CO_2 to the desired pressure, the system was mixed for at least an hour to reach a single phase before performing spectroscopic analysis. The vessel was placed in a

Cary 300E UV-vis spectrophotometer and absorption spectra were recorded to determine the presence of methyl orange solubilized in the surfactant/water/CO_2 mixture. Pressure within the vessel was monitored to approximately ± 0.7 MPa, and temperature was maintained to within ± 0.1 ^{o}C.

4.1.5.2 Spectroscopic Results The peracetyl gluconic surfactants were examined at 0.3 wt% in CO_2 at 40 °C and with water loading of W = 10. In each case, the CO_2-surfactant solutions were compressed to pressures above the reported cloud point pressure. Specifically, the sodium carboxylate, ammonium carboxylate, and ethyl sodium sulfate forms of the peracetyl gluconic were pressurized to 38, 44.8, and 48.3 MPa, respectively. There was no apparent methyl orange absorption, however, indicating that there was no tendency of the surfactants to form reverse micelles or polar microenvironments. Visual observation showed that, while water was dissolved into the CO_2, dry methyl orange was being left on the surface of the vessel, thus indicating that none of the water in the CO_2-rich phase existed in the form of a bulk water pool within the core of reverse micelles.

4.2 IONIC SURFACTANTS WITH PPG TAILS

4.2.1 Materials

Poly(propylene glycol) monobutyl ether (Mn=340, 1000), pyridinium sulfur trioxide, sodium bicarbonate, fumaryl chloride, sodium hydrogen sulfite were purchased from Aldrich and used as received. All other reagent and solvents were obtained from Aldrich and used without further purification. N_2 (99.995%) and CO_2 (99.99%, Coleman grade) were purchased from Penn Oxygen.

4.2.2 Synthesis

Poly (**P**ropylene **G**lycol) **M**ono**B**utyl **E**ther (PPGMBE) is a secondary alcohol containing propylene oxide repeat units. PPGMBE of different molecular weights (Mn=340, 1000) have been identified to be extremely CO_2 soluble at very low pressure. Three kinds of ionic surfactants with sodium sulfate, pyridinium sulfate, and sodium sulfosuccinate head groups were designed and synthesized. The synthesis of PPG-based ionic surfactants with sodium sulfate and pyridinium sulfate head groups were carried out with the help of Dr. Hamilton's group of Chemistry Department at Yale University.[95] AOT (sodium bis-2-ethyl-1-hexyl sulfosuccinate) is a commercially widely used aqueous surfactant, but it doesn't dissolve in CO_2 at all. Sodium bis (3,5,5-trimethyl1-hexyl) sulfosuccinate (AOT-TMH) with highly methyl branched tail as an AOT analogue was first synthesized by Nave and Eastoe,[60] considering that the pendant methyl groups in the outer blocks have a much lower surface energy (cohesive energy density) than the CH_2 group. Therefore, PPGMBE 340 is combined with the sodium sulfosuccinate head to form a twin tailed AOT analogue as an ionic surfactant. The structures of PPG-based single and twin tailed ionic surfactants are shown in Figure 4.10. The reaction scheme is shown as follows in Figure 4.11, with the synthesis of PPGMBE 340 sodium sulfate as an example. The

reaction route for the synthesis of sodium bis(PPGMBE 340) sulfosuccinate (AOT Analogue) is shown in Figure 4.12.

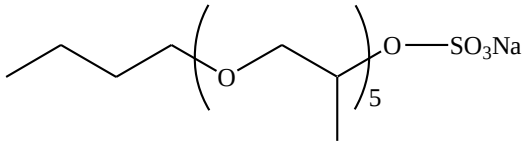

PPGMBE 340 Sodium Sulfate (a)

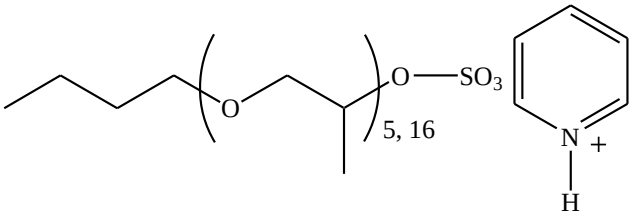

PPGMBE 340, 1000 Pyridinium Sulfate (b, c)

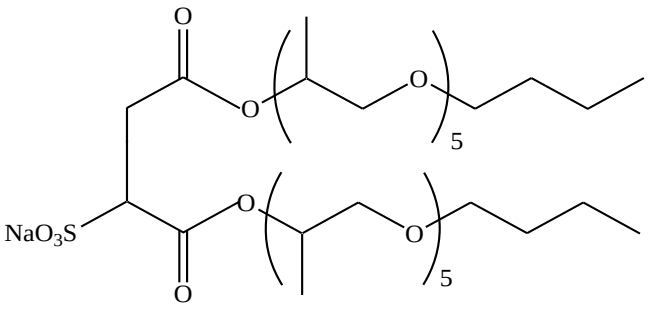

Sodium bis(PPGMBE 340) Sulfosuccinate (d)

Figure 4.10. Structures of peracetyl gluconic-based ionic surfactants.

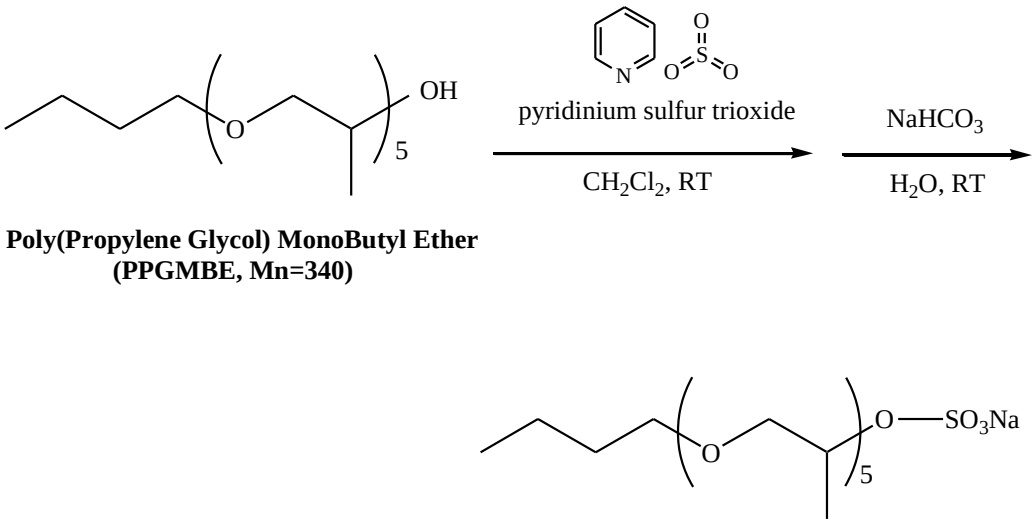

Poly(Propylene Glycol) MonoButyl Ether (PPGMBE, Mn=340)

PPGMBE 340 Sodium Sulfate

Figure 4.11. Reaction scheme for the synthesis of PPGMBE 340 sodium sulfate.

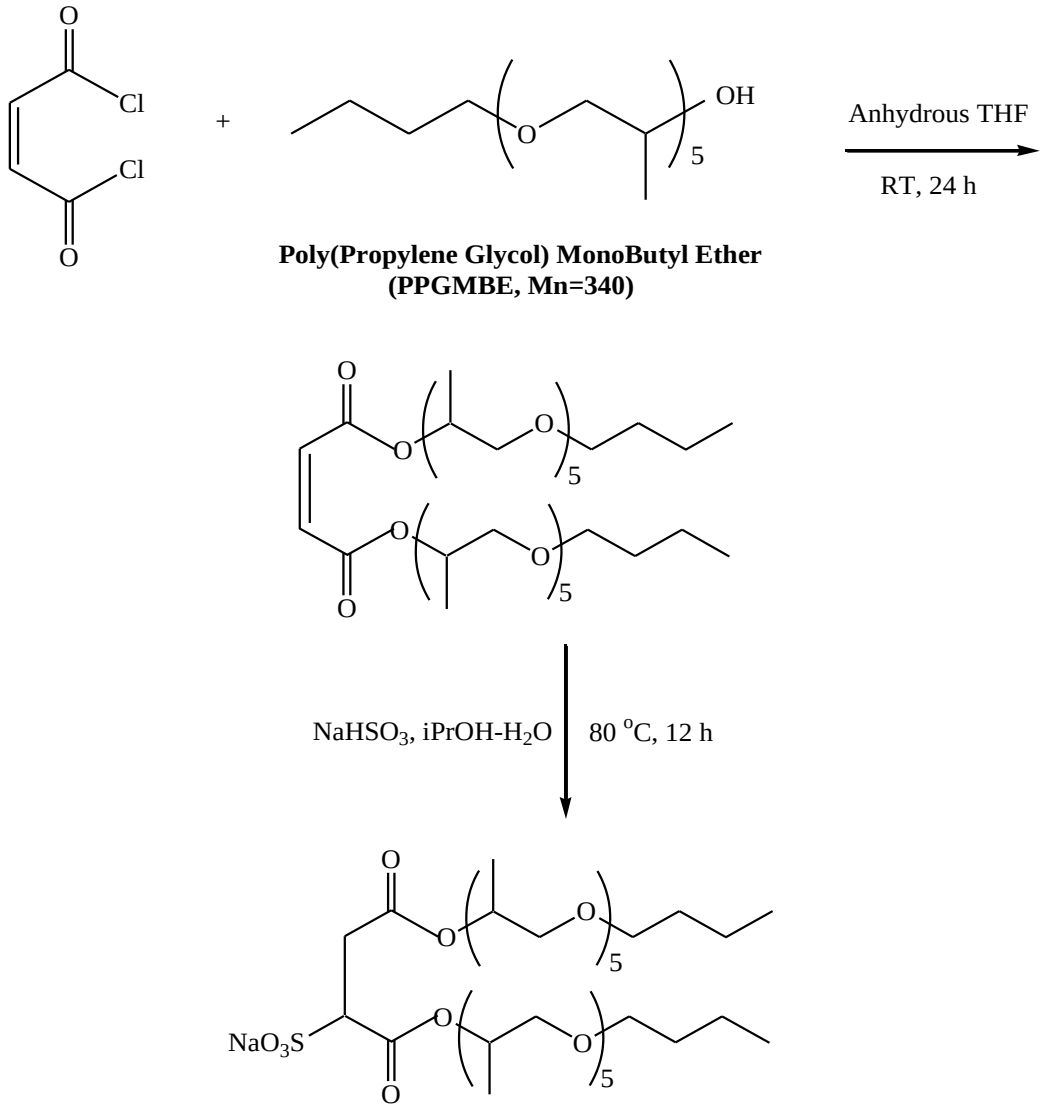

Figure 4.12. Reaction scheme for the synthesis of sodium bis(PPGMBE 340) sulfosuccinate.

Synthesis of PPGMBE 340 Sodium Sulfate (Figure 4.10 a)

Poly(propylene glycol) monobutyl ether (Mn = 340, 10 g, 29.4 mmol) was dissolved in dichloromethane (150 mL), pyridine sulfur trioxide (10 g, 62.83 mmol) was added, and the mixture was stirred at room temperature for 12 h. The reaction mixture was filtered through a pad of Celite and solvent removed to give the pyridinium salt. The pyridinium salt was dissolved in water (100 mL), and sodium bicarbonate was added until no further effervescence was observed. The resultant mixture was frozen and water was removed using a freeze-dryer to give yellow viscous liquid. Mass spectrum showed that the number-average molecular weight for PPGMBE (Mn = 340) sodium sulfate is 445.3. (Appendix A Figure A.7)

Synthesis of PPGMBE 340, 1000 Pyridinium Sulfate (Figure 4.10 b, c)

Poly(propylene glycol) monobutyl ether (Mn = 340, 10 g, 29.4 mmol) was dissolved in dichloromethane (150 mL), pyridine sulfur trioxide (10 g, 62.83 mmol) was added, and the mixture was stirred at room temperature for 12 h. The reaction mixture was filtered through a pad of Celite and solvent removed to give the PPGMBE (Mn = 340) pyridinium salt. PPGMBE (Mn = 1000) pyridinium sulfate was synthesized in the similar way.

Mass spectra showed that the number-average molecular weight for PPGMBE (Mn = 340) pyridinium sulfate and PPGMBE (Mn = 1000) pyridinium sulfate is 515.2 and 1178.6, respectively.

Synthesis of Na Bis(PPGMBE 340) Sulfosuccinate (AOT Analogue) (Figure 4.10 d)

The esterification of alcohol and fumaryl chloride followed the procedure described by Nave et al.[60] Poly(propylene glycol) monobutyl ether (Mn = 340, 10.41 g, 30.62 mmol) and anhydrous THF (60 mL) were charged in a 250 mL three-neck round-bottom flask equipped with a stirring bar and condenser under a steady flow of nitrogen. After cooling to 0 °C, fumaryl chloride (2.81 g, 18.36 mmol) was added dropwise. The reaction mixture was stirred for the next 24 h at room temperature. After rotary evaporation of THF, the mixture was dissolved in 100 mL of diethyl ether and washed with 50 mL of 1 N HCl, 50 mL of saturated $NaHCO_3$, and 50 mL of saturated NaCl solutions sequentially. The ether extract was dried over anhydrous Na_2SO_4 and filtered and then ether was removed by rotary evaporation. A pale yellow oil of diester product was obtained with 89% yield (10.37 g). The diester was subject to sulfonation with sodium hydrogen sulfite following the procedure provided by Baczko et al.[104] Sodium hydrogen sulfite (0.89 g, 8.55 mmol) in water (60 mL) was added dropwise to a solution of the diester (5 g, 6.58 mmol) in 2-propanol (80 mL) (both solutions were previously degassed with nitrogen for 20 min). The reaction mixture was then refluxed for the next 24 h. After rotary evaporation of the solvent, the residue was dissolved in chloroform and dried over Na_2SO_4 followed by removal of the solvent and drying of the resulting paste under a vacuum desiccator overnight. A yellow viscous liquid was obtained (4.2 g, yield 74%) The FTIR spectra showed the disappearance of the OH peak at 3471 cm^{-1} and appearance of carbonyl peak at 1723 cm^{-1}. (Appendix A Figure A.8-9) Mass spectrum showed that the number average molecular weight for sodium bis(PPGMBE 340) sulfosuccinate is 913.5. (Appendix A Figure A.10)

4.2.3 Phase Behavior Results

The PPGMBE 340 pyridinium sulfate was insoluble in CO_2. Figure 4.13 illustrates that the PPGMBE 340 sodium sulfate is CO_2-soluble; however, indicating that the sodium counterion is less CO_2 phobic than the pyridinium counterion. The PPGMBE 1000 pyridinium sulfate can dissolve in CO_2, indicating that the longer PPG segment of the tail made the surfactant with the pyridinium sulfate more CO_2 soluble. The addition of water lowers the cloud point pressure, as shown by the PPGMBE 1000 pyridinium sulfate dissolving in CO_2 at 40 ^oC and concentrations of 0.1-0.6 wt% with at W = 10. W^{corr} is 0 for W value of 10 over PPGMBE 1000 pyridinium sulfate concentrations up to 0.5 wt% at 40 ^oC. In each case, the limiting solubility of this surfactant in CO_2 is approximately 0.5 wt%. Single phase solutions could not be realized at W values of 40, even at surfactant concentrations as low as 0.1 wt%.

The phase behavior of mixtures of CO_2 and a twin tailed sodium bis(PPGMBE 340) sulfosuccinate, Figure 4.10 d, was also determined. This PPG twin tailed AOT analogue surfactant is 2 wt% soluble in CO_2, and its solubility in CO_2 decreases with the addition of water at W value of 10, as shown in Figure 4.13. W^{corr} is 0 for W value of 10 over sodium bis(PPGMBE 340) sulfosuccinate concentrations up to 0.5 wt% at 40 ^oC. Single phase solutions could not be realized at W values of 40, even at surfactant concentrations as low as 0.1 wt%.

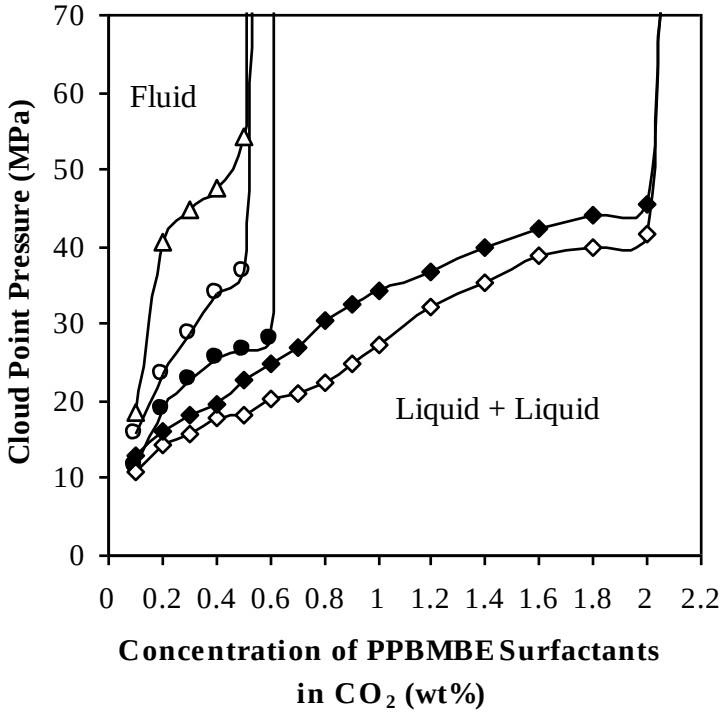

Figure 4.13. Phase behavior of PPGMBE surfactants/CO_2 mixtures at 40 ^{o}C. PPGMBE 340 sodium sulfate, W=0 (Δ); PPGMBE 1000 pyridinium sulfate, W=0 (○); PPGMBE 1000 pyridinium sulfate, W=10 (●); Sodium bis(PPBMBE 340) sulfosuccinate, W=0 (◊); Sodium bis(PPBMBE 340) sulfosuccinate, W=10 (♦). (Appendix A Figure A.11. Surfactant concentration in mM).

4.2.4 Spectroscopic Results

It was difficult to attain a single phase solution with the PPG-based surfactants, possibly due to the less intense mixing in the UV-vis cell and/or the instability of these surfactants exhibited during the weeks between their synthesis and their evaluation for water uptake. Therefore no evidence of reverse micelle formation was obtained for these surfactants.

4.3 IONIC SURFACTANTS WITH OLIGO(VINYL ACETATE) TAILS

4.3.1 Materials

Chlorosulfonic acid, pyridine, sodium hydroxide, sodium carbonate, sodium bicarbonate, fumaryl chloride, sodium hydrogen sulfite were purchased from Aldrich and used as received. The 2,2'-azobisisobutyronitrile (AIBN) was recrystalized in methanol, and vinyl acetate was passed through an inhibitor remover column to remove the inhibitor prior to use. All other reagent and solvents were obtained from Aldrich and used without further purification. N_2 (99.995%) and CO_2 (99.99%, Coleman grade) were purchased from Penn Oxygen.

4.3.2 Synthesis

Oligomerization of vinyl acetate was carried out using AIBN as a free radical initiator with 2-isopropoxyethanol being both the solvent and chain-transfer agent. Hydroxy-functional oligo(vinyl acetate) was then transformed to single tailed oligo(vinyl acetate) sodium sulfate and twin tailed sodium bis(vinyl acetate)8 sulfosuccinat (AOT analogue) surfactants. The structures of oligo(vinyl acetate)-based ionic surfactants are shown in Figure 4.14. The reaction scheme for the synthesis of single-tailed oligo(vinyl acetate) sodium sulfate is shown as follows in Figure 4.15. The reaction route for the synthesis of twin tailed sodium bis(vinyl acetate)$_8$ sulfosuccinate (AOT Analogue) is similar to that of sodium bis(PPGMBE 340) sulfosuccinate as shown previously.

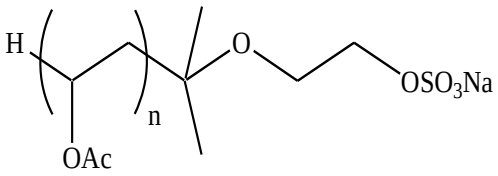

Oligo(Vinyl Acetate) (n=6,10, or 17) Sodium Sulfate (a, b, c)

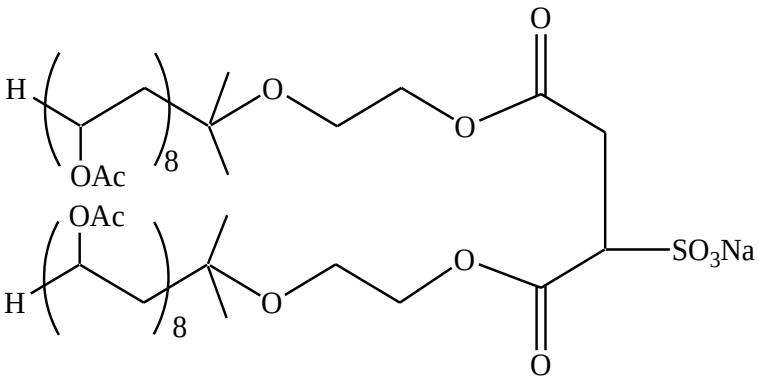

Sodium bis(Vinyl Acetate)8 Sulfosuccinate (d)

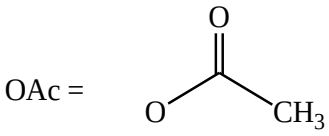

Figure 4.14. Structures of oligo(vinyl acetate)-based ionic surfactants.

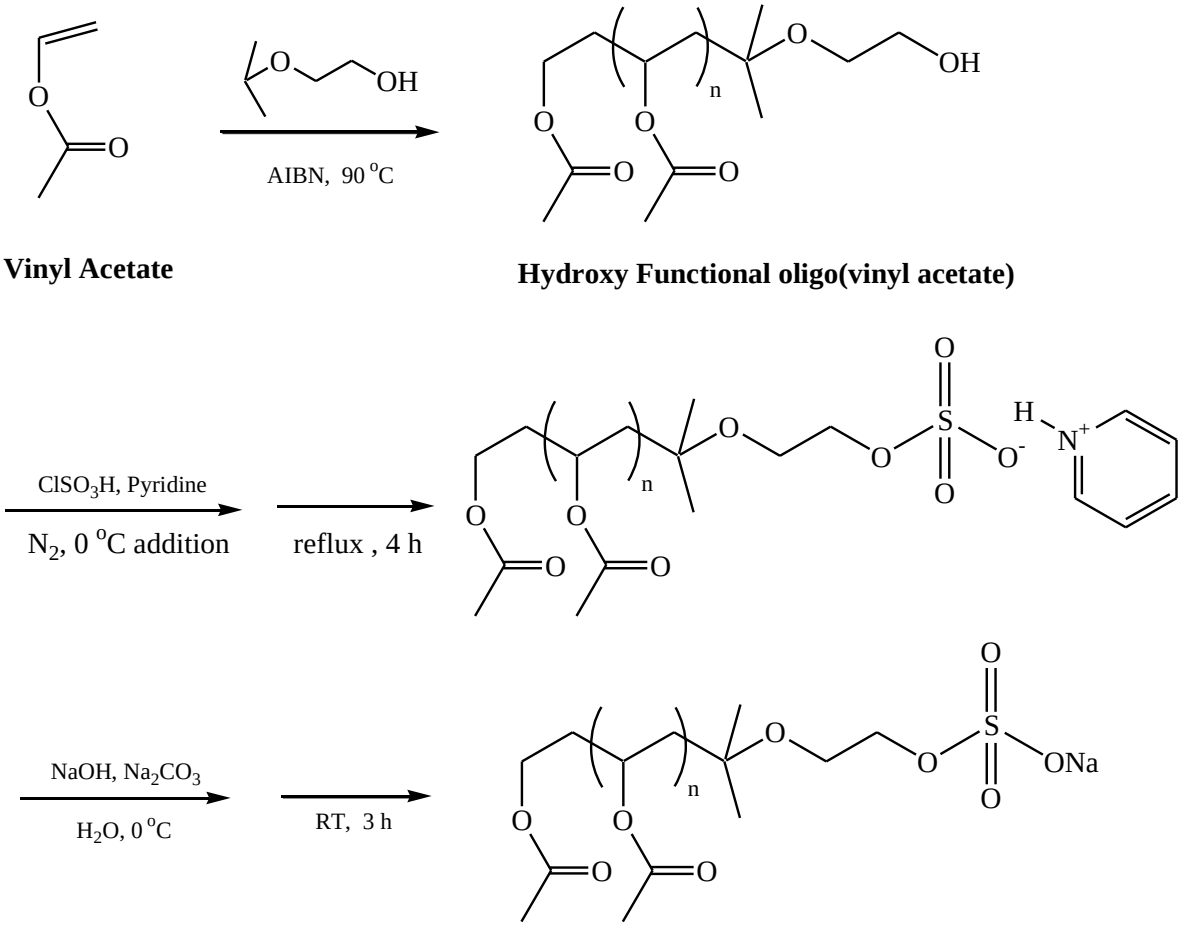

Figure 4.15. Reaction scheme for the synthesis of oligo(Vinyl Acetate) sodium sulfate.

Synthesis of hydroxy-functional oligo(vinyl acetate)

The preparation of hydroxy-functional oligo(vinyl acetate) followed the method of Zimmermann et al.[105] For a typical experiment, a solution of AIBN (0.04 g, 0.24 mmol) in 2-isopropoxyethanol (10 mL) (previously degassed for 15 min) was added to a solution of vinyl acetate (20 g, 232 mmol) in 2-isopropoxyethanol (190 mL) (previously degassed in a 3-neck 500 mL round-bottom flask by bubbling through nitrogen for 30 min). The reaction mixture was refluxed at 90 ^{o}C under a N_2 blanket for 24 h. The solvent was removed by rotary evaporation followed by vacuum desiccation at 90 ^{o}C overnight. A viscous yellow liquid of hydroxyl-functional oligo(vinyl acetate) with 10 repeat units, designated PVAc10, was recovered (15.8g, yield 79%). ^{1}H NMR δ_H ($CDCl_3$): 4.90 (10H, CH), 4.09 (2H, CH_2), 3.59 (2H, CH_2), 3.43 (1H, OH), 2.04 (30H, CH_3), 1.84 (20H, CH_2), 1.20 (6H, CH_3). ^{1}H NMR spectra showed DP_n=10 and Mn=964 g/mol. Table 4.2 lists the experimental data for the number of repeat units and number average molecular weight of four PVAc-OH samples obtained from the NMR spectra by the polymerization of vinyl acetate in 2-isopropoxyethanol. The concentration of vinyl acetate monomer in 2-isopropoxyethanol was varied to control the molecular weight at constant concentration ratio of AIBN to VAc at 0.1%. Hydroxy-functional oligo(vinly acetate) with repeat unit of 6, 8, 10, and 17 as determined through NMR spectra were obtained and represented as PVAc6-OH, PVAc8-OH, PVAc10-OH, and PVAc17-OH respectively. The functional hydroxyl end group was verified by FTIR spectra. (Appendix A Figure A.12-19)

Table 4.2. Experimental Data for PVAc-OH Oligomers from ^{1}H NMR at [AIBN]/[VAc]=0.1%.

	[VAc]^a (mol %)	**DP_n (^{1}H NMR)**	**Mn (^{1}H NMR, g/mol)**
PVAc6-OH	6.3	6	620
PVAc8-OH	8.2	8	792
PVAc10-OH	11.8	10	964
PVAc17-OH	18.6	17	1566

^{a} Molar Ratio of [VAc]/([VAc]+[2-isopropoxyethanol])

Synthesis of oligo(vinyl acetate) sodium sulfate surfactants, Figures 4.14 a,b,c

The oligo(vinyl acetate) sodium sulfate surfactants were prepared according to Murphy and Taggart's procedure.[106] In a typical experiment, chlorosulfonic acid (0.45 mL, 6.76 mmol) was added dropwise to pyridine (10 mL) in a 250 mL round-bottom flask placed in an ice bath. The solution was stirred vigorously during the dropwise addition. A solution of hydroxy-functional oligo(vinyl acetate) PVAc10-OH (5 g, 5.19 mmol) in pyridine (50 mL) was slowly added to the above solution, and cooling and stirring were continued. The contents of the flask were refluxed for about 4 h until a clear yellow solution was formed. The reaction was then quenched and the product converted to the sodium salt by pouring the contents into an ice-cooled sodium hydroxide and sodium carbonate solution (0.27 g NaOH and about 30-40 g Na_2CO_3 in 100 mL deionized water). The reaction mixture was stirred at room temperature for 3 h. The resulting oligo(vinyl acetate) surfactant solution was extracted using n-butanol (2 x 50 mL). The combined organic layers were dried over anhydrous sodium sulfate and filtered. Evaporating the solvents of pyridine and n-butanol by rotary evaporation followed by vacuum desiccation gave a dark yellow product of PVAc10-SO_3Na (4.86 g, yield 87.9 %, Mn= 1066 g/mol). The NMR spectra of PVAc6, 10, 17-OSO_3Na were illustrated in Appendix A Figure A. 20-22.

Synthesis of sodium bis(vinyl acetate)8 sulfosuccinate, Figure 4.14 d

Twin tailed oligo(vinyl acetate) AOT analogue was synthesized using the PVAc8-OH in a similar way as the PPGMBE (Mn=340) twin tailed AOT analogue that was described previously. A yellow viscous liquid was recovered as product and confirmed by the disappearance of the FTIR peak at approximately 3500 cm^{-1} (-OH) and the appearance of carbonyl peak at 1741 cm^{-1}. (Appendix A Figure A. 23-24)

4.3.3 Phase Behavior Results

Single tailed oligo(vinyl acetate) sodium sulfate surfactants, Figures 4.14 a,b,c

Viscous liquid oligo(vinyl acetate) sodium sulfate surfactants (Mn=722, 1066, 1668 g/mol) exhibit remarkably high solubility in CO_2, as shown in Figure 4.1. These levels of CO_2 solubility for an ionic surfactant are comparable to those reported for fluorous surfactants,[11] greater than the other oxygenated hydrocarbon surfactants developed during this work, and greater than those reported for branched hydrocarbon AOT analogs.[62] The PVAc-OSO_3Na surfactants consisting of 6, 10, or 17 repeat units exhibit CO_2 solubility of 4, 7 and 2.5 wt%, respectively, at room temperature and pressure less than 50 MPa. The occurrence of an optimal tail length, 10 repeat units in this case, has been previously observed in the design of surfactants with PFPE tails, and can be attributed to two competing trends. As the number of repeat units in vinyl acetate oligomer decreases, the oligomer itself becomes more CO_2 soluble; however, as the length of the oligomeric tail decreases the surfactant becomes more hydrophilic (and CO_2 phobic) as the influence of the ionic group becomes more pronounced.[59]

The solubility of oligo(vinyl acetate) surfactant decreases with increasing temperature, i.e., the pressure required to achieve miscibility with CO_2 is higher at 40 ^oC than it is at 22 ^oC, as

represented in Figure 4.16. The solubility of the oligo(vinyl acetate) surfactant in CO_2 also decreases with the addition of water at W value of 10. The surfactant solubility drops to 0.5 wt% at these conditions. W^{corr} is 0 for W value of 10 over PVAc10-OSO_3Na concentrations up to 0.5 wt% at 40 ^oC. Single phase solutions could not be realized at W values of 40, even at surfactant concentrations as low as 0.1 wt%.

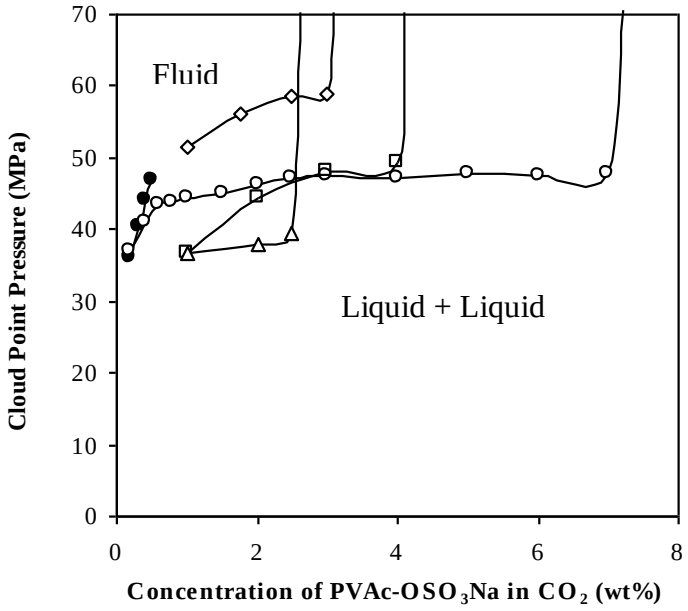

Figure 4.16. Phase behavior of PVAc-OSO_3Na/CO_2 mixtures. PVAc6-OSO_3Na, 22 ^oC, W=0 (□); PVAc10-OSO_3Na, 22 ^oC, W=0 (o); PVAc17-OSO_3Na, 22 ^oC, W=0 (Δ); PVAc10-OSO_3Na, 22 ^oC, W=10 (●); PVAc10-OSO_3Na, 40 ^oC, W=0 (◊). (Appendix A Figure A.25. Surfactant concentration in mM).

Twin tailed sodium bis(vinyl acetate)8 sulfosuccinate, Figure 4.14 d

The sodium bis(vinyl acetate)8 sulfosuccinate AOT analogue consisting of twin tails of 8 repeat units on each tail (Mn= 1747 g/mol) was a viscous liquid that exhibited CO_2 solubility up to 3 wt% at 22 ^oC and pressure less than 40 MPa, as shown in Figure 4.17**.** The solubility

decreases with the addition of water at W= 10. This surfactant was the only one (of those illustrated in Figure 4.14) capable of solubilizing water to W values as high as 50, at surfactant concentrations up to 1 wt%. Table 4.3 lists W and W^{corr} for the sodium bis(vinyl acetate)8 sulfosuccinate surfactant in water and CO_2 mixture at different weight percents and 22 ^{o}C.

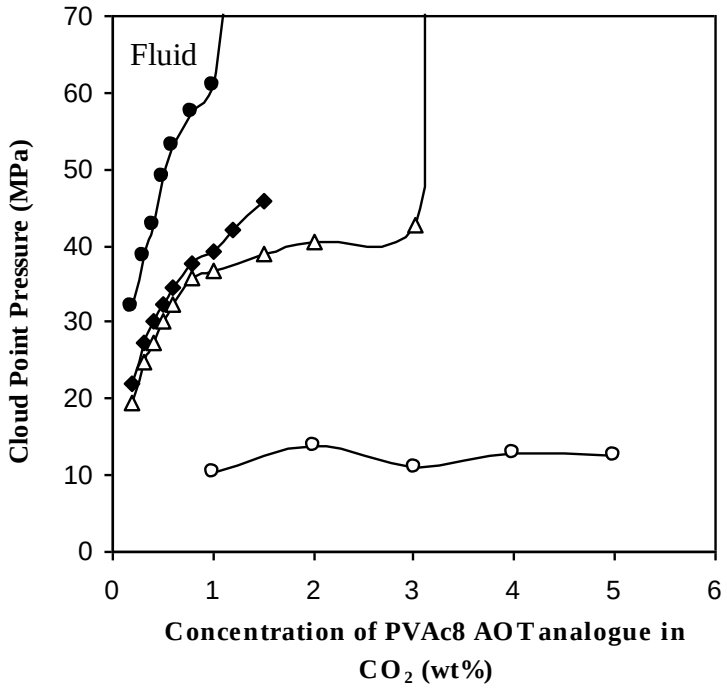

Figure 4.17. Phase behavior of sodium bis(vinyl acetate)8 sulfosuccinate/CO_2 mixtures at 22 ^{o}C. W = 0 (Δ); W = 10 (♦); W = 50 (●). Sodium bis(dodecafluoroheptyl) sulfosuccinate, W=0 (o). [10] (Appendix A Figure A.26. Surfactant concentration in mM).

Table 4.3. W and W^{corr} for sodium bis(vinyl acetate)8 sulfosuccinate in water and CO_2 mixture at different weight percents and 22 ^{o}C. *When the amount of water is not sufficient to saturate the CO_2, W^{corr} is reported as 0.

Sodium bis(vinyl acetate)$_8$ sulfosuccinate Concentration, wt%	Temperature, ^oC	W	W^{corr*}
0.2-1.5	22	10	0
0.15-0.3	22	50	0
0.4	22	50	10.80
0.5	22	50	17.83
0.6	22	50	22.51
0.8	22	50	28.87
1	22	50	32.69

4.3.4 Spectroscopic Results

The single tailed PVAc10-OSO_3Na was loaded at 0.15 wt% with water loading of W = 10 (W^{corr}=0, 0.025 wt%) and methyl orange at 4.7 x 10^{-5} M. The system was pressurized to 38 MPa at 25 °C and stirred for 1 hour. After this mixing period, a methyl orange peak was observed at 422 nm implied the formation of water-in-CO_2 (w/c) reverse microemulsions. The twin tailed sodium bis(vinyl acetate)8 sulfosuccinate AOT analogue was loaded at 0.15 wt% with water loading of W = 10, 20, 30, and 40, respectively, (0.015 wt%, 0.03 wt%, 0.045 wt%, and 0.06 wt%, respectively) at W^{corr} = 0, and methyl orange at 4.7 x 10^{-5} M. After pressurizing to 34.5 MPa at 22 °C, the system was allowed to mix for over an hour to reach a single phase microemulsion. Figure 4.18 shows the UV-vis spectra for the twin tailed sodium bis(vinyl acetate)8 sulfosuccinate w/c reverse microemulsion system. As shown in Figure 4.18, the UV absorption peaks which assigned at about 423 nm indicate the formation of the water-in-CO_2 reverse microemulsions. The intensity of the methyl orange peak increases with the loading

water ranging from W = 10 to 40, which indicates that the concentration of methyl orange within the microemulsions increases as the amount of loading water increases. However, the absorption maximum wavelength, λ_{max}, doesn't shift to higher wavelengths, which implies the polarity of the microenvironment within the reverse micelles doesn't increase as the increasing of water amount loaded to the system. Methyl orange dissolved in bulk water results in an absorption maximum wavelength at 464 nm. The absorption bands of ~423 nm in these studies indicate that the microenvironment within the reverse micelles of the ionic surfactants with PVAc tails is similar to that of neat methanol (methyl orange absorption at ~421 nm), and slightly more polar than that of the cores of dry PFPE–$COONH_4$ reverse micelles (~416 nm).[68, 69] Whereas the twin tailed vinyl acetate based surfactants lead to high water loading values up to W=50, the methyl orange solubilities and polarities are rather limited. This can be attributed to the relatively low corresponding weight percent of water caused by the low surfactant loading concentration and the high molecular weight and the $W^{corr} = 0$ at these conditions, which means the amount of water added to the system would be insufficient to saturate the CO_2.

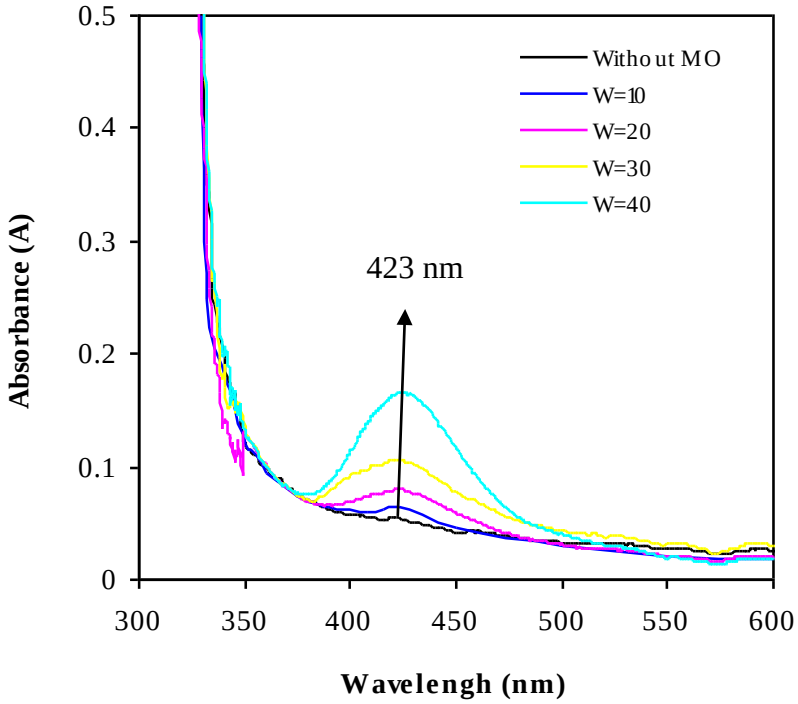

Figure 4.18. UV-vis absorption spectra of methyl orange in 0.15 wt% twin tailed sodium bis(vinyl acetate)8 sulfosuccinate based water-in-CO_2 reverse microemulsions with different loading of water at 34.5 MPa and 25 ^{o}C.

4.4 DISCUSSIONS

4.4.1 Modeling Results

Wang and Johnson[95] have optimized the geometries and calculated the binding energies for a single water molecule interacting with an isopropyl acetate (IPA) molecule. Two different binding modes were found for the IPA/H_2O system. As shown in Figure 4.19, for mode (A) the water molecule mainly interacts with the carbonyl oxygen. For mode (B) H_2O binds mainly with the ether oxygen. The interaction energies for the two modes are listed in Table 4.4. The interactions between IPA and water molecules as shown in Table 4.4 are much stronger than the strongest binding energy between IPA and CO_2.[54] The calculations therefore predict that the tails of the acetate functionalized surfactants (Figure 4.1a-c, Figure 4.14 a-d) are hydrophilic.

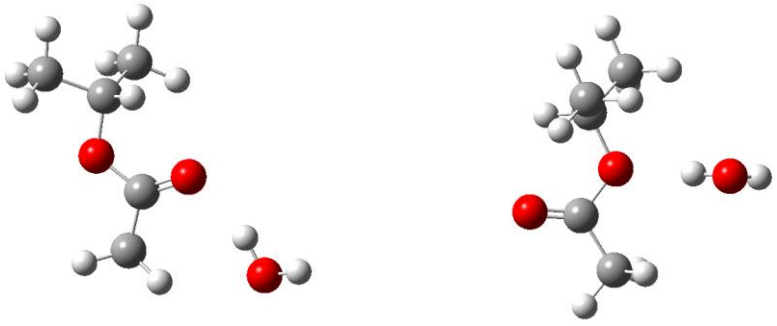

(A) (B)

Figure 4.19. Two different binding modes for the isopropyl acetate/H_2O system. (white = H, gray = C, red = O).

Table 4.4 Interaction energies for several different dimers related to the CO_2/H_2O surfactant systems. The energies are computed at the MP2/aug-cc-pVDZ level of theory.

	IPA/H_2O		IPA/CO_2*	H_2O/H_2O [107]		CO_2/CO_2	
	(A)	(B)				T-shape	Slipped parallel
Interaction energy (kJ/mol)	-27.0	-21.3	-15.9	-19.6	-20.7**	-5.1	-5.8

* There are actually three binding modes for the IPA/CO_2 dimer. We chose the mode that has the strongest interaction energy for comparison.[54]

** The value is calculated at the MP2 level of theory and extrapolated to the complete basis set limit.[107]

4.4.2 Water Solubility Values of Three Acetate Functionalized Surfactants

Furthermore, experiments were performed to measure the water solubility of peracetyl gluconic sodium carboxylate (Figure 4.1b), peracetyl gluconic ammonium carboxylate (Figure 4.1c), and oligo(vinyl acetate)10 sodium sulfate (Figure 4.14b). 20 μL of water was initially added to 0.08 g of surfactant (80 wt%), then water was gradually added to the mixture followed by stirring the mixture using a Vortex-Genie® 2 mixer until the surfactant was completely dissolved. The measured solubilities are reported in Table 4.5 and clearly show that both peracetyl surfactants are significantly more water soluble than the vinyl acetate-based surfactant. The head groups on the peracetyl- and vinyl acetate-based surfactants are not identical. However, the sodium sulfate head group of (Figure 4.14b) should make that surfactant more water soluble than the sodium carboxylate head group of (Figure 4.1b) and ammonium carboxylate head group of (Figure 4.1c).

Therefore, we expect that the differences in water solubility are due to the composition of the tail groups is larger than the head groups indicated by the data in Table 4.5.

Table 4.5. Water solubility values of three acetate functionalized surfactants

Surfactant	Water solubility (wt%)
Peracetyl gluconic sodium carboxylic (Figure 4.1b)	64 %
Peracetyl gluconic ammonium carboxylic (Figure 4.1c)	73 %
Oligo(vinyl acetate)10 sodium sulfate (Figure 4.13b)	40 %

4.4.3 Effects of the Addition of Water in Surfactants/CO_2 Systems

The addition of water to CO_2 mixtures containing acetate-based surfactants resulted in an increase in the cloud point pressures. Water molecules will compete with CO_2 molecules for binding to the acetate groups. The acetate tail groups will preferentially bind with water molecules because of the more favorable binding energies (see Table 4.4), thus lowering the CO_2 solubilities of the surfactants. Experiments have shown that the addition of water does indeed increase the cloud point pressures of two of the peracetyl gluconic-based surfactants (Figure 4.1b,c) and also of the PVAc single/twin tailed surfactants (Figure 4.14a-d). These observations are consistent with our theoretical analysis. However, PGESS (Figure 4.1a) exhibits the opposite behavior, which couldn't dissolve in CO_2 in the absence of water, and its solubility increases as water is added. This may be due to co-solvent effects with water. PGESS is insoluble in CO_2 because of its extremely polar head group. Adding water to the PGESS/CO_2 system acts to shield the sulfate head group from CO_2 and therefore increases the solubility. Therefore, water plays

competing roles in the PGESS/CO_2 system. On one hand, it increases solubility by shielding the head group from the nonpolar CO_2 environment. On the other hand, water competes with CO_2 in binding to the CO_2-philic acetate tail.

4.4.4 Formation of the Reverse Micelles

The experiments have shown that only the PVAc-based surfactants can form reverse micelles. None of the peracetyl gluconic-based surfactants exhibit micelle formation, although their tail groups have similar structures to those of PVAc-based surfactants. The formation of micelles requires a tail that is sufficiently hydrophobic to drive water out of the bulk homogeneous phase into confined micelles. Our calculations indicate that the peracetyl tails are very hydrophilic. We therefore speculate that peracetyl tails do not have a large enough hydrophobic driving force to form micelles. In contrast, the methylene groups in the PVAc tails are relatively hydrophobic, which provides enough of an energetic driving force to stabilize the micelles. The difference in water solubilities of peracetyl gluconic-based surfactants and PVAc-based surfactants (Table 4.5) indicates that peracetyl tails are indeed more hydrophilic than PVAc tails. The difference in water solubilities provides a plausible explanation for the observation that PVAc-based surfactants form micelles while the surfactants with peracetyl gluconic tails do not.

5.0 PREPARATION OF SILVER NANOPARTICLES VIA CO_2-SOLUBLE HYDROCARBON-BASED METAL PRECURSOR

The objectives of this study were to determine the solubility of silver acetylacetonate and (if this solubility was low) to design a novel organometallic complex with much greater CO_2-solubility that could be used to form silver nanoparticles in CO_2 via reduction in the presence of fluorous or non-fluorous stabilizing thiols. Silver bis(3,5,5-trimethyl-1-hexyl)sulfosuccinate (Ag-AOT-TMH) was selected as the metal-ligand candidate because of the ease of its synthesis; simply requiring an ion exchange of the CO_2-soluble ionic surfactant AOT-TMH to yield Ag-AOT-TMH. Ion exchange of other ionic surfactants composed of oxygenated hydrocarbon tails was not successful due to the instability of the Ag^+ counterion during the synthesis.

5.1 MATERIALS

Silver acetylacetonate, fumaryl chloride, 3,5,5-trimethyl-1-hexanol, sodium hydrogensulfite, silver nitrate, tert-nonyl mercaptan, 4-tert butylbenzenethiol, and solvents was purchased from Aldrich. The fluorocarbon thiol 1H,1H,2H,2H-perfluorooctanethiol ($C_6F_{13}C_2H_4SH$) was obtained from Oakwood Product Inc. Poly(mercaptopropyl) methyl siloxane (Mw=4000-7000) was

obtained from Gelest, Inc. Thiol terminated poly(ethylene oxide) (Mn=2000, Mw=2100) was obtained from Polymer Science, Inc. H_2 (99.999), N_2 (99.995%) and CO_2 (99.99%) gases were obtained from BOC gases and perfluorobutylmethyl ether (HFE−7100) was obtained from 3M. All chemicals were used as received.

5.2 Synthesis of a CO_2-Soluble Hydrocarbon-based Silver Precursor

The structures of AOT-TMH and Ag-AOT-TMH are shown in Figure 5.1.

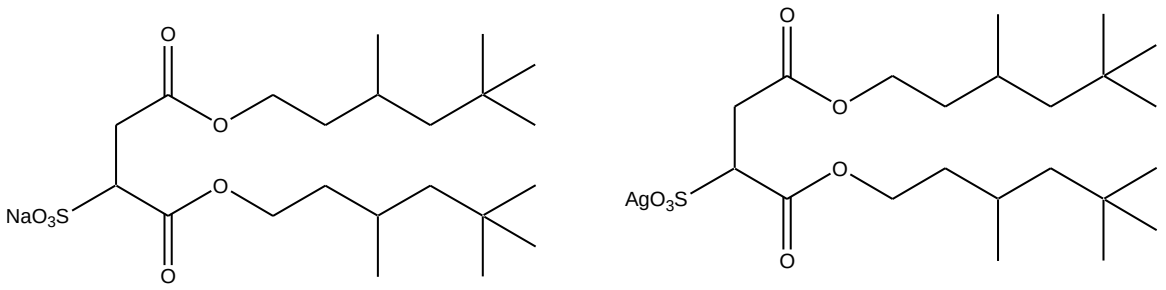

AOT-TMH (a) **Ag-AOT-TMH (b)**

Figure 5.1. Structures of sodium bis(3,5,5-trimethyl-1-hexyl) sulfosuccinate (AOT-TMH) and silver precursor, silver bis(3,5,5-trimethyl-1-hexyl) sulfosuccinate (Ag-AOT-TMH).

Sodium bis (3,5,5-trimethyl-1-hexyl) sulfosuccinate (AOT-TMH) with highly methyl branched tail as an AOT analogue was first synthesized by Nave and Eastoe.[60] Ag-AOT-TMH was synthesized via the esterification of fumaryl chloride and 3,5,5-trimethyl-1-hexanol, sulfonation by sodium hydrogensulfite, then ion exchange by $AgNO_3$, as shown in Figure 5.2.

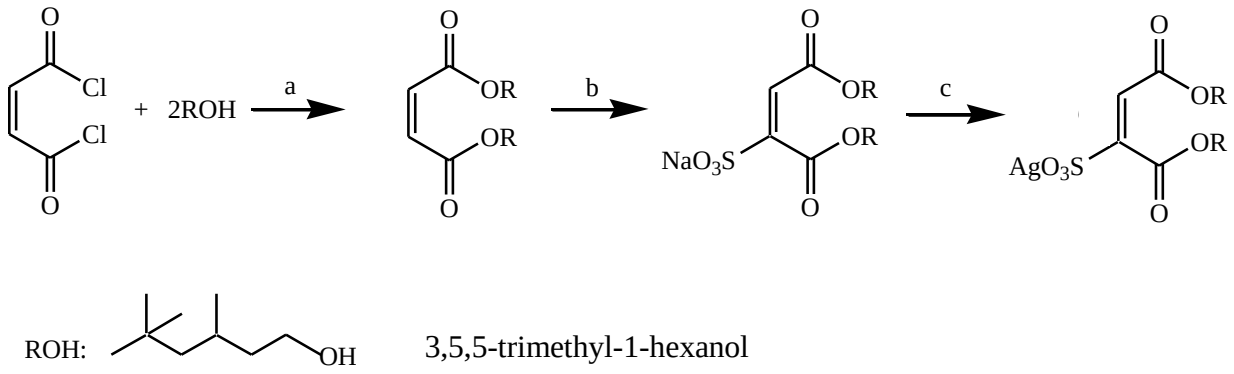

Figure 5.2. Synthesis of Ag-AOT-TMH (a) anhydrous THF, RT, 24 h; (b) $NaHSO_3$, $^{i}PrOH$-H_2O, 80 ^{o}C, 24 h; (c) $AgNO_3$, ethanol–H_2O, RT.

The glassware was oven-dried overnight and purge with ultra-high purity nitrogen before use. 3,5,5-trimethyl-1-hexanol (14.4 g, 100 mmol) and anhydrous THF (150 mL) were charged in a 500 mL 3-neck round-bottom flask equipped with a stirring bar and condenser under a steady flow of nitrogen. After cooling to 0 ^{o}C, fumaryl chloride (7.65 g, 50 mmol) was added dropwise. The reaction mixture was stirred for the next 24 h at room temperature. After rotary evaporation of THF, the mixture was dissolved in 100 mL diethyl ether, washed with 50 mL 1N HCl, 50 mL saturated $NaHCO_3$, and 50 mL saturated NaCl solutions sequentially. The ether extract was dried over anhydrous Na_2SO_4 and filtered, then ether was removed by rotary evaporation. 16.56 g pale yellow oil of diester product was obtained with 90% yield. The obtained diester was subject to sulfonation with sodium hydrogensulfite. A solution of sodium hydrogensulfite (3.45 g, 32.56 mmol) in water (60 mL) (previously degassed for 15 min) was added dropwisely to a solution of the diester (6 g, 16.28 mmol) in isopropanol (80 mL) (previously degassed in a 3-neck round-bottom flask by bubbling through N_2 for 30 min). The reaction mixture was then refluxed for the next 24 h. After rotary evaporation of the solvent, the residue was dissolved in 100 mL ether and the water layer was extracted with ether (2×30 mL).

The combined ether extraction was dried over anhydrous Na_2SO_4 and then filtered. White paste was yielded after removing ether. Traces of water were removed by redissolving the paste in chloroform followed by drying over Na_2SO_4. Chloroform was removed by rotary evaporation and the resulting paste was dried under vacuum oven at 40 ^oC overnight. White solid of AOT-TMH was obtained (5.77 g, yield 75%), which was then transformed to Ag-AOT-TMH via ion exchange. A silver nitrate (5.025 g, 29.58 mmol) aqueous solution (10 mL) was mixed with AOT-TMH (0.8297 g, 1.8 mmol) dissolved in ethanol (5 mL). After mixing for 6 h, ether (6 mL) was added which led to the formation of two separate phases. The lower phase containing $NaNO_3$ and excess $AgNO_3$ was removed to leave the upper phase containing the Ag-AOT-TMH. The upper phase was dried on a rotary evaporator, redissolved in isooctane, and centrifuged to separate any residual solids. Finally, isooctane was removed in a vacuum oven at room temperature, and yellow solid of Ag-AOT-TMH was received as product (0.82 g, 84%). The FTIR and ^1H NMR spectra of the intermediate diester and the sodium bis(3,5,5-trimethyl-1-hexyl) sulfosuccinate (AOT-TMH) are shown in Appendix B.1-3. Soil analysis indicates the Ag^+ exchange for the Na^+ is around 85% (Appendix B.4).

5.3 PHASE BEHAVIOR STUDY

5.3.1 Experimental Apparatus

The experimental setup of the phase behavior study with silver acetylacetonate, AOT-TMH, and Ag-AOT-TMH is the same as shown in Chapter 4.1.4.1.

5.3.2 Phase Behavior Results

The commercially available silver acetylacetonate was tested for CO_2 solubility at 40 ^{o}C. At concentrations as low as 0.01 wt% and pressures as high as 70 MPa, there was no evidence of dissolution, swelling or melting point reduction of the silver acetylacetonate particles.

The solubility of AOT-TMH and Ag-AOT-TMH in CO_2 were then evaluated. Figure 5.3 presents a pressure-composition diagram for this mixture at 40 ^{o}C. Although the AOT-TMH was initially insoluble when CO_2 was introduced, the solid surfactant melted in CO_2 immediately at room temperature and 13.8 MPa and then formed a single transparent solution after 1 h stirring at 1500 rpm. Figure 5.3 illustrates that the cloud point pressure increases with AOT-TMH concentration, reaching a limiting value of about 1 wt% at 50 MPa. Ag-AOT-TMH also melted in CO_2 immediately and reached a limiting solubility of 1.2 wt% at 52 MPa.

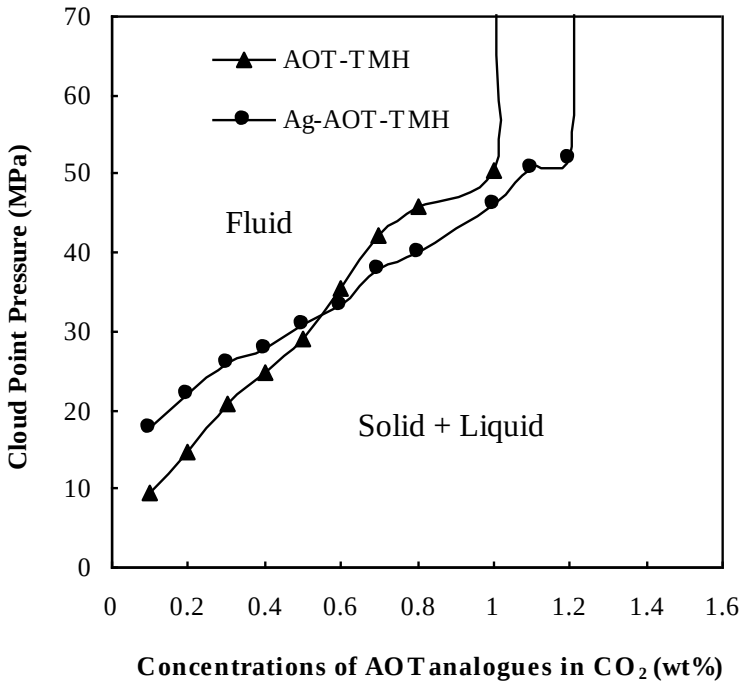

Figure 5.3. Phase behavior of AOT-TMH and Ag-AOT-TMH at 40 ^{o}C. (Appendix B Figure B.4. Surfactant concentration in mM).

5.4 SILVER NANOPARTICLE FORMATION

Silver nanoparticle formation experiment was carried out at Dr. Roberts' group in Chemical Engineering Department at Auburn University.[108]

5.4.1 Experimental Apparatus

Nanoparticles were synthesized in a 32 mL stainless steel high-pressure vessel equipped with pressure gauge, resistance temperature detector (RTD), and parallel quartz windows for UV-vis

characterization. A magnetic stir bar was used to facilitate mixing. The vessel was initially filled with 0.06 wt% Ag-AOT-TMH, 0.5 wt% fluorinated thiol. After sealing the vessel, an ISCO syringe pump was used to add specific quantity of CO_2 to the vessel to reach the desired pressure of 28.6 MPa. The temperature of the vessel was raised to 40 ^{o}C by using a heating tape which was wrapped around the vessel and connected to the temperature controller. The system was mixed for one hour to reach a single phase. Reducing agent was then injected by forcing in 200 μL of a 0.8 M $NaBH_4$/ethanol solution with additional carbon dioxide.

5.4.2 Nanoparticle Formation Results

The CO_2 solution turned into dark red color in less than 2 minutes after the introduction of the reducing agent, but unfortunately, due to the highly optical absorbance of the silver nanoparticles, the collection of accurate UV−vis data was not possible. The particles were stable in solution for 24 h as the solution maintained its visible red color. The vessel was subsequently depressurized, and the particles were redispersed in HFE−7100 and placed onto a transmission electron microscopy (TEM) grid for analysis.

Figure 5.4 shows the TEM image of silver nanoparticles. A statistical analysis of the TEM image yields an average size of 3.5 nm in diameter, a standard deviation of 0.8 nm, and the size distribution is shown in Figure 5.5. Energy dispersive spectroscopy (EDS) was also performed on the particles and identified that the particles consist of silver with the fluorinated thiol ligand present as indicated by the absorbance of silver, fluorine, and sulfur in Figure 5.6. The large copper peak is due to the copper support of the TEM sample grid. This analysis reveals the

effectiveness of the fluorocarbon thiol molecule as a stabilizing ligand on the silver nanoparticles.

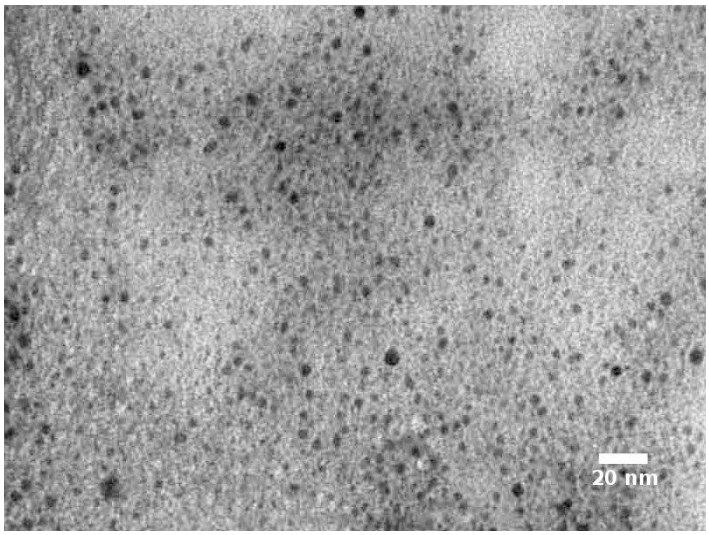

Figure 5.4. TEM Image of silver nanoparticles formed by reducing CO_2 solution containing Ag-AOT-TMH and fluorinated thiol stabilizing ligands using $NaBH_4$ as reducing agent.[108]

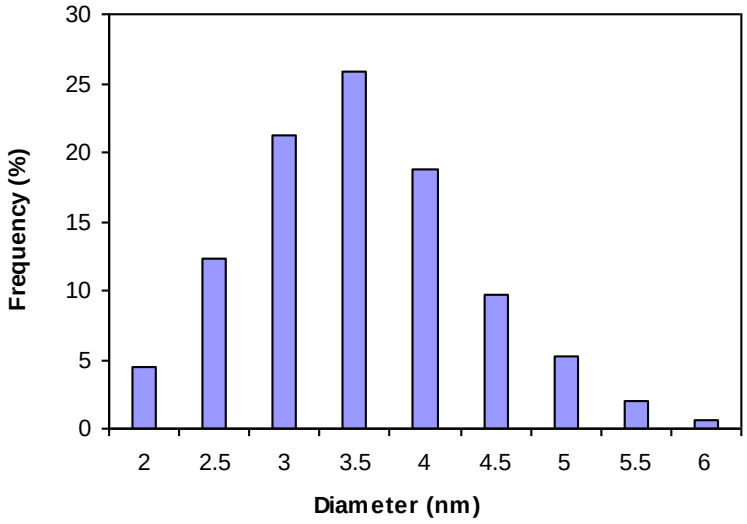

Figure 5.5. Size distribution of silver nanoparticles synthesized in CO_2. P = 28.6 MPa, t = 40 ^oC, [Ag-AOT-TMH] = 0.06 wt%, [Fluorinated Thiol] = 0.5 wt%.[108]

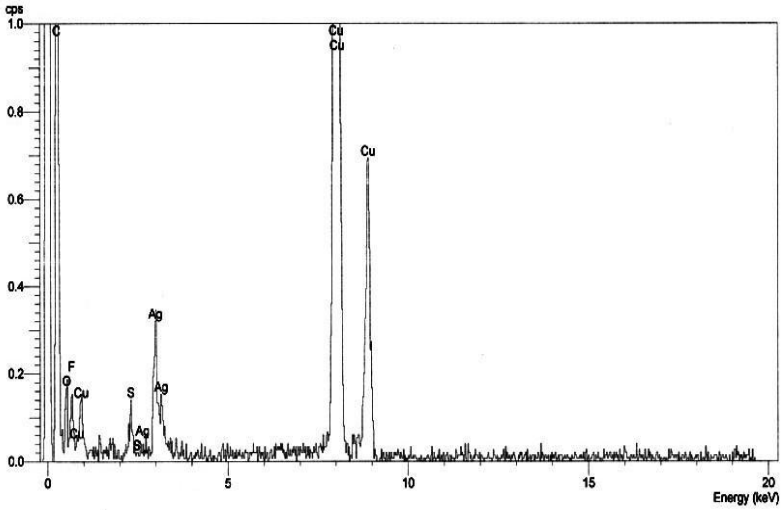

Figure 5.6. EDS measurement of the silver nanoparticles. The spectrum shows the presence of silver along with fluorine and sulfur indicating the presence of the fluorinated thiol stabilizing agent.[108]

5.5 NON-FLUOROUS THIOLS RESULTS

Non-fluorous thiols, including silicone-based, PEG-based, and hydrocarbon-based thiols, were also investigated for CO_2 solubility study and their abilities to stabilize nanoparticles in CO_2. Figure 5.7 shows the structures of silicone-based and PEG-based thiols investigated in this study. Poly(mercaptopropyl) methyl siloxane and thiol terminated poly(ethylene oxide) are insoluble in CO_2 at room temperature at concentrations as low as 1 wt%. Hydrocarbon-based thiols containing tert-butyl group, 4-tert-butylbenzenethiol and tert-nonyl mercaptan, are very miscible with CO_2 at moderate pressure values, as shown in Figure 5.8 and Figure 5.9. Tert-nonyl mercaptan is more branched than the 4-tert-butylbenzenethiol, and therefore is more miscible with CO_2. However, these hydrocarbon-based thiols were unable to disperse and stabilize the silver nanoparticles.

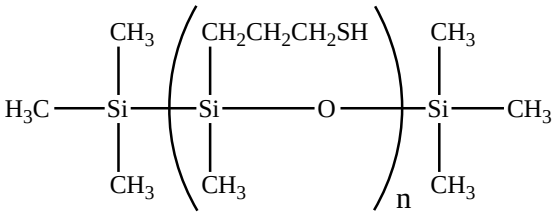

Poly(mercaptopropyl) methyl siloxane

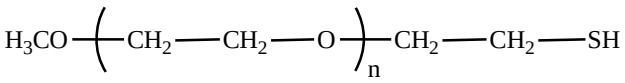

Thiol terminated Poly(ethylene oxide)

Figure 5.7. Structures of silicone-based and PEG-based thiols investigated in this study.

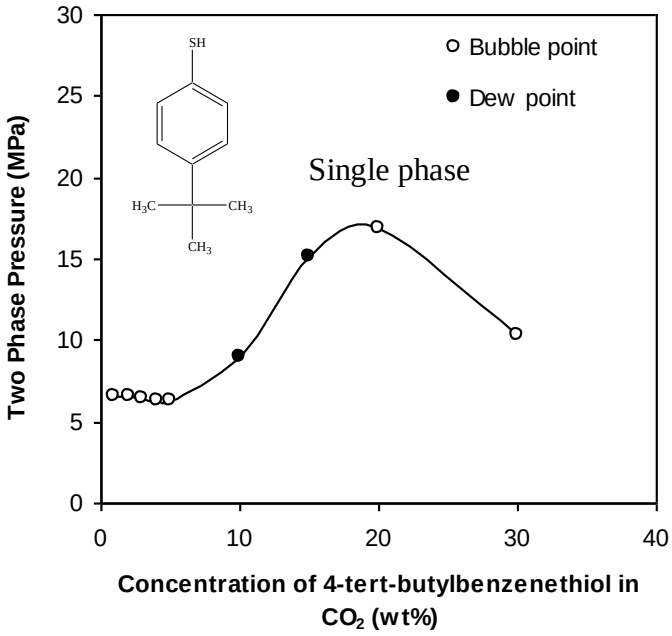

Figure 5.8. Phase behavior of 4-tert-butylbenzenethiol at 22 °C.

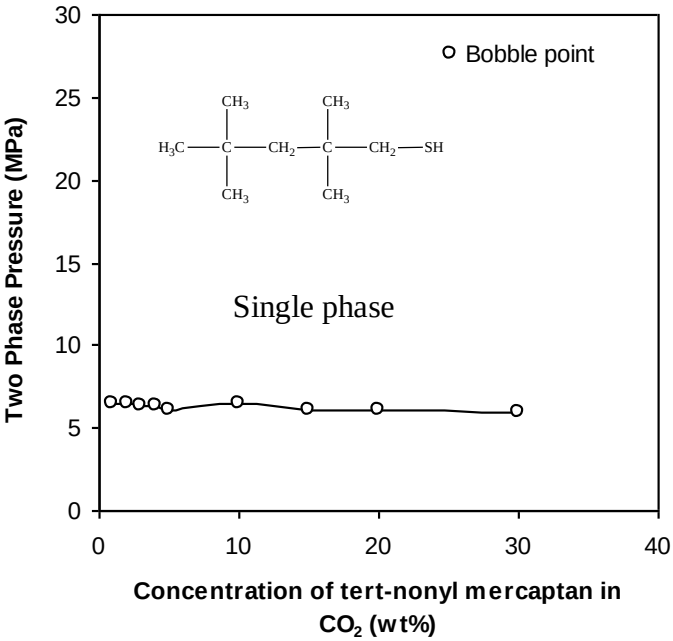

Figure 5.9. Phase behavior of tert-nonyl mercaptan at 22 °C.

5.6 CONCLUSIONS

A previously reported CO_2 soluble hydrocarbon complex, silver acetylacetonate, is less than 0.01 wt% CO_2 soluble at 40 ^oC and 70 MPa, whereas the Ag-AOT-TMH synthesized during this investigation can dissolve in CO_2 up to 1.2 wt% at 40 ^oC and 52 MPa. Silver nanoparticles (1−6 nanometers in diameter) were synthesized at 40 ^oC and 28.6 MPa from Ag-AOT-TMH in CO_2 using $NaBH_4$ as a reducing agent. A CO_2-soluble fluorinated thiol was used to sterically stabilize the silver nanoparticles, as evidenced by TEM and EDS analysis. Attempts to produce the silver nanoparticles in a completely non-fluorous system were unsuccessful because stabilization could not be attained with silicone-, PEG-, or hydrocarbon-based thiols.

6.0 STABLE DISPERSION OF SILVER NANOPARTICLES IN CARBON DIOXIDE WITH HYDROCARBON-BASED LIGANDS

6.1 STABLE DISPERSION OF NANOPARTICLES IN CARBON DIOXIDE WITH LIGANDS

In order to disperse particles in a given solvent, it is common to use ligands extending from the surface of the nanoparticles that can interact with the solvent molecules. Favorable interactions between the solvent molecules and the ligand tails provide enough repulsive force between particles to overcome the attractive Van der Waals forces that occur between particles in solution. Unfortunately, CO_2 is a poor solvent for most commonly available ligands and surfactants. As a result, fluorinated surfactants have been required to stabilize nanoparticles in CO_2 or to form microemulsions for the synthesis of nanoparticles within CO_2. Early studies showed the ability of these fluorinated compounds to support water in CO_2 microemulsions[68, 69] based on better surfactant tail – solvent interactions. These water in CO_2 microemulsion systems have since been used to form a variety of nanoparticles in CO_2[109-115]. The need for surfactants, and a separate water phase, during synthesis of nanoparticles in CO_2 was eliminated by Shah et al.[81, 82] and McLeod et al.[75] They synthesized and subsequently precipitated

nanoparticles in single CO_2 phase. The approach in these studies was to reduce CO_2-soluble metallic precursors in a single CO_2 phase and to prevent agglomeration by capping the particles with CO_2-soluble fluorinated ligands that provide for steric stabilization of the particles. Unfortunately, these processes continue to require the use of fluorinated ligands to disperse the nanoparticles. These CO_2 soluble fluorinated compounds suffer from the disadvantages of being both expensive and environmentally unfriendly[116, 117].

Several research groups[10, 61, 116, 118-126] have sought to find non-fuorinated compounds that would be soluble in CO_2 in the hopes of creating non-fluorinated polymers as well as surfactants where the latter could be used to form microemulsions in CO_2. Research has shown that branched, methylated, and stubby surfactants can be used to form micelles in supercritical CO_2, because of higher tail solvation and smaller tail-tail interactions[44, 45, 61, 127]. Although some success has been reported in forming fluorine-free microemulsions using hydrocarbon surfactants[46, 128] and in making macroemulsions using silica nanoparticles[129], ionic hydrocarbon surfactants[130, 131], or trisiloxane surfactants[127] in CO_2, no reports to date have demonstrated the synthesis or dispersion of nanoparticles within these non-fluorinated surfactant systems in CO_2. To make full use of the advantages of supercritical CO_2, a stable dispersion of fluorine-free nanoparticles in a single CO_2 phase would be ideal. While metallic nanoparticles have been stably dispersed in pure liquid and supercritical CO_2[132, 133], fluorinated ligands were required. The objective of this study is to illustrate the ability to stably disperse ligand coated metal nanoparticles in neat CO_2 without the need for fluorinated constituents. To accomplish this, iso-stearic acid, received from Nissan Chemicals, as structure shown in Figure 6.1, was chosen as a ligand for dispersion of silver nanoparticles in CO_2 solvent.

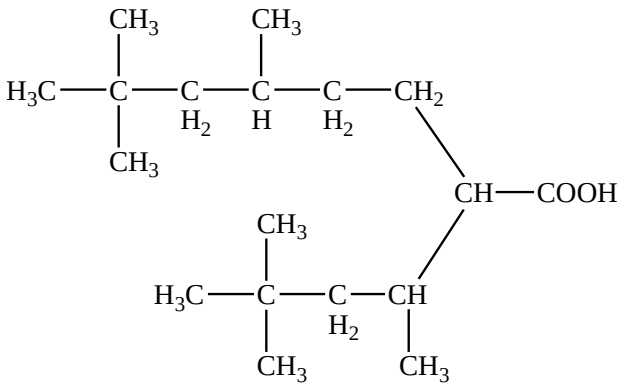

Figure 6.1. Structure of iso-stearic acid, Mn = 284 g/mol.

6.2 EXPERIMENTAL APPARATUS

The experimental setup of the phase behavior study with iso-stearic is the same as shown in Chapter 4.1.4.1.

6.3 PHASE BEHAVIOR RESULTS

Figure 6.2 presents a pressure-composition diagram for the iso-stearic acid-CO_2 mixture demonstrating that iso-stearic acid is highly CO_2-soluble. Iso-stearic acid, a short, stubby compound with branched, methylated tails, is completely miscible with CO_2 at pressures above 13 MPa at 22 ^{o}C, as shown in Figure 6.2. No data was collected for the small VL1 two phase region at the CO_2-rich end of the diagram. The high CO_2 solubility may be attributable to the highly methylated branched tails, in which the surface energy of the pendant methyl groups is much lower than that of the CH_2 groups of linear tails[30]. These interactions between the ligand tails and CO_2 are also what make iso-stearic acid a useful ligand to sterically stabilize metallic nanoparticles in CO_2. Iso-stearic acid coated silver nanoparticles have been stably dispersed in carbon dioxide with hexane cosolvent. Neat carbon dioxide has successfully dispersed iso-stearic

acid coated silver nanoparticles that had been deposited on either quartz or polystyrene surfaces. These results are the first reports of sterically stabilized nanoparticles in carbon dioxide without the use of any fluorinated compounds.[134]

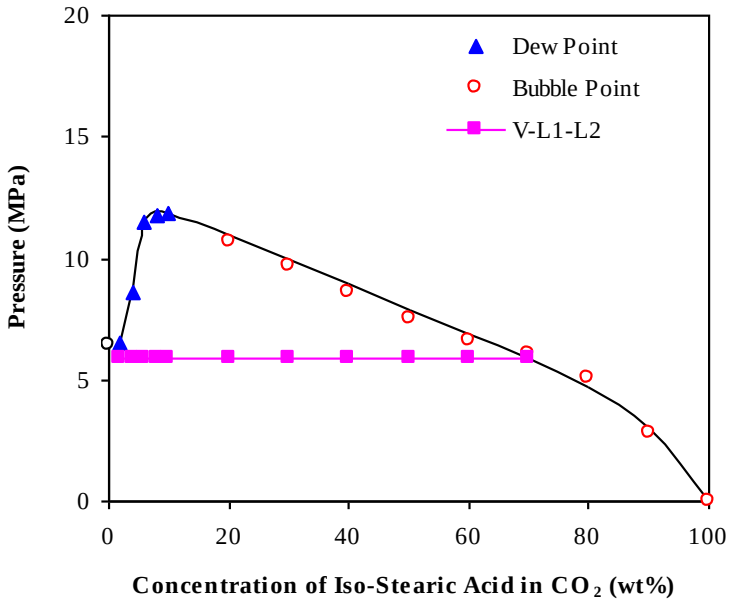

Figure 6.2. Phase behavior of iso-stearic acid/CO_2 mixture at 22 ^{o}C. No data was collected for the small VL1 two phase region at the CO_2-rich end of the diagram.

7.0 STABILITY OF CO_2-WATER EMULSIONS STABILIZED WITH CO_2-SOLUBLE SURFACTANTS

7.1 INTRODUCTION

Carbon dioxide is an attractive fluid for enhanced oil recovery (EOR) processes because it is a good solvent for light crude oils and it is available in large quantities from natural reservoirs at high purity and pressure. Currently, about 1.5 billion standard cubic feet (SCF) per day of CO_2 are injected into domestic reservoirs, resulting in the recovery of nearly 200,000 barrels of oil per day. An inherent disadvantage to this CO_2 flooding process is the low viscosity of CO_2 (0.03-0.1 cp) relative to that of the oil being displaced (0.1-50 cp), causing mobility control problems. The high mobility of CO_2 (permeability/viscosity) in the sandstone or limestone causes CO_2 "fingering" its way towards the production well, bypassing much of the oil in the reservoir and reducing the areal sweep efficiency. Moreover, the low viscosity of CO_2 also contributes to the low vertical sweep efficiency, especially in stratified reservoirs that include two or more layers into which the CO_2 may enter. For example, the formation may contain a highly permeable, water-rich zone caused by decades of prior water flooding, while the other less permeable layer is oil-rich because the water preferred to enter the high permeability zone. The high mobility of CO_2 induces it to preferentially enter the highly permeable water-rich zone, leaving oil residing in the less permeable zone.

The mobility of a CO_2 foam or emulsion (e.g. 80-95 vol% dense CO_2, 1% surfactant, and 9% brine) in porous media is much lower than that of CO_2 alone. Therefore, CO_2 foams have been investigated as a means of reducing fingering by making moderate decreases in mobility, or for diverting CO_2 to low permeability oil-rich zones by initially forming a very low mobility foam in the water-rich zone. CO_2 foams have been studied by both academic groups [42, 88-90, 135-137] and by industrial researchers [91, 92, 138-141]. In all previously reported applications, an aqueous surfactant solution has been injected into the porous media, followed by CO_2 injection in a process referred to as surfactant-alternating-gas (SAG). The in-situ generation of foams results in high phase volume CO_2 foams in which bubbles of the supercritical CO_2 (or droplets of liquid CO_2) are separated by thin aqueous films. Shorter cycles are recommended in the SAG process to obtain a more uniform foam quality. Bernard and coworkers [138] have presented mobility control results indicating that the CO_2 mobility can be reduced by almost 50% using a commercially available surfactant, Alipal CD-128 (ammonium sulfate ester), as the foaming agent. Researchers at Shell Development Company [141, 142] demonstrated a relationship between surfactant compositions and surfactant adsorption, foam stability, and mobility control using a series surfactants of alcohol ethoxy glyceryl sulfonates (AEGS) and alpha olefin sulfonates (AOS). The stability of CO_2 foams formed by water soluble surfactants depends on many factors such as the texture of the foams (bubble size, shape, and distribution), salinity, pH, surfactant concentration, pressure and temperature.[89, 135, 136] The method of foam generation is also a major factor that determines the texture and quality of the foam that will ultimately establish the concentration required to prolong stability.[143] The anionic surfactants used for the SAG process include Chaser CD 1045,[135, 136, 143] Rhodapex CD-128,[143] Witcolate 1276,[88, 89] and Enordet X2001,[88] which have been investigated for

foam stability and mobility control in both the laboratory and field at concentrations ranging from 0.01-0.1 wt%. Problems associated with CO_2 foam flooding or the SAG process include corrosion, surfactant adsorption, and control of foam mobility within the reservoir for extended periods of time. In this work, we propose the dissolution of an ionic surfactant in dense CO_2, rather than the injection of a water-soluble surfactant into the brine slug followed by the injection of a CO_2 slug. The single-phase solution of surfactant in CO_2 would be injected into the reservoir and form CO_2 foams in-situ as it mixes with the brine retained within the formation. These low mobility foams could form in water-out high permeability zones, thereby diverting the subsequently injected neat CO_2 to oil-rich zones. If the mobility decrease induced by the foam could be moderated, then the surfactant-CO_2 solution could also be used for mobility control purposes. The potential advantages of this process include the elimination of aqueous surfactant slug injection and the generation of foams along and at the tips of the CO_2 "fingers" where mobility control is most needed.

The objective of this study was to form emulsions by mixing of CO_2, water, and CO_2-soluble surfactants, and to characterize the stability of the emulsion by measuring its rate of collapse. CO_2-soluble ionic surfactants with CO_2-philic hydrocarbon or oxygenated hydrocarbon tails and conventional ionic head groups that have been presented in Chapter 4, and 5 were investigated for the foam stability study. CO_2-soluble ionic surfactants with oxygenated hydrocarbon or hydrocarbon tails composed of acetylated sugar, PPO, oligo(vinyl acetate), and 3,5,5-trimethyl-1-hexyl were evaluated along with two nonionic surfactants. The structures of these ionic and nonionic surfactants are shown in Figure 7.1 and Figure 7.2, respectively. The ionic surfactants with oxygenated hydrocarbon or hydrocarbon tails were synthesized as described in Chapter 3 and 4, while the nonionic surfactants of iso-stearic carboxylic acid and

PPG-PEG-PPG triblock polymer (Mn=3300) were obtained from Nissan Chemical and Aldrich, respectively. Several prior investigators[30, 56] have noted the CO_2 solubility of oligomeric block copolymers of PPG and PEG. Nonionic surfactants are considered to be low-to-moderate foamers relative to ionic surfactants and were therefore expected to yield less stable emulsions. However, nonionic surfactants have less severe problems associated with adsorption or chemical degradation. The stability of the emulsions stabilized with CO_2 soluble ionic surfactants was then contrasted with the stability of emulsions formed using conventional water soluble ionic surfactants.

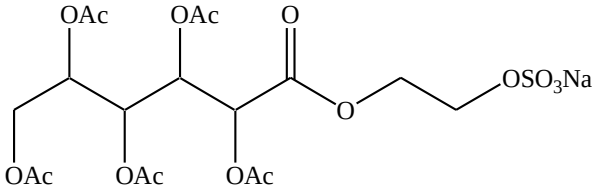

Peracetoxy Gluconate Ethyl Sodium Sulfate (a)

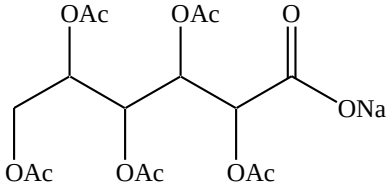

Peracetoxy Gluconate Sodium Carboxylate (b)

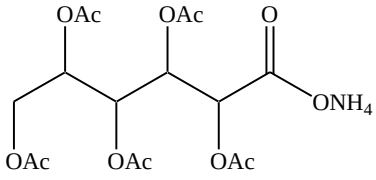

Peracetoxy Gluconate Amonium Carboxylate (c)

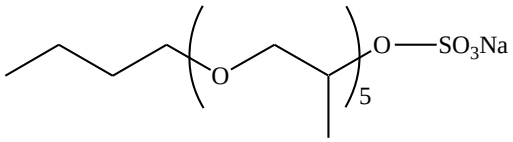

PPGMBE 340 Sodium Sulfate (d)

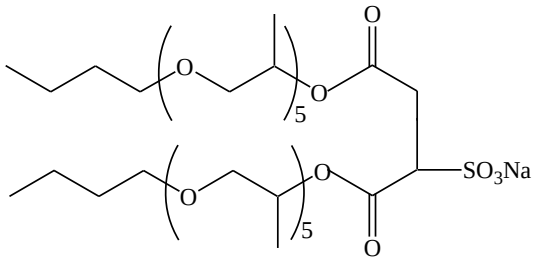

Sodium bis(PPGMBE 340) Sulfosuccinate
(PPGMBE 340 AOT Analogue) (e)

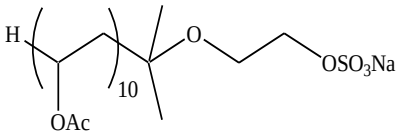

Oligo(Vinyl Acetate)10 Sodium Sulfate (f)

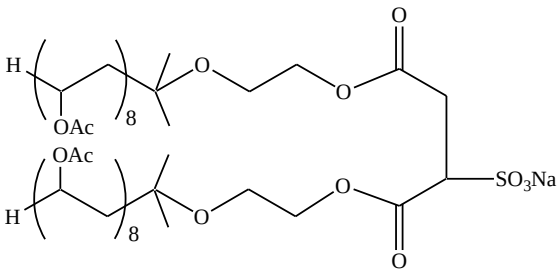

Sodium bis(Vinyl Acetate)8 Sulfosuccinate
(OVAc8 AOT Analogue) (g)

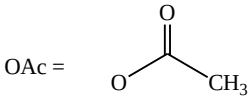

Figure 7.1. Structures of ionic surfactants with oxygenated hydrocarbon CO_2-philic tails.

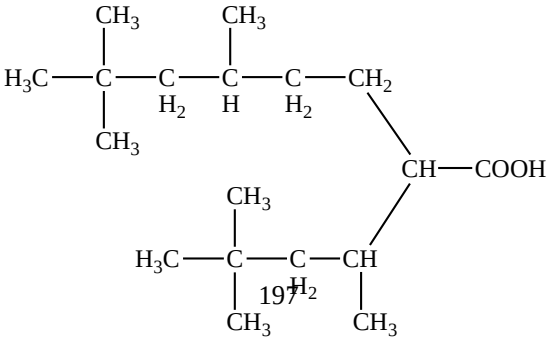

Iso-Stearic Acid (a)

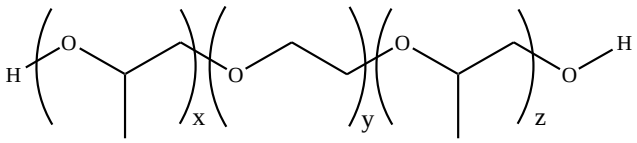

PPG-PEG-PPG (Mn=3300) (b)

Figure 7.2. Structures of nonionic surfactants.

7.2 EXPERIMENTS

Foam stability experiments were conducted in a high pressure, windowed, stirred, variable-volume view cell (DB Robinson & Assoc., 3.18 cm ID, ~120 cm^3 working volume), as described previously for phase behavior study.[95] The sample volume of this apparatus is a cylinder of variable height and fixed diameter. A specified amount of surfactant (e.g., 0.004 ± 0.0001 g) and double distilled and de-ionized water (e.g., 45.9 ± 0.1 mL) were added to the sample volume of the view cell and followed by the introduction of equal volume of CO_2 (e.g., 45.90 ± 0.1 mL) at 2000 psi. The amount of surfactant corresponded to 0.01 wt% based on the mass of CO_2. In this cell, the sample volume is separated from the overburden fluid by a steel cylinder (floating piston) that retains an O-ring around its perimeter. The O-ring permits the cylinder to move easily while retaining a seal between the sample volume and the overburden fluid. The sample volume was minimized by displacing the floating piston to the highest possible position within the cell that did not result in the displacement of surfactant-water mixture out of the sample volume. High pressure liquid carbon dioxide (22 ^oC, 13.8 MPa) was then introduced to the sample volume as the silicone oil overburden fluid (which was maintained at the same pressure

as the CO_2) was withdrawn at the equivalent flow rate using a dual-proportioning positive displacement pump (DB Robinson). This technique facilitated the isothermal, isobaric addition of a known volume of CO_2 into the sample volume. The mass of CO_2 introduced was determined from the displaced volume, temperature, and pressure using an accurate equation of state for carbon dioxide.[96] Pressure within the vessel was monitored to approximately ± 0.5 MPa, and temperature was measured with a type K thermocouple to an accuracy of ± 0.1 ^{o}C. The system was then compressed to 34.5 MPa. The surfactants are both CO_2 soluble and water soluble at these conditions, and no attempts were made to quantify the partitioning of the surfactant between the phases.

The cell was inverted, allowing the mixer to be at the bottom of the sample volume. The position of the original interface between water and liquid CO_2 prior to mixing (and emulsion generation) was then measured using a ruler that was adjacent to the window. The mixture was then mixed thoroughly for 10 minutes at 2000 rpm using a slotted propeller-type impeller magnetic stirrer on the bottom of the sample volume (DB Robinson, max. 2500 rpm). After the mixing ceased, a white, creamy, opaque emulsion formed immediately within the entire sample volume. Subsequently, clear CO_2-rich upper phase and aqueous lower phase appeared. The emulsion stability and volume were evaluated by periodically measuring the position of the top (CO_2-emulsion) and bottom (water-emulsion) interfaces of the white emulsion. The volume of the foam was measured as the percentage of the original CO_2 and aqueous phases that were occupied by the emulsion.

$$\text{Foam volume} = \frac{H(t)}{H(0)} \times 100\% \qquad (1)$$

where t is time, H(t) is the height of the CO_2 or H_2O emulsion layers with time, and H(0) is the initial height of the CO_2 or H_2O layer. In all cases, the foam volume was initially 100% of both

the CO_2 and water layers, but the foam decayed thereafter. The final volume corresponded to either 0, which corresponded to the complete collapse of the foam, or a finite % value that was indicative of a stable middle phase emulsion. Stable foams were characterized by slow collapse and the occurrence of a stable middle phase emulsion.

7.3 RESULTS AND DISCUSSIONS

Peracetyl Gluconic-based Ionic Surfactants, Figures 7.1a,b,c

Foam stabilities of peracetyl gluconic-based ionic surfactants with an ethyl spacer and a sodium sulfate, sodium carboxylate or ammonium carboxylate head group (Figures 7.1a,b,c) are shown in Figure 7.3. The emulsion generated by peracetyl gluconic ammonium carboxylate is much more stable than those generated by the other two peracetyl gluconic-based ionic surfactants, taking about 250 minutes to collapse to a stable middle phase emulsion that occupied about 22% of the original CO_2 volume. The emulsion formed by the peraceyl gluconic ethyl sodium sulfate required about 200 minutes to collapse to a middle phase emulsion that occupied about 15% of the CO_2 volume. The emulsion formed by the peracetyl gluconic sodium carboxylate collapsed in about 120 minutes to a volume that was 5% of the CO_2 volume. In all cases, the emulsion percentage in the aqueous phase collapsed quickly from 100% to 0%.

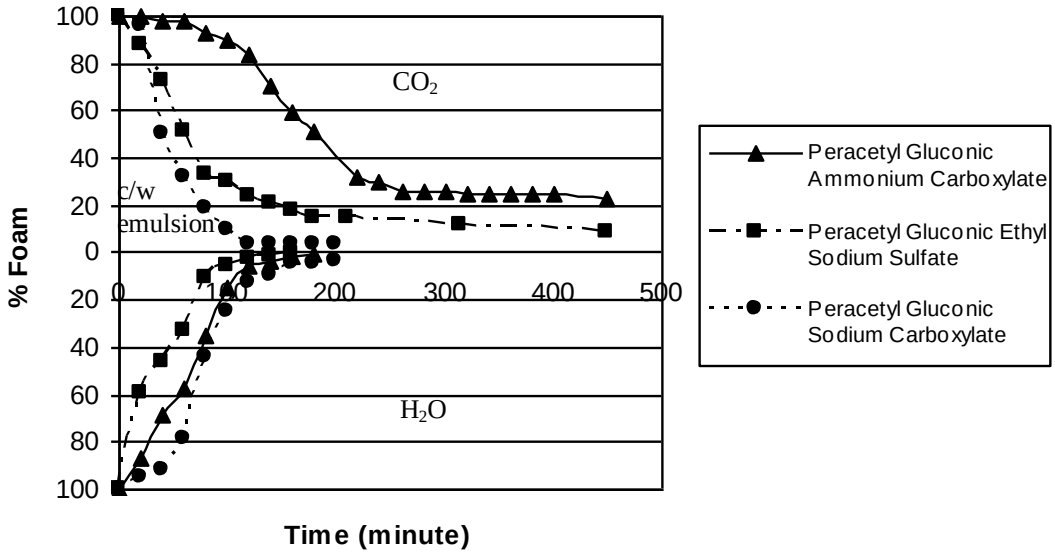

Figure 7.3. Foam stability of peracetyl gluconic-based ionic surfactants at concentration of 0.01 wt% in CO_2, 22 ^oC and 34.5 MPa.

Poly(Propylene Glycol) MonoButyl Ether(PPGMBE)-based Ionic Surfactants, Figures 7.1d,e

Emulsions formed by twin tailed AOT analogue of sodium bis(PPGMBE 340) sulfosuccinate are slightly more stable than those formed by the single-tailed PPGMBE 340 sodium sulfate, as shown in Figure 7.4 in that the emulsions collapsed at comparable rates, requiring about 160 minutes to reach steady state values of 15% and 5% of the original CO_2 volume, respectively. The portion of the emulsion that originally formed in the aqueous phase collapsed at a comparable rate, and a portion of the final emulsion volume, about 5% of the water volume, resided below the original CO_2-water boundary.

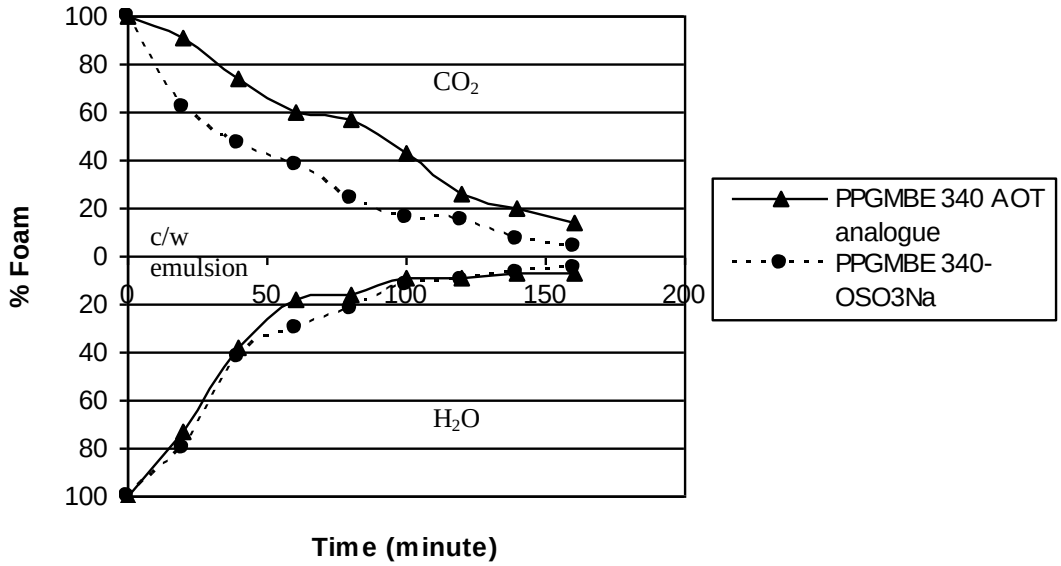

Figure 7.4. Foam stability of PPGMBE-based ionic surfactants at concentration of 0.01 wt% in CO_2, 22 ^oC and 34.5 MPa.

Oligo(Vinyl Acetate)-based Ionic Surfactants, Figures 7.1f,g

Single-tailed oligo(vinyl acetate)10 sodium sulfate (OVAc10-OSO_3Na) formed emulsions that were only slightly more stable than the twin-tailed AOT analogue of sodium bis(vinyl acetate)8 sulfosuccinate (OVAc8 AOT analogue). As shown in Figure 7.5, it took roughly 400 minutes for the emulsion formed by 0.01 wt% OVAc10-OSO_3Na to collapse to about 10% of the orignial CO_2 volume, while emulsions formed by OVAc8 AOT analogue took about 300 minutes to collapse to a comparable volume. The portion of the emulsion in the aqueous layer decayed first and collapsed to 0.

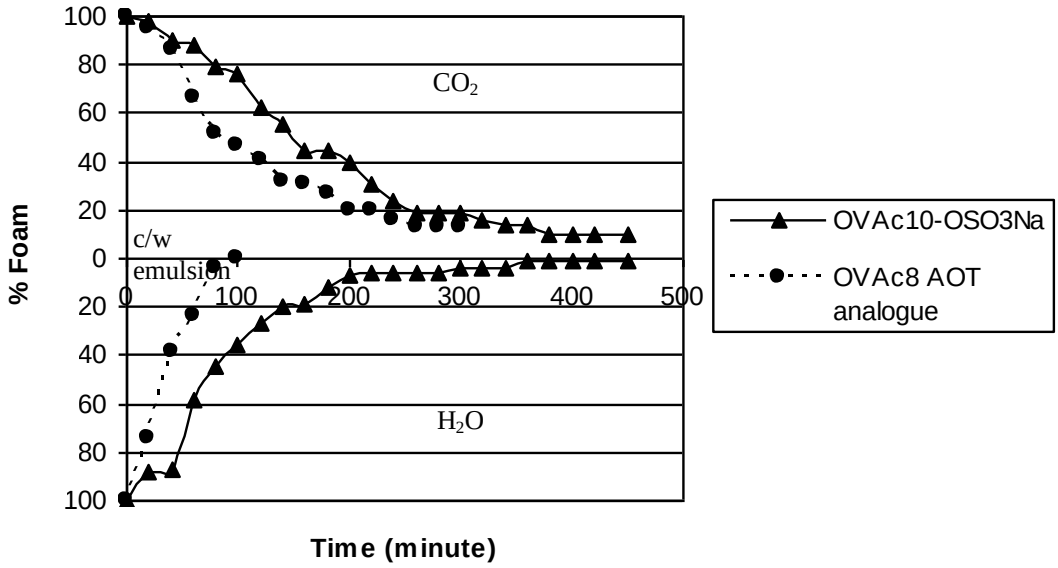

Figure 7.5. Foam stability of oligo(vinyl acetate)-based ionic surfactants at concentration of 0.01 wt% in CO_2, 22 ^oC and 34.5 MPa.

Comparison of Oligo(Vinyl Acetate)10 Sodium Sulfate and Commercial Chaser CD 1045

The oligo(vinyl acetate)10 sodium sulfate demonstrated the best foam stability in both CO_2 and H_2O layers, which was chosen for comparison with the commercial water soluble ionic surfactant of Chase CD 1045. The foam stability comparison was presented in Figure 7.6. The stability of CO_2 emulsions formed by both surfactants at 0.01 wt% are comparable. It took roughly 400 minutes for the CO_2 emulsions to collapse to about 10% of the orignial CO_2 volume. The portion of the emulsion in the aqueous layer formed by Chaser CD 1045 decayed faster and collapsed to 0 at about 200 minutes, while that of oligo(vinyl acetate)10 sodium sulfate lasted 400 minutes to collapse to 0.

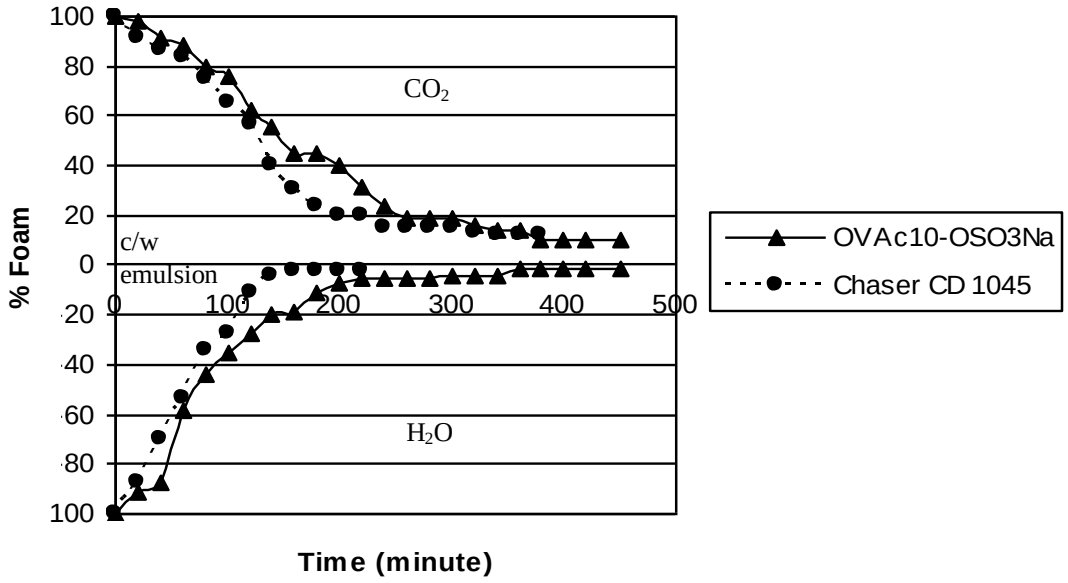

Figure 7.6. Foam stability of OVAc10-OSO_3Na and Chaser CD 1045 at concentration of 0.01 wt% in CO_2, 22 ^oC and 34.5 MPa.

Nonionic surfactants, Figures 7.2a,b

The emulsions generated by the nonionic surfactants decayed at a much faster rate than the ionic surfactants, as shown in Figure 7.7. The emulsion formed by the iso-stearic acid collapsed completely in less than an hour. The emulsion formed by the PPG-PEG-PPG reached its steady-state value of about 10% of the aqueous phase volume in just over an hour.

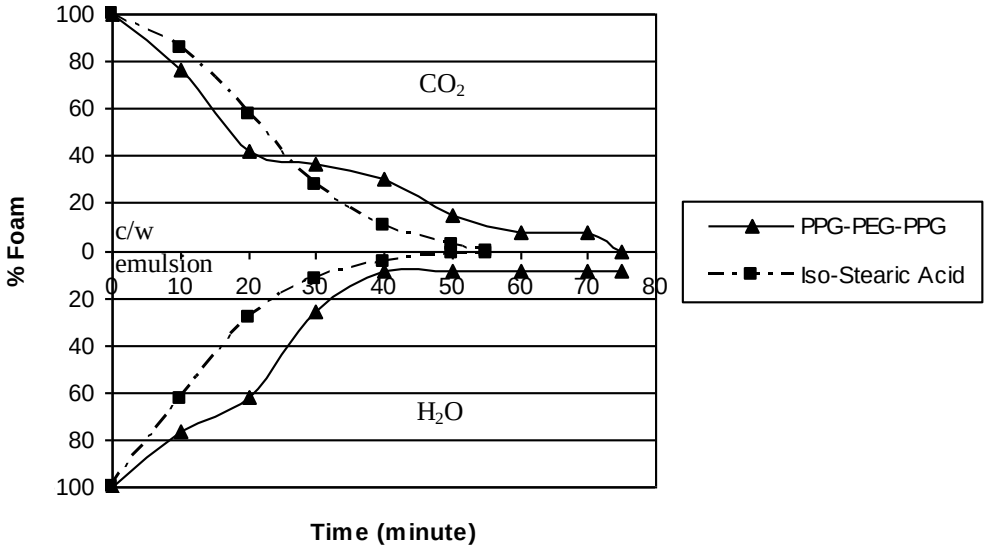

Figure 7.7. Foam stability of iso-stearic acid and PPG-PEG-PPG nonionic surfactants at cncentration of 0.01 wt% in CO_2, 22 ^oC and 34.5 MPa.

7.4 CONCLUSIONS

At constant conditions of 0.01 wt% surfactant in CO_2, 22 ^oC and 34.5 MPa, it is apparent that the emulsions formed by the ionic surfactants displayed a significantly greater stability than those formed by the nonionic compounds. Of the ionic surfactants, the peracetyl gluconic ammonium carboxylate demonstrated the best CO_2 foam stability, with around 20% of the CO_2 foams lasting for over 450 min. The oligo(vinyl acetate)10 sodium sulfate demonstrated the best foam stability in both CO_2 and H_2O layers, with around 10% and 1% of foams respectively remaining stable for over 450 min. Further tests on the salinity of the H_2O present, pressure, temperature, and varied surfactant concentrations would be evaluated further for the most potential candidate of oligo(vinyl acetate)10 sodium sulfate to be used in EOR processes.

8.0 NONIONIC SURFACTANTS

8.1 EFFECT OF ALKYL CHAIN LENGTH

Some commercially available nonionic surfactants were also investigated for CO_2 solubility. First, the effect of alkyl chain length to surfactants solubility in CO_2 was investigated. Poly (propylene) butyl ether and poly(propylene) stearyl ether (Chemron) have almost the same PPO repeat units while different alkyl chains length; see their structures in Figure 8.1. PBE-14 is extremely CO_2 soluble up to 80wt%. PSE-15 is much less CO_2 soluble, only up to 15wt% could be dissolved in CO_2 at much higher pressure (Figure 8.2). That means short alkyl chain is much more CO_2-philic than longer alkyl chain.

Poly (propylene) Butyl Ether, PBE-14

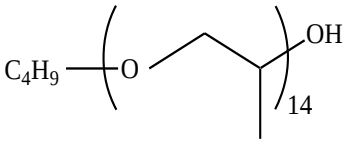

Poly (propylene) Stearyl Ether, PSE-15

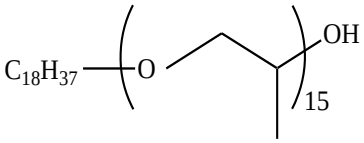

Figure 8.1. Structures of PBE-14 and PSE-15.

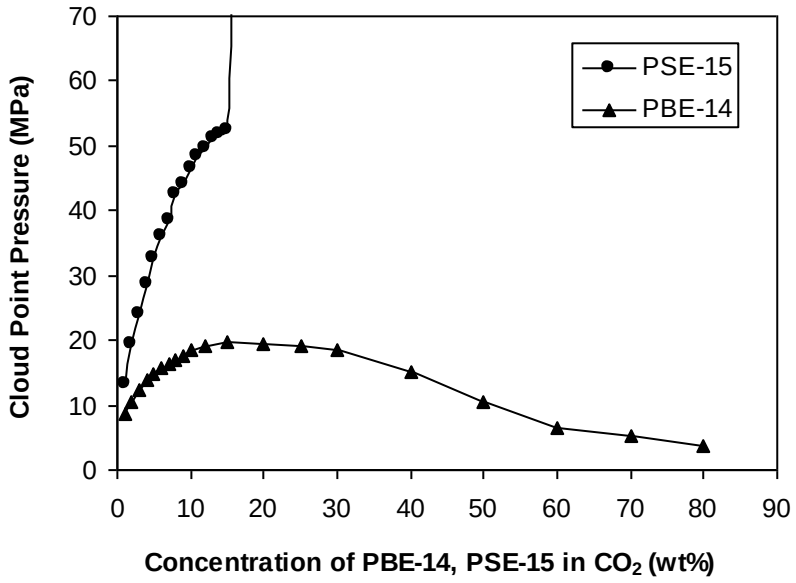

Figure 8.2. Phase behavior of PBE-14, PSE-15/CO_2 mixtures at 22 ^{o}C.

8.2 EFFECT OF ETHYLENE OXIDE AND PROPYLENE OXIDE

The function of PEO and PPO to CO_2 solubility was also studied. The solubility of commercial nonionic surfactants containing ethylene oxide and propylene oxide including Vanwet9N9, LS-54 (Cognis), TD-23 and TD-29 (Chemron) were compared at room temperature. Water in TD-23 and TD-29 was removed by vacuum distillation before the phase behavior study. Figure 8.3 shows their structures. Phase behavior results in Figure 8.4 illustrate that Vanwet9N9 is the least soluble because it contains only PEO repeat units, while the LS-54, TD-23 and TD-29 are much more CO_2 soluble due to the CO_2 philic PPO units. Further, TD-29 is more soluble than LS-54 and TD-23 because its relatively higher composition of PPO.

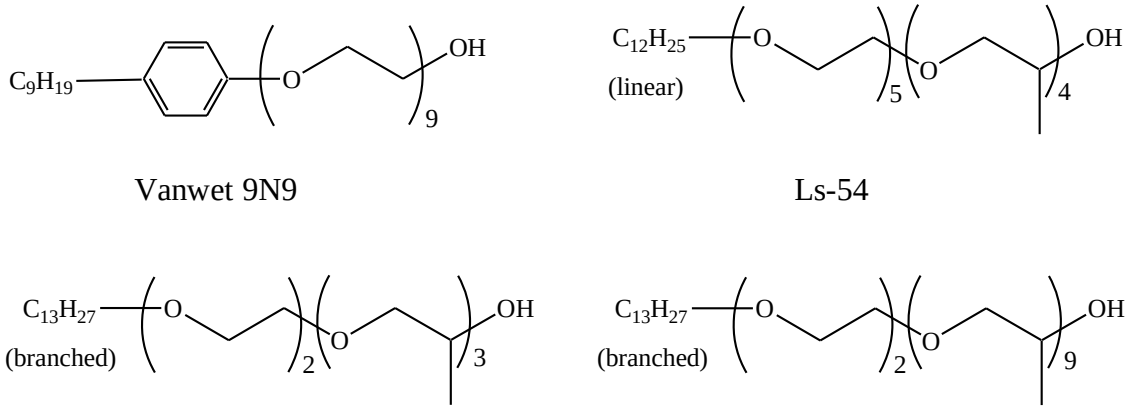

Figure 8.3. Structures of Vanwet9N9, LS-54, TD-23 and TD-29.

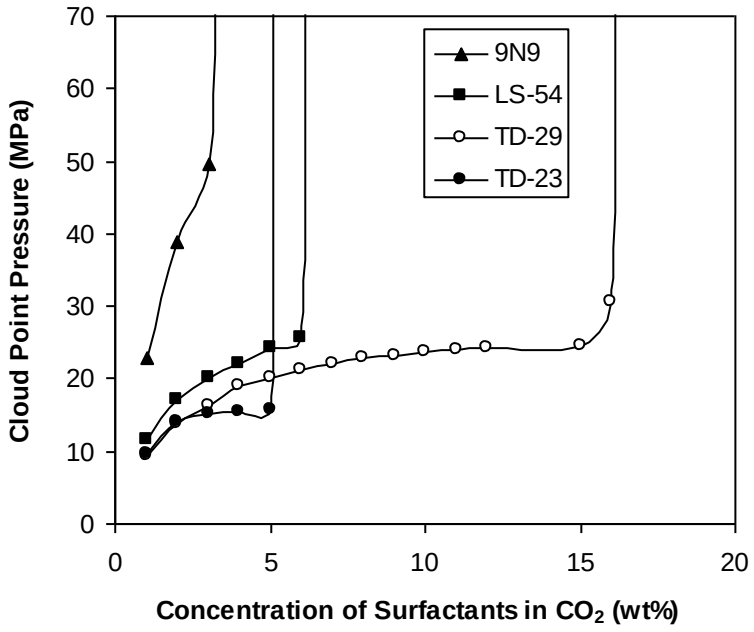

Figure 8.4. Phase behavior of Vanwet9N9, LS-54, TD-23 and TD-29/CO_2 mixtures at 22 ^{o}C.

9.0 CONCLUSIONS

(1) Oxygenated hydrocarbon based ionic surfactants composed of acetylated sugars, poly(propylene oxide) tails are 0.1-2 wt% soluble in CO_2.

(2) Oxygenated hydrocarbon based ionic surfactants composed of oligo(vinyl acetate) tails are highly CO_2 soluble.

   i. Single-tailed OVAc-OSO_3Na are 2-7 wt% soluble in CO_2

   ii. Twin-tailed OVAc8 AOT analogue is 3 wt% soluble in CO_2

   iii. Both single and twin-tailed OVAc ionic surfactants can form water-in-CO_2 microemulsions at W values as high as 40.

   iv. OVAc ionic surfactants represent the first reports of highly CO_2 soluble ionic surfactants with tails composed solely of C, H and O that can form water-in-CO_2 microemulsions.

(3) Ag-AOT-TMH, a hydrocarbon-based metal precursor, is 1.2 wt% soluble in CO_2. It was reduced to silver nanoparticles in CO_2.

(4) Iso-stearic acid, a highly branched nonionic surfactant, is completely miscible with CO_2 and it is the first report of metallic nanoparticles dispersed in pure CO_2 without the use of fluorinated ligands.

(5) The oligo(vinyl acetate)10 sodium sulfate demonstrated the best foam stability in both CO_2 and H_2O layers, with around 10% and 1% of foams respectively remaining stable for over 450 min.

(6) Short alkyl chain is much more CO_2-philic than long alkyl chain and poly (propylene oxide)

(PPO) is much more CO_2-philic than poly (ethylene oxide) (PEO).

10.0 FUTURE WORK

Our future work will continue to design oxygenated hydrocarbon-based or hydrocarbon-based CO_2 soluble surfactants for nanoparticle formation, foam generation, interfacial tension reduction and other chemical engineering applications. The interactions between the tail and the CO_2 must be strong enough to impart CO_2-philicity to the surfactant that contains a CO_2-phobic segment. Further, the CO_2 soluble surfactant must be able to form water-in-CO_2 microemulsions, stabilize nanoparticles, generate foams, increase viscosity or reduce interfacial tension.

APPENDIX A

SPECTRA AND PHASE BEHAVIOR OF SURFACTANTS IN CHAPTER 4

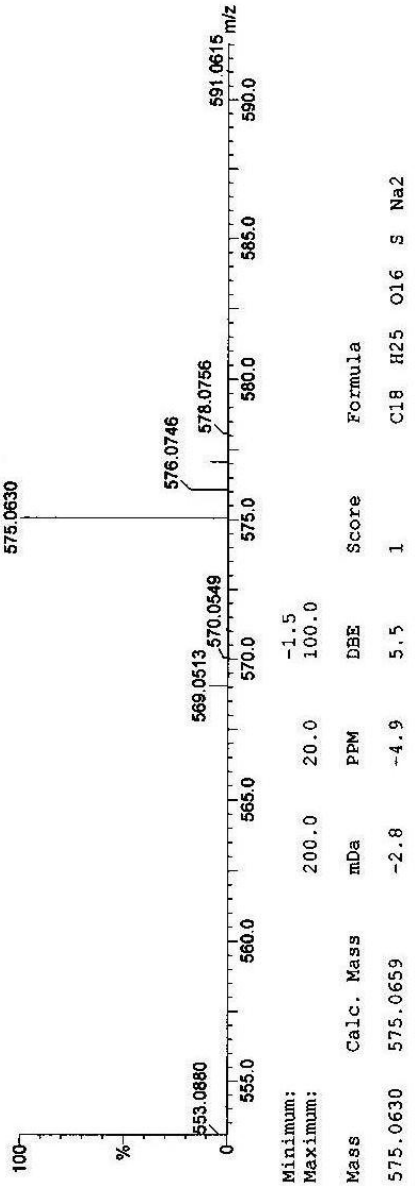

Figure A.1. Mass spectrum of peracetyl gluconic ethyl sodium sulfate

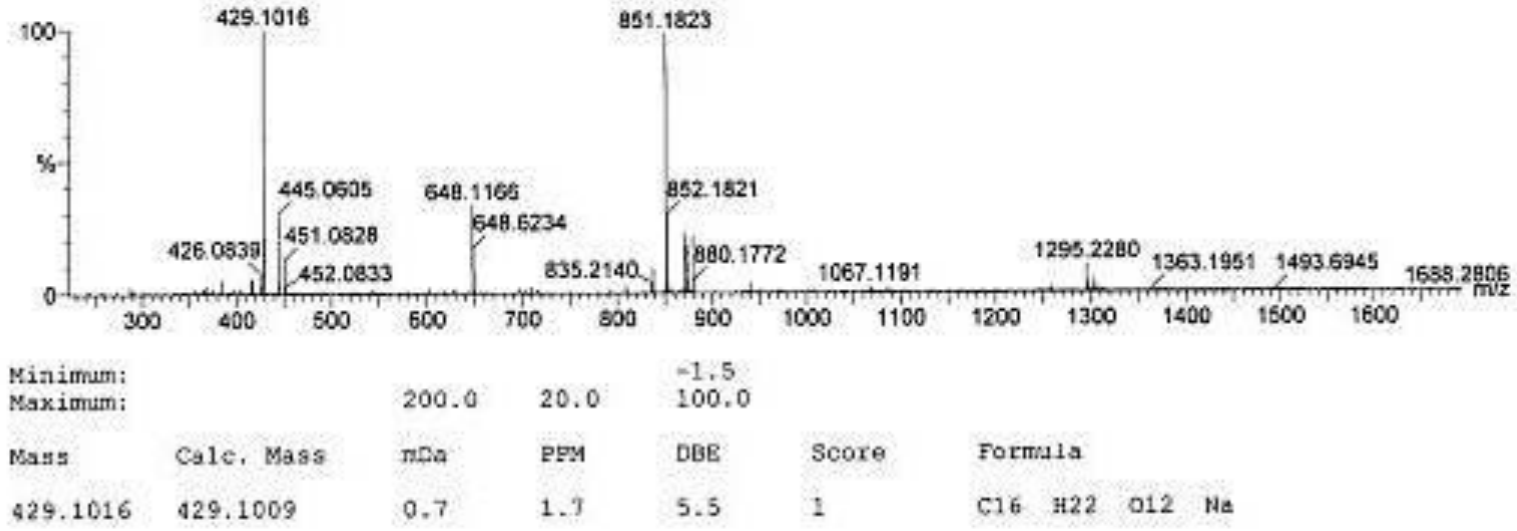

Minimum:				-1.5		
Maximum:		200.0	20.0	100.0		
Mass	Calc. Mass	mDa	PPM	DBE	Score	Formula
429.1016	429.1009	0.7	1.7	5.5	1	C16 H22 O12 Na

Figure A.2. Mass spectrum of peracetyl gluconic sodium carboxylate

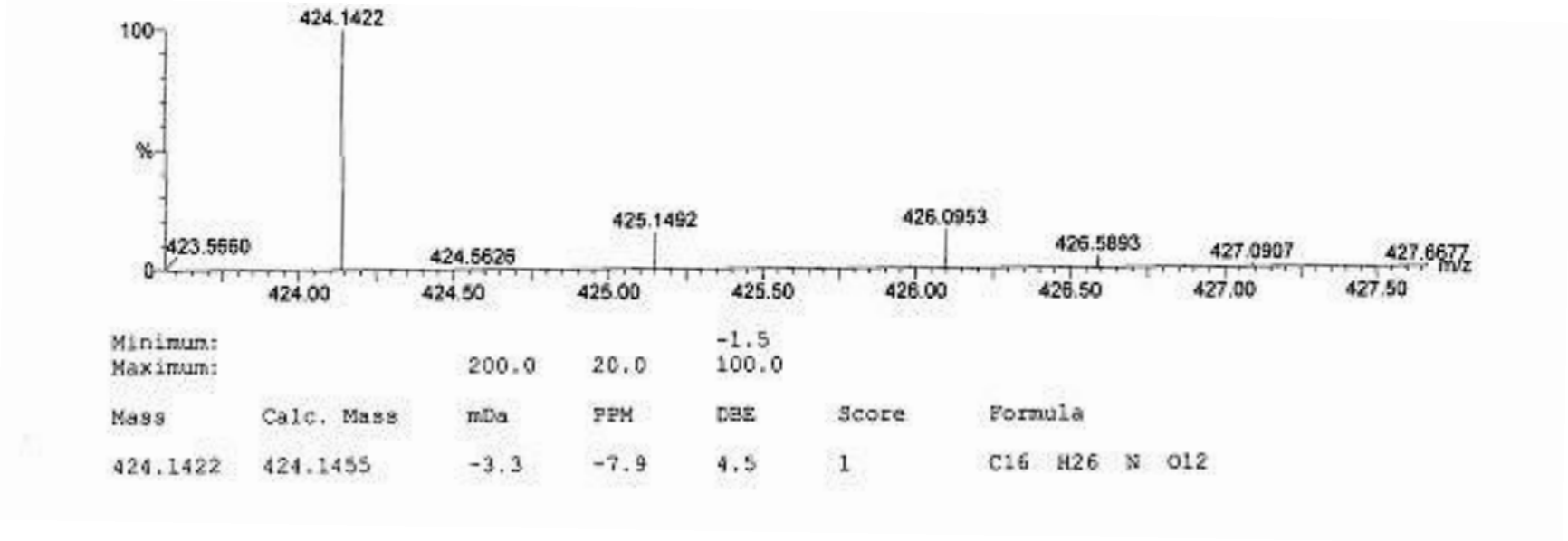

Minimum:				-1.5		
Maximum:		200.0	20.0	100.0		
Mass	Calc. Mass	mDa	PPM	DBE	Score	Formula
424.1422	424.1455	-3.3	-7.9	4.5	1	C16 H26 N O12

Figure A.3. Mass spectrum of peracetyl gluconic ammonium carboxylate

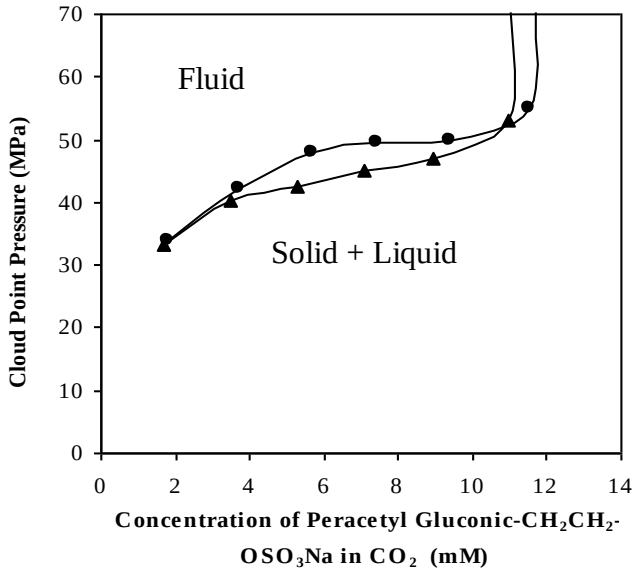

Figure A.4. Phase behavior of peracetyl gluconic-CH_2CH_2-OSO_3Na/CO_2 mixtures. Insoluble at W = 0; 25 ^oC, W =10 (●); 40 ^oC, W=10 (▲). (Surfactant concentration in mM).

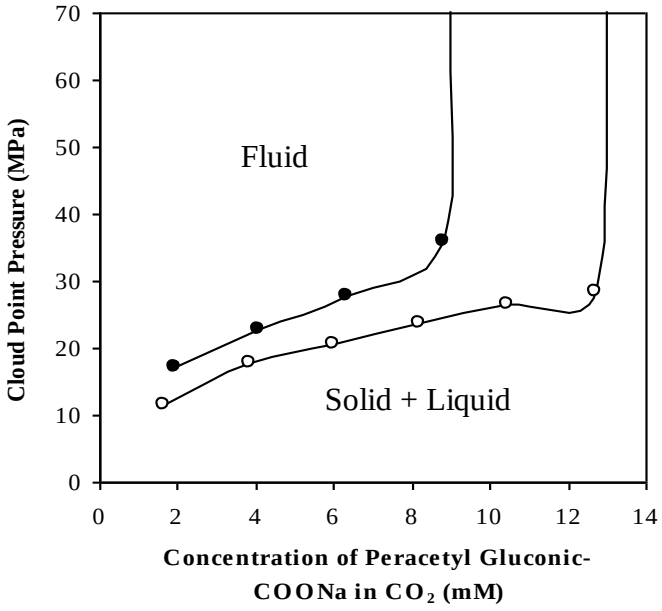

Figure A.5. Phase behavior of peracetyl gluconic-$COONa/CO_2$ mixtures at 40 ^oC. W=0 (o); W=10 (•). (Surfactant concentration in mM).

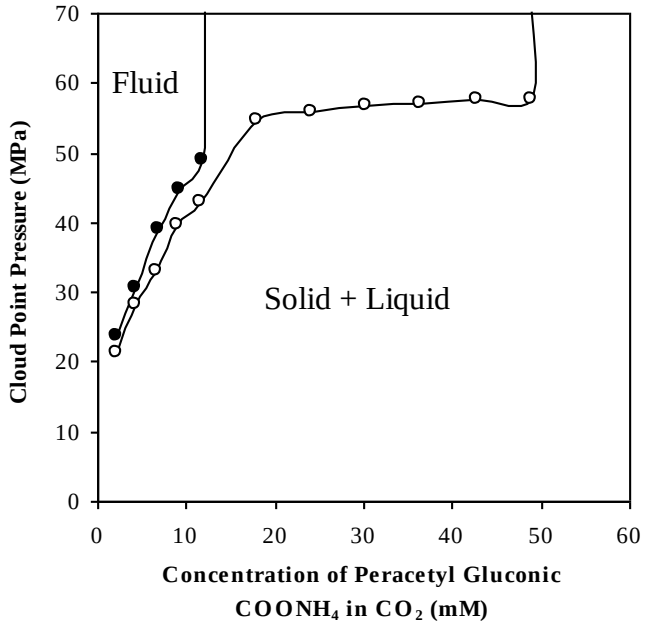

Figure A.6. Phase behavior of peracetyl gluconic-$COONH_4/CO_2$ mixtures at 40 ^oC. W =0 (o); W =10 (•). Surfactant concentration in mM. (Surfactant concentration in mM).

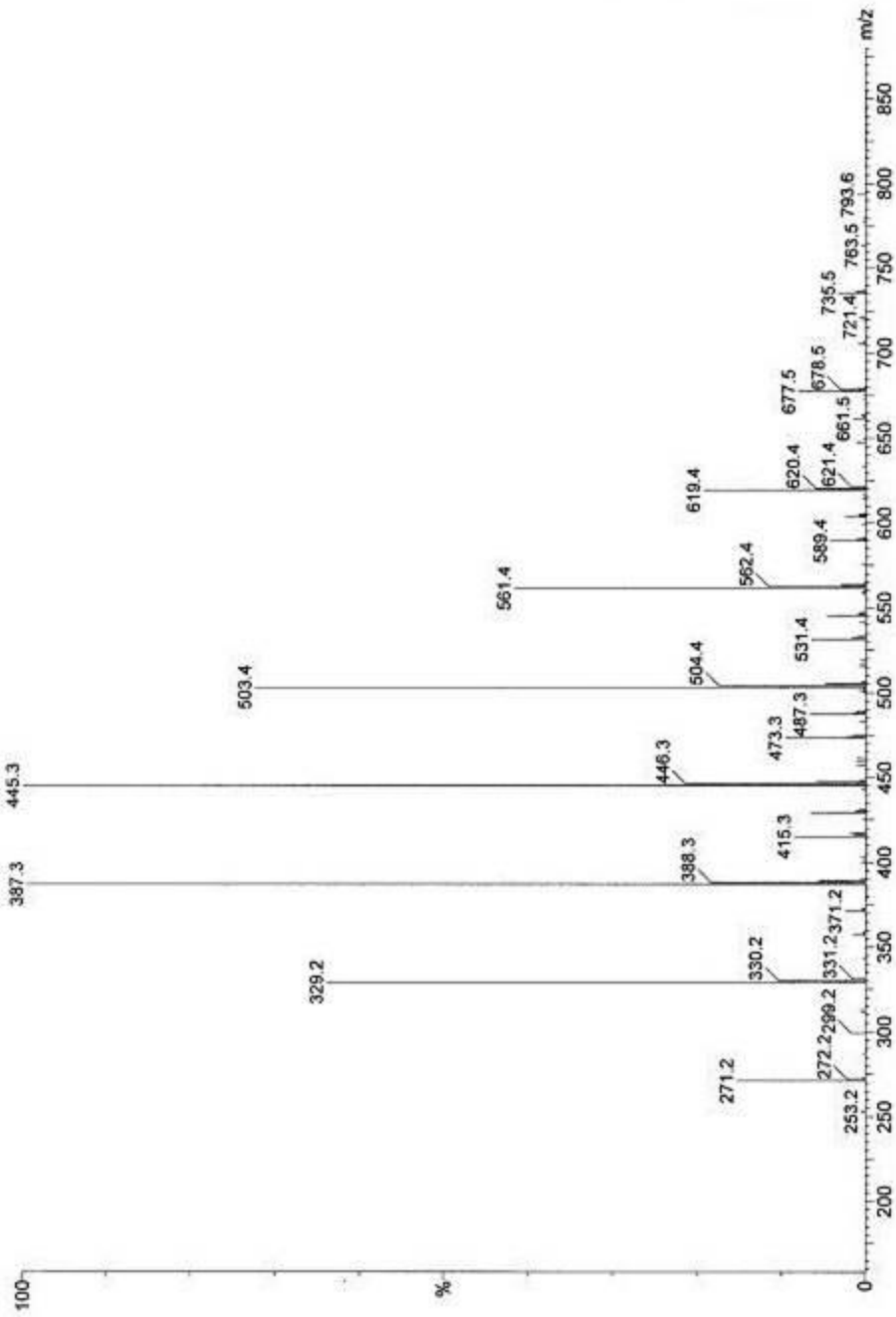

Figure A.7. Mass spectrum of PPGMBE 340 sodium sulfate

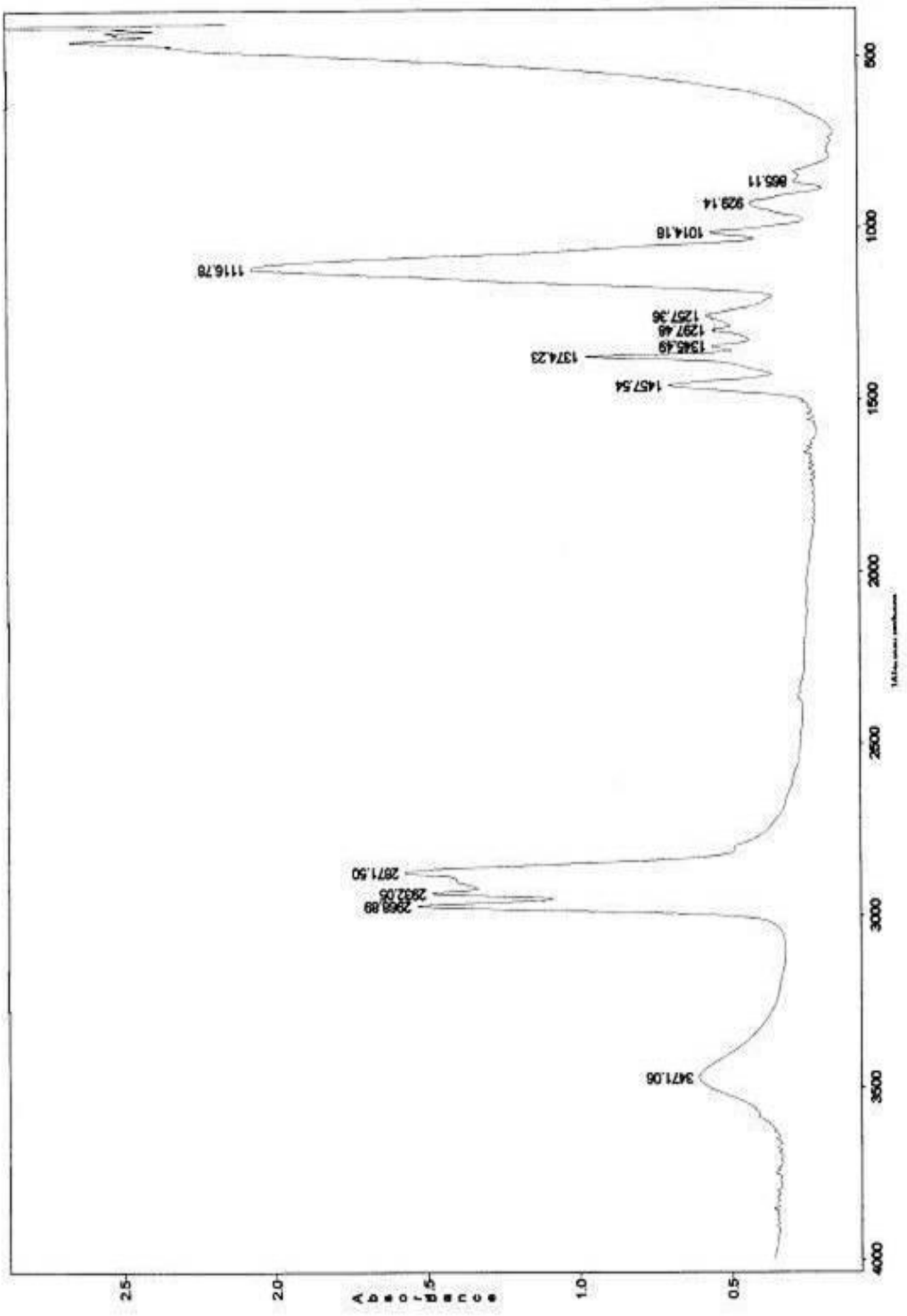

Figure A.8. FTIR spectrum of PPGMBE 340

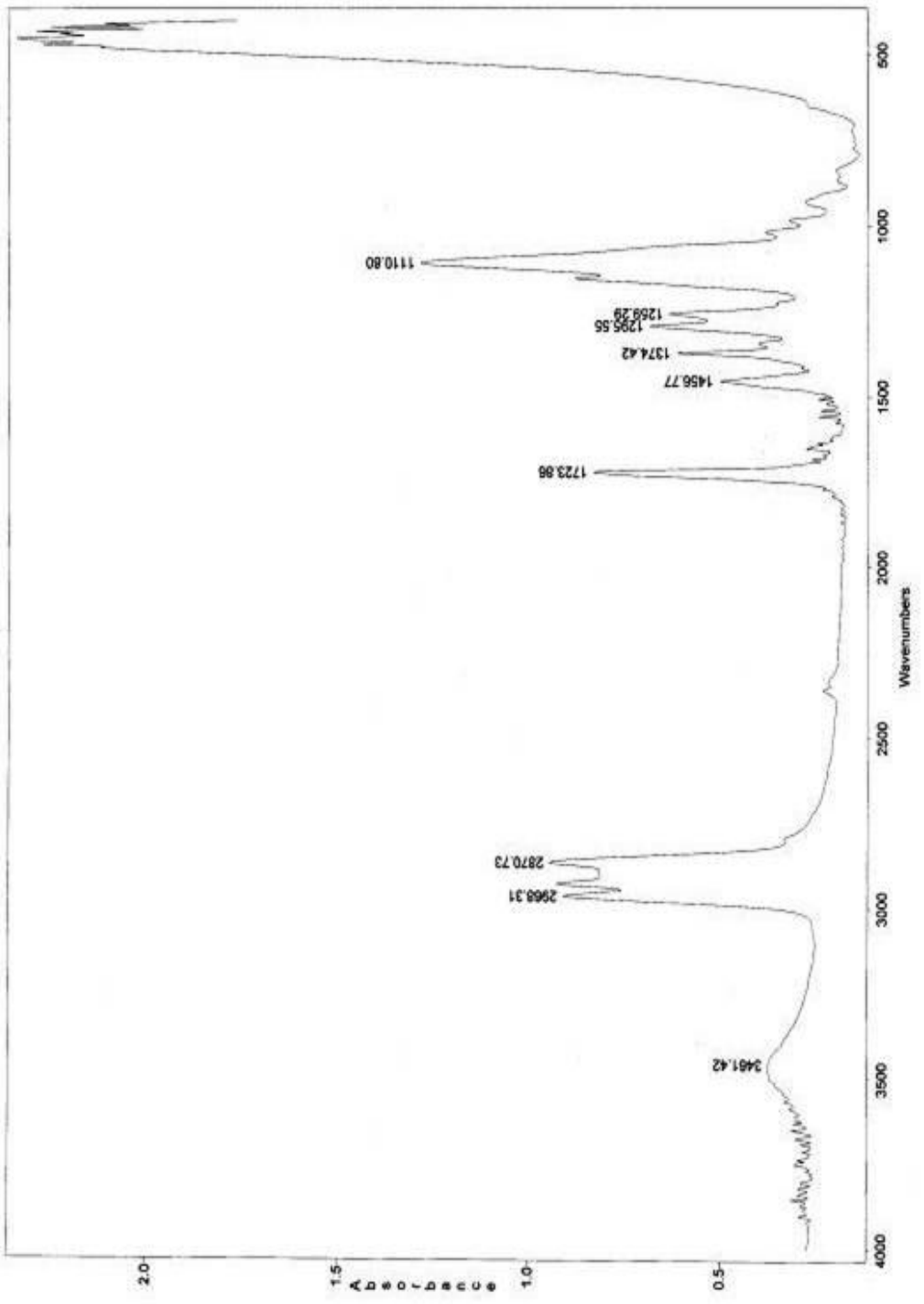

Figure A.9. FTIR spectrum of PPGMBE 340 diester

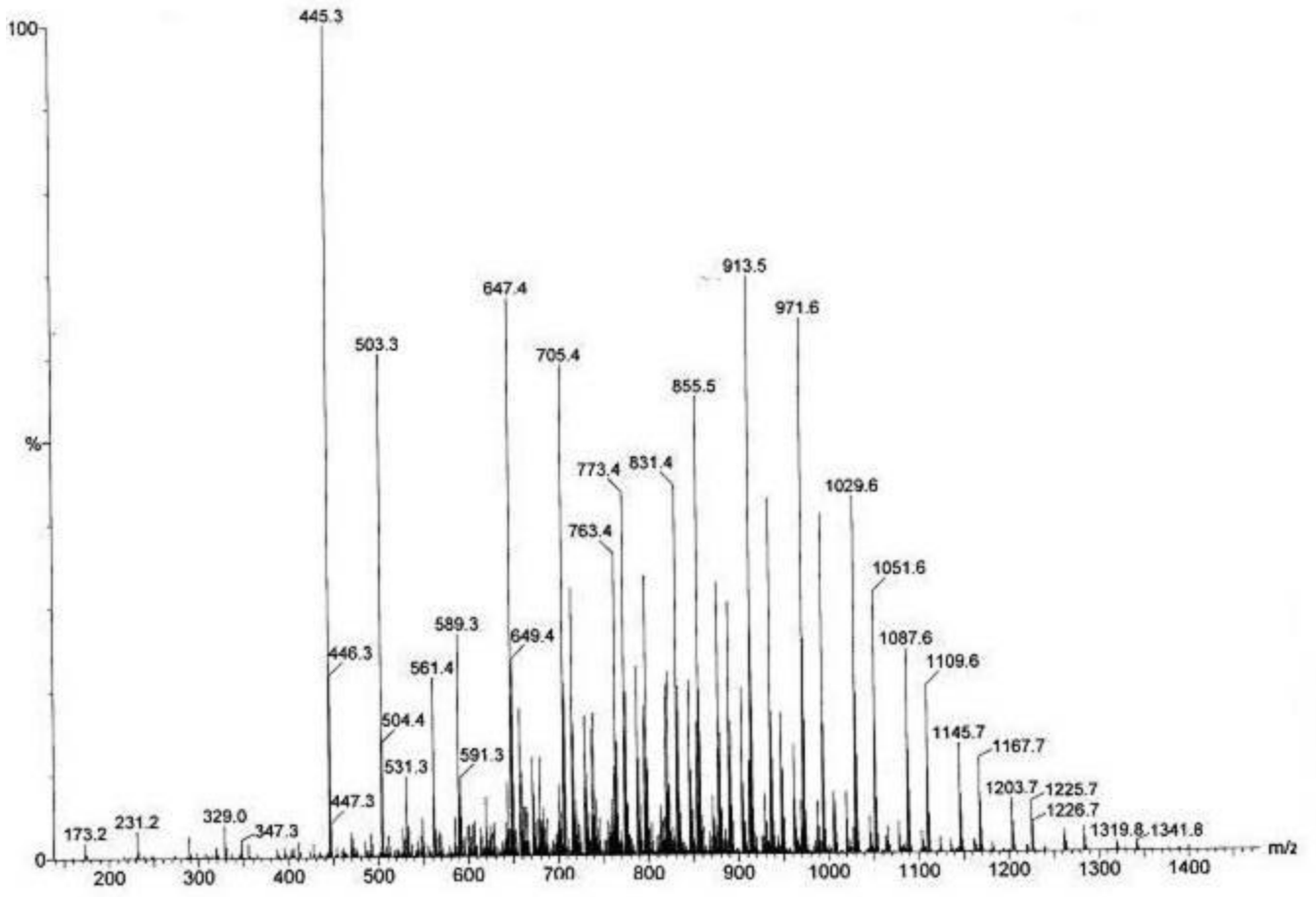

Figure A.10. Mass spectra of sodium bis(PPGMBE 340) sulfosuccinate

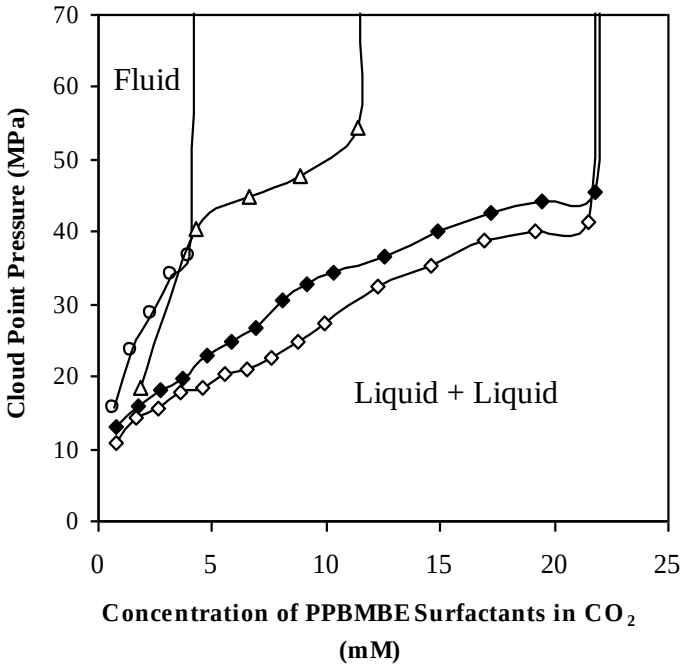

Figure A.11. Phase behavior of PPGMBE surfactants/CO_2 mixtures at 40 ^{o}C. PPGMBE 340 sodium sulfate, W=0 (Δ); PPGMBE 1000 pyridinium sulfate, W=0 (o); PPGMBE 1000 pyridinium sulfate, W=10 (●); Sodium bis(PPBMBE 340) sulfosuccinate, W=0 (◊); Sodium bis(PPBMBE 340) sulfosuccinate, W=10 (♦). (Surfactant concentration in mM).

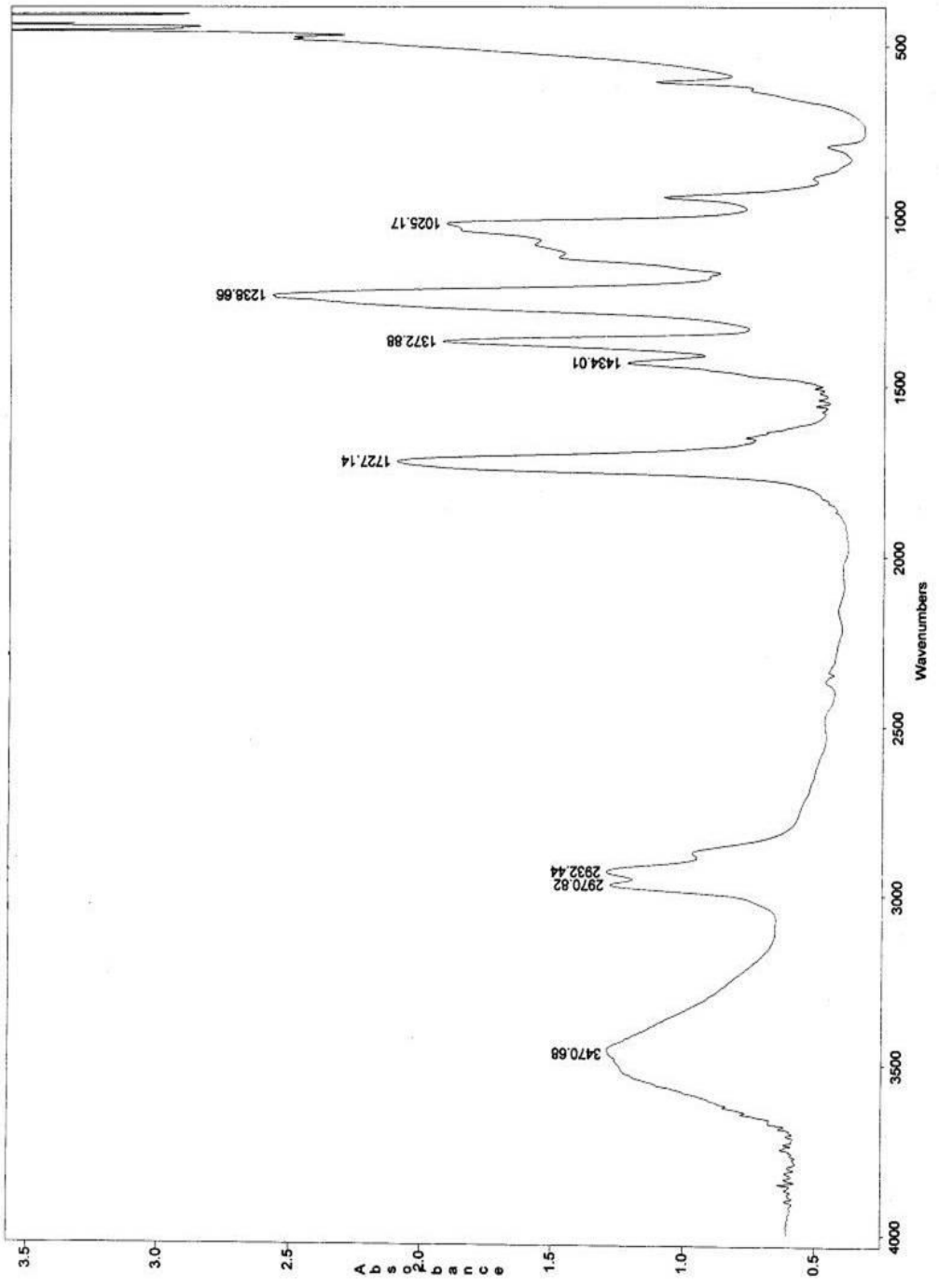

Figure A.12. FTIR spectrum of OVAc6-OH

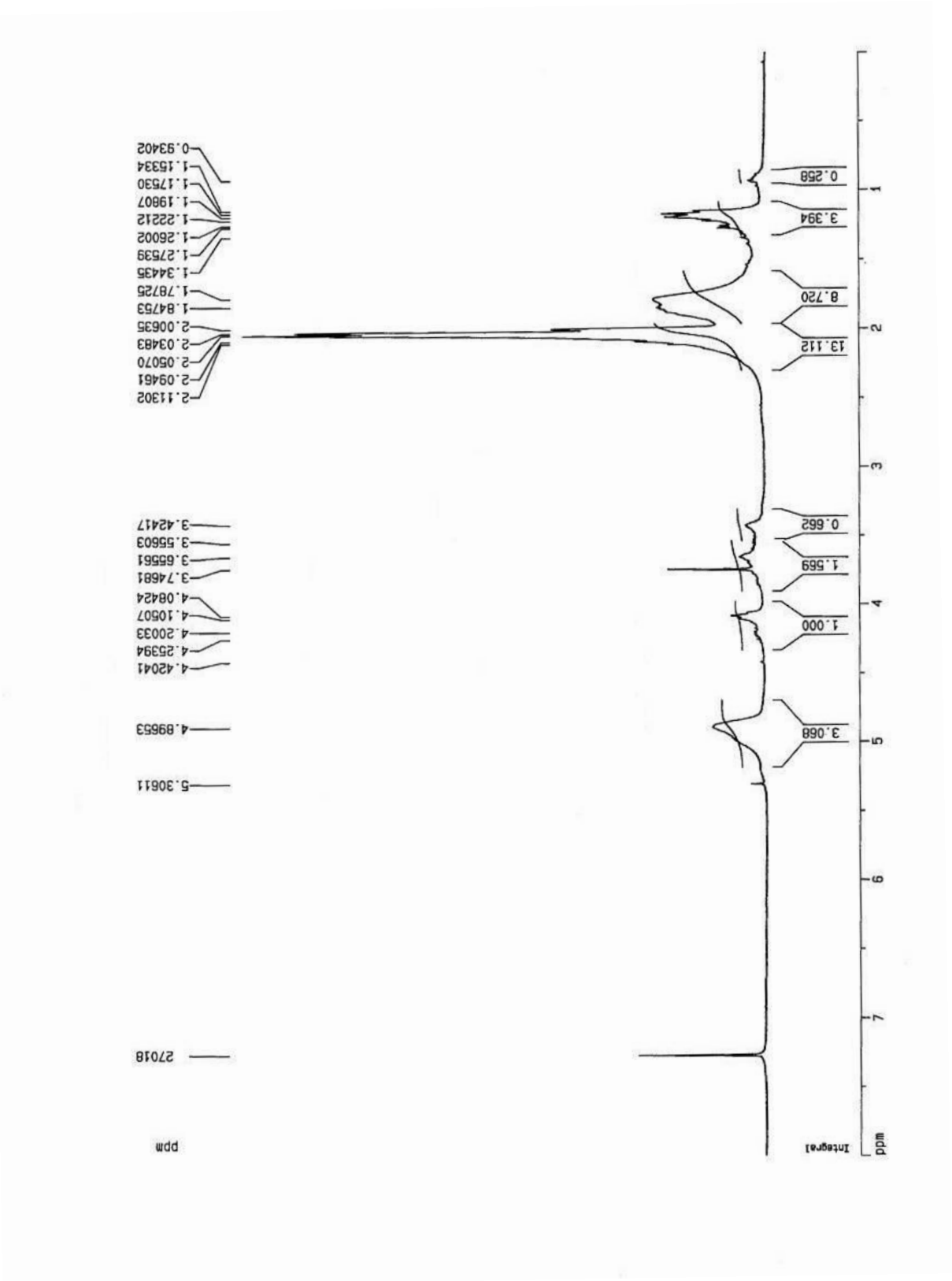

Figure A.13. ^{1}H-NMR spectrum of OVAc6-OH

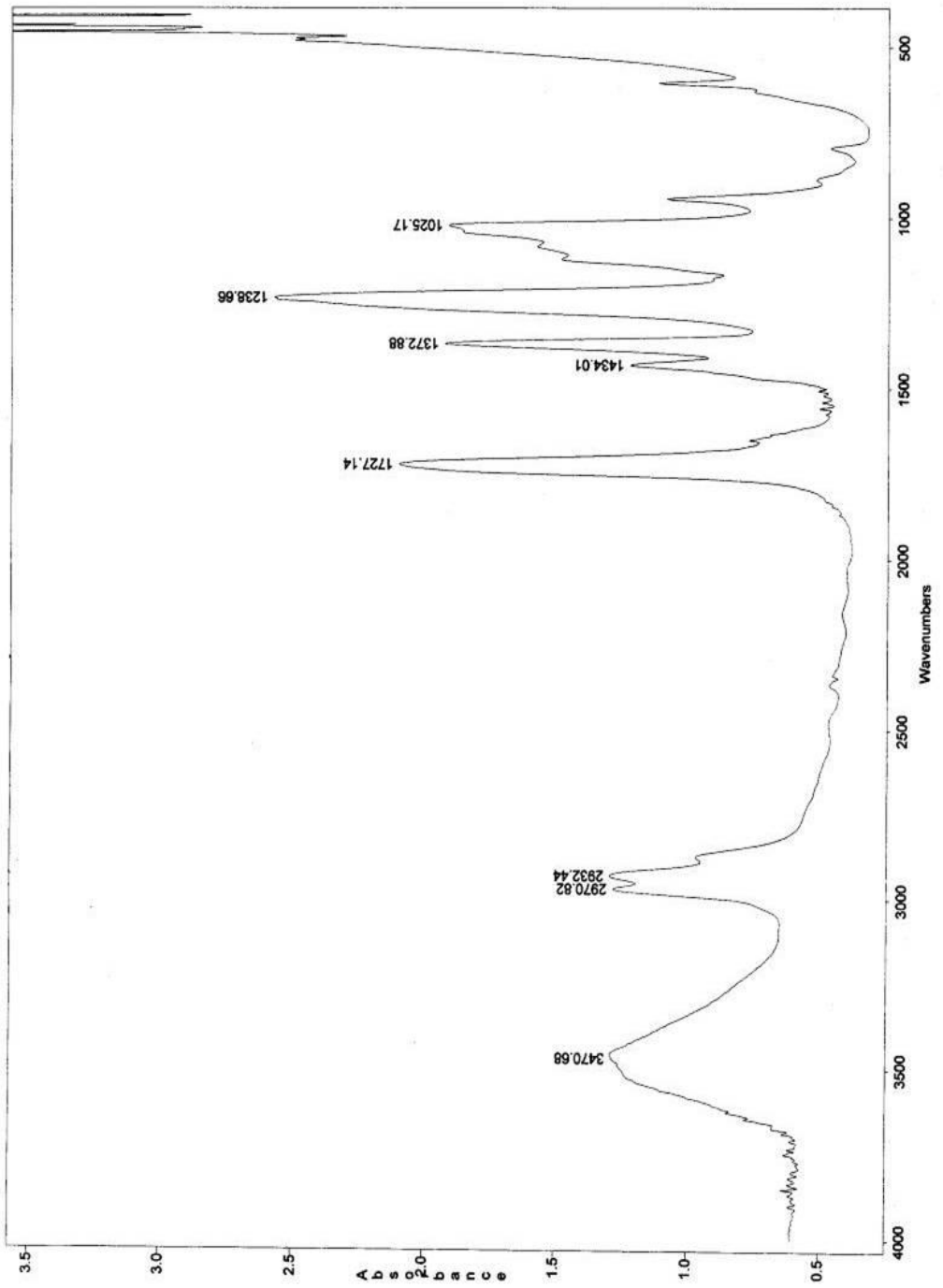

Figure A.14. FTIR spectrum of OVAc8-OH

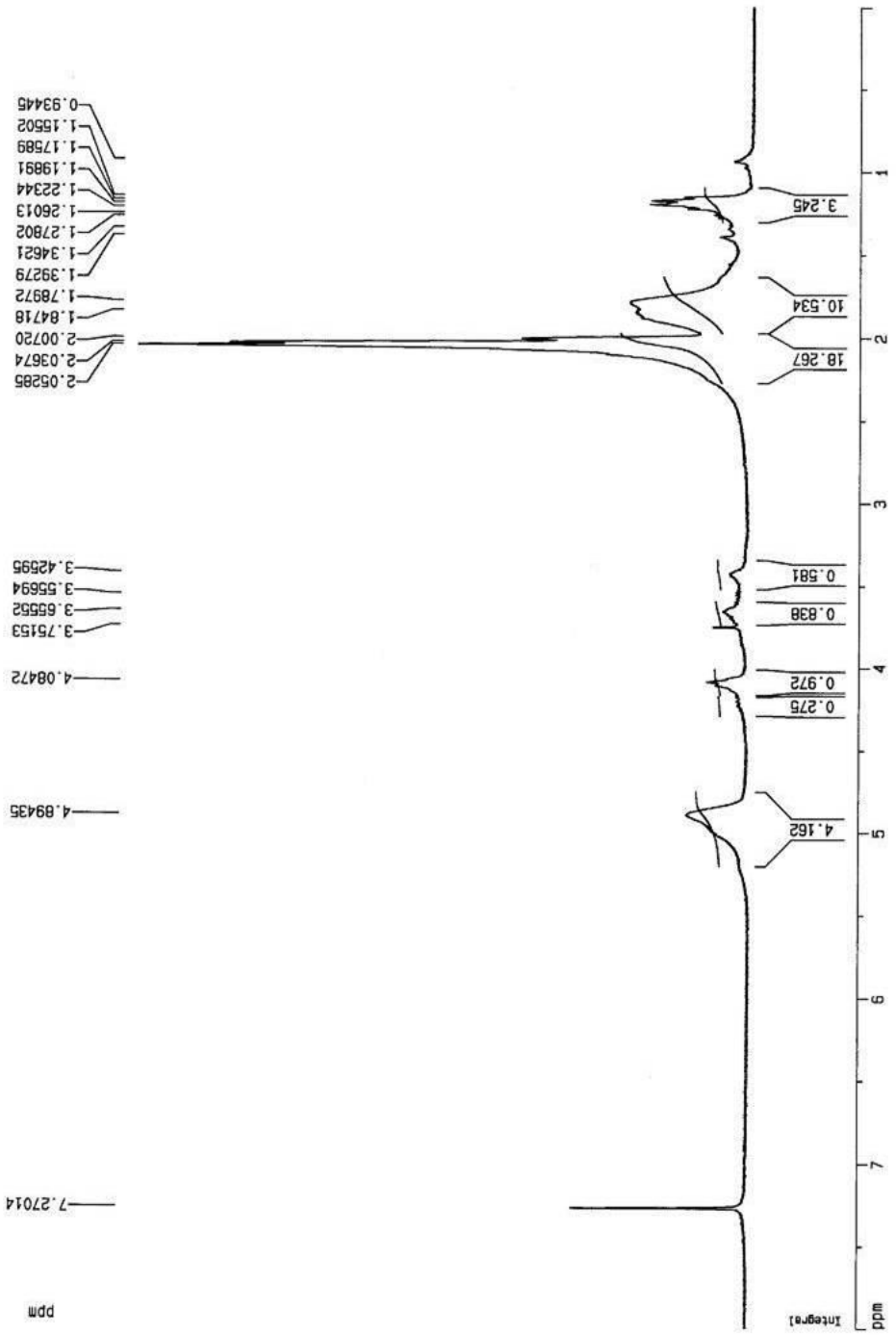

Figure A.15. ^{1}H-NMR spectrum of OVAc8-OH

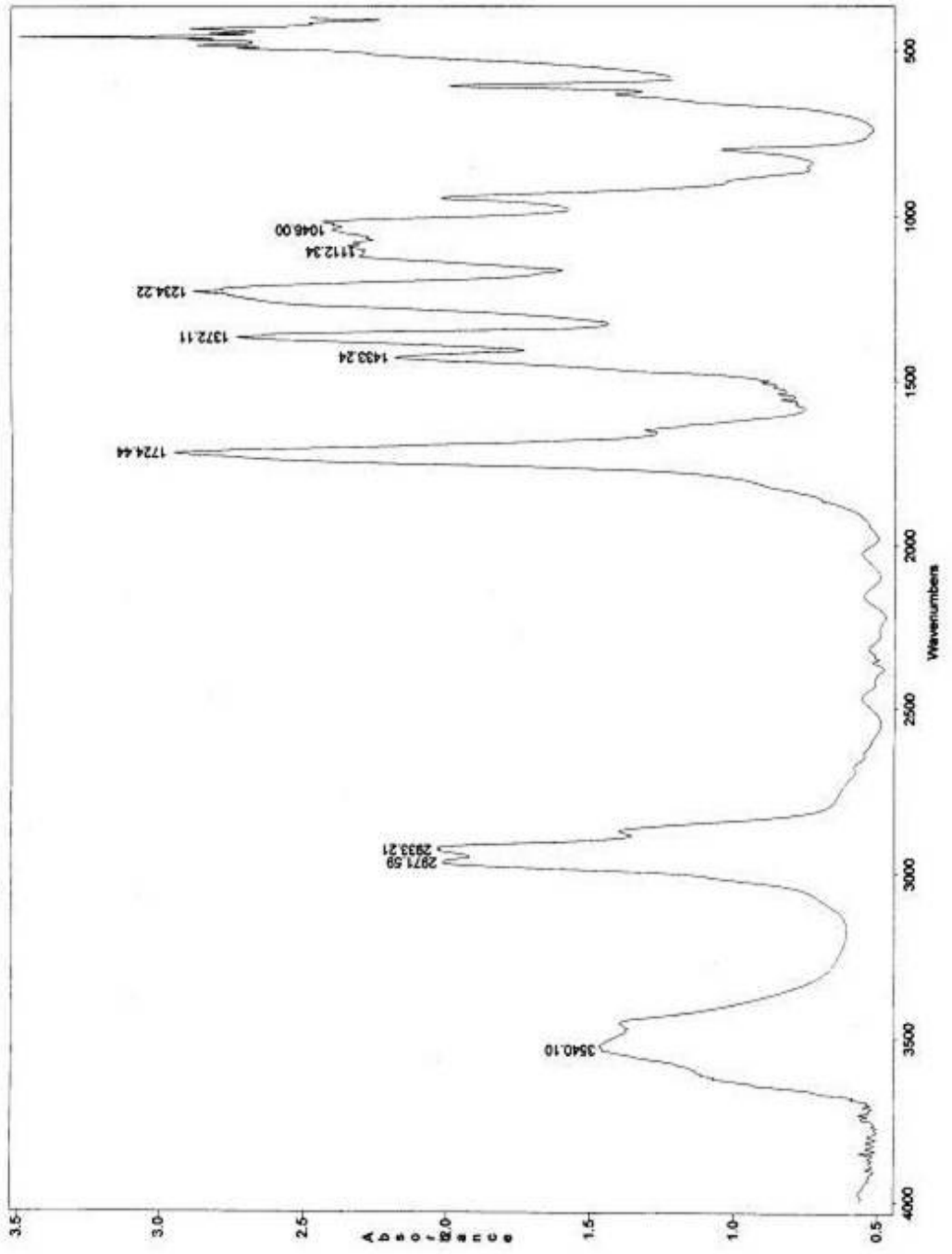

Figure A.16. FTIR spectrum of OVAc10-OH

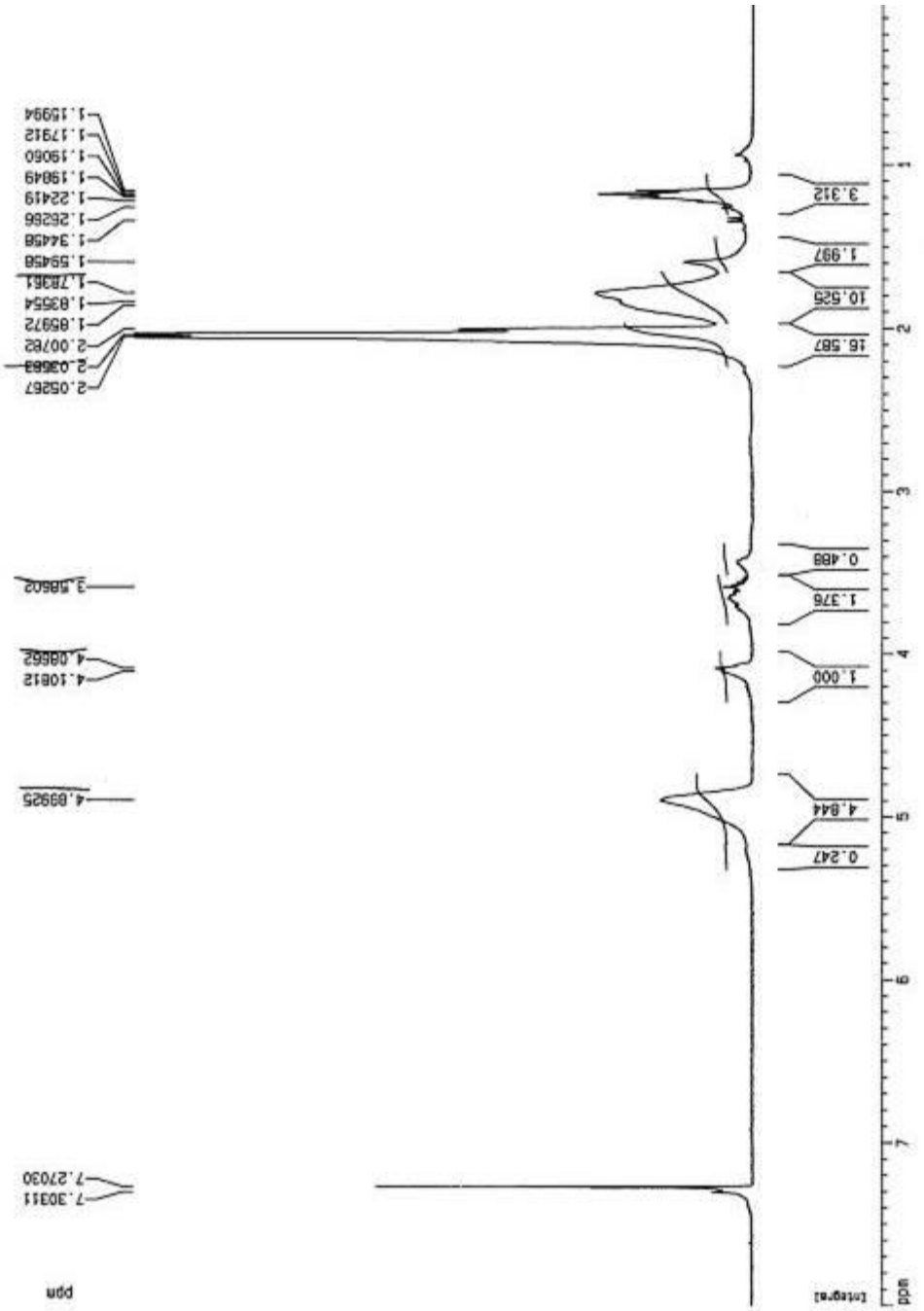

Figure A.17. ^{1}H-NMR spectrum of OVAc10-OH

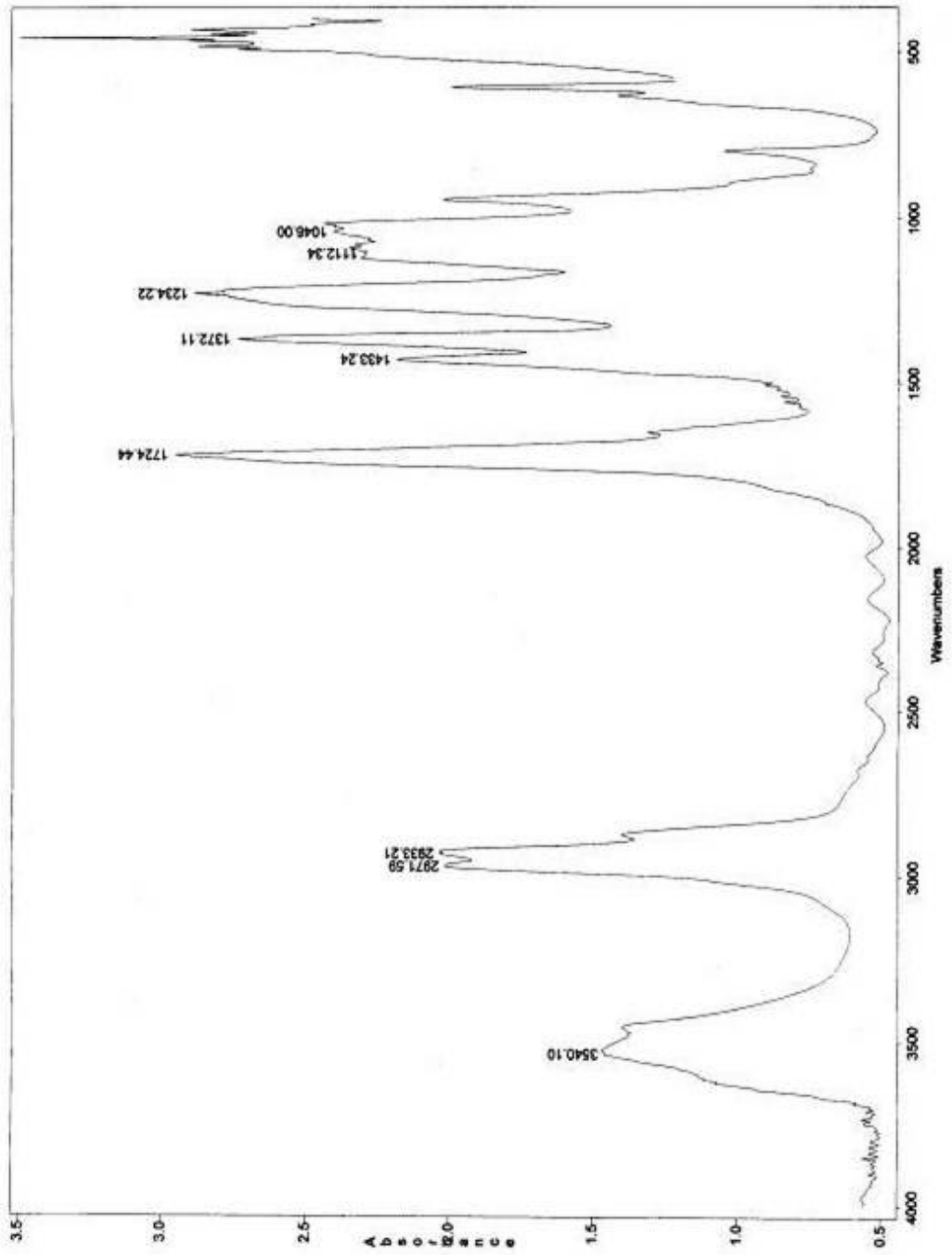

Figure A.18. FTIR spectrum of OVAc17-OH

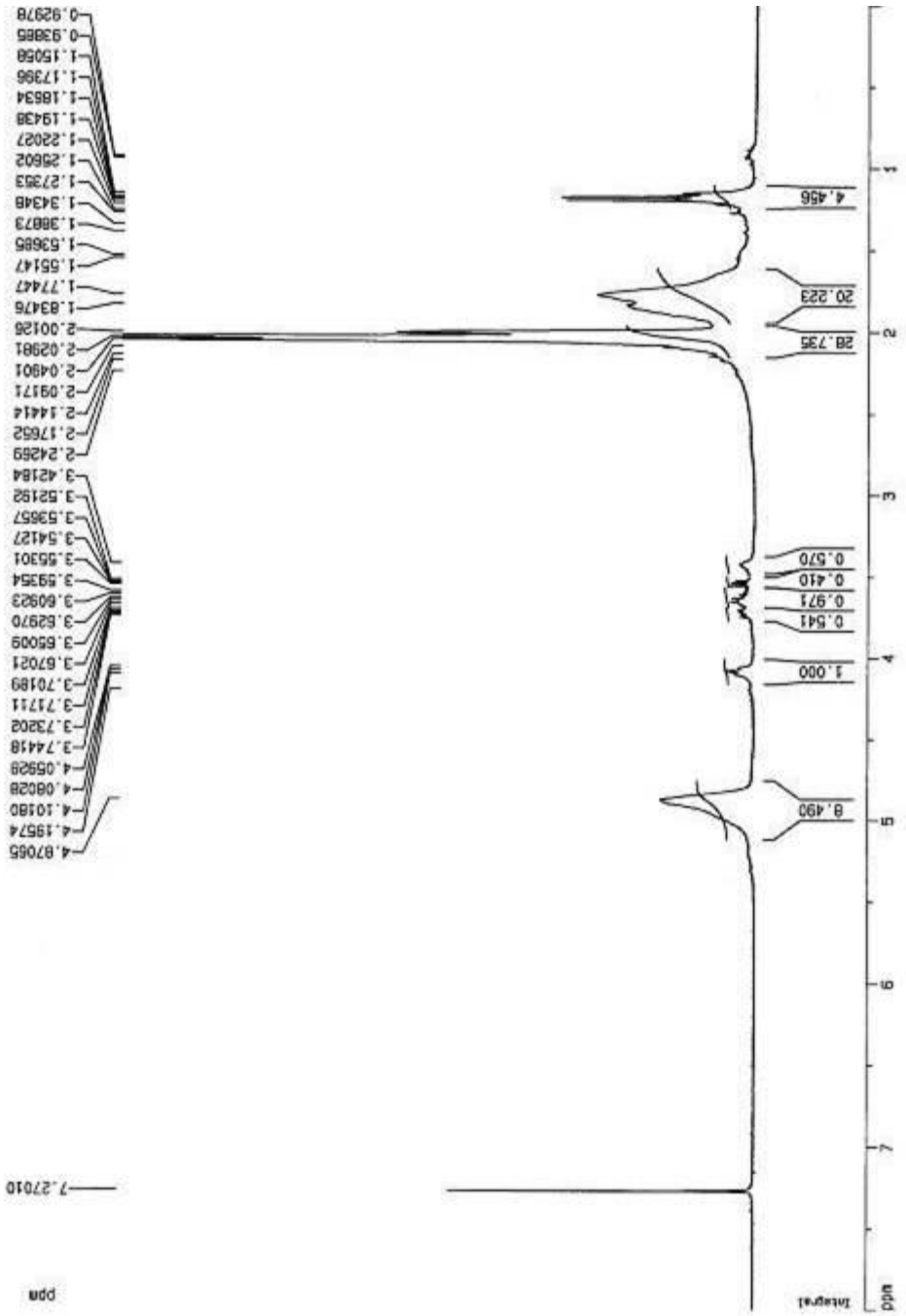

Figure A.19. ^{1}H-NMR spectrum of OVAc17-OH

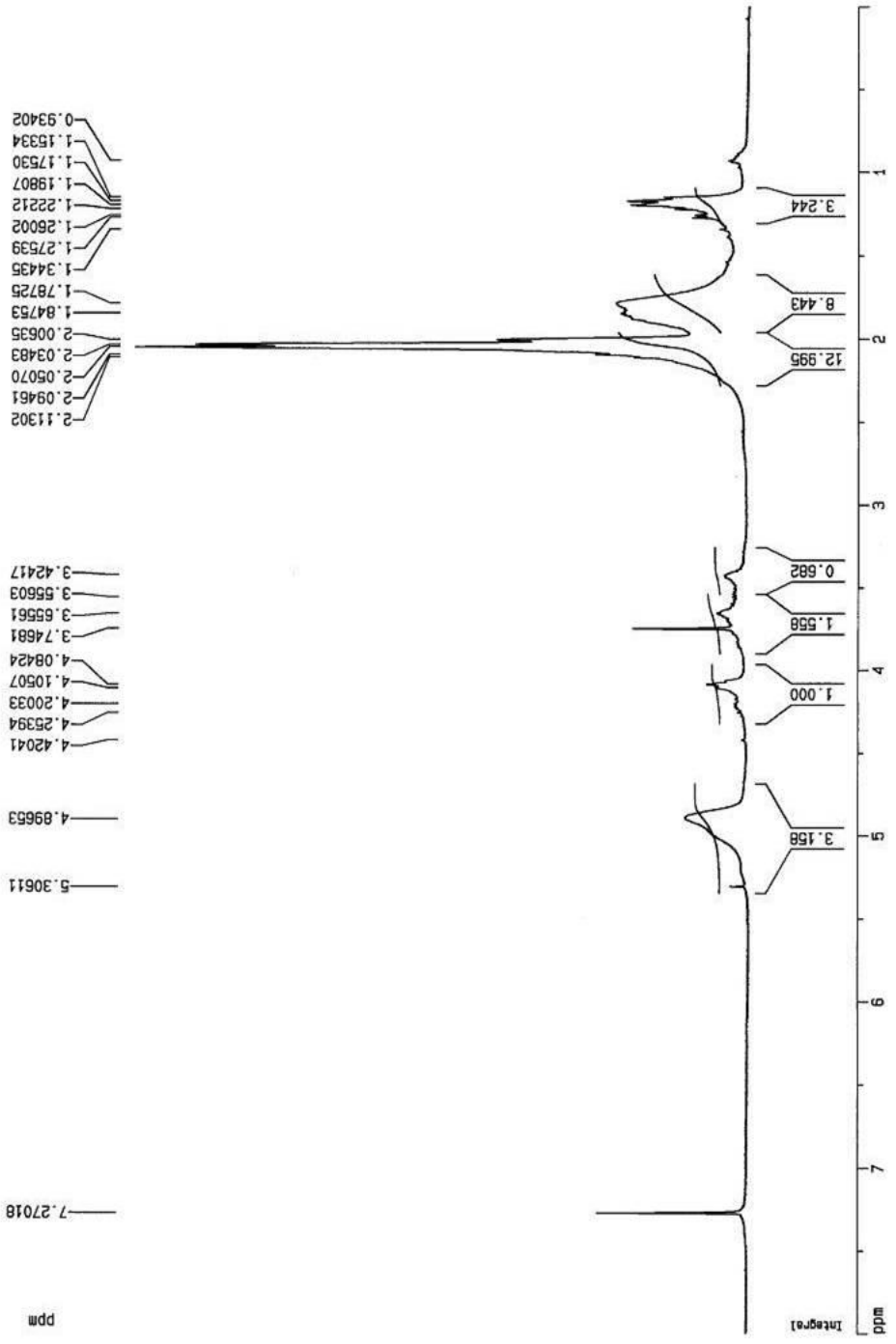

Figure A.20. ^{1}H-NMR spectrum of OVAc6-OSO_3Na

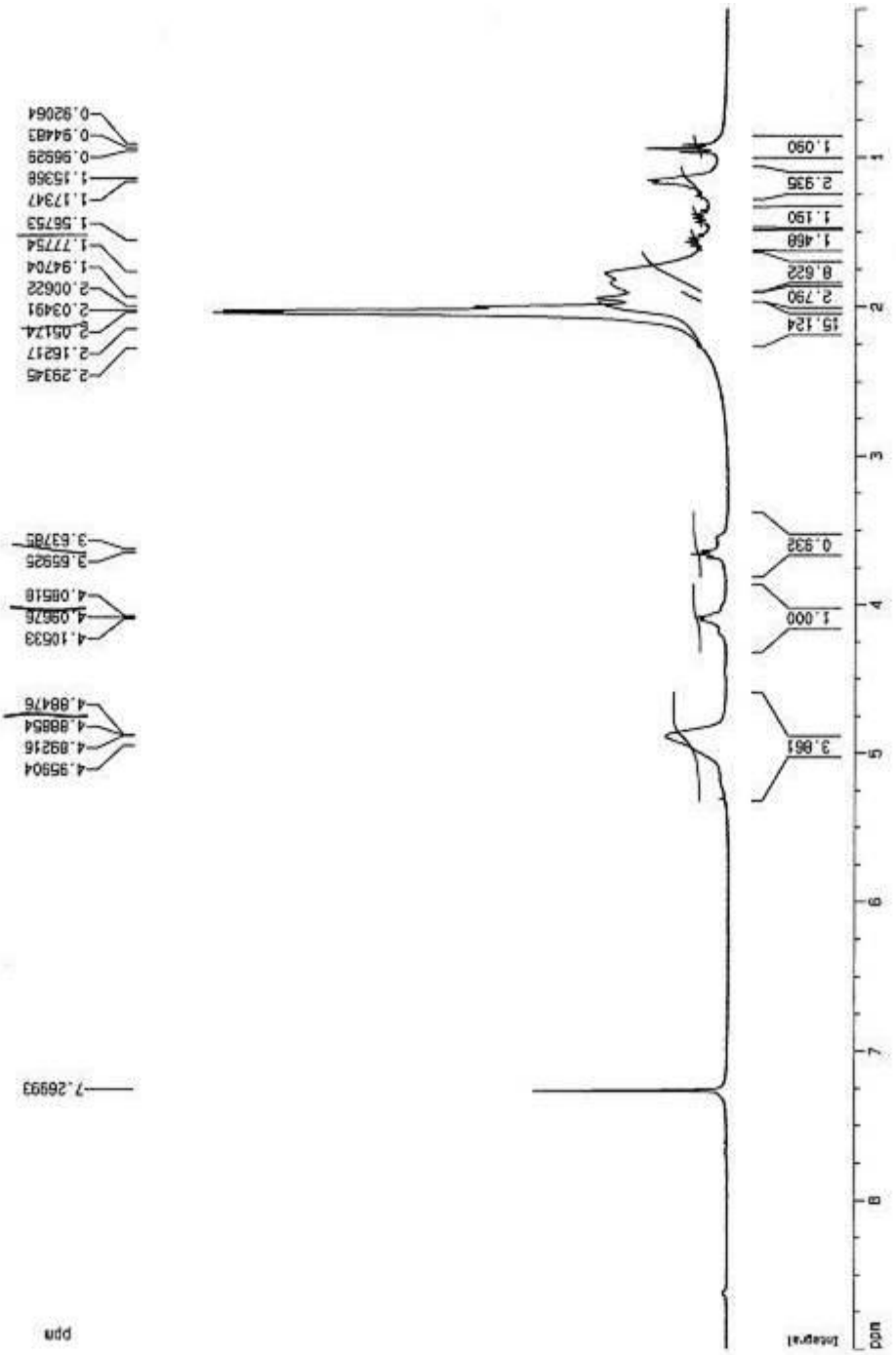

Figure A.21. ^{1}H-NMR spectrum of OVAc10-OSO_3Na

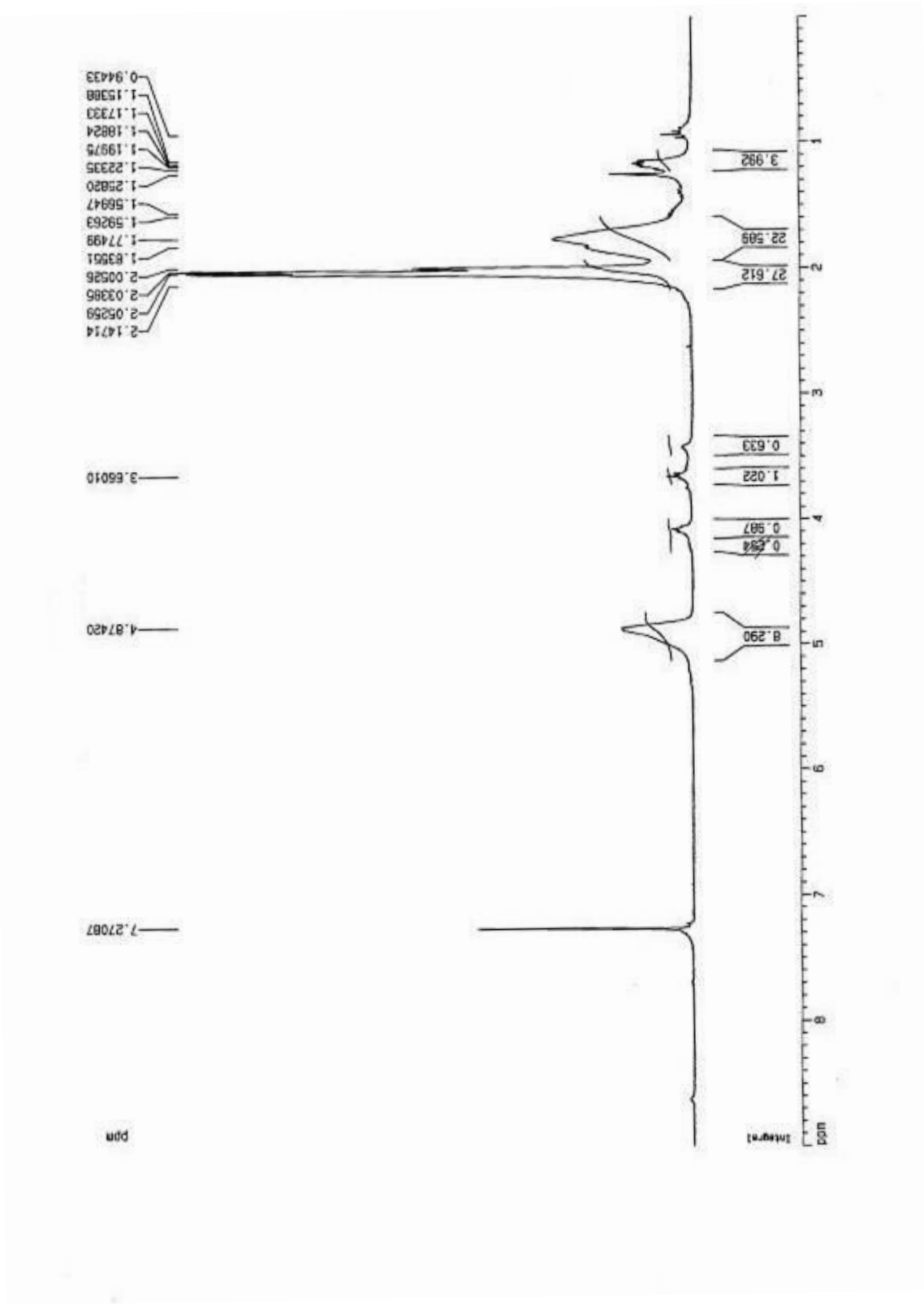

Figure A.22. ^{1}H-NMR spectrum of OVAc17-OSO_3Na

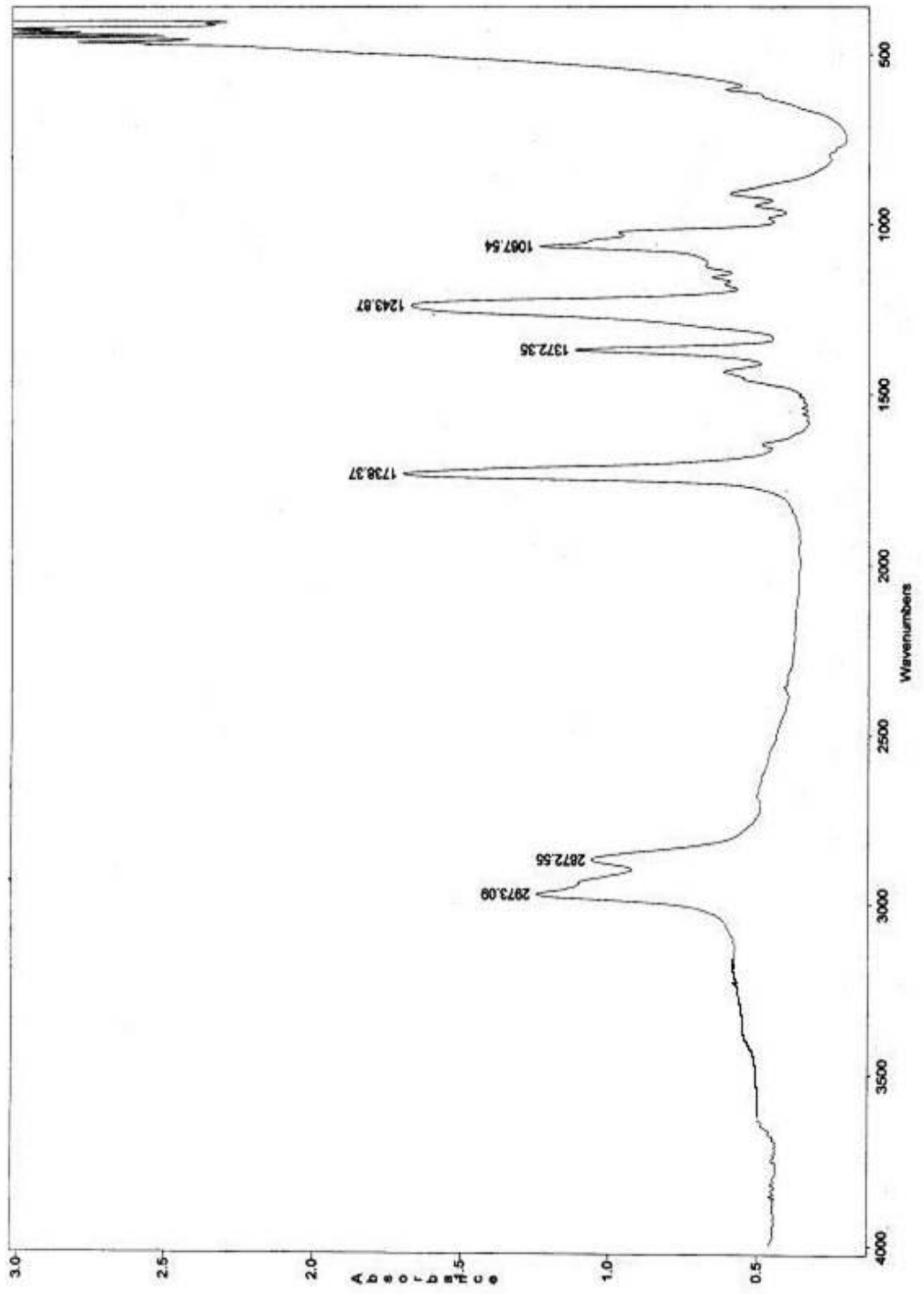

Figure A.23. FTIR spectrum of OVAc8 diester

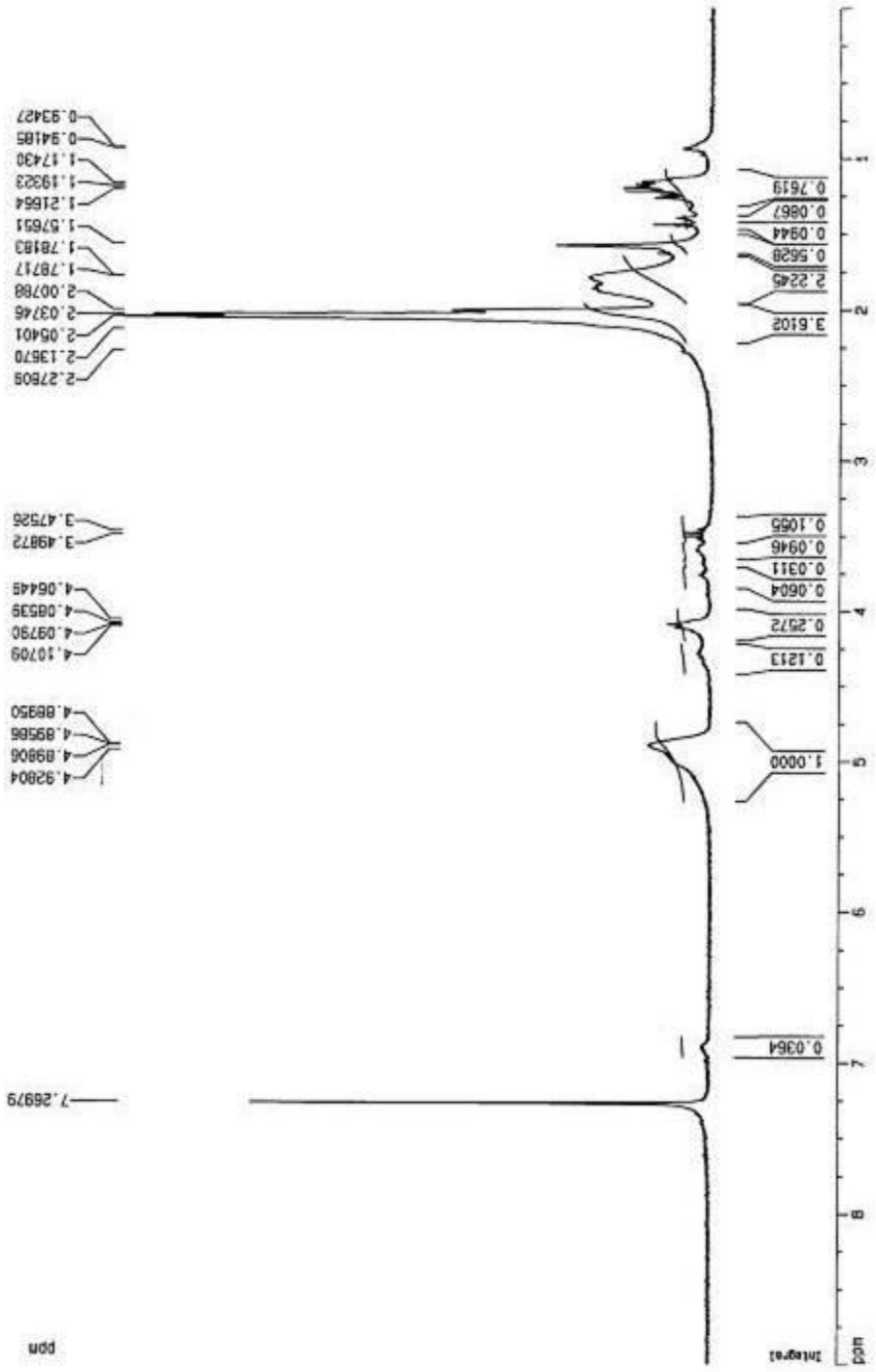

Figure A.24. ^{1}H-NMR spectrum of OVAc8 diester

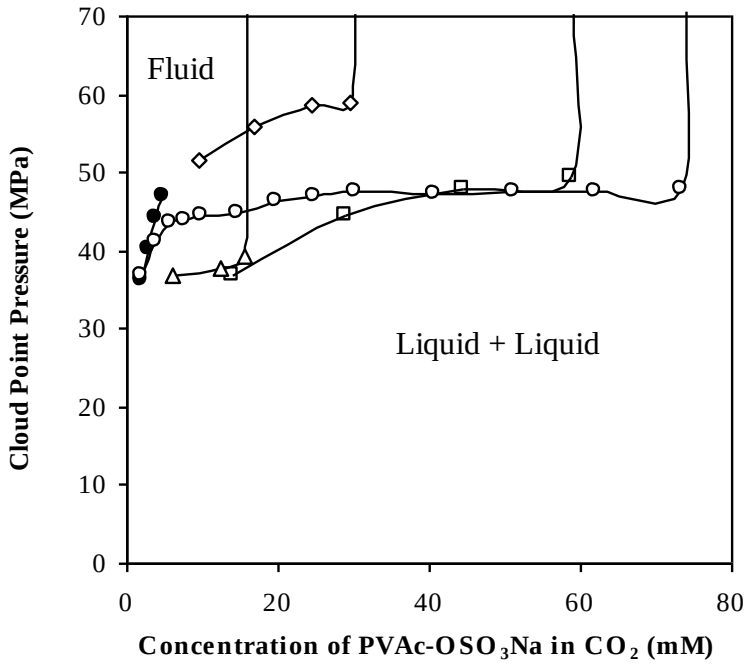

Figure A.25. Phase behavior of PVAc-OSO_3Na/CO_2 mixtures. PVAc6-OSO_3Na, 25 ^oC, W=0 (□); PVAc10-OSO_3Na, 25 ^oC, W=0 (o); PVAc17-OSO_3Na, 25 ^oC, W=0 (Δ); PVAc10-OSO_3Na, 25 ^oC, W=10 (●); PVAc10-OSO_3Na, 40 ^oC, W=0 (◊). (Surfactant concentration in mM).

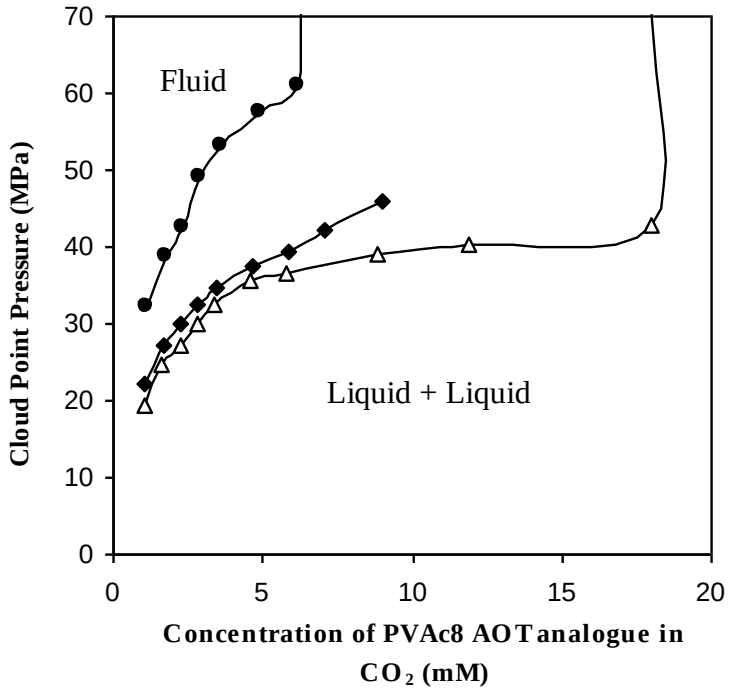

Figure A.26. Phase behavior of sodium bis(vinyl acetate)8 sulfosuccinate/CO_2 mixtures at 25 ^{o}C. W = 0 (Δ); W = 10 (♦); W = 50 (●). (Surfactant concentration in mM).

APPENDIX B

SPECTRA AND PHASE BEHAVIOR OF SURFACTANTS IN CHAPTER 5

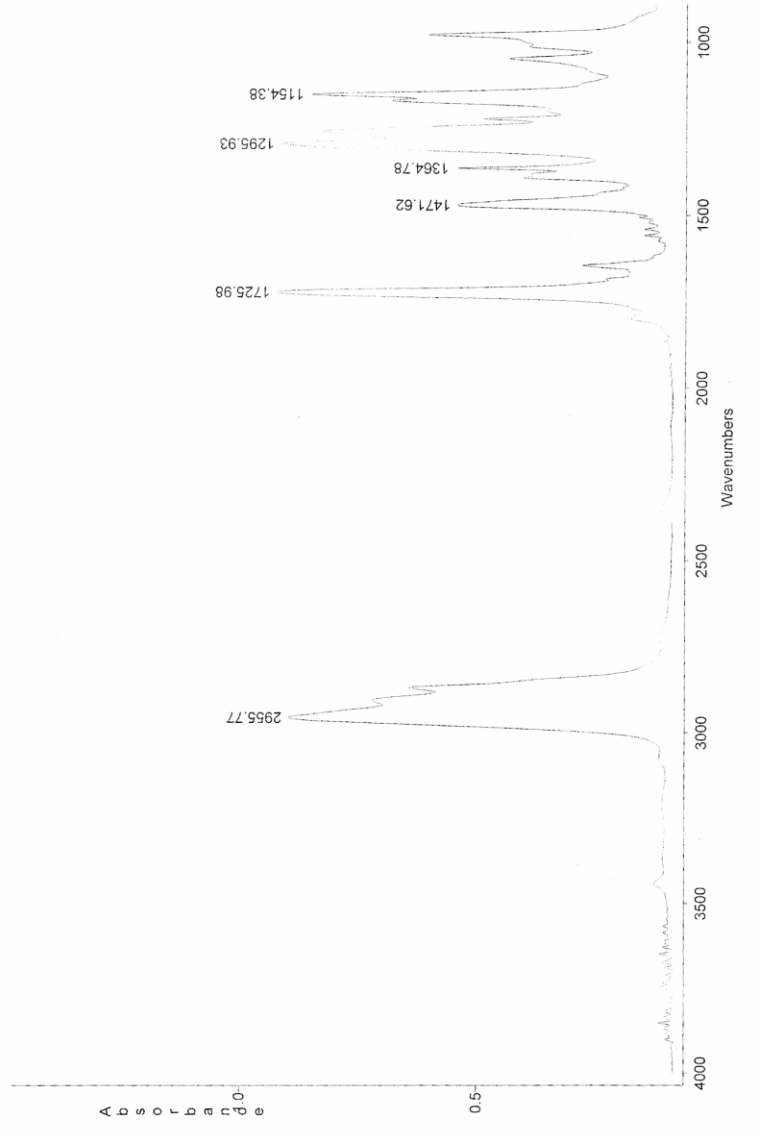

Figure B.1. FTIR spectrum of diester of AOT-TMH

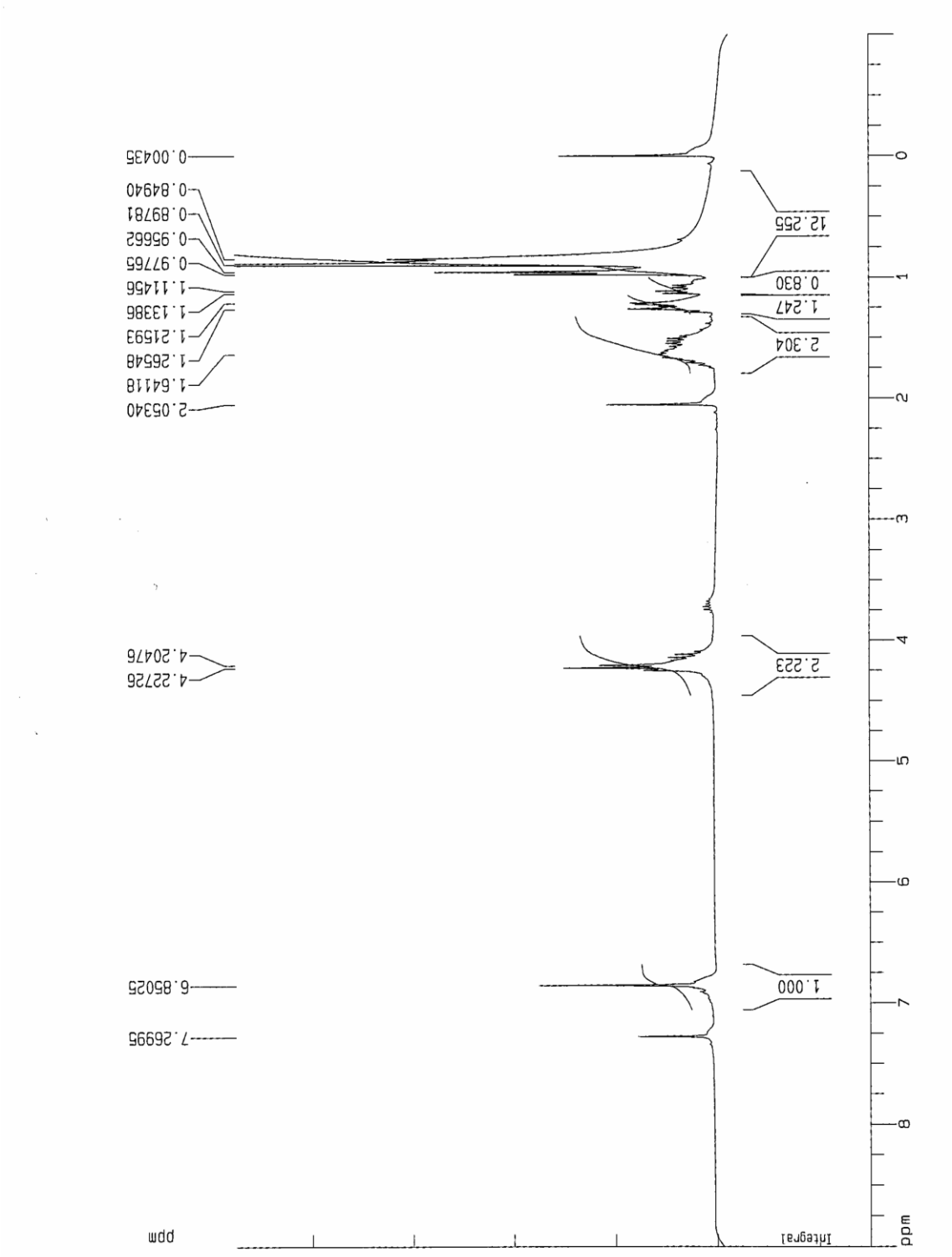

Figure B.2. ^{1}H-NMR spectrum of diester of AOT-TMH

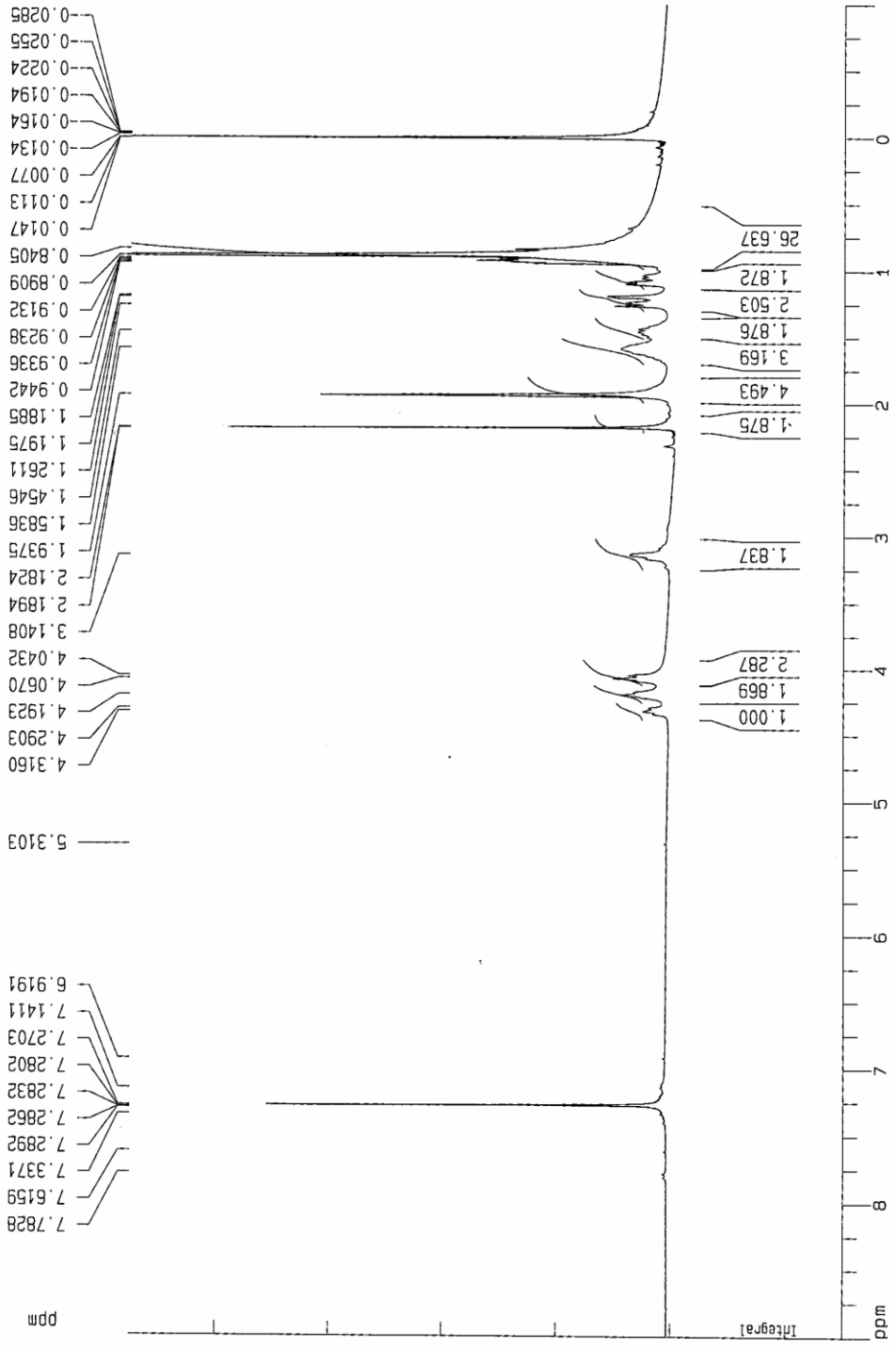

Figure B.3. ^{1}H-NMR spectrum for AOT-TMH

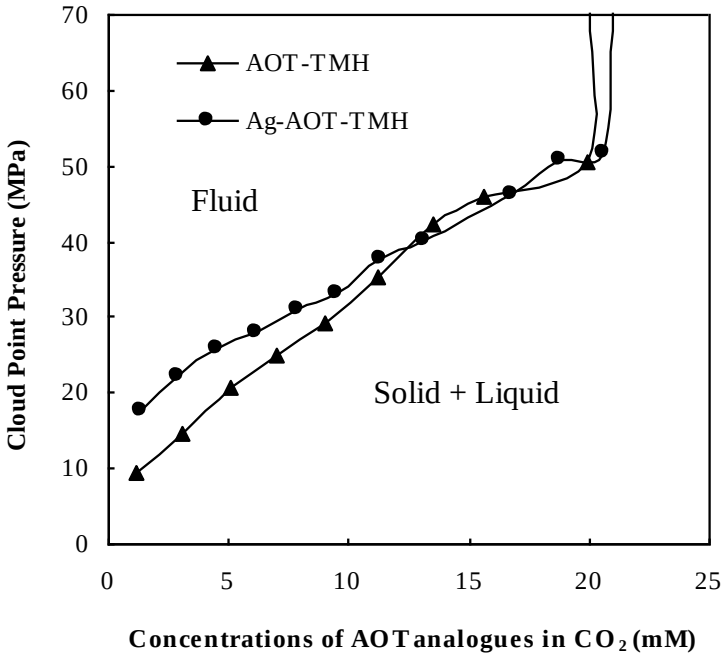

Figure B.4. Phase behavior of AOT-TMH and Ag-AOT-TMH at 40 ^{o}C. (Surfactant concentration in mM).

Table B.1. Soil analysis results of Ag-AOT-TMH

original dissolved Ag-AOT-TMH	0.0154	g
AOT dissolved in volume H_2O	10	mL
moles Ag-AOT-TMH=	3.343E-05	moles
moles H_2O=	0.5555556	moles
original ppm AOT in solution=	60.178749	
assuming all sodium not present exchanged to silver=	85.237314	% exchange

-- ppm in solution --						
Ca	K	Mg	P	Al	B	Cd
8.2	10.0	7.9	7.8	5.4	2.1	<0.1
-- ppm in solution --						
Cr	Cu	Fe	Mn	Na	Ni	Pb
<0.1	0.1	8.2	<0.1	8.9	0.5	2.4

BIBLIOGRAPHY

References for CO_2 Soluble Surfactants

1. Panza, J.L. and E.J. Beckman, *Surfactants in Supercritical Fluids*, in *Supercritical Fluid Technology in Materials Science and Engineering: Syntheses, Properties, and Applications*, Y.P. Sun, Editor. 2002, Marcel Dekker: New York. p. 255-284.
2. Eastoe, J., et al., *Design and Performance of Surfactants for Carbon Dioxide*, in *Supercritical Carbon Dioxide: Separation and Processes*, A.S. Gopalan, C.M. Wai, and H.K. Jacobs, Editors. 2003, ACS Symposium Series 860; American Chemical Society: Washington, DC. p. 285-309.
3. Desimone, J.M., et al., *Dispersion Polymerizations in Supercritical Carbon-Dioxide*. Science, 1994. **265**(5170): p. 356-359.
4. Shaffer, K.A., et al., *Dispersion Polymerizations in Carbon Dioxide Using Siloxane-Based Stabilizers*. Macromolecules, 1996. **29**(7): p. 2704-2706.
5. Yazdi, A.V. and E.J. Beckman, *Design, Synthesis, and Evaluation of Novel, Highly CO_2-Soluble Chelating Agents for Removal of Metals*. Industrial & Engineering Chemistry Research, 1996. **35**(10): p. 3644-3652.
6. Yazdi, A.V. and E.J. Beckman, *Design of Highly CO_2-Soluble Chelating Agents .2. Effect of Chelate Structure and Process Parameters on Extraction Efficiency*. Industrial & Engineering Chemistry Research, 1997. **36**(6): p. 2368-2374.
7. Xu, J.H., A. Wlaschin, and R.M. Enick, *Thickening Carbon Dioxide with the Fluoroacrylate-Styrene Copolymer*. SPE Journal, 2003. **8**(2): p. 85-91.
8. Mistele, C.D., H.H. Thorp, and J.M. Desimone, *Ring-Opening Metathesis Polymerizations in Carbon Dioxide*. Journal of Macromolecular Science-Pure and Applied Chemistry, 1996. **A33**(7): p. 953-960.
9. Consani, K.A. and R.D. Smith, *Observations on the Solubility of Surfactants and Related Molecules in Carbon Dioxide at 50°C*. Journal of Supercritical Fluids, 1990. **3**(2): p. 51-65.
10. Hoefling, T.A., R.M. Enick, and E.J. Beckman, *Microemulsions in Near-Critical and Supercritical CO_2*. J. Phys. Chem., 1991. **95**: p. 7127.
11. Newman, D.A., et al., *Phase-Behavior of Fluoroether-Functional Amphiphiles in Supercritical Carbon-Dioxide*. Journal of Supercritical Fluids, 1993. **6**(4): p. 205-210.
12. Desimone, J.M., Z. Guan, and C.S. Elsbernd, *Synthesis of Fluoropolymers in Supercritical Carbon-Dioxide*. Science, 1992. **257**(5072): p. 945-947.
13. Hoefling, T.A., et al., *Effect of Structure on the Cloud-Point Curves of Silicone-Based Amphiphiles in Supercritical Carbon-Dioxide*. Journal of Supercritical Fluids, 1993. **6**(3): p. 165-171.
14. Hoefling, T.A., et al., *Design and Synthesis of Highly CO_2-Soluble Surfactants and Chelating-Agents*. Fluid Phase Equilibria, 1993. **83**: p. 203-212.
15. Eastoe, J., A. Paul, and A. Downer, *Effects of Fluorocarbon Surfactant Chain Stucture on Stability of Water-in-Carbon Dioxide Microemulsions. Links between Aqueous Surface Tension and Microemulsion Stability*. Langmuir, 2002. **18**(8): p. 3014-3017.
16. Fink, R. and E.J. Beckman, *Phase Behavior of Siloxane-based Amphiphiles in Supercritical Carbon Dioxide*. Journal of Supercritical Fluids, 2000. **18**(2): p. 101-110.
17. Psathas, P.A., et al., *Water-in-Carbon Dioxide Emulsions with Poly(dimethylsiloxane)-based Block Copolymer Ionomers*. Industrial & Engineering Chemistry Research, 2000. **39**(8): p. 2655-2664.
18. McNally, M.P. and F.V. Bright, *"Supercritical Fluid Technology"*. ACS Symposium Series, 1992. **488**.
19. Kumar, S.K. and K.P. Johnston, *Modelling the Solubility of Solids in Supercritical Fluids with Density as the Independent Variable*. Journal of Supercritical Fluids, 1988. **1**(1): p. 15-22.
20. Technical Insights, I., *Supercritical Fluids Processing: Emerging Opportunities*. Emerging Technologies. Vol. no. 15. 1985, Fort Lee, N.J.
21. McHugh, M.A. and V.J. Krukonis, *Supercritical Fluid Extraction: Principles and Practice, 2nd Edition*, ed. H. Brenner. 1994, Stoneham, MA: Butterworth-Heinemann.
22. Schneider, G.M., *Physiochemical Principles of Extraction with Supercritical Gases*. Angew. Chem. Int. Ed. Engl., 1978. **17**: p. 716.
23. Hyatt, J.A., *Liquid and Supercritical Carbon Dioxide as Organic Solvents*. Journal of Organic Chemistry, 1984. **49**(26): p. 5097-5101.
24. Mcfann, G.J., et al., *Carbon-Dioxide Regeneration of Block-Copolymer Micelles Used for Extraction and Concentration of Trace Organics*. Industrial & Engineering Chemistry Research, 1993. **32**(10): p. 2336-2344.

25. Mcfann, G.J., K.P. Johnston, and S.M. Howdle, *Solubilization in Nonionic Reverse Micelles in Carbon-Dioxide.* AIChE Journal, 1994. **40**(3): p. 543-555.
26. Kazarian, S.G., et al., *Specific Intermolecular Interaction of Carbon Dioxide with Polymers.* Journal of the American Chemical Society, 1996. **118**(7): p. 1729-1736.
27. Meredith, J.C., et al., *Quantitative Equilibrium Constants between CO_2 and Lewis bases from FTIR Spectroscopy.* Journal of Physical Chemistry, 1996. **100**(26): p. 10837-10848.
28. Mertdogan, C.A., T.P. DiNoia, and M.A. McHugh, *Impact of Backbone Architecture on the Solubility of Fluorocopolymers in Supercritical CO_2 and Halogenated Supercritical Solvents: Comparison of Poly(vinylidene fluoride-co-22 mol % hexafluoropropylene) and Poly(tetrafluoroethylene-co-19 mol % hexafluoropropylene).* Macromolecules, 1997. **30**(24): p. 7511-7515.
29. Rindfleisch, F., T.P. DiNoia, and M.A. McHugh, *Solubility of Polymers and Copolymers in Supercritical CO_2.* Journal of Physical Chemistry, 1996. **100**(38): p. 15581-15587.
30. O'Neill, M.L., et al., *Solubility of Homopolymers and Copolymers in Carbon Dioxide.* Industrial & Engineering Chemistry Research, 1998. **37**(8): p. 3067-3079.
31. Jacobson, G.B., et al., *Organic Synthesis in Water/Carbon Dioxide Emulsions.* Journal of Organic Chemistry, 1999. **64**: p. 1207-1210.
32. Jacobson, G.B., et al., *Enhanced Catalyst Reactivity and Separations Using Water/Carbon Dioxide Emulsions.* Journal of the American Chemical Society, 1999. **121**: p. 11902-11903.
33. Ohde, H., F. Hunt, and C.M. Wai, *Synthesis of Silver and Copper Nanoparticles in a Water-in-Supercritical Carbon Dioxide Microemulsion.* Chemistry of Materials, 2001. **13**(11): p. 4130-4135.
34. Ohde, H., et al., *Hydrogenation of Olefins in Supercritical CO_2 Catalyzed by Palladium Nanoparticles in a Water-in-CO_2 Microemulsion.* Journal of the American Chemical Society, 2002. **124**(17): p. 4540-4541.
35. Iezzi, A., *Supercritical Fluid Science and Technology*, in *ACS Symposium Series 406*, J.M.L.P. Keith P. Johnson, Editor. 1989, American Chemical Society: Washington DC. p. 122.
36. Harrison, K., et al., *Water-in-Carbon Dioxide Microemulsions with a Fluorocarbon-Hydrocarbon Hybrid Surfactant.* Langmuir, 1994. **10**(10): p. 3536-3541.
37. Eastoe, J., et al., *Fluoro-Surfactants at Air/Water and Water/CO_2 Interfaces.* Physical Chemistry Chemical Physics, 2000. **2**(22): p. 5235-5242.
38. Heitz, M.P., et al., *Water Core within Perfluopolyether-based Microemulsions formed in Supercritical Carbon Dioxide.* J. Phys. Chem. B, 1997. **101**: p. 6707.
39. Chillura-Martino, D., et al., *Neutroon Scattering Characterization of Homopolymer and Graft-Copolymer Micelles in Supercritical Carbon Dioxide.* J. Mol. Struct., 1997. **383**: p. 3.
40. McClain, J.B., et al., *Design of Nonionic Sufactants for Spercritical Carbon Dioxide.* Science, 1996. **274**(5295): p. 2049-2052.
41. Fulton, J.L., et al., *Aggregation of Amphiphilic Molecules in Supercritical Carbon-Dioxide - a Small-Angle X-Ray-Scattering Study.* Langmuir, 1995. **11**(11): p. 4241-4249.
42. Heller, J.P., D.K. Dandge, and R.J. Card, *Direct Thickners for Mobility Control of CO_2 Floods.* Society of Petroleum Engineers Journal, 1985. **25**(5): p. 679-686.
43. Kirby, C.F. and M.A. McHugh, *Phase Behavior of Polymers in Supercritical Fluid Solvents.* Chemical Reviews, 1999. **99**(2): p. 565-602.
44. Stone, M.T., et al., *Molecular Differences between Hydrocarbon and Fluorocarbon Surfactants at the CO2/Water Interface.* Journal of Physical Chemistry B, 2003. **107**(37): p. 10185-10192.
45. Stone, M.T., et al., *Low interfacial free volume of Stubby surfactants stabilizes water-in-carbon dioxide microemulsions.* Journal of Physical Chemistry B, 2004. **108**(6): p. 1962-1966.
46. Ryoo, W., S.E. Webber, and K.P. Johnston, *Water-in-Carbon Dioxide Microemulsions with Methylated Branched Hydrocarbon Surfactants.* Industrial & Engineering Chemistry Research, 2003. **42**(25): p. 6348-6358.
47. Raveendran, P. and S.L. Wallen, *Sugar Acetates as Novel, Renewable CO_2-Philes.* Journal of the American Chemical Society, 2002. **124**(25): p. 7274-7275.
48. Potluri, V.K., et al., *Peracetylated Sugar Derivatives Show High Solubility in Liquid and Supercritical Carbon Dioxide.* Organic Letters, 2002. **4**(14): p. 2333-2335.
49. Hong, L., M.C. Thies, and R.M. Enick, *Global Phase Behavior for CO_2-philic Solids: the CO_2 + ß-D-Maltose Octaacetate System.* Journal of Supercritical Fluids, 2005. **34**(1): p. 11-16.
50. Potluri, V.K., et al., *The High CO_2-Solubility of per-Acetylated Alpha-, Beta-, and Gamma-Cyclodextrin.* Fluid Phase Equilibria, 2003. **211**(2): p. 211-217.

51. Raveendran, P. and S.L. Wallen, *Cooperative C-H···O Hydrogen Bonding in CO_2-Lewis Base Complexes: Implications for Solvation in Supercritical CO_2.* Journal of the American Chemical Society, 2002. **124**(42): p. 12590-12599.
52. Blatchford, M.A., P. Raveendran, and S.L. Wallen, *Spectroscopic Studies of Model Carbonyl Compounds in CO_2: Evidence for Cooperative C-H Center dot center dot center dot O interactions.* Journal of Physical Chemistry A, 2003. **107**(48): p. 10311-10323.
53. Shen, Z., et al., *CO_2-Solubility of Oligomers and Polymers that Contain the Carbonyl Group.* Polymer, 2003. **44**(5): p. 1491-1498.
54. Kilic, S., et al., *Effect of Grafted Lewis Base Groups on the Phase Behavior of Model Poly(dimethyl siloxanes) in CO_2.* Industrial & Engineering Chemistry Research, 2003. **42**(25): p. 6415-6424.
55. da Rocha, S.R.P., K.L. Harrison, and K.P. Johnston, *Effect of Surfactants on the Interfacial Tension and Emulsion Formation between Water and Carbon Dioxide.* Langmuir, 1999. **15**(2): p. 419-428.
56. Sarbu, T., T. Styranec, and E.J. Beckman, *Non-Fluorous Polymers with very High Solubility in Supercritical CO_2 down to Low Pressures.* Nature, 2000. **405**(6783): p. 165-168.
57. Liu, J.C., et al., *Solubility of Ls-36 and Ls-45 Surfactants in Supercritical CO_2 and Loading Water in the CO_2/Water/Surfactant Systems.* Langmuir, 2002. **18**(8): p. 3086-3089.
58. Liu, J.C., et al., *Formation of Water-in-CO_2 Microemulsions with Non-Fluorous Surfactant Ls-54 and Solubilization of Biomacromolecules.* Chemistry-A European Journal, 2002. **8**(6): p. 1356-1360.
59. Drohmann, C. and E.J. Beckman, *Phase Behavior of Polymers Containing Ether Groups in Carbon Dioxide.* Journal of Supercritical Fluids, 2002. **22**(2): p. 103-110.
60. Nave, S., J. Eastoe, and J. Penfold, *What is So Special about Aerosol-OT? 1. Aqaueous Systems.* Langmuir, 2000. **16**(23): p. 8733-8740.
61. Eastoe, J., et al., *Micellization of Hydrocarbon Surfactants in Supercritical Carbon Dioxide.* Journal of the American Chemical Society, 2001. **123**(5): p. 988-989.
62. Johnston, K.P., et al., *Water in Carbon Dioxide Macroemulsions and Miniemulsions with a Hydrocarbon Surfactant.* Langmuir, 2001. **17**(23): p. 7191-7193.
63. Gale, R.W., J.L. Fulton, and R.D. Smith, *Organized Molecular Assemblies in the Gas Phase: Reverse Micelles and Microemulsions in Supercritical Fluids.* Journal of the American Chemical Society, 1987. **109**(3): p. 920-921.
64. Bartscherer, K.A., M. Minier, and H. Renon, *Microemulsions in Compressible Fluids.* Fluid Phase Equilibria, 1995. **107**(93-150).
65. Johnston, K.P., G.J. Mcfann, and D.G. Peck, *Design and Characterization of the Molecular Environment in Supercritical Fluids.* Fluid Phase Equilibria, 1989. **52**: p. 337-346.
66. Johnston, K.P., et al., *Water-in-Carbon Dioxide Microemulsions: An Environment for Hydrophiles Including Proteins.* Science, 1996. **271**: p. 624-626.
67. Heitz, M.P., et al., *Water Core within Perfluoropolyether-Based Microemulsions Formed in Supercritical Carbon Dioxide.* Journal of Physical Chemistry B, 1997. **101**(34): p. 6707-6714.
68. Clarke, M.J., et al., *Water in Supercritical Carbon Dioxide Microemulsions: Spectroscopic Investigation of a New Environment for Aqueous Inorganic Chemistry.* Journal of the American Chemical Society, 1997. **119**(27): p. 6399-6406.
69. Johnston, K.P., et al., *Water-in-Carbon Dioxide Microemulsions: an Environment for Hydrophiles including Proteins.* Science (Washington, D. C.), 1996. **271**(5249): p. 624-6.
70. Lee, C.T., et al., *Droplet interactions in Water-in-Carbon Dioxide Microemulsions Near the Critical Ppoint: A Small-Angle Neutron Scattering Study.* Journal of Physical Chemistry B, 2001. **105**(17): p. 3540-3548.
71. Zielinski, R.G., et al., *A small-angle neutron scattering study of water in carbon dioxide microemulsions.* Langmuir, 1997. **13**(15): p. 3934-3937.
72. Sun, Y.P., P. Atorngitjawat, and M.J. Meziani, *Preparation of Silver Nanoparticles via Rapid Expansion of Water in Carbon Dioxide Microemulsion into Reductant Solution.* Langmuir, 2001. **17**(19): p. 5707-5710.
73. McLeod, M.C., et al., *Synthesis and Stabilization of Silver Metallic Nanoparticles and Premetallic Intermediates in Perfluoropolyether/CO_2 Reverse Micelle Systems.* Journal of Physical Chemistry B, 2003. **107**(12): p. 2693-2700.
74. Ji, M., et al., *Synthesizing and Dispersing Silver Nanoparticles in a Water-in-Supercritical Carbon Dioxide Microemulsion.* Journal of the American Chemical Society, 1999. **121**(11): p. 2631-2632.
75. McLeod, M.C., W.F. Gale, and C.B. Roberts, *Metallic nanoparticle production utilizing a supercritical carbon dioxide flow process.* Langmuir, 2004. **20**(17): p. 7078-7082.
76. Esumi, K., S. Sarashina, and T. Yoshimura, *Synthesis of Gold Nanoparticles from an Organometallic Compound in Supercritical Carbon Dioxide.* Langmuir, 2004. **20**(13): p. 5189-5191.

77. Morley, K.S., et al., *Clean Preparation of Nanoparticulate Metals in Porous Supports: a Supercritical Route*. Journal of Materials Chemistry, 2002. **12**(6): p. 1898-1905.
78. Ohade, H., M. Ohde, and C.M. Wai, *Swelled Plastics in Supercritical CO_2 as Media for Stabilization of Metal Nanoparticles and for Catalytic Hydrogenation.* Chemical Communications, 2004(8): p. 930-931.
79. Watkins, J.J., J.M. Blackburn, and T.J. McCarthy, *Chemical Fluid Deposition: Reactive Deposition of Platinum Metal from Carbon Dioxide Solution.* Chemistry of Materials, 1999. **11**(2): p. 213-215.
80. Blackburn, J.M., et al., *Deposition of Conformal Copper and Nickel Films from Supercritical Carbon Dioxide.* Science, 2001. **294**(5540): p. 141-5.
81. Shah, P.S., et al., *Nanocrystal Arrested Precipitation in Supercritical Carbon Dioxide*. Journal of Physical Chemistry B, 2001. **105**(39): p. 9433-9440.
82. Shah, P.S., et al., *Role of Steric Stabilization on the Arrested Growth of Silver Nanocrystals in Supercritical Carbon Dioxide.* Journal of Physical Chemistry B, 2002. **106**(47): p. 12178-12185.
83. Taber, J.J., F.D. Martin, and R.S. Seright, *EOR Screening Criteria Revisited .1. Introduction to Screening Criteria and Enhanced Recovery Field Projects.* SPE Reservoir Engineering, 1997. **12**(3): p. 189-198.
84. Enick, R., G. Holder, and B. Morsi, *A Thermodynamic Correlation for the Minimum Miscibility Pressure in CO_2 Flooding of Petroleum Reserviors.* SPE Reservoir Engineering, 1988.
85. Carcoana, A., *Applied Enhanced Oil Recovery*. 1992: Prentice Hall.
86. Xu, J., *Carbon Dioxide Thickening Agents for Reducing CO_2 Mobility*, in *Department of Chemical and Petroleum Engineering*. 2003, University of Pittsburgh: Pittsburgh.
87. Caudle, B.H. and A.B. Dyes, *Improving Miscible Displacement by Gas-Water Injection.* Trans AIME, 1958. **213**: p. 281-284.
88. Lee, H.O. and J.P. Heller, *Laboratory Measurements of CO_2-Foam Mobility*. SPE Reservoir Engineering, 1990. **5**(2).
89. Lee, H.O., J.P. Heller, and A. Hoefer, *Change in Apparent Viscosity of CO_2 Foam with Rock Permeability.* SPE Reservoir Engineering, 1991. **6**(4): p. 421-428.
90. Schramm, L.L., ed. *Foams: Fundamentals and Applications in the Petroleum Industry*. Chapter 5. CO_2 Foams in Enhanced Oil Recovery, ed. J.P. Heller. 1994, American Chemical Society, Advances in Chemistry Series: Washington, DC.
91. Wellington, S.L., *Reservoir-Tailored CO_2-Aided Oil Recovery Process*. 1983, Shell Oil Company (Houston, TX): United States.
92. Wellington, S.L., et al., *Polyalkoxy Sulfonate, CO_2 and Brine Drive Process for Oil Recovery*. 1985, Shell Oil Company: United States.
93. McClain, J.B., et al., *Solution Properties of a CO_2-Soluble Fluoropolymer via Small Angle Neutron Scattering.* Journal of the American Chemical Society, 1996. **118**(4): p. 917-918.
94. Huang, Z.H., et al., *Enhancement of the Viscosity of Carbon Dioxide using Styrene/Fluoroacrylate Copolymers.* Macromolecules, 2000. **33**(15): p. 5437-5442.
95. Fan, X., et al., *Oxygenated Hydrocarbon Ionic Surfactants Exhibit CO_2 Solubility.* Journal of the American Chemical Society, 2005. **Web Released**(35).
96. Span, R. and W. Wagner, *A New Equation of State for Carbon Dioxide Covering the Fluid Region from the Triple-Point Temperature to 1100 K at Pressures up to 800 MPa.* Journal of Physical and Chemical Reference Data, 1996. **25**(6): p. 1509-1596.
97. Panagiotopoulos, A.Z. and R.C. Reid, *New Mixing Rule for Cubic Equations of State for Highly Polar, Asymmetric System*, in *Equations of State: Theories and Applications*, K.C. Chao and R.L. Robinson, Editors. 1986, ACS symposium series 300; American Chemical Society: Washington, D.C. p. 577.
98. Hutton, B.H., et al., *Investigation of AOT Reverse Microemulsions in Supercritical Carbon Dioxide.* Colloids and Surfaces, A: Physicochemical and Engineering Aspects, 1999. **146**(1-3): p. 227-241.
99. Lee, C.T., Jr., et al., *Formation of Water-in-Carbon Dioxide Microemulsions with a Cationic Surfactant: A Small-Angle Neutron Scattering Study.* Journal of Physical Chemistry B, 2000. **104**(47): p. 11094-11102.
100. Maury, E.E., et al., *Graft Copolymer Surfactants for Supercritical Carbon Dioxide Applications.* Polymer Preprints (American Chemical Society, Division of Polymer Chemistry), 1993. **34**(2): p. 664-5.
101. Zhu, D.M. and Z.A. Schelly, *Investigation of the Microenvironment in Triton X-100 Reverse Micelles in Cyclohexane, using Methyl Orange as a Probe.* Langmuir, 1992. **8**(1): p. 48-50.
102. McFann, G.J., *Ph.D. Dissertation Thesis*. 1993, The University of Texas at Austin.
103. Liu, J., et al., *Investigation of Nonionic Surfactant Dynol-604 Based Reverse Microemulsions Formed in Supercritical Carbon Dioxide.* Langmuir, 2001. **17**(26): p. 8040 - 8043.

104. Baczko, K., X. Chasseray, and C. Larpent, *Synthesis and Surfactant Properties of Symmetric and Unsymmetric Sulfosuccinic Diesters, Aerosol-OT Homologues.* Journal of the Chemical Society-Perkin Transactions 2, 2001(11): p. 2179-2188.
105. Zimmermann, J., A. Sunder, and R. Mulhaupt, *Preparation of Partially Hydrolyzed Oligo(vinylacetate) as Polyol for Polyurethane Formation.* Journal of Polymer Science Part a-Polymer Chemistry, 2002. **40**(12): p. 2085-2092.
106. Murphy, A. and G. Taggart, *Synthesis and Characterisation of a Novel Surfactant, Sodium Geranyl Sulphate.* Colloids and Surfaces a-Physicochemical and Engineering Aspects, 2001. **180**(3): p. 295-299.
107. Feller, D., *Application of Systematic Sequences of Wave-Functions to the Water Dimer.* Journal of Chemical Physics, 1992. **96**(8): p. 6104-6114.
108. Fan, X., et al., *Preparation of Silver Nanoparticles via Reduction of a Highly CO_2-Soluble Hydrocarbon-based Metal Precursor.* Industrial & Engineering Chemistry Research, 2005. **In print**.
109. Liu, J., et al., *Synthesis of Ag and AgI Quantum Dots in AOT-stabilized Water-in-CO_2 Microemulsions.* Chemistry--A European Journal, 2005. **11**(6): p. 1854-1860.
110. Ohde, H., et al., *Synthesizing Silver Halide Nanoparticles in Supercritical Carbon Dioxide Utilizing a Water-in-CO_2 Microemulsion.* Chemical Communications (Cambridge), 2000(23): p. 2353-2354.
111. McLeod, M.C., et al., *Synthesis and Stabilization of Metallic Nanoparticles and Pre-metallic Intermediates in PFPE/CO_2 Reverse Micelle Systems.* Phys. Chem. B, 2003. **107**(12): p. 2693.
112. Ji, M., et al., *Synthesizing and Dispersing Silver Nanoparticles in a Water-in-Supercritical Carbon Dioxide Microemulsion.* Journal of the American Chemical Society, 1999. **121**(11): p. 2631-2632.
113. Holmes, J.D., et al., *Synthesis of Cadmium Sulfide Q Particles in Water-in-CO2 Microemulsions.* Langmuir, 1999. **15**(20): p. 6613-6615.
114. Dong, X., D. Potter, and C. Erkey, *Synthesis of CuS Nanoparticles in Water-in-Carbon Dioxide Microemulsions.* Industrial & Engineering Chemistry Research, 2002. **41**(18): p. 4489-4493.
115. Zhang, R., et al., *Organic Reactions and Nanoparticle Preparation in CO_2-induced Water/P104/p-Xylene Microemulsions.* Chemistry--A European Journal, 2003. **9**(10): p. 2167-2172.
116. Sarbu, T., T.J. Styranec, and E.J. Beckman, *Non-Fluorous Polymers with Very High Solubility in Supercritical CO_2 Down to Low Pressures.* Nature, 2000. **405**: p. 165.
117. Dimitrov, S., et al., *Predicting the Biodegradation Products of Perfluorinated Chemicals using CATABOL.* SAR and QSAR in Environmental Research, 2004. **15**(1): p. 69-82.
118. Hoefling, T.A., et al., *Design and Synthesis of Highly CO_2-Soluble Surfactants and Chelating Agents.* Fluid Phase Equilibria, 1993. **83**: p. 203.
119. Sarbu, T., T.J. Styranec, and E.J. Beckman, *Design and Synthesis of Low Cost, Sustainable CO_2-philes.* Ind. Eng. Chem. Res., 2000. **39**(12): p. 4678.
120. Potluri, V.K., et al., *Peracetylated Sugar Derivatives Show High Solubility in Liquid and Supercritical Carbon Dioxide.* Org. Lett., 2002. **4**(14): p. 2333.
121. Rindfleisch, F., T. DiNoia, and M.J. McHugh, *Solubility of Polymers and Copolymers in Supercritical CO2.* J. Phys. Chem., 1996. **100**: p. 15581.
122. Shen, Z., et al., *CO_2-Solubility of Oligomers and Polymers that Contain the Carbonyl Group.* Polymer, 2003. **44**(5): p. 1491-1498.
123. Lora, M., F. Rindfleisch, and M.A. McHugh, *Influence of the Alkyl Tail on the Solubility of Poly(Alkyl Acrylates) in Ethylene and CO_2 at High Pressures: Experiments and Modeling.* Journal of Applied Polymer Science, 1999. **73**(10): p. 1979-1991.
124. Johnston, K.P., et al., *Water in Carbon Dioxide Macroemulsions and Miniemulsions with a Hydrocarbon Surfactant.* Langmuir, 2001. **17**(23): p. 7191-7193.
125. Raveendran, P. and S.L. Wallen, *Dissolving Carbohydrates in CO_2: Renewable Materials as CO_2-philes.* ACS Symposium Series, 2003. **860**(Supercritical Carbon Dioxide): p. 270-284.
126. Eastoe, J., et al., *Micellization of Economically Viable Surfactants in CO_2.* Journal of Colloid and Interface Science, 2003. **258**(2): p. 367-373.
127. da Rocha, S.R.P., et al., *Surfactants for Stabilization of Water and CO_2 Emulsions: Trisiloxanes.* Langmuir, 2003. **19**(8): p. 3114-3120.
128. Liu, J., et al., *Investigation of Nonionic Surfactant Dynol-604 Based Reverse Microemulsions Formed in Supercritical Carbon Dioxide.* Langmuir, 2001. **17**(26): p. 8040-8043.
129. Dickson, J.L., B.P. Binks, and K.P. Johnston, *Stabilization of Carbon Dioxide-in-Water Emulsions with Silica Nanoparticles.* Langmuir, 2004. **20**(19): p. 7976-7983.

130. Dickson, J.L., et al., *Interfacial Properties of Fluorocarbon and Hydrocarbon Phosphate Surfactants at the Water-CO2 Interface.* Industrial & Engineering Chemistry Research, 2005. **44**(5): p. 1370-1380.
131. Fan, X., et al., *Oxygenated Hydrocarbon Ionic Surfactants Exhibit CO_2 Solubility.* Journal of the American Chemical Society, 2005. **127**(33): p. 11754-11762.
132. Saunders, A.E., et al., *Solvent Density-Dependent Steric Stabilization of Perfluoropolyether-Coated Nanocrystals in Supercritical Carbon Dioxide.* Journal of Physical Chemistry B, 2004. **108**(41): p. 15969-15975.
133. Shah, P.S., et al., *Steric Stabilization of Nanocrystals in Supercritical CO2 Using Fluorinated Ligands.* Journal of the American Chemical Society, 2000. **122**(17): p. 4245-4246.
134. Bell, P.W., et al., *Stable Dispersions of Silver Nanoparticles in Carbon Dioxide with Fluorine-Free Ligands.* Langmuir, 2005. **21**(25): p. 11608-11613.
135. Liu, Y., R.B. Grigg, and R.K. Svec, *CO_2 Foam Behavior: Influence of Temperature, Pressure, and Concentration of Surfactant.* SPE 94307, 2005. **SPE Production and Operations Symposium, Oklahoma, OK, 17-19 April, 2005**.
136. Liu, Y., R.B. Grigg, and B. Bai, *Salinity, PH, and Surfactant Concentration Effects on CO_2-Foam.* SPE 93095, 2005. **SPE International Symposium on Oilfield Chemistry, Houston, TX, 2-4 February, 2005**.
137. Yaghoobi, H. and J.P. Heller, *Laboratory Investigation on Parameters Affecting CO2-Foam Mobility in Sandstone at Reservoir Conditions.* SPE 29168, 1994. **Eastern Regional Conference & Exhibition, Charleston, WV, 8-10 November, 1994**: p. 107-121.
138. Bernard, G.G., L.W. Holm, and C.P. Harvery, *Use of Surfactant to Reduce CO2 Mobility in Oil Displacement.* SPE Journal, 1980. **20**(4): p. 281-292.
139. Casteel, J.F. and N.F. Djabbarah, *Sweep Improvement in CO2 Flooding by Use of Foaming Agents.* SPE Reservoir Engineering, 1988. **3**: p. 1186-1192.
140. Holt, T., F. Vassenden, and I. Svorstol, *Effects of Pressure on Foam Stability; Implications for Foam Screening.* SPE 35398, 1996. **SPE/DOE Tenth Symposium on Improved Oil Recovery, Tulsa, OK**: p. 21-24 Aprial, 1996, 543-552.
141. Kuhlman, M.I., H.C. Lau, and A.H. Falls, *Surfactant Criteria for Successful Carbon Dioxide Foam in Sanstone Reservoirs.* SPE Reservoir Evaluation and Engineering, 2000. **3**(1): p. 35-41.
142. Borchardt, J.K., et al., *Surfactants for CO_2 Foam Flooding.* SPE 14394, 1985. **Annual Technical Conference and Exhibition, 22-26 September, Las Vegas, Nevada**.
143. Hoefner, M.L. and E.M. Evans, *CO_2 Foam: Results from Four Developmental Field Trials.* SPE Reservoir Engineering, 1995. **10**(4): p. 273-281.

References for CO_2 Soluble Polymers and Small Hydrogen Bonding Compounds

[1]. Drilling and production, Special report: CO_2 injection gains momentum, *Oil and gas journal* April 17 **2006**.
[2] Holm, L. W., and Josendal, V. A: "Effect of oil composition on miscible –type displacement by CO2," Soc. Pet. Enj. J. 1982 p87-98.]
[3]. Holm.L.W and Josendal. V. A. Mechanism of oil displacement by CO_2, *J. Pet. Tech*. **1974**, 1427-36.
[4]. ECL Technology, CO_2 Injection for Heavy Oil Reservoirs, DTI Sharp, CO_2 Dissemination April 2001
[5]. **Klins**, M., Carbon Dioxide Flooding – Basic Mechanisms and Project Design, International Human Resources Development Corporation, Boston, 1984.
[6]. Bernard, G. G., L. W. Holm, et al. (1980). "Use of Surfactant to Reduce CO2 Mobility in Oil Displacement." SPE Journal **20**(4): 281-292.
[7]. Borchardt, J. K., D. B. Bright, et al. (1985). "Surfactants for CO_2 Foam Flooding." SPE 14394 Annual Technical Conference and Exhibition, 22-26 September, Las Vegas, Nevada
[8]. Tullo, A. ICI enters CO_2 dry cleaining. *Chem.Eng.News*. **2002**, 80 (35), 12.
[9]. Jessop, P.G. Leitner, W., Eds Chemical Synthesis using supercritical CO_2, Wiley-VCH, Weinnnheim, 1999
[10]. Cooper, A.I. Polymer synthesis and processing using supercritical CO_2, *J. Mater. Chem.* **2000**, 10 (2) 207-234.
[11]. Behles, J.A. DeSimone,J.M. Developments in CO_2 research. *Pure Appl. Chem.* **2001**, 73 (8), 1281-1285.
[12]. Fulton, J. L.; Yee, G. G.; Smith, R. D. J. Am. Chem. SOC. 1991, 113,8327-8334
[13] Christopher F. Kirby and Mark A. McHugh, PhaseBehavior of Polymer in Supercritical Fluid Solvents, Chem. Rev.,1999, 99, 565-602
[14] Prausnitz.J.M, Lichtennthaler. R.N, Azevedo E.G, Molecular Thermodynamics of Fluid Phase Equilibria, 2nd ed, Prentice Hall, Englewood Cliffs, NJ,1986.

[15] Jucks, K. W; Huang, Z. S; Miller, R. E; Lafferty, W. J. The Structure of CO2 Dimer from Near Infrared Spectroscopy. J. Chem. Phys. 1987, 86, 4341-4346.
[16]. Kazarian, S. G.; Vincent, M. F.; Bright, F. V.; Liotta, C. L.; Eckert, C. A. Specific Intramolecular Interaction of Carbon Dioxide with Polymers, J. Am. Chem. Soc. 1996, 118, 1729.
[17]. Poovathinthodiyil Raveendran and Scott L. Wallen, Cooperative C-H…O hydrogen Bonding in CO_2-Lewis Base Complexes: Implication in Solvation in Supercritical CO_2, J. Am. Chem. Soc., 2002, 124, 12590-12599.
[18]. Kazariann, S. G., Vincent, M. V., Bright, F. V., Liotta, C. L. and Eckert, C. A., Specific Intermolecular Interaction of CO_2 with Polymers, J. Am. Chem. Soc., 1996, 118, 1729-1736.
[19]. Shen, Z., McHugh, M. A., Xu, J., Belardi, J., Kilic, S., Mesiano, A., Bane, S., Karnikas, C., Beckman, E., and Enick, R., CO_2-solubility of oligomers and polymers that contain the carbonyl group, Polymer, 2003, 44, 1491-1498.
[20] Heller J.P, Dandge D.K, Card R.J, and Donaruma L.G, Direct Thickners for Mobility Control of CO2 floods, Society of Petroleum Engineers Journal, 1985, 25(5), 679-86.
[21] Heller J.P, and Martin F.D. Improvement in CO2 Performance – Quarterly Report, April-June, Sept. 1990, PRRC.
[22] Gullapalli P.T, Heller J.P, Gelling Behaviour of HAS in organic Fluids and Dense CO2, SPE International Symposium on Oilfield Chemistry, 1995.
[23] Heller John P, Lien Cheng Li, Kuntamukkula Murty S, Foamlike dispersion for mobility control in carbon dioxide floods, Society of Petroleum Engineers Journal, 1985, 25(4), 603-13.
[24] Terry R, Zaid A, Angelos C, Polymerization in scCO2 to improve CO2/Oil Mobility Ratio, Society of Petroleum Engineers Journal, 1987, 16270
[25] Llave F, Chung F and Burchfield T, Use of Entrainers in improving mobility control scCO2, Society of Petroleum Engineers Journal, 1990, 47-51.
[26] Bae, J.H., Irani. C. A., Society of Petroleum Engineers Journal, 1990, 73.
[27] DeSimone, J., Guan, Z., Combes, J., Menceloglu, Y., Macromolecules, 1993, 26, 2663
[28] McClain, J. B., Betts, D. E., DeSimone, J. M., Poly. Preprints, 1996, 74,234.
[29] Enick, R. M., Beckman, E. J., Shi, C., Karmana, E., J Supercrit. Fl. 1998, 13, 127.
[30]. Huang, H., Shi, C., Xu, J., Kilic, S., Enick, R. M., Beckman, E. J., Macromolecules, 2000, 33, 5437.
[31]. Xu JH, Wlaschin A, Enick R.M, Thickening CO_2 with fluoroacrylate-styrene copolymer, SPE journal, 8(2), 85-91, 2003
[32]. C. Shi, Z. Huang, S. Kilic, J. Xu, R. M. Enick, E. J. Beckman, A. J. Carr, R. E. Melendez, A. D. Hamilton, The Gelation of CO_2: A Sustainable Route to the Creation of Microcellular Materials, *Science* **1999**, *286*, 1540 - 1543.
[33]. Stephen J. Michalik , Design, synthesis and optimization of non-fluorous,CO_2-philic polymers: A systematic approach. Thesis, University of Pittsburgh, 2003
[34]. Huang, H., Shi, C., Xu, J., Kilic, S., Enick, R. M., Beckman, E. J., Macromolecules, 2000, 33, 5437.

National Energy Technology Laboratory

626 Cochrans Mill Road

P.O. Box 10940

Pittsburgh, PA 15236-0940

3610 Collins Ferry Road

P.O. Box 880

Morgantown, WV 26507-0880

13131 Dairy Ashford, Suite 225

Sugar Land, TX 77478

1450 Queen Avenue SW
Albany, OR 97321-2198

2175 University Ave. South

Suite 201

Fairbanks, AK 99709

Visit the NETL website at:

www.netl.doe.gov

Customer Service:

1-800-553-7681